Understanding the relationship between central metabolism and virulence in the human pathogen *Streptococcus pneumoniae*

Sandra M. Carvalho

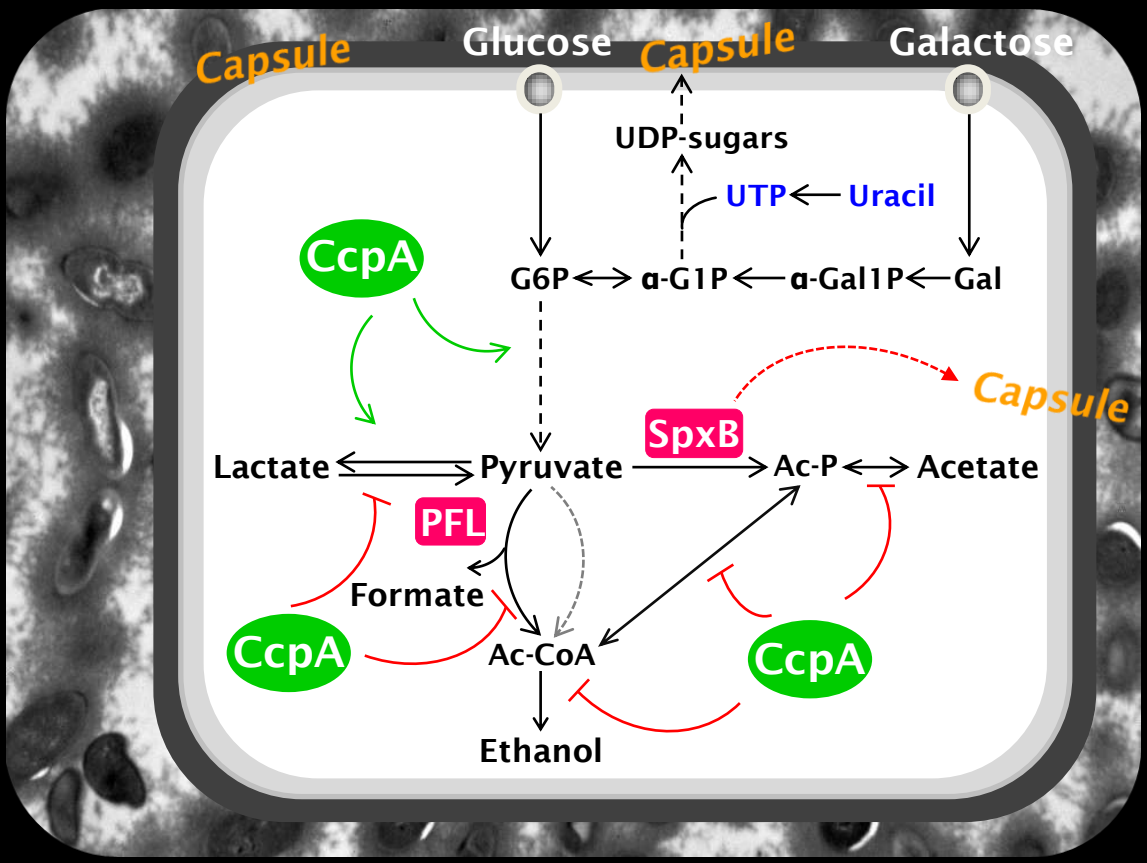

Dissertation presented to obtain the Ph.D. degree in Biochemistry

Instituto de Tecnologia Química e Biológica | Universidade Nova de Lisboa

Oeiras,
September, 2012

INSTITUTO
DE TECNOLOGIA
QUÍMICA E BIOLÓGICA
/UNL
Knowledge Creation

Understanding the relationship between central metabolism and virulence in the human pathogen *Streptococcus pneumoniae*

Sandra M. Carvalho

Supervisor: Dr. Ana Rute Neves

Co-supervisor: Professor Oscar Kuipers

Dissertation presented to obtain the Ph.D. degree in Biochemistry

Instituto de Tecnologia Química e Biológica | Universidade Nova de Lisboa

Oeiras, September, 2012

FCT Fundação para a Ciência e a Tecnologia
MINISTÉRIO DA CIÊNCIA, TECNOLOGIA E ENSINO SUPERIOR

INSTITUTO DE TECNOLOGIA QUÍMICA E BIOLÓGICA /UNL
Knowledge Creation

From left to right: Mário Ramirez, Paula Fareleira, Reinhold Brückner, Oscar Kuipers, Sandra Carvalho, Ana Rute Neves, Isabel Sá Nogueira, Helena Santos.

Apoio financeiro da Fundação para a Ciência e Tecnologia e do FSE no âmbito do Quadro Comunitário de apoio, Bolsa de Doutoramento com a referência SFRH/BD/35947/2007

Cover page figure: Schematic illustration of the pathways for glucose and galactose metabolism in a *Streptococcus pneumoniae* cell. Uracil, an important constituent of the capsule building blocks, and the non-classical virulence proteins (CcpA, SpxB and PFL) studied in this thesis are highlighted in different colours.
Background of the cover page figure: Transmission electron micrograph of *S. pneumoniae* cells grown in liquid medium. The picture was obtained by our collaborator JJE Bijlsma in the University of Groningen during the course of this thesis.

To my mother, father, brother and Nuno

Acknowledgements

In 2006, at the Lactic Acid Bacteria & *in vivo* NMR laboratory, I was introduced to scientific research and really enjoyed the experience. The excitement led me to accept the opportunity to integrate a PhD project to study central metabolism in *S. pneumoniae*, offered by my supervisor, Dr. Ana Rute Neves. During the course of the thesis I experienced a lot of emotions: the excitement and joy of new ideas and results, the disappointments of bad or confusing results, the persistence of not giving up and now the relief and happiness of achieving the final product. The present thesis would have never been possible without the help and encouragement of many people.

I thank my supervisor, Dr. Ana Rute Neves, for the opportunity to join her group and for introducing me to research and to the field of microbial physiology and biochemistry. I am grateful for her intellectual and scientific support, good ideas, advices, discussions and critical reading and writing of this thesis. I also thank her guidance during this PhD project.

I thank my co-supervisor, Prof. Dr. Oscar Kuipers, for the stimulating and pleasant collaboration with Dr. Ana Rute Neves, and the fruitful discussions and ideas. I also thank him for accepting me in the Molecular Genetics (MolGen) group, at the University of Groningen (The Netherlands), where I have been for 6 months, learning several techniques. I thank him all the support provided during this stay, which contributed not only to my research experience but also to my personal development.

I thank Prof. Dr. Helena Santos for the fruitful collaboration with Dr. Ana Rute Neves during my first year as a research student and for all the help provided during the course of this thesis. I acknowledge Prof. Dr. Helena Santos for the valuable discussions in lab meeting presentations and for the critical reading of the abstract of this thesis.

I thank Prof. Dr. Jan Martinussen for supervising me during a short stay at the Technical University of Denmark (DTU), Lyngby, and for the determination of pyrimidine nucleotides. I also thank him and his family for the warm reception and generous hospitality.

I thank Prof. Dr. Peter Andrew and Dr. Hasan Yesilkaya for the collaboration that led to the “PFL publication”.

I thank Dr. Jetta Bijlsma (UMCG, Groningen) for the good collaboration in the work involving pyruvate oxidase (SpxB) and for all the helpful discussions.

I thank Dr. Susana Vinga for the good collaboration in the development of descriptive and predictive models of *S. pneumoniae* metabolism. I thank José Caldas for the fast assistance in microarray analysis.

When I started my PhD, in 2007, I was the only student working with *S. pneumoniae* in the LAB & *in vivo* NMR group, but I was never alone, I found good company among the people at the Cell Physiology and NMR group. In 2008/9, during 6 months, I got settled in Groningen, and in the MolGen group I got support from many people, especially the “Strep” group. When I got back, the LAB & *in vivo* NMR group started to flourish and I have gotten company from many new

people, my enthusiastic and “Streptococcal” lab mates and my daily lunch partners. Having more people working with *S. pneumoniae* in the lab and sharing many questions, “Strep” related, was an additional excitement. I am truly thankful for the help and friendship of many of you.

I thank Patrícia Almeida, Ana Manso and Cristiana Faria for being helpful colleagues and good friends. Thank you for listening to me and motivating me when I needed it.

I thank Mafalda Cavaleiro, Joana Oliveira, Anabela Vieira, Irene Gonzalez and João Jorge for the stimulating and fun environment inside and outside the lab. Thank you all for the support and help provided.

I thank Nuno Borges, Rute Castro and Ana Lúcia Carvalho for their invaluable help in the lab and for being always available to teach. I thank Luís Fonseca for the useful discussions and for always being available to help.

All my other colleagues in the LAB & *in vivo* NMR and Cell Physiology and NMR groups and short-stay lab visits: Ana Esteves, Dusica Rados, Nelson, Claudia Sanchez, Marta Rodrigues, Teresa Maio, Paula Gaspar, Ricardo Sequeira, Ana Isabel Mingote, Ana Laura Paixão, Luís Gafeira, Tiago Pais, Tiago Faria, Pedro Lamosa, Marta Conchinha, Carla Jorge, Melinda Noronha, Tony Collins, Pedro Quintas, Teresa Ferreira, Margarida Santos, Catarina Silva, Sónia Neto, Márcia, Andreia, Alexandre, Eva Lourenço, Francesca Spissu, Ana Belém, Alessandro Bidossi and Karina Pokusaeva, for creating a good working atmosphere.

I thank all my colleagues in MolGen for all the assistance provided during my stay there. In particular, I would like to acknowledge the “Strep” group for making Groningen a nice place to remember. I thank Tomas Kloosterman for the supervision of my work at the MolGen, for all the help provided during this thesis and for the nice and friendly talks. I thank Sulman Shafeeq for being a great colleague and friend, for helping me finding things in the lab and for the useful discussions. I also thank him and Munir for the delicious and spicy Pakistani food. I thank Asia, Rutger, Agata and Michael for all the help and company.

During this thesis, I have crossed with many other great people. I thank Nicolas Bernier, Manuel Marques Pita, Daniela, Yuki Miyagaki and Chantal Fernandes for the pleasant talks and excursion activities.

I thank the invaluable technical support of many people, Teresa Batista, Luís Gonçalves, Miguel Loureiro, people from the academic services, D. Fátima and Ana Maria Portocarrero, and from the washing room of the 5th floor and D. Alice.

I thank Fundação para a Ciência e Tecnologia (FCT) for the financial support that made this doctoral work possible (SFRH/BD/35947/2007).

Agradeço aos meus pais e ao meu irmão o amor incondicional, a compreensão nos meus momentos de ausência involuntários, e o apoio em todas as circunstâncias. A toda a minha família e amigos, obrigada por tudo.

Finalmente gostaria de agradecer ao Nuno, com quem partilho de todo o coração a minha vida. Obrigada pela tua paciência, incentivo, conselhos, inspiração e motivação durante esta jornada. Obrigada por estares sempre presente.

Abstract

Streptococcus pneumoniae is a normal inhabitant of the human nasopharynx, but it is better known for its role in a plethora of human diseases. Growing emergence of antibiotic-resistant streptococci and non-type vaccine strains increases the urgency of finding new targets for the development of novel therapeutic and preventive drugs. As a major concern for global public health, *S. pneumoniae* has always attracted great attention from the scientific community, which has translated into knowledge on pathogenesis and virulence and the development of a considerable “toolbox” for genetic manipulation and genomic analysis, as well as a large number of deciphered genome sequences. Interestingly, genome-wide studies have consistently pinpointed genes involved in carbohydrate uptake and metabolism as essential for the virulence of *S. pneumoniae*. These global studies offered the opportunity to investigate in greater depth the potential connections between basic physiology, and in particular central metabolism, and pneumococcal virulence and pathogenesis. The general goal of this thesis is to achieve a deeper understanding of the molecular mechanisms underlying sugar metabolism and their relation to virulence factors in *S. pneumoniae*, with a special focus on capsule production. In the present work, glucose (Glc) and galactose (Gal) were used as carbon sources for the study of pneumococcal sugar metabolism. This choice was made for two reasons: Firstly, Glc is a common preferred sugar and is also found as a major carbon source in niches potentially occupied by *S. pneumoniae* during host inflammation or hyperglycaemia. Secondly, Gal, generally a slowly metabolized non-preferred sugar, is a major carbohydrate in the human nasopharynx, the non-pathological colonization niche of *S. pneumoniae*.

The study of complex regulatory mechanisms such as those involved in sugar metabolism is largely facilitated by the use of well-defined conditions. We developed a chemically defined medium and growth conditions for high yield streptococcal growth, applicable to *in vivo* NMR studies. Time series data on metabolite pools have been obtained *in vivo* by ^{13}C- and ^{31}P- NMR, during Glc metabolism of *S. pneumoniae*. The major end-product formed from the metabolism of [1-^{13}C]Glc by resting cells of *S. pneumoniae* acapsular strain R6 was lactate (about 35 mM). Fructose 1,6-bisphosphate (FBP) was the only glycolytic intermediate detected. The pool of FBP increased at the expense of Glc, reached a steady concentration and decreased to undetectable levels before Glc exhaustion. In ^{31}P-NMR experiments, upon Glc addition, the levels of inorganic phosphate (P_i) decreased, accompanying the consumption of Glc, and the levels of NTP reached very small values (*circa* 2 mM). Moreover, during the optimization of growth conditions for *S. pneumoniae*, an extensive comparative metabolic characterization between strains D39 and its non-encapsulated derivative R6 was obtained under different environmental and nutritional conditions. The effect of oxygen, Glc and nucleobases on the physiology of growth of these strains was studied under controlled conditions of pH, temperature and gas atmosphere (anaerobic, semi-aerobic or aerobic) in 2-l bioreactors. Independently of the growth conditions tested, both strains displayed a typical homolactic behavior. However, the growth rates of D39 and R6 were stimulated under semi-aerobic and strictly anaerobic conditions, respectively. This difference was mainly attributed to lower activity of pyruvate oxidase in strain D39, in the presence of oxygen. It was notable that the maximal biomass reached by strain D39 was substantially enhanced by supplementation of the culture medium with extra uracil, whereas in strain R6 no effect was observed, suggesting a link between uracil and capsule production.

The synthesis of the NDP-sugars, precursors of D39 capsule, requires UTP and dTTP. UTP is formed from UMP in the salvage pathway of pyrimidine biosynthesis. UMP may also be synthesized *de novo* from amino acids and CO_2 or via the salvage pathway using external pyrimidine nucleobases (*e.g.* uracil) or nucleosides. A remarkable adaptation of *S. pneumoniae* to fluctuating environmental conditions in the human host consists in the switch between opaque and transparent phenotypes, distinguished by different capsule amounts. In this work, the role of uracil on capsule expression and production was assessed by studying D39 and a spontaneous non-reversible D39 mutant displaying an underproducing capsule phenotype. A comparative transcriptome analysis between these strains in medium with and without uracil suggested a connection between pyrimidine metabolism and capsule production. In medium lacking uracil, strain D39 exhibited a long lag phase, decreased growth rate and higher biomass than in the presence of the nucleobase. In accordance, capsule promoter activity and capsule amounts were decreased under uracil-deprived conditions in strain D39. In contrast, uracil showed no effect on the mutant strain. Growth and CFU analysis of co-cultures of both strains in medium without uracil clearly showed a prevalence of the mutant strain at mid-exponential phase of growth, independently of the initial cell concentrations used for inoculation. Thus, we propose that sensing uracil is a potential mechanism by which *S. pneumoniae* alters capsule production.

Other than uracil, oxygen variability in host niches may also trigger the capsular phenotype switch in *S. pneumoniae*. Pyruvate oxidase (SpxB) is an oxygen-consuming enzyme involved in the aerobic metabolism of *S. pneumoniae*. SpxB converts pyruvate, the end-product of glycolysis, O_2 and P_i into CO_2, H_2O_2 and acetyl-phosphate. We show that inactivation of *spxB* in D39 leads to increased production of capsule amounts in medium with Glc. This increase was

partially mediated by induction of *cps2A*, the first gene of the capsule *locus*. In addition, the *spxB* mutation increased the expression of two putative operons involved in carbohydrate uptake and processing, leading to altered sugar utilization capabilities of D39, as shown by a combination of metabolite profiling analysis and growth experiments. In environments with oxygen and Glc as major carbon source, SpxB activity presumably minimizes the use of alternative sugar utilization pathways and the amount of capsule, hence improving the fitness of *S. pneumoniae*.

Besides SpxB, pyruvate formate-lyase (PFL) is also a competing activity for the glycolytic end-product, pyruvate. This oxygen-sensitive enzyme is involved in mixed-acid fermentation and requires post-translational activation by the pyruvate formate-lyase activating enzyme (PFL-AE). PFL activity is associated with formation of formate and acetyl-CoA. The sequenced genome of D39 possesses two copies of *pfl* and *pfl-ae*. Mutant strains disrupted in these genes were created, and their Glc and Gal metabolism was analyzed. In the presence of Glc, all strains, including D39, exhibited homolactic fermentation. However, in Gal, strain D39 produced formate, acetate and ethanol in a 2:1:1 ratio, denoting activity of PFL, but no formate production was observed by mutants defective in *spd_0420* and *spd_1774*, indicating that *spd_0420* codes for PFL and *spd_1774* for PFL-AE. The *spd_0420* and *spd_1774* mutants showed impaired colonization and infection in mouse studies, indicating a direct link between pneumococcal fermentative metabolism and virulence.

S. pneumoniae has to adapt to changing carbon sources in the fluctuating environments of the human host. Pathways metabolizing sugars other than the preferred one are silenced through mechanisms of catabolite repression. A global regulator involved in this process in several Gram-positive bacteria is CcpA. In *S. pneumoniae*, a systemic appraisal of the role of CcpA in the physiology of this

bacterium was missing. We clearly demonstrate that CcpA is a global regulator, affecting the expression of up to 19% of the genome, covering multiple cellular functions. Remarkably, CcpA was not only a major repressor in response to Glc, but also to Gal. Additionally, we show that Leloir and tagatose 6-phosphate pathways for Gal metabolism are functionally active, despite repression of the Leloir genes by CcpA. Of surprise was the shift from mixed-acid towards a more homolactic fermentation in the *ccpA* mutant during growth on Gal, as genes involved in mixed-acid fermentation were mostly under CcpA repression. This result indicates regulation at other cellular layers, which is further supported by dissimilar accumulation in the *ccpA* and parent strain of intracellular metabolites potentially involved in metabolic regulation. Interestingly, capsule amounts were higher in response to Gal than to Glc, regardless of CcpA. Overall, the whole-genome transcriptome analyses provided solid evidence that *S. pneumoniae* optimizes basic metabolic processes in a CcpA-mediated manner. This view is further corroborated by the metabolic profiles obtained under the conditions studied. Moreover, integration of transcriptional and metabolic data revealed a link between CcpA and the association of surface molecules (capsule and phosphorylcholine) recognized as virulence factors, to the cell wall. This finding indicates an important role of CcpA in modulating the interaction of *S. pneumoniae* with its host.

Overall, the work presented in this thesis represents an important step towards the understanding of basic metabolic processes and, in particular, sugar metabolism, in *S. pneumoniae*. We believe that the insights gained from this study will help to better comprehend the role of metabolism in the interaction between *S. pneumoniae* and its host. In this light, the work here described makes a unique bridge between the often disconnected fields of fundamental physiology, and virulence and infection.

Resumo

A bactéria *Streptococcus pneumoniae* é uma habitante normal da nasofaringe humana, conhecida principalmente por ser a causa de várias doenças humanas. Em ambientes hospitalares bem como na comunidade, o aparecimento galopante de estreptococos resistentes a antibióticos bem como de estirpes não integradas no programa de vacinação incentiva novos estudos com o objectivo de identificar alvos para o desenvolvimento de novas drogas terapêuticas ou preventivas. Dado o seu impacto ao nível de saúde pública mundial, *S. pneumoniae* tem atraído desde sempre a atenção da comunidade científica. Este grande interesse permitiu grandes avanços no conhecimento da patogenicidade e virulência deste organismo, e levou ao desenvolvimento de muitas ferramentas de manipulação genética e análise genómica e à descodificação de um número elevado de sequências genómicas. Em estudos de análise pangenómica, genes envolvidos no transporte e metabolismo de hidratos de carbono foram consistentemente identificados como sendo essenciais para a virulência de *S. pneumoniae*. Estes estudos globais ofereceram a oportunidade de investigar em profundidade uma ligação potencial de processos metabólicos básicos, em particular envolvidos no metabolismo central, com a virulência e patogenicidade de pneumococos. Assim sendo, este trabalho de tese tem por objectivo geral elucidar fundamentos necessários para a compreensão de mecanismos moleculares relacionados com o metabolismo de açúcares e sua ligação a factores de virulência de *S. pneumoniae*, em especial a cápsula. As hexoses glucose (Glc) e galactose (Gal) foram seleccionadas como fontes de carbono para o estudo do metabolismo de açúcares. Esta escolha baseou-se no seguinte: i), a Glc é o açúcar preferido por excelência e é a principal fonte de carbono encontrada em nichos potencialmente ocupados por *S. pneumoniae*

durante estados inflamatórios ou de hiperglicémia; ii), a Gal, geralmente um açúcar não preferido e de metabolismo lento, é um dos hidratos de carbono em maior quantidade na nasofaringe humana, o nicho de colonização de *S. pneumoniae*.

O estudo de mecanismos de regulação complexos, como os envolvidos em metabolismo de açúcares, é grandemente facilitado pelo uso de condições bem definidas. Neste trabalho, foram desenvolvidos um meio quimicamente definido e condições de crescimento para produção de biomassa elevada de estreptococos, aplicável também a estudos de NMR *in vivo*. Pela primeira vez, as concentrações de metabolitos formados e consumidos ao longo do tempo, durante o metabolismo de Glc em *S. pneumoniae*, foram obtidas *in vivo* recorrendo a NMR de ^{13}C e ^{31}P. O produto final maioritário do metabolismo de [1-^{13}C]Glc pelas células R6 em repouso foi o lactato (cerca de 35 mM). A frutose 1,6-bisfosfato (FBP) foi o único intermediário glicolítico detectado. Os níveis de FBP aumentaram à custa do consumo de Glc, atingiram uma concentração estacionária e decresceram para níveis não detectáveis antes da exaustão de Glc. Nas experiências de ^{31}P-NMR, após a adição de Glc, os níveis de fosfato inorgânico (P_i) decresceram, acompanhando o consumo de Glc, e os níveis de NTP atingiram valores muito baixos (cerca de 2 mM). Além disso, durante a optimização das condições para crescimento de *S. pneumoniae*, uma caracterização metabólica comparativa entre as estirpes D39 e a sua derivada não encapsulada R6 foi obtida em diferentes ambientes manipulados. O efeito do oxigénio, Glc e nucleobases na fisiologia do crescimento destas estirpes foi estudado em condições controladas de pH, temperatura e atmosfera gasosa (anaeróbica, semi-aeróbica e aeróbica), em reactores de 2-l. Independentemente das condições de crescimento testadas, ambas as estirpes exibiram um comportamento tipicamente homoláctico. Contudo, as taxas de crescimento das

estirpes D39 e R6 foram estimuladas em condições semi-aeróbicas e estritamente anaeróbicas, respectivamente. Esta diferença foi atribuída essencialmente à baixa actividade de piruvato oxidase na primeira estirpe, na presença de oxigénio. Curiosamente, a biomassa máxima atingida pela estirpe D39 foi substancialmente melhorada suplementando o meio de cultura com uracilo adicional, enquanto na estirpe R6 nenhum efeito foi observado, indicando uma ligação entre a quantidade de uracilo e produção de cápsula.

A síntese dos açúcares ligados quimicamente a NDP, precursores da cápsula da estirpe D39, requer UTP e dTTP. O UTP é sintetizado a partir de UMP na via de salvamento de síntese de pirimidinas. O UMP pode ser sintetizado *de novo* a partir de aminoácidos e CO_2 ou na via de salvamento das nucleobases (*e.g.* uracilo) ou nucleósidos de pirimidinas exógenas. Um mecanismo notável de adaptação do *S. pneumoniae* a condições ambientais inconstantes no hospedeiro humano consiste na permuta entre fenótipos opaco e transparente, que se distinguem pela quantidade diferente de cápsula exibida. Neste trabalho, o papel do uracilo na expressão e produção de cápsula foi demonstrado usando D39 e um mutante não reversível da D39 exibindo características associadas à baixa produção de cápsula. Uma análise de transcriptómica comparativa entre estas estirpes em meio com e sem uracilo sugeriu uma ligação entre o metabolismo de pirimidinas e produção de cápsula. Em meio sem uracilo, a estirpe D39 exibiu uma fase de adaptação (lag) longa, taxa de crescimento reduzida e biomassa mais elevada do que em meio contendo a nucleobase. Em conformidade, a actividade do promotor do operão que codifica para a cápsula bem como a quantidade de cápsula decresceram em meio sem uracilo na estirpe D39. Em contraste, o uracilo não teve qualquer efeito na estirpe mutante. O crescimento e análise de CFUs de co-culturas de ambas as estirpes mostrou claramente a predominância da estirpe mutante em fase exponencial de crescimento, em meio

sem uracilo, independentemente das concentrações iniciais de células usadas para inoculação das co-culturas. Posto isto, propomos que a detecção de quantidades variáveis de uracilo no ambiente constitui um mecanismo pelo qual o *S. pneumoniae* poderá alterar a produção de cápsula.

Para além do uracilo, o oxigénio poderá também desencadear a permuta dos fenótipos relacionados com diferentes quantidades de cápsula em *S. pneumoniae*. A piruvato oxidase (SpxB) é uma enzima consumidora de oxigénio envolvida no metabolismo aeróbio de *S. pneumoniae*. A SpxB converte piruvato, o produto final da glicólise, O_2 e P_i em CO_2, H_2O_2 e acetil-fosfato. Neste trabalho, mostramos que a inactivação de *spxB* em D39 leva a um aumento na quantidade de cápsula produzida em meio com Glc. Este aumento foi parcialmente mediado pela indução de *cps2A*, o primeiro gene do *locus* capsular. Adicionalmente, a mutação da *spxB* aumentou a expressão de dois operões putativamente envolvidos no transporte e processamento de hidratos de carbono, levando a uma alteração da capacidade de utilização de açúcares na estirpe D39, como indicado pela combinação de análise de perfis de metabolitos e experiências de crescimento. Em ambientes com oxigénio e Glc como principal fonte de carbono, a actividade de SpxB minimiza presumivelmente o uso de vias alternativas de utilização de açúcares e a quantidade de cápsula, melhorando assim a aptidão fisiológica de *S. pneumoniae*.

Para além da SpxB, a piruvato formato-liase (PFL) também compete por piruvato. Esta enzima sensível ao oxigénio, está envolvida na fermentação a ácidos mistos e sofre activação pós-traducional pela enzima activadora da piruvato formato-liase (PFL-AE). A actividade de PFL está associada à formação de formato e acetil-coenzima A. O genoma de D39 apresenta duas cópias de *pfl* e *pfl-ae*. Neste trabalho, estirpes mutantes inactivadas nestes genes foram construídas e o metabolismo de Glc e Gal foi analisado. Em Glc, todas as

estirpes, incluindo a D39, exibiram fermentação homoláctica. Em Gal, a estirpe D39 produziu formato, acetato e etanol na razão 2:1:1, indicando actividade de PFL, mas não se observou formação de formato nos mutantes com inactivação dos genes *spd_0420* e *spd_1774*, indicando que *spd_0420* codifica para a PFL e *spd_1774* para a PFL-AE. Os mutantes *spd_0420* e *spd_1774* mostraram deficiências na colonização e infecção de ratos, indicando uma ligação directa entre o metabolismo fermentativo de pneumococos e patogenicidade.

Nos ambientes inconstantes do hospedeiro humano *S. pneumoniae* é forçado a adaptar-se a variações na acessibilidade de fontes de carbono. As vias envolvidas no metabolismo de açúcares, que não o preferido, são silenciadas através de mecanismos de repressão catabólica. Um regulador global envolvido neste processo em várias bactérias é a CcpA. Em *S. pneumoniae*, uma avaliação sistémica do papel da CcpA na fisiologia desta bactéria não existia. Neste trabalho, mostrou-se claramente que a CcpA é um regulador global que afecta a expressão de cerca de 19% do genoma, abrangendo inúmeros processos celulares. Curiosamente, o papel repressor da CcpA não foi observado apenas em Glc, mas também em Gal. Adicionalmente, mostrou-se que as vias Leloir e tagatose 6-fosfato envolvidas no metabolismo de Gal estão funcionalmente activas, apesar da CcpA reprimir os genes da via de Leloir. Considerando que os genes envolvidos na fermentação a ácidos mistos estão sob repressão pela CcpA, o desvio do metabolismo de Gal de ácidos mistos para fermentação homoláctica no mutante da *ccpA* foi claramente surpreendente. Esta observação indica regulação ao nível de outras camadas celulares, e é fortemente corroborada pelos diferentes conteúdos intracelulares no mutante e na estirpe parental potencialmente envolvidos em regulação metabólica. Notavelmente, os níveis de cápsula foram maiores em Gal do que em Glc, independentemente da presença da CcpA. Em geral, as análises globais de transcriptómica

providenciaram evidência sólida de que *S. pneumoniae* optimiza processos metabólicos básicos através da CcpA. Esta observação é corroborada pelos perfis metabólicos obtidos nas condições estudadas. Mais ainda, a integração dos dados de transcriptómica e de metabolismo revelaram uma ligação entre a CcpA e a associação de moléculas da superfície celular (cápsula e fosforilcolina), reconhecidas como factores de virulência, com a parede celular. Desta forma, a CcpA pode ter um papel preponderante nas interações hospedeiro-micróbio.

Em suma, o trabalho apresentado nesta tese representa um passo importante para a compreensão de processos metabólicos básicos e, em particular, metabolismo de açúcares, em *S. pneumoniae*. Estamos convictos que os conhecimentos adquiridos neste estudo contribuirão para um conhecimento mais profundo do papel do metabolismo na interacção entre *S. pneumoniae* e o hospedeiro. O trabalho aqui descrito estabelece uma ponte única entre duas áreas, muitas vezes desconectadas, ou sejam, a fisiologia fundamental e virulência e infecção.

Contents

Thesis outline

Diseases caused by *Streptococcus pneumoniae* constitute a major global health problem. The ever-increasing emergence of antibiotic resistant strains exacerbates the need to find new targets for the development of effective therapeutic and prophylactic drugs. The work in this thesis aimed at gaining further knowledge on central metabolism and its connections to virulence in *S. pneumoniae*.

Chapter 1 starts with an introduction to the pneumococcus and its virulence factors. Next, an overview of carbohydrate metabolism, including capsule synthesis in the pneumococcus, is presented. Finally, a detailed description of the current knowledge concerning regulation of sugar metabolism in *Streptococcaceae* and links between basic physiology in *S. pneumoniae* and virulence is provided.

Chapter 2 describes the development of a culture medium and growth conditions for high yield pneumococcal growth, that enable the application of *in vivo* NMR techniques to study metabolism in *S. pneumoniae*. During this optimization a comparative metabolic characterization between the model strain D39 and its unencapsulated derivative R6 was performed.

In Chapter 3, the effect of uracil in the physiology of growth and capsule expression/production of D39 and D39SM, a spontaneous mutant displaying characteristics of underproducing capsule phenotype, was analyzed. Additionally, a genome wide transcriptional response of both strains to uracil and uracil limitation was studied by using DNA microarrays.

In Chapter 4, the transcriptional response of *S. pneumoniae* to *spxB*, encoding pyruvate oxidase, deletion was examined. The effect of this mutation in the profile of intracellular metabolites, end-products accumulation and capsule

amount was determined by resorting to ^{31}P-NMR, HPLC and capsule quantification, respectively. The effect of the *spxB* knock-out on the utilization of a number of sugars was also studied.

The identification of *S. pneumoniae* pyruvate formate-lyase (PFL) and the PFL activating enzyme (PFL-AE) is described in Chapter 5. Deletion of putative genes coding for these proteins was performed and functional assignment was determined by measuring the fermentation products of the mutant strains during metabolism of Glc and Gal.

Chapter 6 describes the carbon catabolite protein A (CcpA) regulon on Glc and Gal and the impact of this transcriptional regulator on the expression of virulence factors. In this work CcpA is demonstrated to act as a global regulator in *S. pneumoniae*. Overall, our results support the hypothesis that *S. pneumoniae* optimizes basic metabolic processes, likely enhancing *in vivo* fitness, in a CcpA-mediated manner.

A general discussion of the findings resulting from this work is presented in Chapter 7.

Abbreviations

ABC	ATP-binding cassette
ACKA	Acetate kinase A
Ac-P	Acetyl-phosphate
ADH	Alcohol dehydrogenase
BgaA	β-galactosidase A
CBP	Choline-binding protein
CcpA	Carbon catabolite protein A
CCR	Carbon catabolite repression
CDM	Chemically defined medium
CDP-Cho	CDP-Choline
CFU	Colony forming unit
COG	Clusters of Orthologous Groups
Cre	Catabolite responsive element
DHAP	Dihydroxyacetone phosphate
D39SM	D39 spontaneous mutant
dTDP-Rha	dTDP-rhamnose
EMP	Embden-Meyerhof-Parnas
Eno	Enolase
FAD	Flavine adenine dinucleotide
FBP	Fructose 1,6-bisphosphate
Gal	Galactose
Gal1P	Galactose 1-phosphate
GAP	Glyceraldehyde 3-phosphate
GAPDH	Glyceraldehyde 3-phosphate dehydrogenase
Glc	Glucose

GlcA	Gluconic acid
GlcNAc	N-acetylglucosamine
GlcUA	Glucuronic acid
G1P	Glucose 1-phosphate
G6P	Glucose 6-phosphate
H_2O_2	Hydrogen peroxide
HPLC	High Performance Liquid Chromatography
HPr	Histidine-containing phosphocarrier protein
$HPr_{(His15)}$~P	HPr phosphorylated at histidine 15
HPrK/P	HPr kinase/phosphorylase
$HPr_{(Ser46)}$~P	HPr phosphorylated at serine 46
LAB	Lactic acid bacteria
LDH	Lactate dehydrogenase
LOX	Lactate oxidase
MIC	Minimal inhibitory concentration
NAD^+	Nicotinamide adenine dinucleotide
NADH	Dihydronicotinamide adenine dinucleotide
NMR	Nuclear magnetic resonance
*P*Cho	Phosphorylcholine
PDHc	Pyruvate dehydrogenase complex
PEP	Phospho*enol*pyruvate
PFK	6-Phosphofructokinase
PFL	Pyruvate formate-lyase
PFL-AE	Pyruvate formate-lyase activating enzyme
3-PGA	3-Phosphoglycerate
6-PGD	6-Phosphogluconate dehydrogenase
PGM	Phosphoglucomutase

P_i	Inorganic phosphate
PK	Pyruvate kinase
PRDs	PTS-regulatory domains
PTA	Phosphotransacetylase
PTS	Phospho*enol*pryruvate:carbohydrate phosphotransferase system
PTS^{Man}	Mannose-PTS (domains IIA^{Man}, IIB^{Man}, IIC^{Man} and IID^{Man})
RT-PCR	Real time PCR
SpxB	Pyruvate oxidase
TBP	Tagatose 1,6-bisphosphate
TEM	Transmission electron microscopy
UDP-Gal	UDP-galactose
UDP-Glc	UDP-glucose
UDP-GlcUA	UDP-glucuronic acid
Und-P	Undecaprenyl-phosphate
WT	Wild-type

Chapter 1

General introduction

Chapter 1 – Contents

Streptococcus pneumoniae

Streptococcus pneumoniae, also called the pneumococcus, was first isolated and identified independently by George M. Sternberg and Louis Pasteur, in 1880 (Gray and Musher, 2008). During the following decade the pneumococcus would be recognized as the major cause of human lobar pneumonia (Gray and Musher, 2008). In the beginning of the 20th century the pneumococcus was among the leading causes of human death and a major concern in medicine (Gray and Musher, 2008). For this reason, *S. pneumoniae* was the subject of intensive research in a number of groundbreaking scientific discoveries, including the discovery of DNA as the carrier of genetic inheritance, and the therapeutic efficacy of the antibiotic penicillin (Avery *et al.*, 1944; Watson *et al.*, 1993). In the present time, an increase in antibiotic-resistant pneumococcal strains due to the widespread and uncontrolled antibiotic usage encourages the scientific community to find and develop novel preventive and prophylactic drugs (López, 2006).

General characteristics of *S. pneumoniae*

S. pneumoniae is a Gram-positive, low-GC microorganism. The pneumococcus may appear singly, as two joined cells (diplococcus) or in short or long chains (Fig. 1.1). The individual cells are ovoid, spherical or lancet-shaped with a size of 0.5 – 1.25 µm, and display a capsule surrounding the cell wall (Fig. 1.1). *S. pneumoniae* is non-motile and non-spore forming. This organism is a non-respiring, catalase-negative, aerotolerant fermentative anaerobe that requires several nutrients for growth, normally supplied by its natural habitats (mucosal secretions or blood); it produces mainly lactic acid from fermentation of carbohydrates (Tuomanen, 2006). The ideal temperature and pH for growth of the

pneumococcus is 37ºC and 6.5 – 7.5, respectively. In batch cultures, this microorganism undergoes autolysis at stationary phase (Severin *et al.*, 1997).

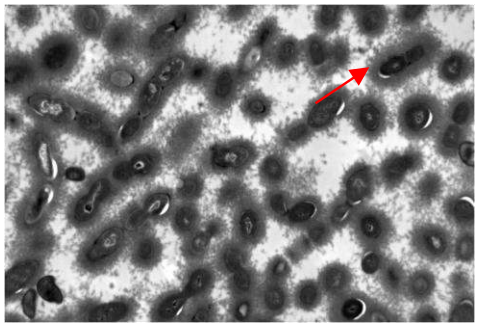

Fig. 1.1. Transmission electron micrograph of *S. pneumoniae* cells grown in liquid medium. The red arrow points to the polysaccharide capsule. This image was obtained at the University of Groningen during the course of this work (Chapter 4).

Due to its appearance as pairs of cocci under the microscope the pneumococcus was generally known as *Diplococcus pneumoniae*. This denomination remained official until 1974, when the bacterium was reclassified as *Streptococcus pneumoniae* based on its growth as chains in liquid media and the proximity with other streptococcal species (López, 2006; Gray and Musher, 2008). The genus *Streptococcus* includes other highly relevant pathogenic bacteria (*e.g. S. agalactiae*, *S. pyogenes*, *S. mutans, S. mitis*, *S. gordonii*, *S. sanguis*, *S. bovis*, and *S. suis*), infecting humans and/or animals, and a dairy bacterium, *S. thermophilus* (reviewed in Facklam, 2002). Some of these microorganisms colonize niches (oral cavity) in close proximity to that of *S. pneumoniae* (nasopharynx). Differentiation of nasopharyngeal swab isolated pneumococci from other streptococci, is provided by dissimilarities in bile solubility, fermentation

of inulin, sensitivity to optochin, agglutination with anti-polysaccharide capsule antibodies (Quellung reaction) and alpha-haemolytic activity in blood agar plates, namely the formation of a green halo surrounding pneumococcal colonies (Dowson, 2004). The genus *Streptococcus* belongs to the family *Streptococcaceae*, which also includes the genus *Lactococcus* (Schleifer *et al.*, 1985).

S. pneumoniae is a frequent colonizer of the human nasopharynx of healthy individuals, especially children (Obaro and Adegbola, 2002; Bogaert *et al.*, 2004; Cardozo *et al.*, 2006). Prevalence of carriage as high as 90% has been reported for children in some African regions, whereas in western societies the values can be as high as 70% (Bogaert *et al.*, 2004; Cardozo *et al.*, 2006). Hence, children are believed to be an important vehicle for the horizontal spread of *S. pneumoniae* within the communities (Obaro and Adegbola, 2002; Bogaert *et al.*, 2004; Cardozo *et al.*, 2006). The transmission of the pneumococcus occurs through direct droplet contact with colonized individuals. *S. pneumoniae* is also an opportunistic bacterium, therefore, when the host immune system is immature (*e.g.* in children) or debilitated (*e.g.* in elderly and immuno-compromised people), it can migrate from the nasopharynx to normal sterile parts of the human body, such as middle ear, paranasal sinuses, lungs, blood or meninges, causing otitis media and sinusitis, or other less prevalent, but more severe conditions such as pneumonia, septicaemia and meningitis (Obaro and Adegbola, 2002; Mitchell, 2003; Cardozo *et al.*, 2006). The mortality caused by pneumococcal infections is very high and is often age-associated. For instance, in the developed world serious pneumococcal infections occur in children below two years of age and in the elderly (> 65 years); in developing countries (*e.g.* African and South Asian) *S. pneumoniae* kills more than 1 million children under the age of 5 years anually, including newborn infants (Obaro and Adegbola, 2002; Bogaert *et al.*, 2004;

Cardozo *et al.*, 2006). In these countries, pneumonia is the leading cause of children death, earning the name of "The Forgotten Killer of Children" (UNICEF/WHO, Pneumonia: The Forgotten Killer of Children, 2006 (http://www.unicef.org/publications/files/Pneumonia_The_Forgotten_Killer_of_Children.pdf). The progression from carriage to invasive disease is often associated with changes in the expression of pneumococcal virulence factors (reviewed in Mitchell, 2003). Virulence factors enable the microorganism to overcome host defence mechanisms and survive in different host niches. The properties presented by some of these factors make them potential candidates for vaccine design.

Virulence factors

In classical terms, a virulence factor is any molecule of a pathogen that damages the host (Casadevall and Pirofski, 1999). In *S. pneumoniae* most of these factors are surface exposed proteins that interact directly with the host, soluble toxins and structures protecting the pneumococcus from the host immune system (reviewed in Jedrzejas, 2001). The role of many virulence factors in the pathogenicity of *S. pneumoniae* has been reported (reviewed in Jedrzejas, 2001; Kadioglu *et al.*, 2008; Mitchell and Mitchell, 2010). Major pneumococcal virulence factors are described below (Table 1.1 and Fig. 1.2).

Table 1.1. Pneumococcal virulence factors and their main role in virulence (adapted from Kadioglu *et al.*, 2008)

Main role in virulence	Virulence factors
Upper airway colonization	Capsule, *P*Cho, PspC (or CbpA), NanA, BgaA, StrH, Hyl, PavA, Eno, GAPDH
Competition in upper airway	Bacteriocins, H_2O_2
Respiratory tract infection and pneumonia	Ply, PspA, LytA, PsaA, PiaA, PiuA, NanA, NanB, IgA1 protease

*P*Cho, phosphorylcholine; PspC, pneumococcal surface protein C (or CbpA, choline-binding protein A); NanA, neuraminidase A; BgaA, β-galactosidase A; StrH, β-N-acetylglucosaminidase; Hyl, hyaluronidase; PavA, pneumococcal adhesion and virulence A; Eno, enolase; GAPDH, glyceraldehyde 3-phosphate dehydrogenase; H_2O_2, hydrogen peroxide; Ply, pneumolysin; PspA, pneumococcal surface protein A; LytA, autolysin A; PsaA, pneumococcal surface antigen A; PiaA, pneumococcal iron acquisition A; PiuA, pneumococcal iron uptake A; NanB, neuraminidase B; IgA1, immunoglobulin A1.

Of all classical virulence factors, capsule is the only one meeting the criteria of condition *sine qua non* of virulence (Iannelli *et al.*, 1999; Ogunniyi *et al.*, 2002). Capsule is a hydrophilic polysaccharide structure surrounding the cell wall (see the red arrow in Fig. 1.1, Fig. 1.2). The pneumococcal serotypes are defined by the composition of the capsular polysaccharide. When this work started 90 serotypes were documented, but currently at least 3 more have been described (Song *et al.*, 2012), denoting the high genetic plasticity of this microorganism. The intrinsic properties of each capsule type, *i.e.*, carbohydrate chemical nature, degree of electronegative charge and thickness, confer specific host anti-phagocytic and neutrophil responses and therefore, different ability to cause invasive disease (Lee *et al.*, 1991; AlonsoDeVelasco *et al.*, 1995; Wartha *et al.*, 2007; Kadioglu *et al.*, 2008; Mitchell and Mitchell, 2010). Capsule interferes with the binding of antibodies (*e.g.* Fc of IgG) and complement system (*e.g.* iC3b protein) proteins, attached to the surface of the pneumococcal cells, to the

specific receptors in phagocytic cells (AlonsoDeVelasco *et al.*, 1995; Abeyta *et al.*, 2003; Kadioglu *et al.*, 2008; Mitchell and Mitchell, 2010). Capsule has also been shown to reduce transformation (Weiser and Kapoor, 1999) and spontaneous or antibiotic-induced lysis, contributing to tolerance to antibiotics (Fernebro *et al.*, 2004; Kadioglu *et al.*, 2008). Moreover, capsule is essential for colonization since it prevents mechanical exclusion of the pneumococcal cells by the mucus in mucosal surfaces (Nelson *et al.*, 2007; Kadioglu *et al.*, 2008; Mitchell and Mitchell, 2010). Intra-strain and serotype-dependent variation of the amount of capsule is also an important feature in colonization and disease: a very thick capsule is detrimental for adhesion of *S. pneumoniae* surface proteins to host cell receptors. On the other hand, in blood a thick capsule contributes to persistence of the pneumococcus in this planktonic environment (Weiser *et al.*, 1994; Cundell *et al.*, 1995; Hardy *et al.*, 2001; Magee and Yother, 2001).

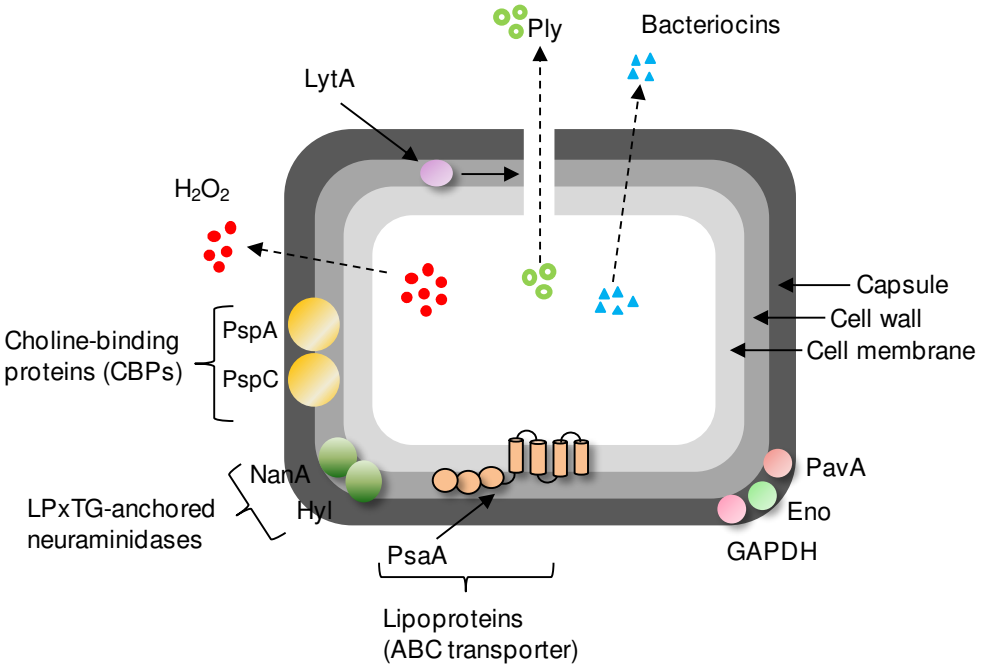

Fig. 1.2. Schematic representation depicting pneumococcal virulence factors and their localization in the cell. Abbreviations: LytA, autolysin A; Ply, pneumolysin; PspA and PspC, pneumococcal surface proteins A and C; NanA, neuraminidase A; Hyl, hyaluronidase; PsaA, pneumococcal surface antigen A; PavA, pneumococcal adhesion and virulence A; Eno, enolase; GAPDH, glyceraldehyde 3-phosphate dehydrogenase; H_2O_2, hydrogen peroxide.

The nasopharynx is a densely populated niche. In assymptomatic individuals, and particularly in children, various *S. pneumoniae* serotypes may cohabit with other species, including *Haemophilus influenzae*, *Moraxella catarrhalis*, *Neisseria meningitidis* and even *Staphylococcus aureus* (Pericone *et al.*, 2000; García-Rodríguez and Martínez, 2002; Pettigrew *et al.*, 2008; Brugger *et al.*, 2009; Margolis *et al.*, 2010). In such communities, intra- and inter-strain

competition phenomena may occur. Among the streptococcal virulence factors, the bactericidal bacteriocins (*e.g.* the bacterial pneumocins BlpM and BlpN) and hydrogen peroxide (H_2O_2) are known for their roles targeting others bacteria in the upper airway (Fig. 1.2) (Pericone *et al.*, 2000; Dawid *et al.*, 2007; Pettigrew *et al.*, 2008). The H_2O_2 produced by *S. pneumoniae* may reach extracellular concentrations in the mM range, higher than those generated by many other species, and sufficient to kill the competitors (Pericone *et al.*, 2000). Interestingly, H_2O_2 was also shown to have cytotoxic effects on epithelial cells (Duane *et al.*, 1993; Hirst *et al.*, 2000; Braun *et al.*, 2002). Another important virulence factor is pneumolysin (Ply). Ply is a pore-forming cytotoxin belonging to the family of cholesterol-dependent cytolysins (CDCs). Pneumococcal autolysis triggers the release of this cytoplasmic soluble protein (Fig. 1.2), which displays multiple functions important for infection. In short, Ply oligomers polymerize in cholesterol-containing host cell membranes forming a transmembrane pore inducing cell lysis; Ply activates and binds the complement of the host immune system, *e.g.* C3b protein, diverting it from the surface of pneumococcal cells; it affects host cell activities at sub-lytic concentrations (reviewed in Kadioglu *et al.*, 2008; Mitchell and Mitchell, 2010). The major autolysin inducing pneumococcal lysis, and thus, release of intracellular content (*e.g.* pneumolysin and DNA), is autolysin A (LytA) (Fig. 1.2) (reviewed in Kadioglu *et al.*, 2008; Mitchell and Mitchell, 2010). LytA is also a virulence factor and belongs to the group of choline-binding proteins (CBPs). CBPs are surface exposed proteins that anchor non-covalently to the cell wall teichoic acid and membrane-bound lipoteichoic acids through residues of phosphorylcholine (*P*Cho). *P*Cho is an atypical bacterial cell wall component, present in *S. pneumoniae*, that stimulates adherence of bacterial cells to the platelet-activating factor receptor (rPAF) in epithelial surfaces of the nasopharynx (reviewed in Bergmann and Hammerschmidt, 2006; Kadioglu *et al.*, 2008). LytA is

an N-acetylmuramoyl-L-alanine-amidase that digests peptidoglycan; its major role in virulence is presumably mediated by the release of pneumolysin and cell wall (Fig. 1.2) (reviewed in Kadioglu *et al.*, 2008; Mitchell and Mitchell, 2010). Cell wall has a pivotal function in triggering inflammatory processes (reviewed in Kadioglu *et al.*, 2008; Mitchell and Mitchell, 2010). Other two known virulent CBPs are the pneumococcal surface proteins C (PspC, also known as choline-binding protein A, CbpA) and A (PspA) (Fig. 1.2), with function in colonization and infection, respectively. During transcytosis across the surface epithelium, PspC binds the immunoglobulin A (IgA) receptor and the complement factor H-binding protein, inhibiting complement activation (reviewed in Kadioglu *et al.*, 2008; Mitchell and Mitchell, 2010). PspA binds the bactericidal protein lactoferrin and the C3 protein of the complement system preventing its deposition on the surface of pneumococcal cells (reviewed in Kadioglu *et al.*, 2008; Mitchell and Mitchell, 2010). Among the surface proteins, several LPxTG-proteins, which are anchored by an amino acid LPxTG motif to peptidoglycan, are well described virulence factors (Fig. 1.2) (reviewed in Bergmann and Hammerschmidt, 2006; Kadioglu *et al.*, 2008). Of these, neuraminidase A (NanA), also called sialidase A, is a good example. NanA cleaves N-acetylneuraminic acid or sialic acid from glycosylated proteins or lipids and oligosaccharides in the mucosal cell surfaces. By cleaving these residues, NanA unmasks potential receptors in the host surface epithelium, promoting colonization, and modifies the function of sialidated proteins of the host involved in clearance of bacteria, stimulating invasion (reviewed in Kadioglu *et al.*, 2008; Mitchell and Mitchell, 2010). The pneumococcal surface antigen A (PsaA), a lipoprotein that is part of the Psa(ABC) transporter (Fig. 1.2), is involved in the translocation of manganese ions into the cell. The contribution of this protein in the resistance to oxidative stress and in increased adhesion has been shown (reviewed in Kadioglu *et al.*, 2008; Mitchell and Mitchell, 2010). Other key surface

proteins involved in adherence to host cells and/or invasion are the pneumococcal adherence and virulence A (PavA), enolase (Eno), glyceraldehyde 3-phosphate dehydrogenase (GAPDH), 6-phosphogluconate dehydrogenase (6-PGD), β-galactosidase A (BgaA), β-N-acetylglucosaminidase (StrH) and hyaluronate lyase A (HylA) (Fig. 1.2) (Berry and Paton, 2000; Bergmann *et al.*, 2001; Holmes *et al.*, 2001; Bergmann *et al.*, 2003; Pracht *et al.*, 2005; King *et al.*, 2006; Daniely *et al.*, 2006; Terra *et al.*, 2010; Dalia *et al.*, 2010; Limoli *et al.*, 2011). BgaA, StrH and HylA are involved in the hydrolysis of surface glycoproteins and unmasking of host receptors, which ultimately facilitates pneumococcal adherence to epithelial cells. Remarkably, BgaA and Hyl were also found to be important for growth in certain media (van Opijnen *et al.*, 2009; Marion *et al.*, 2012). The glycolytic enzymes Eno and GAPDH bind the host plasminogen, which prevents activation of plasmin and cleavage of fibrin clots (Henderson and Martin, 2011). The moonlighting facet of these proteins suggests a more relevant role of sugar metabolic enzymes than previously imagined (Henderson and Martin, 2011). In accordance, a number of studies showed that deletion of genes involved in sugar metabolism and regulation (*e.g.* pyruvate oxidase (SpxB)) and the global regulator CcpA leads to virulence attenuation (Giammarinaro and Paton, 2002; Iyer *et al.*, 2005; Ramos-Montañez *et al.*, 2008). Although not classical virulence factors, these proteins, also common to non-pathogenic bacteria, are very important for the fitness of *S. pneumoniae* in host niches. The study of sugar metabolism may therefore disclose unforeseen metabolic factors as potential targets for the development of new preventive and therapeutic drugs.

Carbohydrate metabolism in *S. pneumoniae*

Over the past few decades, most investigators centered their attention in trying to understand the mechanisms by which *S. pneumoniae* classical virulence factors interact with the host (reviewed in Kadioglu *et al.*, 2008). However, factors involved in basic metabolic physiology, allowing for fitness and adaptation of this strictly fermentative bacterium in the microenvironments of the host, have been largely ignored. In the nasopharynx, free sugars, and in particular the often preferred hexose glucose ($[Glc]_{nasopharynx}$ < 1 mM), are scarce (Shelburne *et al.*, 2008a). In this environment, *S. pneumoniae* most likely relies on wide range of glycosylated proteins (mucins) present in the mucus lining the epithelial cell surfaces of airway structures (*e.g.* nasopharynx, tracheae, bronqui) (Rose and Voynow, 2006; Yesilkaya *et al.*, 2008). The most abundant mucin present in mucus contains a chain of different sugars (N-acetylgalactosamine, N-acetylglucosamine, fucose, sialic acid, galactose and sulfated sugars) in varied proportions that is O-glycosydically linked to the polypeptide (apomucin) (Yesilkaya *et al.*, 2008; Terra *et al.*, 2010). The determination of the relative proportion of each sugar in these chains showed that Gal is one of the sugars present at higher concentrations (Holmén *et al.*, 2004; Yesilkaya *et al.*, 2008; Terra *et al.*, 2010). Release of Gal from deglycosylation of human mucins by exoglycosidases expressed by *S. pneumoniae* has been reported (King *et al.*, 2006). Contrastingly, in other host niches, such as blood, *S. pneumoniae* encounters Glc as major carbon source, $[Glc]_{blood}$ ~ 4-6 mM (Shelburne *et al.*, 2008a). Glc and Gal are thus relevant sugars for the study of sugar metabolism in *S. pneumoniae*.

Complete genome sequences of *S. pneumoniae* are available since 2001 (Tettelin *et al.*, 2001; Hoskins *et al.*, 2001; Lanie *et al.*, 2007). Deciphering of the

genomes brought to light the importance of sugars to the lifestyle of *S. pneumoniae* and provided the framework for the development of a number of genome-wide analysis (*e.g.* microarray analysis and signature-tagged mutagenesis) (Hava and Camilli, 2002; Orihuela *et al.*, 2004a; Shelburne *et al.*, 2008a). Interestingly, studies designed to identify genes essential for virulence at the genome level consistently revealed genes involved in sugar catabolism. Capitalizing on these genome-wide studies, several research efforts have shown that non-classical virulence factors such as carbohydrate uptake systems, metabolic enzymes and a global regulator of carbon metabolism (CcpA) directly contribute to *S. pneumoniae* colonization and disease (Giammarinaro and Paton, 2002; King *et al.*, 2004; Iyer *et al.*, 2005; King *et al.*, 2006; Iyer and Camilli, 2007; Burnaugh *et al.*, 2008; Ramos-Montañez *et al.*, 2008; Yesilkaya *et al.*, 2009; Trappetti *et al.*, 2009; Marion *et al.*, 2011; Marion *et al.*, 2012).

Although the value of sugar metabolic proteins for the infectivity of *S. pneumoniae* is starting to be recognized, the need for in depth studies enabling integration of basic metabolic processes, regulation and connections to virulence in *S. pneumoniae* is evident. In the following subsections a genome and literature based overview of the putative sugar transport and metabolic capabilities, particularly for the sugars Glc and Gal, of *S. pneumoniae* will be presented. Subsequently, the cross talk between the synthesis of the polysaccharide capsule and the metabolism of these sugars will be discussed.

Transport of glucose and galactose

The transport of any exogenous carbohydrate across the sugar-impermeable lipidic membrane is the first step committed to its metabolism. In the *Streptococacceae* family this translocation may occur through three different types of carbohydrate uptake systems: secondary carriers (uniporters, symporters and antiporters), ABC-transporters and phospho*enol*pyruvate: carbohydrate phosphotransferase systems (PTS-systems) (Fig. 1.3) (Lorca *et al.*, 2007). The driving force impelling the transport of carbohydrates through secondary carriers is an electrochemical gradient of other solutes across the cell membrane (Poolman and Konings, 1993). In ABC transporters, also called ATP-binding cassettes, this driving force is the intracellular hydrolysis of ATP (reviewed in Rees *et al.*, 2009). The PTS systems are multiprotein complexes comprising both cytoplasmatic and transmembranar proteins (reviewed in Postma *et al.*, 1993). Although more complex, this system is more efficient in energetic terms, since rather than ATP it utilizes phospho*enol*pyruvate (PEP) to phosphorylate the incoming sugar (Fig. 1.3) (reviewed in Postma *et al.*, 1993). In *S. pneumoniae*, a genome survey revealed the occurrence of twenty-one PTS systems, seven ABC-transporters, one symporter and a permease (uniporter) for carbohydrate uptake (Bidossi *et al.*, 2012). The number of sugar transporters in the pneumococcus is higher than for any other prokaryote relative to genome size (Tettelin *et al.*, 2001; Bidossi *et al.*, 2012) and is variable between serotypes (Bidossi *et al.*, 2012). The ensemble of transporters have specificity for several sugars, such as Glc, Gal, N-acetylglucosamine, mannose, fructose, sialic acid, cellobiose, fructose and β-glucosides (Bidossi *et al.*, 2012). However, firm functional assignments are only available for some of the transporters (Marion *et al.*, 2011; Bidossi *et al.*, 2012).

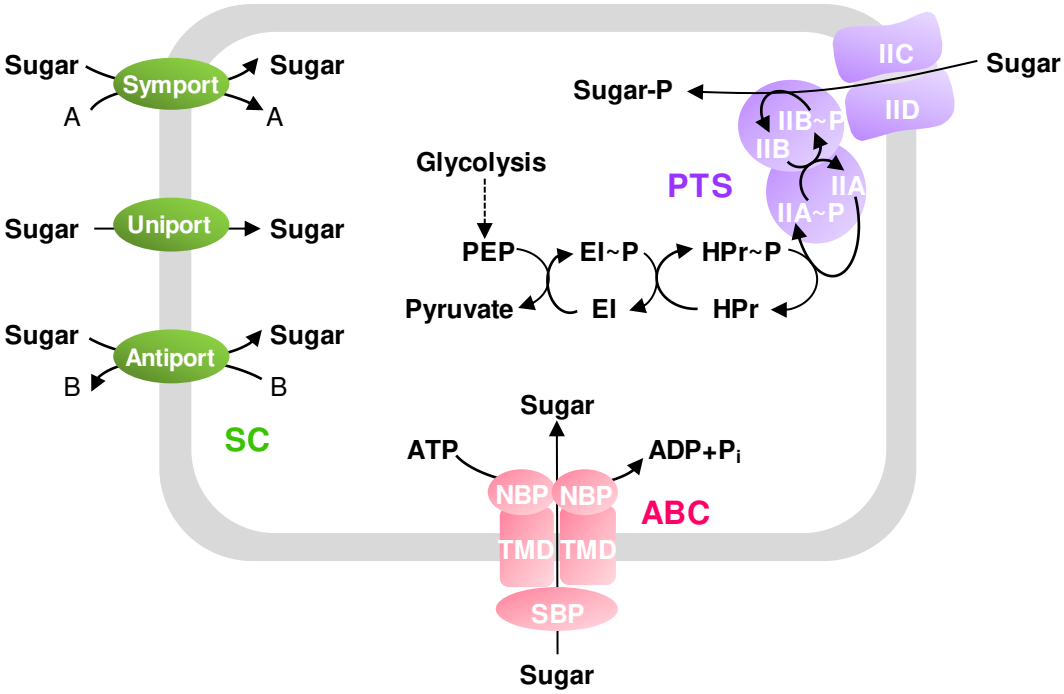

Fig. 1.3. Schematic figure showing the three classes of carbohydrate uptake systems in *Streptococcaceae*. SC (in green), secondary carriers; ABC (in pink), ABC-transporters; PTS (in purple), phospho*enol*pyruvate: carbohydrate phosphotransferase system. Abbreviations: NBP, nucleotide-binding protein; TMD, transmembrane domain; SPB, sugar/solute-binding protein; PEP, phospho*enol*pyruvate; EI, HPr are the cytoplasmatic proteins of the PTS-system; IIAB and IICD are the cytoplasmatic and transmembranar proteins of the carbohydrate-specific PTS, respectively. The PTS-system depicted here represents a PTS-system from the PTS mannose-fructose-sorbose family (PTS^{Man}).

As for the hexose Glc, its transport is not fully elucidated in *S. pneumoniae,* but a PTS system (*spd_0264-2* or *manLMN*) of the PTS mannose-fructose-sorbose (Man) family, referred as PTS^{Man}, is presumably the major transporter of Glc in *S. pneumoniae* (Bidossi *et al.*, 2012). Growth on Glc

was, however, not abolished by a *manLMN* mutation, a result consistent with the presence of other uptake systems (Bidossi *et al.*, 2012). Furthermore, the ability of a *ptsI* mutant, disrupted for the general PTS protein EI, to grow on Glc supports the occurrence of non-PTS systems for Glc transport (Bidossi *et al.*, 2012). Current work in our laboratory is aimed at identifying additional Glc uptake routes in *S. pneumoniae*.

Transport of Gal in *S. pneumoniae* is even more obscure; however, the PTS system of the family PTS-galactitol (Gat) encoded by *spd_0559-61 aka gatABC* was pointed out in two independent studies as playing a role on Gal uptake (Kaufman and Yother, 2007; Bidossi *et al.*, 2012). Confirmation has been hampered by the weak phenotype of the null mutant. Which other transporters are involved in Gal uptake remain to be elucidated, but Bidossi *et al.* reported a decreased ability of a *manLMN* mutant to grow on Gal (Bidossi *et al.*, 2012). Hitherto, firm identification of Glc and Gal transporters and their ensuing biochemical characterization in *S. pneumoniae* is still missing. Interestingly, PTS sugar transporters are only present in prokaryotes. Considering their location in bacterial cells (superficial), these transporters could be good targets for the development of drugs.

Metabolism of glucose and galactose

S. pneumoniae is a strictly fermentative bacterium, relying on sugar substrates for growth. Since it lacks a respiratory chain, this organism depends on substrate-level phosphorylation to form ATP (Tettelin *et al*., 2001; Hoskins *et al*., 2001; Lanie *et al*., 2007). In this process, ATP is originated from the direct transfer of a phosphoryl group from phosphorylated reactive intermediates to ADP (Nelson and Cox, 2000).

S. pneumoniae is a homofermentative bacterium that converts hexoses to pyruvate via the Embden-Meyerhof-Parnas (EMP) pathway; recycling of reducing equivalents is achieved mainly through reduction of pyruvate to lactate (Fig. 1.4).

Glc can be transported and concomitantly phosphorylated by PTS systems or enter the cell via non-PTS transporters and be subsequently phosphorylated to G6P by intracellular glucokinases (Fig. 1.4). The ensuing processing of G6P is as in Fig. 1.4.

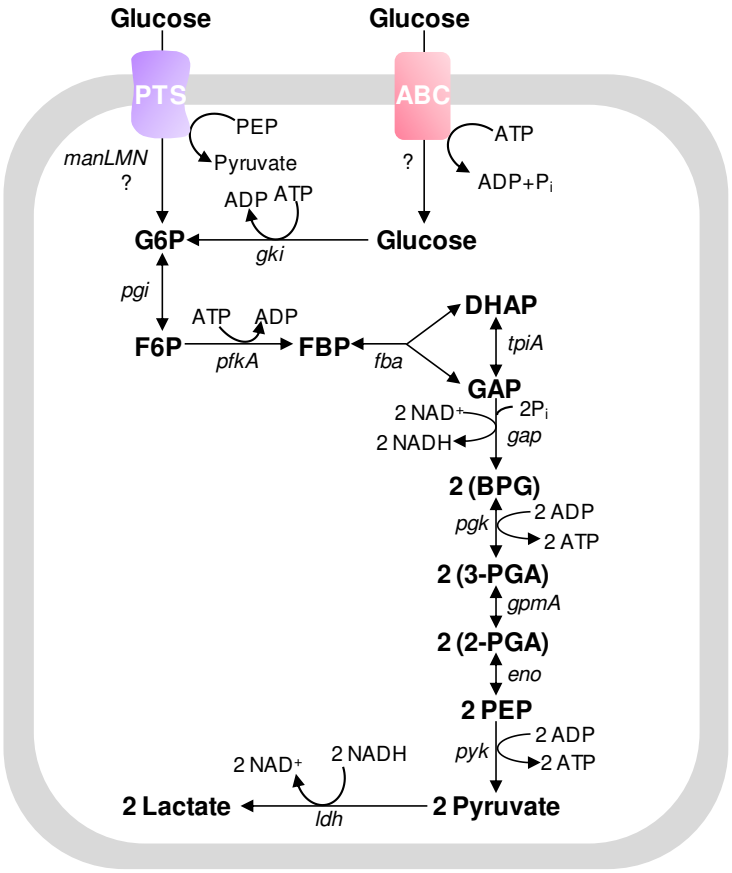

Fig. 1.4. Glucose catabolism in *S. pneumoniae* via the Embden-Meyherhof-Parnas (EMP) pathway. Glc can be imported by the PTS^{Man} or other PTS systems and non-PTS transporters (Bidossi *et al.*, 2012). The intracellular reactions depicted are catalyzed by the following enzymes (the genes that code for the enzymes are in parenthesis): glucokinase (*gki*), phosphoglucose isomerase (*pgi*), 6-phosphofructokinase (*pfkA*), fructose 1,6-bisphosphate aldolase (*fba*), triosephosphate isomerase (*tpiA*), glyceraldehyde 3-phosphate dehydrogenase (*gap*), phosphoglycerate kinase (*pgk*), phosphoglyceromutase (*gpmA*), enolase (*eno*), pyruvate kinase (*pyk*), lactate dehydrogenase (*ldh*). Abbreviations: G6P, glucose 6-phosphate; F6P, fructose 6-phosphate; FBP, fructose 1,6-bisphosphate; GAP, glyceraldehyde 3-phosphate; DHAP, dihydroxyacetone phosphate; BPG, 1,3-bisphosphoglycerate; 3-PGA, 3-phosphoglycerate; 2-PGA, 2-phosphoglycerate; PEP, phospho*enol*pyruvate.

Gal is generally recognized as a slowly metabolized carbohydrate (reviewed in Deutscher *et al.*, 2006). The metabolism of Gal is well documented for a number of *Streptococcaceae*, including *S. mutans*, *S. pyogenes*, *L. lactis, and S. salivarius*) (Steele *et al.*, 1954; Pierce, 1957; Thomas *et al.*, 1980; Abranches *et al.*, 2004; Neves *et al.*, 2010). In these organisms, Gal can be metabolized by the Leloir and/or tagatose 6-phosphate pathways (Fig. 1.5). In *S. mutans*, Gal can only be efficiently metabolized when both pathways are operating simultaneously (Abranches *et al.*, 2004). In *L. lactis*, the use of the Leloir and/or the tagatose 6-phosphate pathway for Gal utilization is currently viewed as strain-dependent, but the relative efficacy in the degradation of the sugar has not been established (Thomas *et al.*, 1980; Neves *et al.*, 2010). In *S. salivarius*, due to absence of Gal-PTS transporters only the Leloir pathway is functional (Chen *et al.*, 2002). In *S. pneumoniae*, the functionality of the two pathways is yet to be proven, but the enzymatic steps of both pathways can be inferred from the genome (Fig. 1.5) (Tettelin *et al.*, 2001; Hoskins *et al.*, 2001; Lanie *et al.*, 2007).

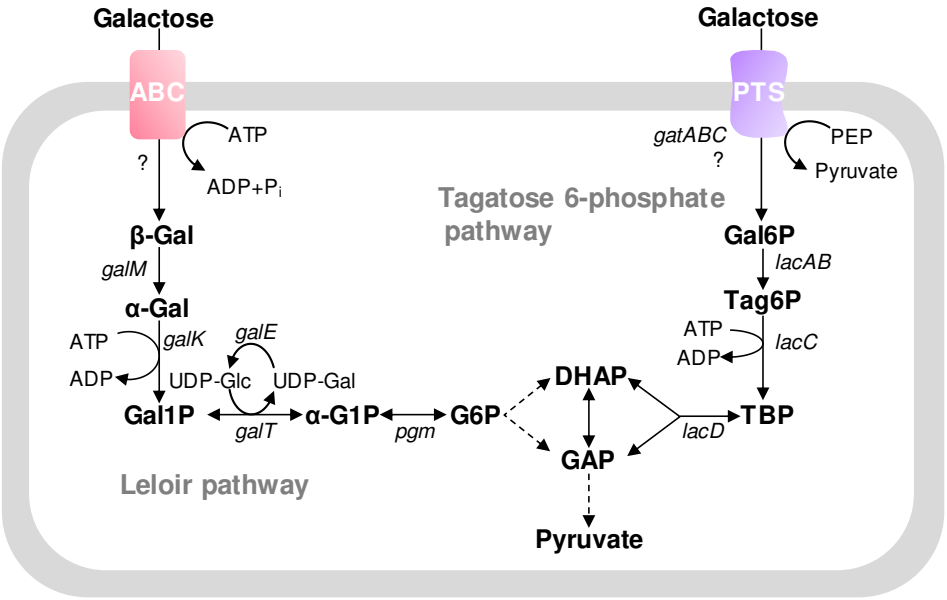

Fig. 1.5. Putative routes for galactose transport and catabolism in *S. pneumoniae*. Gal can be imported by PTS and non-PTS systems (Kaufman and Yother, 2007; Bidossi *et al.*, 2012). The intracellular reactions depicted are catalyzed by the following enzymes (the genes that code for the enzymes are in parenthesis): galactose 6-phosphate isomerase (*lacAB*), tagatose 6-phosphate kinase (*lacC*), tagatose 1,6-diphosphate aldolase (*lacD*), galactose mutarotase (*galM*), galactokinase (*galK*), galactose 1-phosphate uridylyltransferase (*galT*), UDP-galactose 4-epimerase (*galE*), α-phosphoglucomutase (*pgm*). Abbreviations: Gal, galactose; Gal6P, galactose 6-phosphate; Gal1P, galactose 1-phosphate; Tag6P, tagatose 6-phosphate; TBP, tagatose 1,6-bisphosphate; G6P, glucose 6-phosphate; α-G1P, α-glucose 1-phosphate; GAP, glyceraldehyde 3-phosphate; DHAP, dihydroxyacetone phosphate; UDP-Glc, UDP-glucose; UDP-Gal, UDP-galactose.

The type of Gal uptake system dictates to a large extent the intracellular pathway used to process the incoming Gal. Often, but not always, Gal imported and concomitantly phosphorylated to galactose 6-phosphate (Gal6P) via a PTS-system follows the tagatose 6-phosphate pathway. In short, Gal6P is converted to

glycolytic triose-phosphates via the sequential action of three enzymes, galactose 6-phosphate isomerase (LacAB), Tag6P kinase (LacC) and tagatose 1,6-diphosphate aldolase (LacD) (Fig. 1.5). Gal taken up by non-PTS transporters (second carriers or ABC-transporters) converges into the Leloir pathway. In this route, Gal is converted to α-glucose 1-phosphate (α-G1P), which in turn forms the glycolytic intermediate G6P by the action of α-phosphoglucomutase (*pgm*) (Fig. 1.5). However, Gal6P, the product of Gal-PTSs, can also be processed via the Leloir pathway, upon dephosphorylation by yet unknown Gal6P phosphatases (Neves *et al.*, 2010; Solopova *et al.*, 2012).

Pyruvate metabolism in *S. pneumoniae*

Independently of which sugar is metabolized, the end-product of the EMP pathway is pyruvate. Genes encoding the pyruvate consuming enzymes lactate dehydrogenase (LDH), pyruvate oxidase (SpxB), and pyruvate formate-lyase (PFL) are present in genome sequences of *S. pneumoniae* (Tettelin *et al.*, 2001; Hoskins *et al.*, 2001; Lanie *et al.*, 2007). Biochemical characterization of the enzymes is missing, but the functions of LDH and SpxB have been experimentally validated by product and activity measurements, and loss-of-function mutants for SpxB (Spellerberg *et al.*, 1996; Chapuy-Regaud *et al.*, 2001; Ramos-Montañez *et al.*, 2008; Taniai *et al.*, 2008; Ramos-Montañez *et al.*, 2010). Furthermore, the identification of a functional PFL encoding gene was achieved during the course of this work (Chapter 5).

Many *Streptococcaceae* also possess a pyruvate dehydrogenase complex (PDHc), which catalyzes the conversion of pyruvate to acetyl-CoA and CO_2 at the expense of NAD^+ (Snoep *et al.*, 1993; Seki *et al.*, 2004). Homologues of the PDHc proteins were not found in the genomes of *S. pneumoniae* (Tettelin *et al.*, 2001; Hoskins *et al.*, 2001; Lanie *et al.*, 2007), but recent reports suggest the presence

of a functional pyruvate dehydrogenase (Taniai *et al.*, 2008; Ramos-Montañez *et al.*, 2010).

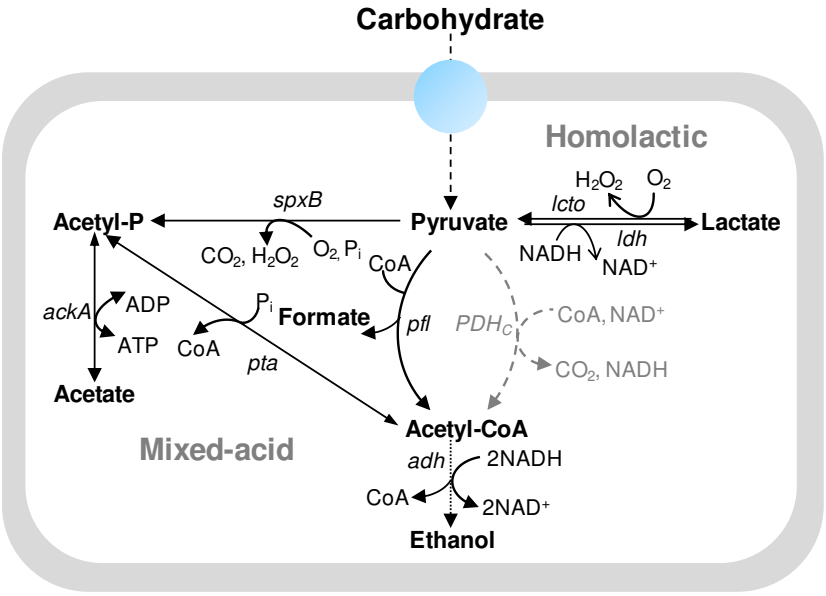

Fig. 1.6. Schematic representation of pyruvate metabolism in *S. pneumoniae*. The reactions depicted are catalyzed by the following enzymes (the genes that code for the enzymes are in parenthesis): pyruvate oxidase (*spxB*), pyruvate formate-lyase (*pfl*), bifunctional acetaldehyde-CoA/alcohol dehydrogenase (*adh*), phosphotransacetylase (*pta*), acetate kinase (*ackA*), pyruvate dehydrogenase complex (*PDHc*), L-lactate dehydrogenase (*ldh*), lactate oxidase (*lcto*). The reaction catalyzed by *PDHc* is in grey because its occurrence remains to be proved.

LDH, which activity originates lactate and NAD^+ at the expense of pyruvate and NADH (homolactic fermentation) (Fig. 1.6), is one of the most ubiquitous activities, and *ldh* genes are present in all genomes of lactic acid bacteria (LAB), frequently in several copies (reviewed in Garvie, 1980). Curiously,

S. pneumoniae possesses a single copy of *ldh* (Tettelin *et al.*, 2001; Hoskins *et al.*, 2001; Lanie *et al.*, 2007) and so far null mutants have not been reported. PFL catalyses the conversion of pyruvate to formate and acetyl-CoA (mixed-acid fermentation); the latter is the precursor for ethanol and acetate production via ADH and PTA/ACKA activities, respectively (Fig. 1.6). Formation of ethanol leads to NAD^+ regeneration, whereas acetate production results in extra ATP (Fig. 1.6). PFL is synthesized as an inactive enzyme. The enzyme is activated post-translationally via a PFL-activating enzyme (PFL-AE) that introduces a glycyl radical in PFL (Melchiorsen *et al.*, 2000; Buis and Broderick, 2005). Due to the presence of this radical, the active form of PFL is highly sensitive to molecular oxygen, explaining its better performance in hypoxia (Yamada *et al.*, 1985; Melchiorsen *et al.*, 2000; Takahashi-Abbe *et al.*, 2003; Buis and Broderick, 2005). The degree of sensitivity to O_2 is strain-dependent and is related to different self-protecting mechanisms of bacteria (Yamada *et al.*, 1985; Takahashi *et al.*, 1987; Melchiorsen *et al.*, 2000; Takahashi-Abbe *et al.*, 2003). The genome of *S. pneumoniae* revealed the presence of two copies each of *pfl* and *pfl-ae* (Tettelin *et al.*, 2001; Hoskins *et al.*, 2001; Lanie *et al.*, 2007), but in Chapter 5 we show that only one copy of each enzyme is functional. SpxB is a FAD and thiamine requiring flavoprotein that converts pyruvate, oxygen and phosphate (P_i) into CO_2, H_2O_2 and acetyl-phosphate (Fig. 1.6) (Spellerberg *et al.*, 1996). Acetyl-phosphate is a highly energetic compound and is the substrate for acetate kinase, which produces acetate and ATP (Fig. 1.6). SpxB is expressed during all phases of growth and has presumably a prominent role in the aerobic metabolism of *S. pneumoniae* (Taniai *et al.*, 2008). In agreement, the expression of SpxB in *S. pneumoniae* is higher in the nasopharynx, an oxygen-rich environment, than in blood, where O_2 is mostly associated with haemoglobin (LeMessurier *et al.*, 2006). In *S. pneumoniae*, a number of studies describe the involvement of SpxB

in virulence and colony phenotypic variation (Spellerberg *et al.*, 1996; Pericone *et al.*, 2000; Overweg *et al.*, 2000; Belanger *et al.*, 2004; Ramos-Montañez *et al.*, 2008; Allegrucci and Sauer, 2008). The role of SpxB in virulence is in part mediated by the potential deleterious effects of its product, H_2O_2 (Duane *et al.*, 1993; Spellerberg *et al.*, 1996; Hirst *et al.*, 2000; Pericone *et al.*, 2000). However, SpxB was also shown to be differentially expressed in phenotypic variants of *S. pneumoniae* displaying different capsule amounts (Overweg *et al.*, 2000; Belanger *et al.*, 2004; Ramos-Montañez *et al.*, 2008; Allegrucci and Sauer, 2008). In this light, a potential function of SpxB in virulence may be on the regulation of capsule production. In this work, we directed efforts to assess the role of this enzyme in capsule production and sugar utilization in *S. pneumoniae* (Chapter 4).

Synthesis of capsule

Capsules are composed of carbohydrate repeating units and are widely distributed and diversified among bacteria (*e.g. S. aureus*, *S. haemolyticus*, *S. agalactiae*, *S. pneumoniae*, *E. coli*, *Bacteroides fragilis*) (Tsui *et al.*, 1988; Bhasin *et al.*, 1998; Cieslewicz *et al.*, 2005; Bentley *et al.*, 2006; Flahaut *et al.*, 2008; Patrick *et al.*, 2010; Yother, 2011). Capsule synthesis in bacteria occurs through one of three existing mechanisms, the Wzy-, the synthase- or the ABC-transporter-dependent mechanisms. The three are observed in Gram-negative bacteria, but only the first two are described in Gram-positive bacteria (reviewed in Yother, 2011). In *S. pneumoniae*, 93 different capsular types are recognized. Remarkably, all pneumococcal capsular serotypes are synthesized by a Wzy-dependent mechanism, except serotypes 3 and 37, which are synthesized by a synthase-dependent mechanism (reviewed in Yother, 2011). The diversity of Wzy-dependent capsule is conferred by the existence of multiple distinct sugars

forming the repeating units, glycosydic bonds and branching points. The repeating units are polymerized in a non-processive way, *i.e.* the polymerizing enzyme breaks free after adding each repeating unit to the polymer (reviewed in Yother, 2011). In *S. pneumoniae*, the capsular Wzy-dependent genes are localized within a fixed region in the chromosome, *i.e.* between the *dexB* and *aliA* genes (Fig. 1.7-B) (Iannelli *et al.*, 1999; Bentley *et al.*, 2006; Yother, 2011). The capsular (*cps*) operon is transcribed as a single transcript; the promoter region is localized upstream of the *wzg* gene (Guidolin *et al.*, 1994; Moscoso and Garcia, 2009; Yother, 2011). CpsA coded by this gene (*wzg*) is believed to affect transcription of the *cps* operon, since its deletion reduces capsule production (Guidolin *et al.*, 1994; Morona *et al.*, 2000; Bender *et al.*, 2003; Yother, 2011).

S. pneumoniae serotype 2 strain D39 is a good example of a strain that uses the Wzy-dependent mechanism for capsule synthesis (Figs. 1.7 and 1.8). Furthermore, D39 is a historical and model strain used frequently in the study of pneumococcal physiology and pathogenesis, and is also the model strain used in this work. Its capsule is composed of repeating units of glucuronic acid, glucose and rhamnose in the proportion of 1:2:3 (Fig. 1.7-A) (Iannelli *et al.*, 1999; Yother, 2011).

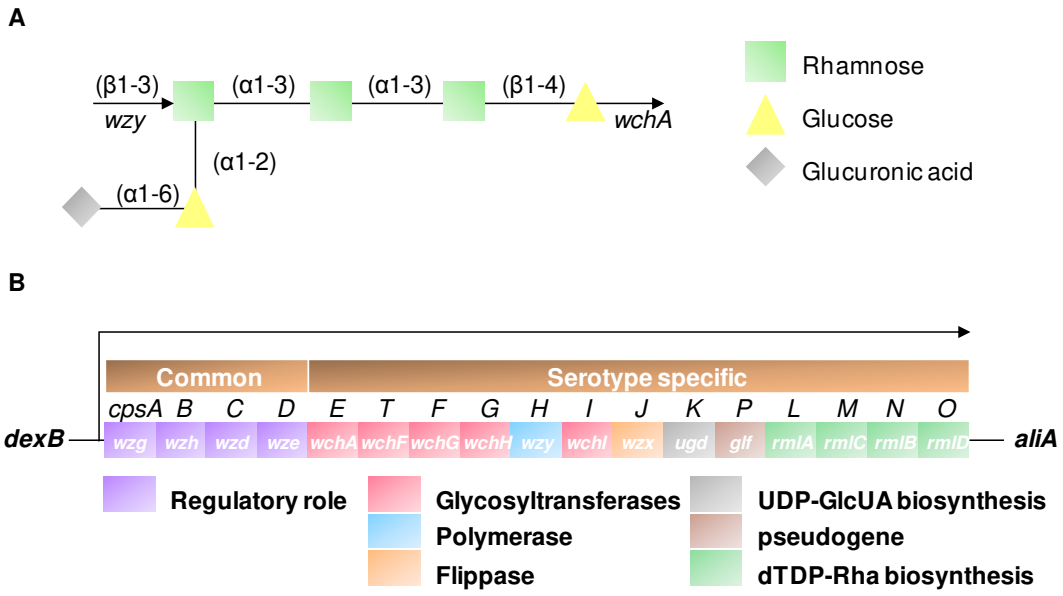

Fig. 1.7. Carbohydrate repeating unit (A) and genetic *locus* (B) of the Wzy-dependent *S. pneumoniae* serotype 2 (strain D39) polysaccharide capsule. A) The type of glycosydic bond between sugars is shown in parenthesis. Symbols: ◆, D-glucuronic acid; ■, L-rhamnose; ▲, D-glucose. B) The capsule *locus* is transcribed as a single operon; the arrow indicates the transcript (Guidolin *et al.*, 1994). The first four genes are common to all serotypes and the next thirteen are serotype-specific. Purple, regulatory genes; Pink, glycosyltransferases; Blue, polymerase; Orange, flippase; Grey and Green, NDP-sugar biosynthesis genes; Brown, pseudogene; NDP-sugar, nucleotide diphospho-sugar; GlcUA, glucuronic acid; Rha, rhamnose. Adapted from Yother, 2011 and Bentley *et al.*, 2006.

In strain D39, likewise in many other serotypes, α-G1P is the primary precursor in the biosynthesis of capsule. α-G1P can arise by the action of the housekeeping enzyme α-phosphoglucomutase (*pgm*) on the glycolytic intermediate G6P or can derive directly from the metabolism of other sugars, such as Gal (Fig. 1.8). Deletions in *pgm* and *galU* genes, located outside the *cps locus*,

lead to a drastic decrease in capsule amounts, growth defects and attenuation of virulence of *S. pneumoniae* (Mollerach *et al.*, 1998; Hardy *et al.*, 2000; Hardy *et al.*, 2001). The enzymes that convert UDP-glucose to UDP-glucuronic acid and α-G1P to dTDP-rhamnose (serotype 2 activated NDP-sugars), required to form the capsular repeating units, are encoded by the downstream regions of the *cps locus* (Fig. 1.7-B and Fig. 1.8).

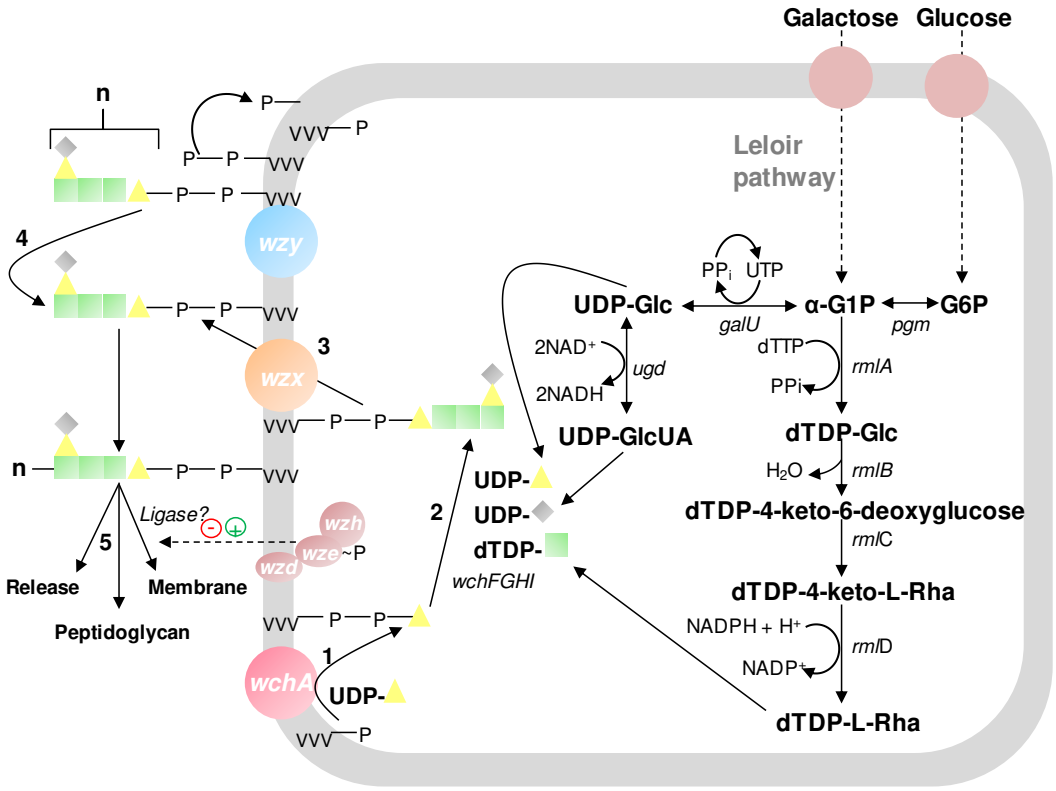

Fig. 1.8. Capsule synthesis in *S. pneumoniae* D39. The metabolism of Glc and Gal originate α-G1P, the primary precursor of capsule production. The reactions depicted are catalyzed by the following enzymes (the genes that code for the enzymes are in parenthesis): α-phosphoglucomutase (*pgm*), glucose 1-P uridylyltransferase (*galU*), UDP-

glucose 6-dehydrogenase CpsK (*ugd*), glucose 1-P thymidylyltransferase CpsL (*rmlA*), dTDP-glc 4,6-dehydratase CpsN (*rmlB*), dTDP-4-keto-6-deoxy-D-glc 3,5-epimerase CpsM (*rmlC*), dTDP-4-keto-L-rhamnose reductase CpsO (*rmlD*), undecaprenylphosphate glucosephosphotransferase CpsE (*wchA*), tyrosine-protein phosphatase CpsB (*wzh*), integral membrane regulatory protein CpsA (*wzg*), chain length determinant protein/polysaccharide export protein, MPA1 family protein, CpsC (*wzd*), tyrosine-protein kinase CpsD, cytosolic ATPase (*wze*), glycoside hydrolase family protein CpsT (*wchF*), glycoside transferase family protein CpsF (*wchG*), glycoside hydrolase family protein CpsG (*wchH*), polysaccharide polymerase CpsH (*wzy*), glycoside hydrolase family protein CpsI (*wchI*), UDP-galactopyranose mutase CpsP (*glf*). GlcUA, glucuronic acid; Rha, rhamnose. Symbols: ◆, D-glucuronic acid; ■, L-rhamnose; ▲, D-glucose. Part of this figure was adapted from Yother, 2011.

The synthesis of D39 capsule, and of most Wzy-dependent polymers, initiates with the transfer of glucose 1-phosphate from UDP-Glc to a membrane undecaprenyl-phosphate (Und-P) acceptor, catalyzed by CpsE (*wchA*) (Cartee *et al.*, 2005a; Cartee *et al.*, 2005b; Bentley *et al.*, 2006; Yother, 2011). The subsequent sugars are added by the remaining glycosyltransferases (CpsTFG and CpsI in serotype 2), forming a repeating unit (Fig. 1.8) (Bentley *et al.*, 2006; Yother, 2011). The transfer of the repeating unit from the inner membrane to the outer membrane and its polymerization in the outer membrane is catalyzed by a flippase (CpsJ coded by *wzx*) and a polymerase (CpsH coded by *wzy*), respectively (Fig. 1.8) (Bentley *et al.*, 2006; Kadioglu *et al.*, 2008; Yother, 2011). Mutations in these proteins are lethal unless accompanied by the occurrence of suppressor mutations in *wchA* (CpsE) (Xayarath and Yother, 2007; Yother, 2011). Most of the capsule polymer binds covalently to peptidoglycan or membrane, but some can also be released from the cell (Fig. 1.8) (Bender *et al.*, 2003; Morona *et al.*, 2006; Yother, 2011). The enzyme(s) linking the polymer to the cell wall remain unknown (reviewed in Kadioglu *et al.*, 2008; Yother, 2011). However, it is assumed that the polymer attaches to N-acetylglucosamine residues in the cell

wall or the membrane (reviewed in Yother, 2011). Polysaccharides not attached to the cell wall or membrane are called exopolysaccharides and their existence is very well documented in other *Streptococcaceae*, such as *L. lactis* and *S. thermophilus* (De Vuyst *et al.*, 1998; Boels *et al.*, 2001). In *S. pneumoniae,* the length of the capsular polymers is modulated by a tyrosine kinase phosphoregulatory system (CpsBCD) encoded by the genes *wzh*, *wzd* and *wze*, common to all Wzy-dependent capsular serotypes (Fig. 1.8) (Bender and Yother, 2001; Morona *et al.*, 2002; Morona *et al.*, 2003; Bender *et al.*, 2003; Kadioglu *et al.*, 2008; Yother, 2011). The autophosphorylation of CpsD induces a conformational change in CpsC, which in turn slows down the capsule polymerization. The polymer is attached to the cell wall or membrane by a putative ligase. Dephosphorylation of CpsD by the CpsB phosphatase accelerates the polymerization process (Fig. 1.8). The phosphorylation and dephosphorylation cycles allow the complete synthesis of capsule (Bender and Yother, 2001; Bender *et al.*, 2003; Yother, 2011). Deletion of *wzd* (*cpsC*) or *wze* (*cpsD*) reduces capsule amounts and the length of the chains (Bender *et al.*, 2003; Xayarath and Yother, 2007; Kadioglu *et al.*, 2008; Yother, 2011). Inactivation of *wzh* (*cpsB*) leads to increased CpsD phosphorylation and increased amounts of capsule; size is apparently not affected (Bender and Yother, 2001; Yother, 2011). High levels of oxygen decrease phosphorylation of CpsD and therefore, decrease capsule amounts in *S. pneumoniae* (Weiser *et al.*, 2001; Yother, 2011). In a recent review manuscript, J. Yother proposed that an elevated oxygen tension leads to decreased CpsC activity and increased CpsB phosphatase activity (reviewed in Yother, 2011). Despite the advances, the molecular mechanism by which this system controls capsule synthesis is not completely unraveled. Mutations in the genes coding the regulatory enzymes lead to attenuation of pneumococcal virulence (Morona *et al.*, 2003; Morona *et al.*, 2004).

Curiously, D39 pneumococcal *ugd* mutants, which lost the ability to form UDP-glucuronic acid, are only viable in the presence of a suppressor mutation in the *wchA* gene (Xayarath and Yother, 2007). These mutants show a reduction in capsule synthesis. The inability to synthesize or process a complete repeating unit is detrimental to the cell due to failure to transfer the carbohydrate polymers to the cell wall, indicating that UDP-glucuronic acid is essential in this process (Xayarath and Yother, 2007). Polymer chain length is affected by the availability of NDP-sugars (Ventura *et al.*, 2006). Pyrimidine nucleotides, and in particular UTP and dTTP in serotype 2, are required for the activation of NDP-sugars (Fig. 1.8). In this thesis we directed efforts to prove the importance of the pyrimidine nucleobase uracil in capsule expression and production in *S. pneumoniae* (Chapters 2 and 3).

Regulation of carbohydrate metabolism

During its lifecycle in the host *S. pneumoniae* is exposed to a multitude of environmental conditions and specific microenvironments, such as the nasopharynx, lungs, blood, etc. To survive fluctuating environments bacteria evolved regulatory systems that sense extra- and intracellular conditions to mount appropriate cellular responses (reviewed in Brooks *et al.*, 2011; Hindré *et al.*, 2012). At the molecular level, these responses are characterized by a readjustment of components at every layer of biological complexity, ultimately resulting in shaping of the cellular physiology to the new condition.

Metabolic adaption to changing nutritional conditions is of central importance to bacterial survival, and thus is among the best studied functional responses in microorganisms (reviewed in Kilstrup *et al.*, 2005; Deutscher *et al.*, 2006; Görke and Stülke, 2008; Amon *et al.*, 2010). The *in vivo* capacity of

metabolic enzymes to realize catalytic fluxes is a function of their abundance and kinetic properties (Gerosa and Sauer, 2011). The layers of cellular regulatory mechanisms, transcription, post-transcription, translation and post-translation (degradation mechanisms) modulate enzyme abundance (Fig. 1.9) (Gerosa and Sauer, 2011). Post-translational modification, *e.g.* protein phosphorylation, may also affect enzymatic kinetic parameters (Fig. 1.9). On the other hand, allosteric regulation by effector molecules mediates exclusively enzyme kinetic parameters (Fig. 1.9). The *in vivo* reaction rates (*i.e.* metabolic flux) are the result of all the above mechanisms, plus the *in vivo* substrate (reactant) concentrations and competitive substrate inhibitors (Fig. 1.9). Feedback regulation of metabolite pools on the cellular regulatory layers increase tremendously the complexity of metabolism and its regulation (Fig. 1.9) (Gerosa and Sauer, 2011). Of all regulatory mechanisms, large-scale efforts were mostly directed towards transcriptional regulation, since mRNA abundance and DNA-binding are easier to measure than protein abundance and activity (Herrgård *et al.*, 2004; Gerosa and Sauer, 2011).

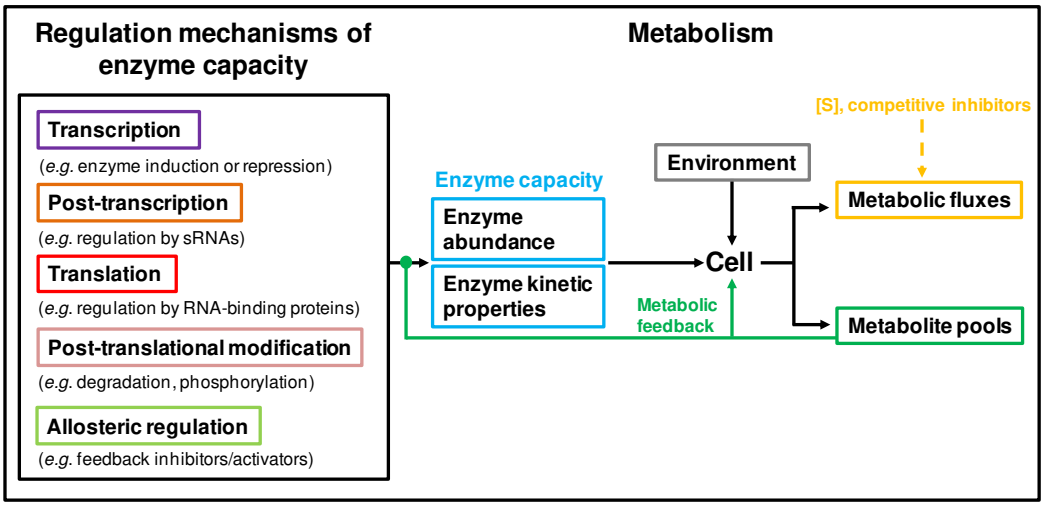

Fig. 1.9. Metabolism and points of regulation. Interplay between cellular regulation (transcriptional, post- transcriptional, translational, post-translational, allosteric) of enzyme capacities (enzyme abundance and kinetic properties), the environment and the metabolite pools, which feedbacks to all modes of enzyme regulation. Part of this figure was adapted from Gerosa and Sauer, 2011.

Therefore, it is without surprise that in *S. pneumoniae* regulation of sugar metabolic enzymes has mainly been shown at the level of transcription. A number of transcriptional regulators, namely CcpA, CelR, SusR and ScrR, RafR and RafS, MalR, and two-component systems, such as TCS08 and CiaRH, affect the expression of sugar metabolic enzymes in *S. pneumoniae* (Nieto *et al.*, 1997; Rosenow *et al.*, 1999; Iyer *et al.*, 2005; McKessar and Hakenbeck, 2007; Iyer and Camilli, 2007; Halfman *et al.*, 2007; Shafeeq *et al.*, 2011). MalR belongs to the LacI-GalR family of transcriptional repressors. In the presence of maltose, maltotriose or maltotetraose, the binding of MalR to operator sequences of operons involved in maltosaccharide uptake (*malXCD*) and utilization (*malMP*) is

inhibited (Nieto *et al.*, 1997). RafR and RafS, identified in a gene cluster for raffinose metabolism, activate and repress, respectively, the *aga* (α-galactosidase) gene in the presence of raffinose (trisaccharide of galactose, fructose and glucose) (Rosenow *et al.*, 1999). SusR (coded by *susR*) and ScrR (coded by *scrR*) repress the expression of the downstream genes in the *sus* and *scr* operons, respectively, involved in sucrose transport and catabolism, in the absence of sucrose (Iyer and Camilli, 2007). CelR activates the expression of the gene cluster for utilization of cellobiose (Shafeeq *et al.*, 2011). On the other hand, TCS08, in its active form (*i.e.* phosphorylated), downregulates cellobiose metabolism (McKessar and Hakenbeck, 2007). The results concerning the effect of the carbon catabolite protein A (CcpA) on sugar metabolism of *S. pneumoniae* are apparently strain-dependent: in strain D39 CcpA was shown to affect the growth rate on Glc and repress β-galactosidase activity in lactose-containing medium, independently of Glc, while in TIGR4 CcpA showed no effect on growth in Glc-medium, and repression of β-galactosidase in lactose-medium was only observed when Glc or sucrose (repressing sugars) were added (Giammarinaro and Paton, 2002; Iyer *et al.*, 2005). The CiaR response regulator of the CiaRH two-component system controls various genes unrelated to sugar metabolism (*e.g.* sRNAs). Furthermore, it represses the *manLMN* operon (PTS^{Man}) and weakly activates the *malMP* operon for maltosaccharide utilization (Halfmann *et al.*, 2007). From these studies a model of the transcriptional regulatory networks controlling sugar metabolism is emerging. On the contrary, little is known about metabolic regulation of sugar metabolism in *S. pneumoniae*. To our knowledge, kinetic and other properties of central pathway (glycolysis and fermentation) enzymes remain largely unknown. Furthermore, predicting direct regulation in this organism is to a great extent hampered by the limited knowledge on intracellular metabolite pool sizes and dynamics. In other *Streptococcaceae*, such as *L. lactis*,

S. bovis and the oral streptococci (*S. mutans*, *S. pyogenes*, *S. sanguis*) regulation of glycolysis and pyruvate fermentation has been intensively investigated (Steele *et al.*, 1954; White *et al.*, 1955; Pierce, 1957; Yamada and Carlsson, 1975a; Yamada and Carlsson, 1975b; Keevil *et al.*, 1984; Neves *et al.*, 2002a; Neves *et al.*, 2002b; Neves *et al.*, 2005). Despite numerous research efforts, questions as to what controls the glycolytic flux or the shift from homolactic to mixed-acid fermentation remain unanswered. The wealth of data accumulated throughout the years permitted however to determine that the fate of pyruvate is dependent at least on sugar composition/concentration, levels of intracellular metabolites, oxygen content and transcriptional regulation (Yamada and Carlsson, 1975a; Yamada and Carlsson, 1975b; Keevil *et al.*, 1984; Garrigues *et al.*, 1997; Melchiorsen *et al.*, 2000; Neves *et al.*, 2002a; Cocaign-Bousquet *et al.*, 2002; Neves *et al.*, 2002b; van Niel *et al.*, 2004; Neves *et al.*, 2005; Abranches *et al.*, 2008). In the following subsections we will provide information about allosteric and transcriptional regulation of Glc and Gal metabolism in other *Streptococcaceae*, based on genome and literature surveys. Then we will focus on global transcriptional regulation and end with links between basic physiology and virulence.

Control of glucose and galactose metabolism in *Streptococcaceae*

In *Streptococcaceae* the metabolism of Glc is typically homolactic, whereas the metabolism of Gal tends to mixed-acid fermentation (Fig. 1.10) (Cocaign-Bousquet *et al.*, 2002; Neves *et al.*, 2005). Under anaerobic conditions, this metabolic shift results from diminished flux through LDH combined with decreased flux through PFL, as evaluated by the end-products profile (Fig. 1.10). However, the mechanisms controlling these fluxes remain to be elucidated. Initially, in a number of *Streptococcaceae* (*S. mutans*, *S. bovis*, *L. lactis, S.*

sanguis), the metabolic shift to mixed-acid was viewed as a consequence of allosteric metabolic regulation over the enzymes involved in the metabolism of pyruvate. In these studies, the production of lactate as major end-product from the anaerobic metabolism of Glc was explained as due to accumulation of the upper glycolytic metabolites G6P and FBP, which activate LDH and PK, and GAP and DHAP, potent PFL inhibitors (Fig. 1.10) (Wolin, 1964; Yamada and Carlsson, 1975b; Thomas *et al.*, 1980; Bender *et al.*, 1985; Takahashi *et al.*, 1991).

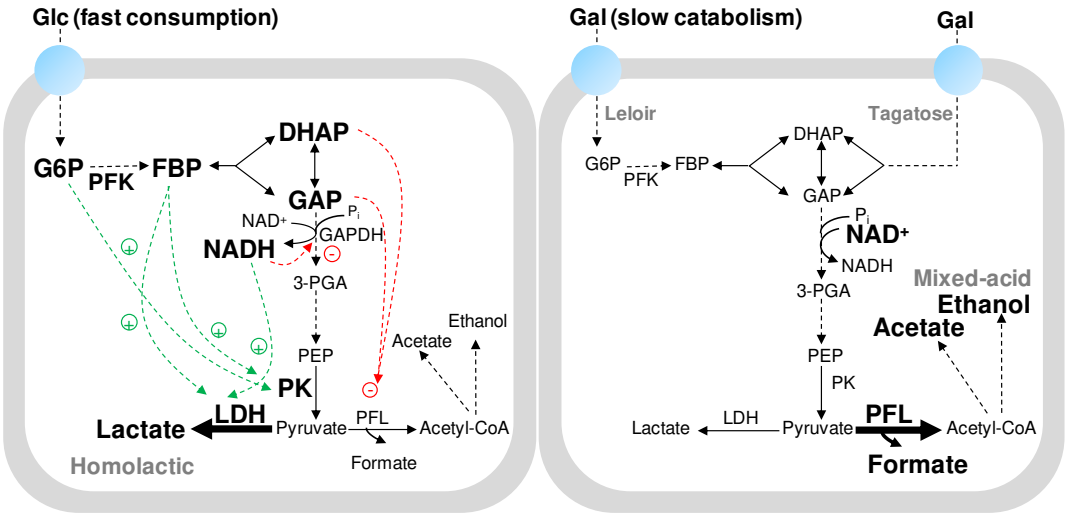

Fig. 1.10. Fate of pyruvate during anaerobic Glc and Gal metabolism in *Streptococcaceae*. Allosteric activation and inhibition of enzymes by glycolytic intermediates are shown in dashed green and red arrows, respectively. Abbreviations: G6P, glucose 6-phosphate; PFK, phosphofructokinase A; FBP, fructose 1,6-bisphosphate; DHAP, dihydroxyacetone phosphate; GAP, glyceraldehyde 3-phosphate; 3-PGA, 3-phosphoglycerate; PEP, phospho*enol*pyruvate; PK, pyruvate kinase; LDH, lactate dehydrogenase; PFL, pyruvate formate-lyase; Acetyl-CoA, acetyl-coenzyme A. The information displayed in this figure derives from data obtained for Glc and Gal metabolism and allosteric regulation in different *Streptococcaceae* species.

A later study suggested that the NADH/NAD^+ ratio determines the pattern of end-products by affecting LDH and glyceraldehyde 3-phosphate dehydrogenase (GAPDH) activities (Garrigues *et al.*, 1997). It was also suggested that homolactic fermentation is a consequence of high glycolytic flux (Garrigues *et al.*, 1997), which in turn was proposed to be controlled at the level of sugar transport (Even *et al.*, 2001). More recently, LDH activity in *L. lactis* was shown to be modulated both by the FBP/P_i and the NADH/NAD^+ ratios. These findings allowed putting forward the idea that the fate of pyruvate is determined by the simultaneous operation of both (van Niel *et al.*, 2004).

Besides the allosteric control of metabolic enzymes, the transcriptional regulation of glycolytic enzymes and enzymes downstream of pyruvate also influences the distribution of end-products. For instance, in *S. mutans* and *L. lactis*, *pfl* expression is strongly activated on Gal when compared to Glc (Melchiorsen *et al.*, 2000; Abranches *et al.*, 2008). In *L. lactis*, the *las* operon, comprising *pfk, pyk* and *ldh* genes, was shown to be activated on Glc by the global transcriptional regulator CcpA, while *pfl*, *ackA* and *adh* genes involved in mixed-acid fermentation where strongly repressed by this regulator (Luesink *et al.*, 1998; Zomer *et al.*, 2007). The shift from homolactic towards mixed-acid fermentation under aeration observed in *L. lactis* in a null *ccpA* mutant led to the hypothesis that CcpA is a mixed-acid repressor (Gaudu *et al.*, 2003; Lopez de Felipe and Gaudu, 2009). In *S. mutans*, *pfl* was also strongly repressed by CcpA on Glc (Abranches *et al.*, 2008). In *S. bovis*, inactivation of *ccpA* also renders a more mixed-acid profile in Glc containing medium (Asanuma *et al.*, 2004). Thus, CcpA presumably plays a chief role in the control of the fermentation type in *Streptococcaceae*. The mechanisms by which CcpA regulates gene expression will be described in the next subsection.

In summary, the factors governing the shift in fermentation are complex and involve at least allosteric and transcriptional regulation.

Despite the relatedness between *Streptococcaceae* species, regulatory mechanisms specific to each species seem to be in effect (reviewed in Görke and Stülke, 2008). This view is even more relevant when considering the pathogenic members. Thus, in this thesis we investigated the metabolism of Glc and Gal in *S. pneumoniae* (Chapters 5 and 6).

Carbon catabolite repression (CCR) and CcpA

One of the topics of this thesis is the transcriptional regulation of the adaptive response to Glc and Gal by the global transcriptional regulator CcpA (Chapter 6). Most fermentative bacteria, including *S. pneumoniae*, can use several sugars as sources of carbon. Each sugar has a specific set of enzymes dedicated to its transport and initial catabolism. Generally, when encountering a variety of carbon sources bacteria use them in a hierarchical manner, *i.e.* selectively and sequentially. Using all sugars simultaneously would be metabolically inefficient and a waste of energy (reviewed in Brückner and Titgemeyer, 2002; Deutscher, 2008; Görke and Stülke, 2008; Fujita, 2009). In Gram-positive bacteria, Glc is generally the selected or preferred sugar (repressing sugar), since it confers fastest growth. The process of repressing the expression of enzymes involved in the metabolism of alternative or less preferred carbon sources is termed carbon catabolite repression (CCR) (reviewed in Brückner and Titgemeyer, 2002; Deutscher, 2008; Görke and Stülke, 2008). CCR has been extensively studied in *E. coli* and Gram-positive bacteria (*e.g. Bacillus subtilis*, *L. lactis*, *S. mutans*, *S. pyogenes*). CCR may be achieved by global or operon/carbohydrate-specific regulatory mechanisms (*e.g.* inducer exclusion and inducer expulsion) (reviewed in Brückner and Titgemeyer, 2002; Deutscher, 2008;

Görke and Stülke, 2008). In the model Gram-positive bacterium *B. subtilis* as well as in pathogenic streptococci and the dairy *L. lactis* the main global regulator of gene expression involved in Glc-mediated CCR is CcpA. This protein is a LacI-GalR family regulator and was initially discovered in *B. subtilis* (reviewed in Warner and Lolkema, 2003; Fujita, 2009). Other key players involved in CCR are the PTS component HPr protein, HPr kinase/phosphorylase (HPrK/P) and the glycolytic metabolites FBP and G6P (reviewed in Görke and Stülke, 2008).

When a preferred sugar like Glc is in excess, the Glc-PTS components predominate in the unphosphorylated form and G6P, FBP and ATP accumulate to a high extent due to high glycolytic flux (Fig. 1.11). The high levels of FBP and ATP stimulate the activity of kinase of the bifunctional HPrK/P, which phosphorylates HPr in a Ser46 residue (Fig. 1.11) (Nessler *et al.*, 2003). In turn, G6P and FBP stimulate allosterically the interaction of $HPr_{(Ser46)}$~P with CcpA (Fig. 1.11) (Seidel *et al.*, 2005; Schumacher *et al.*, 2007; Görke and Stülke, 2008). The binding of $HPr_{(Ser46)}$~P induces a conformational change in the dimeric protein CcpA that brings the N-terminal DNA-binding domain of CcpA into a position capable of binding DNA (Schumacher *et al.*, 2004; Görke and Stülke, 2008). CcpA binds to operator sites called carbon catabolite responsive elements (*cre*) and interacts positively or negatively with RNA polymerase (RNAP) depending on the location of the *cre* site (Miwa *et al.*, 2000; Kim *et al.*, 2005; Zomer *et al.*, 2007). Binding of CcpA to a *cre* in the promoter region blocks the binding of RNA polymerase, thus repressing the expression of the catabolic genes (Fig. 1.11) (Zomer *et al.*, 2007). For instance, in *S. mutans* Glc-mediated CCR of the virulence factor fructanase (*fruA*) is to a great extent regulated directly by the binding of CcpA to the *fruA cre* site localized in the transcription initiation site of the gene (Abranches *et al.*, 2008). In several Gram-positive bacteria, CcpA was

found to repress its own expression in Glc (Egeter and Brückner, 1996; Mahr *et al.*, 2000; Zomer *et al.*, 2007).

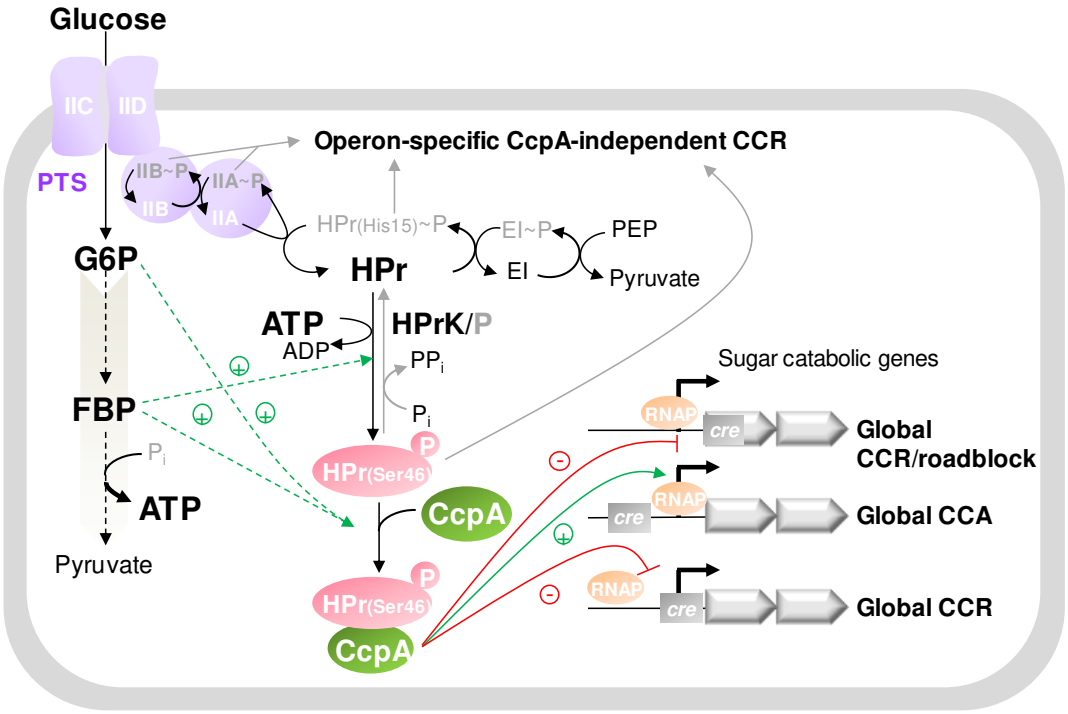

Fig. 1.11. Carbon catabolite control mediated by CcpA in Gram-positive bacteria. Under Glc-excess, the complex $HPr_{(Ser46)}$~P/CcpA is formed and regulates the expression of catabolic genes. Grey lines: $HPr_{(His15)}$~P, EIIAB~P and $HPr_{(Ser46)}$~P modulate the expression of operon-specific catabolic genes, in a CcpA-independent manner. Allosteric activation by glycolytic intermediates is shown in dashed green arrows. Gene repression and activation are represented by red and green arrows, respectively. Abbreviations: G6P, glucose 6-phosphate; FBP, fructose 1,6-bisphosphate; PEP, phospho*enol*pyruvate; EI and HPr are the cytoplasmatic proteins of the PTS-system; IIAB and IICD are the cytoplasmatic and transmembranar proteins of carbohydrate-specific PTS, respectively. RNAP, RNA polymerase; *cre*, catabolite responsive element; CCR, carbon catabolite repression; CCA, carbon catabolite activation.

When the *cre* site is within the gene, CcpA forms a roadblock for RNAP, thus repressing transcription (Fig. 1.11). Good examples are provided by the negative control exerted over the *araB* gene for the utilization of L-arabinose and the *sigL* structural gene controlling the levanase operon in *B. subtilis* (Inácio *et al.*, 2003; Choi and Saier, 2005; Görke and Stülke, 2008; Fujita, 2009).

On the other hand, binding of CcpA to a *cre* site upstream of the promoter region may enhance the RNAP binding-activity leading to activation of gene expression (Fig. 1.11). This event is well described for the *ackA* and *pta* genes of *B. subtilis* and the *las* operon of *L. lactis* (Grundy *et al.*, 1993; Luesink *et al.*, 1998; Presecan-Siedel *et al.*, 1999; Zomer *et al.*, 2007). Generally, transcriptome studies comparing wild-type and *ccpA* strains grown on Glc show that CcpA acts primarily as a repressor (Tobisch *et al.*, 1999; Zomer *et al.*, 2007; Lulko *et al.*, 2007; Abranches *et al.*, 2008; Shelburne *et al.*, 2008b).

Most studies concerning CCR/CcpA focused on the repression exerted by the preferred sugar Glc. However, CcpA-dependent CCR triggered by less preferred carbon sources has also been reported (Singh *et al.*, 2008). In this study, it was demonstrated that the extent to which a variety of carbon sources exert CCR correlates with the amount of $HPr_{(Ser46)}$~P in the cell. In view of these results, the authors hypothesized that the extent of the CcpA-dependent responses depends on the size of the glycolytic metabolite pools, and consequently the degree of HPrK activity, induced by each carbon source.

Carbon catabolite regulation is not necessarily mediated by CcpA. Indeed, CCR mechanisms independent of CcpA have been described (reviewed in Brückner and Titgemeyer, 2002; Deutscher, 2008; Görke and Stülke, 2008). These mechanisms prevent operon/carbohydrate-specific induction of catabolic genes and include inducer exclusion and inducer expulsion processes and transcription regulators containing PTS-regulatory domains (PRDs) (reviewed in

Brückner and Titgemeyer, 2002; Deutscher, 2008; Görke and Stülke, 2008). In Gram-positive bacteria, the key players involved in these regulatory events are the PTS elements $HPr_{(His15)}$~P, EII~P and $HPr_{(Ser46)}$~P (Fig. 1.11) (reviewed in Brückner and Titgemeyer, 2002; Deutscher, 2008; Görke and Stülke, 2008). An example of an inducer exclusion process has been reported for *S. thermophilus*: in the presence of lactose and absence of Glc, the phosphorylation of the lactose permease (LacS) by $HPr_{(His15)}$~P activates the transport of lactose; if Glc becomes available HPr is phosphorylated on Ser46, preventing the activation of LacS. Thus, in the presence of Glc the uptake of the inducer (lactose) is excluded (Gunnewijk and Poolman, 2000; Görke and Stülke, 2008). $HPr_{(Ser46)}$~P was also shown to be involved in inducer exclusion phenomena by repressing non-PTS permeases in *L. casei* and *L. lactis* (Dossonet *et al.*, 2000; Monedero *et al.*, 2001; Brückner and Titgemeyer, 2002).

Inducer expulsion events are less common and not so well characterized. Classical examples of these phenomena are the expulsion of the non-metabolizable thiomethyl-β-galactoside (TMG) and 2-deoxy-D-glucose carbohydrates, which accumulate intracellularly, in the presence of a fast metabolizable substrate (Reizer and Panos, 1980; Thompson and Saier, 1981).

The third mechanism controlling operon-specific induction of catabolic genes involves PRDs. PRDs are present in several proteins, including transcriptional regulators and transport systems. Direct phosphorylation of PRDs by $HPr_{(His15)}$~P and EII~P changes the activity of the PRD-containing protein, which can act as transcriptional activator or RNA-binding anti-terminator protein (Stülke *et al.*, 1998; Brückner and Titgemeyer, 2002; Görke and Stülke, 2008). A good example is provided by the LicT system in *B. subtilis*: in the absence of Glc and beta-glucosides, the PRD-containing anti-terminator LicT is phosphorylated by EII~P (from beta-glucoside PTS) and $HPr_{(His15)}$~P in its two domains (PRD1~P

and PRD2~P), becoming inactive (Krüger *et al.*, 1996; Stülke *et al.*, 1998; Lindner *et al.*, 1999; Tortosa *et al.*, 2001; Lindner *et al.*, 2002; Görke and Stülke, 2008). In the presence of beta-glucosides (inducer), EII~P phosphorylates the incoming sugar, leading to PRD dephosphorylation in one domain (PRD1). $HPr_{(His15)}$~P maintains the remaining domain phosphorylated (PRD2~P). In this form, LicT activates a catabolic operon for the utilization of beta-glucosides (*bglPH*). If Glc becomes available, $HPr_{(His15)}$~P phosphorylates the incoming Glc, thus leading to complete dephosphorylation of PRD, which renders LicT inactive (Krüger *et al.*, 1996; Stülke *et al.*, 1998; Lindner *et al.*, 1999; Tortosa *et al.*, 2001; Lindner *et al.*, 2002; Görke and Stülke, 2008).

In summary, the hierarchical utilization of sugars is conferred by a plethora of CcpA-dependent and independent CCR mechanisms.

In the recent past a few studies appeared in the literature covering some aspects of carbon catabolite regulation in *S. pneumoniae*, and in particular of the role of CcpA in CCR. In this bacterium, CcpA was found to repress the activities of α-glucosidase and β-galactosidase in a Glc-independent manner (Giammarinaro and Paton, 2002). Later on, Iyer and co-workers showed that in the pneumococcus CcpA is involved in Glc-mediated CCR of lactose-inducible β-galactosidase activity, but fails to regulate the expression of maltose-inducible α-glucosidase, raffinose-inducible α-galactosidase and cellobiose-inducible β-glucosidase (Iyer *et al.*, 2005). More recently, Kaufman and Yother showed that the *pts-bgaA* operon, coding for a galactitol family PTS and β-galactosidase A, is directly controlled by CcpA, as denoted by the position of a *cre* site between -35 and -10 promoter regions (Kaufman and Yother, 2007). The involvement of a second regulator in the control of the *pts-bgaA* operon was also postulated (Kaufman and Yother, 2007). In the above mentioned studies, CcpA-independent CCR mechanisms were a recurrent observation, which initially led to the idea that

in pneumococcus CcpA was not a global regulator of gene expression. In Chapter 6 of this thesis we show that CcpA is indeed a global transcriptional regulator in *S. pneumoniae*.

Links to virulence

The primary goal of pathogenic bacteria, including *S. pneumoniae*, in transition between different niches is to gain access to nutrients for growth and cell division (reviewed in Görke and Stülke, 2008). A consequence of the adaptation to different environmental cues is the expression of virulence genes (reviewed in Görke and Stülke, 2008). The identification of regulators and their regulons helps understanding how *S. pneumoniae* responds to signals encountered during colonization and disease (reviewed in Hava *et al*., 2003). Several regulators and their role in virulence of *S. pneumoniae* have been described. Some of these regulators influence directly classical virulence genes, but others affect virulence indirectly by controlling the expression of metabolic pathways and other regulators. Regulators affecting sugar metabolic enzymes and influencing virulence are listed in Table 1.2.

Table 1.2. Important regulators of *S. pneumoniae* affecting sugar metabolism and virulence.

Regulators	Main known regulatory role	References
CelR	Activates the expression of the cellobiose-utilization gene cluster	Lau *et al*., 2001; Hava and Camilli, 2002; Shafeeq *et al*., 2011
RegR	Represses hyaluronidase expression, which besides being involved in the metabolism of hyaluronic acid is a cell wall anchored protein and virulence factor	Berry and Paton, 2000; Chapuy-Regaud *et al*., 2003; Marion *et al*., 2012
RegM/CcpA	Impacts on sugar metabolic capabilities; the effect on capsule is serotype-dependent; the authors undermine the pleiotropic effect of this regulator	Giammarinaro and Paton, 2002; Iyer *et al*., 2005
SpxR	Regulates positively *spxB* transcription; SpxB is an enzyme involved in the aerobic metabolism of *S. pneumoniae* and H_2O_2 virulence factor is the product of its activity	Ramos-Montañez *et al*., 2008
CiaRH	Activates *htrA* coding for a surface exposed serine protease, important for colonization and virulence; influences competence; slightly activates genes involved in sugar and choline metabolism; activates strongly 5 genes coding sRNAs	Sebert *et al*., 2002; Ibrahim *et al*., 2004; Halfmann *et al*., 2007
TCS08	Involvement in cellobiose metabolism	Throup *et al*., 2000; McKessar and Hakenbeck, 2007
TCS09	This system is involved in regulation of several genes in a strain-dependent manner; activates genes involved in sugar metabolism in serotype 2 and 4.	Throup *et al*., 2000; Lau *et al*., 2001; Hava and Camilli, 2002; Hendriksen *et al*., 2007

The significance of in-depth studies on basic metabolic processes, and in particular those involved in sugar catabolism, is strengthened by the growing evidence connecting basic metabolism to virulence in *S. pneumoniae*. As depicted in Table 1.2, several transcriptional regulators control the expression of genes involved in sugar catabolic pathways as well as virulence factors. On the other hand, key metabolic enzymes, such as glyceraldehyde 3-phosphate dehydrogenase and enolase are also implicated in virulence. The work described in this thesis was devised to gain insight into basic physiology and sugar metabolism in *S. pneumoniae*, a still relatively unexplored and exciting field of study.

Chapter 2

Environmental and nutritional factors that affect growth and metabolism of the pneumococcal serotype 2 strain D39 and its non-encapsulated derivative strain R6

The results of this chapter will be submitted for publication:
SM Carvalho, OP Kuipers, AR Neves (2012) "Environmental and Nutritional Factors that Affect Growth and Metabolism of the Pneumococcal Serotype 2 strain D39 and its non-encapsulated derivative Strain R6". Manuscript in preparation.

Chapter 2 – Contents

Summary

Links between carbohydrate metabolism and virulence in *Streptococcus pneumoniae* have been recurrently established. Nevertheless, a deep understanding of basic physiology and metabolism of this human pathogen is missing. We developed a chemically defined medium (CDM) and growth conditions that allow high yield of strains D39 and R6 and application of NMR to study metabolism. The utilization of the defined medium enabled the evaluation of different environmental and nutritional factors on growth and fermentation pattern of strains D39 and R6 under controlled conditions of pH, temperature and gas atmosphere. Surprisingly, the same growth conditions impacted differently on D39 capsulated, and its isogenic nonencapsulated derivative R6. A semi-aerobic atmosphere and a raised concentration of uracil, a fundamental component of D39 capsule, improved considerably D39 growth rate and biomass, respectively. In contrast, in strain R6, the growth rate was enhanced by strictly anaerobic conditions and uracil had no effect on biomass. In the presence of oxygen, the difference in the growth rates was mainly attributed to lower activity of pyruvate oxidase in strain D39. Moreover, our data indicate an intricate connection between capsule production in strain D39 and uracil availability. In this study, we have successfully applied the *in vivo* NMR technique to study sugar metabolism in *S. pneumoniae* R6. Glucose consumption, end-products formation and evolution of intracellular metabolite pools were monitored online by ^{13}C-NMR. Additionally, the pools of NTP and inorganic phosphate were followed by ^{31}P-NMR after a pulse of Glc. These results represent the first metabolic profiling data obtained non-invasively for *S. pneumoniae*, and pave the way to understand regulation of central metabolism.

Introduction

Streptococcus pneumoniae is a commensal organism of the human nasopharynx, and an opportunistic bacterium that can cause a number of serious diseases such as pneumonia, meningitis and septicaemia (reviewed in Mitchell, 2003). According to the World Health Organization (WHO), diseases caused by *S. pneumoniae* constitute a major global public health problem, leading to an estimated 1 million deaths per year in children under the age of five (http://www.who.int/nuvi/pneumococcus/en/). This high mortality is exacerbated by the rate at which the organism acquires resistance to traditional antibiotics. Therefore, it is without surprise that the study of *S. pneumoniae* pathogenesis has focused on attributes influencing host-pathogen interactions, such as toxins, cell wall components and capsule (reviewed in Kadioglu *et al.*, 2008). However, factors that enable persistence and proliferation of the pneumococcus in different host niches, as well as the mechanisms coordinating expression of genes required to adapt have been largely neglected. As a strictly fermentative bacterium, carbohydrates are most likely the only nutrients from which the pneumococcus can obtain sufficient energy to support growth. This view is strengthened by the large portion of the pneumococcal genome that is devoted to carbohydrate uptake and metabolism (Tettelin *et al.*, 2001; Hoskins *et al.*, 2001; Lanie *et al.*, 2007). It is, therefore, not surprising that genes involved in central metabolic processes, namely carbohydrate transport and utilization, recurrently appear in genome-wide studies aimed at identifying genes essential for virulence (Shelburne *et al.*, 2008a). Growing evidence adds to these findings by showing that carbohydrate transport systems, metabolic enzymes and a global regulator of carbon metabolism (CcpA) directly contribute to *S. pneumoniae* colonization and disease (Giammarinaro and Paton, 2002; Iyer *et al.*, 2005; Kaufman and Yother,

2007; Iyer and Camilli, 2007; Trappetti *et al.*, 2009; Yesilkaya *et al.*, 2009; Marion *et al.*, 2011; Marion *et al.*, 2012). These studies establish a link between regulation of virulence and carbohydrate metabolism, denoting a far greater importance of basic metabolic physiology than previously imagined. Recently, it was recognized that a true understanding of metabolism is perhaps more difficult to attain than that of any other cellular system (Heinemann and Sauer, 2010), because metabolism is influenced by a vast number of regulatory activities at different cellular levels, and metabolism itself feeds back to all the other cellular processes, including metabolic networks. In accordance, lack of correlation between metabolic behaviors and changes in transcript levels (Griffin *et al.*, 2002; Daran-Lapujade *et al.*, 2007; Hathaway *et al.*, 2012), emphasize the importance of examining in detail metabolic operation. Capturing the essence of complex regulatory mechanisms as those involved in carbohydrate metabolism demands the use of well-defined physiological conditions.

A powerful technique for studying metabolism in a non-invasive way is *in vivo* NMR spectroscopy. This methodology provides real time information on the pools of intracellular metabolites and metabolic fluxes and can also be used to identify metabolic bottlenecks and regulatory sites (reviewed in Neves *et al.*, 2005). The application of NMR to study metabolism is largely facilitated by the use of a proper chemically defined medium (CDM) for growth (Neves *et al.*, 1999). In CDM all the components and respective concentrations are defined facilitating data interpretation and improving reproducibility between experiments (Cocaign-Bousquet *et al.*, 1995; Zhang *et al.*, 2009). CDM formulations for *S. pneumoniae* are available, but the maximal pneumococcal biomass formed in these media is generally below an optical density value of 1 (Tomasz, 1964; Sicard, 1964; Kloosterman *et al.*, 2006a). Low biomass yields are inadequate when *in vivo* NMR is to be used for metabolic studies, as this technique requires the utilization of

dense cell suspensions. Furthermore, paramagnetic ions (*e.g.* Mn^{2+}, Fe^{2+}), which are well known for lowering the sensitivity of NMR spectroscopy (reviewed in Neves *et al.*, 2005), are generally present in relatively high concentrations in the defined media for the pneumococcus.

Most cultivation optimizations for streptococcal growth were performed in complex media with the goal of producing capsular polysaccharide on a large-scale for industrial application (*e.g.* manufactured vaccines) (Gonçalves *et al.*, 2003; Massaldi *et al.*, 2010). To our knowledge, there is no specific data on growth and cultivation conditions in CDM supporting high biomass production of the laboratory model *S. pneumoniae* serotype 2 strain D39 and its acapsular derivative R6 (Avery *et al.*, 1944; Tomasz, 1964; Hoskins *et al.*, 2001; Lanie *et al.*, 2007). Curiously, and despite the historical significance of these two strains, a thorough comparative metabolic characterization is missing. In this work, we optimized a CDM and growth conditions that support high yields of strains D39 and R6. Growth and fermentation profiles in the improved CDM were obtained for both strains under controlled conditions of pH, gas atmosphere and temperature. The effect of oxygen, Glc and nucleobases on the growth physiology of the two strains was assessed. Dissimilarities in growth profiles were tentatively interpreted on the basis of the reported differences in the genetic content of strains D39 and R6 (Lanie *et al.*, 2007). Finally, the optimized cultivation conditions achieved for strain R6 were proven suitable for *in vivo* NMR experiments. The metabolism of Glc was studied non-invasively in real time. Time series for the consumption of Glc, end-products formation and accumulation of the glycolytic intermediate fructose 1,6-bisphosphate (FBP) were obtained by ^{13}C-NMR with a time resolution of 30 s, while the pools of NTP and inorganic phosphate were followed by ^{31}P-NMR. The application of this technique to *S. pneumoniae* is expected to extend our knowledge on the intricate metabolic operation of this human pathogen.

Materials and Methods

Bacterial strains, stocks preparation and storage

The *S. pneumoniae* strains used in this study were a serotype 2 D39 and its unencapsulated derivative R6 obtained from the Department of Molecular Biology of the University of Groningen. This strain D39 displays characteristics of the D39 Lilly isolate (Avery *et al*., 1944; Lanie *et al*., 2007). ***Long-term storage of strains D39 and R6.*** Permanent stock cultures (1 ml) were prepared in cryogenic vials from cells grown in M17 broth (Difco) supplemented with 0.5% (wt/vol) Glc (Glc-M17), harvested in exponential phase, and were maintained at -80ºC in 25% (vol/vol) glycerol. ***Stocks preparation.*** D39 and R6 cells scraped from the permanent frozen stocks were grown overnight (~14 h) in 5 ml Glc-M17, at 37ºC and stored as 1 ml aliquots in 10% (vol/vol) glycerol at -80ºC. ***Preparation of working stocks.*** Strains D39 and R6 were cultured by transferring 1 ml aliquot of the frozen stock cultures into 50 ml of Glc-M17, followed by incubation at 37ºC until late-exponential phase (OD_{600} 0.8 - 1.0). Cultures were then centrifuged (5750 × *g*, 7 min, 4ºC), the supernatants discarded and the pellets were concentrated 2-fold in fresh M17. Aliquots of 1 ml were stored in 10% (vol/vol) glycerol at -80ºC.

S. pneumoniae growth studies

S. pneumoniae was grown in the CDM described in Table 2.1 prepared in bi-distilled water (Millipore E-POD), except when stated otherwise. Growth was monitored hourly by measuring the optical density at 600 nm (OD_{600}). Batch cultivations were initiated at an OD_{600} of 0.05-0.06 by the addition of a preculture (3-4% vol/vol). The precultures were prepared as follows: 1 ml working stock (D39 or R6) was used to inoculate 80 ml of CDM buffered with disodium β-

glycerophosphate and containing 60 mM Glc, in 100-ml static rubber-stoppered bottles; cultures were incubated 6-7 h (OD_{600} 0.8 - 1.0) at 37ºC, without pH control (initial pH 6.5). Incubation was kept below 7 h to avoid using stationary phase cells for inoculation. Preculturing allows for adjustment of the bacteria to the culture medium and decreases culture variability. Specific growth rates (μ) were calculated through linear regressions of the plots of ln(OD_{600}) *versus* time during the exponential growth phase. Figures throughout this chapter show individual growth curves from representative experiments.

Batch cultivations without pH control. For *S. pneumoniae* cultures grown without pH control (initial pH 6.5) the CDM was buffered with disodium β-glycerophosphate (higher buffering capacity than phosphate buffer) and supplemented with 60 mM Glc. Routinely, cells were cultivated in static rubber-stoppered bottles (semi-aerobic conditions, 80 ml in 100-ml bottles); for aerobic conditions cells were grown in shake flasks (CDM volume 1/5 of the flasks total capacity) in an orbital shaker (AGITORB 200, Aralab) at 150 rpm. For each growth condition at least two independent experiments were performed. The error in each point of the growth curves was always below 15%.

The uracil-dependency on growth of strain D39 was assessed by cultivating cells in semi-aerobic conditions as above, except that uracil was omitted or added to the medium in the following concentrations: 0.67, 1, 3.3, 5, 10, 30 and 40 mg l^{-1}. Two independent experiments were performed at least for each growth condition. The error in each point of the growth curves was always below 10%.

The effect of nucleobases (xanthine, adenine, guanine and uracil) on the growth of strain D39 was tested as follows: cultures of 250 μl were prepared in CDM containing 0.25% (wt/vol) Glc and each nitrogenous base was added individually to a final concentration of 30 mg l^{-1}. Cultures were started at an initial

OD_{595} of 0.25-0.3, by addition of an exponential growing preculture suspended in fresh CDM without nucleobases, and grown for 24 h at 37°C in 96-well microtiter plates. Growth was monitored every 30 min at 595 nm with a ELx808 microplate spectrophotometer (BioTek Instruments, Inc.), and growth curves generated by using Gen5^{TM} (BioTek Instruments, Inc.). Each growth condition was done in triplicate using two independent precultures. The error in each point of the growth curves was always below 5%.

Batch cultivations in bioreactors with pH control. D39 and R6 strains were grown in CDM in a 2-l bioreactor (Sartorius Biostat® B plus) with the pH-controlled at 6.5, and under anaerobic (argon atmosphere), semi-aerobic (initial specific air tension of 50-60%) or aerobic (continuous specific air tension of 40%) conditions. For anaerobic growth, the medium was degassed by flushing argon overnight preceding inoculation, and the headspace was continuously sparged with argon at a rate of 50 ml min^{-1} during growth. For the semi-aerobic conditions and aerobic growth, dissolved oxygen was monitored with a polarographic oxygen electrode (Mettler-Toledo International). The electrode was calibrated to zero or 100% by bubbling sterile argon or air through the medium, respectively. The continuous specific air tension of 40% in the culture medium was maintained by automatic control of the airflow and agitation. Specific air tension consumption over time in growth under semi-aerobic conditions was registered in the MFCS/DA software (B. Braun Biotech International) coupled to the fermentation unit. Independently of the growth condition, Glc was used as carbon source at a final concentration of about 60 mM, except when the effect of Glc concentration on growth was tested. For these experiments, Glc was added to the medium at concentrations of 0.5%, 1% and 3% (wt/vol). To investigate the effect of nucleobases (Table 2.1) on growth, their concentrations were raised from 10 to 30 mg l^{-1} in the culture medium. To test the effect of uracil *per se* on growth of strains

D39 and R6 the concentration of this nucleobase was increased from 10 to 30 mg l^{-1}. The pH was kept at 6.5 by the automatic addition of 10 M NaOH, and the temperature was set to 37ºC. Under anaerobic and semi-aerobic conditions culture homogenization was achieved by maintaining an agitation speed of 70 rpm. For each growth condition at least two independent experiments were performed. The error in each point of the plotted growth curves was always below 20%.

Kinetics of oxygen consumption

Oxygen concentration in the culture medium was calculated using the equation of Henry's Law: X_{O2} (mol O_2 mol^{-1} H_2O) = P_{O2}/H. The partial pressure of oxygen (P_{O2}, atm) in the culture medium was calculated by multiplying the percentage of air in the culture medium by the percentage of O_2 in an atmosphere saturated with air (20.95% (vol/vol) of O_2). The Henry's Law constant (H) for O_2 at 37ºC is 5.18 x 10^{-4} atm mol^{-1} O_2 mol^{-1} H_2O. Water concentration (mol H_2O l^{-1} H_2O) is 55.5 M. The oxygen consumption rate (q_s^{max} in Fig. 2.5) was estimated from a first-order derivative of a polynomial fit of the observed O_2 consumption time series. Dry weight (DW) was used as a measure of cell mass.

Quantification of glucose and fermentation products

Strains were grown in CDM supplemented with Glc and with pH control. Culture samples (2 ml) were taken at different time-points of growth, centrifuged (16,000 × *g*, 2 min, 4ºC), filtered (Millex-GN 0.22 µm filters) and the supernatant solutions were stored at -20ºC until analysis by high performance liquid chromatography (HPLC). Substrates and end-products were quantified in an HPLC apparatus equipped with a refractive index detector (Shodex RI-101, Showa Denko K. K.) using an HPX-87H anion exchange column (Bio-Rad

Laboratories Inc.) at 60ºC, with 5 mM H_2SO_4 as the elution fluid and a flow rate of 0.5 ml min^{-1}. Alternatively, quantification of metabolites in the supernatant solutions was performed by ^{1}H-NMR in a Bruker AMX300 spectrometer (Bruker BioSpin GmbH). Formic acid (sodium salt) was added to the samples and used as an internal concentration standard. The ATP yield was calculated as the ratio of ATP produced to Glc consumed. The global yields of ATP were calculated from the fermentation products determined at the time-point of growth arrest assuming that all ATP was synthesized by substrate-level phosphorylation. A factor of 0.39, determined from a DW (mg ml^{-1}) *versus* OD_{600} curve, was used to convert OD_{600} into dry weight (mg biomass ml^{-1}). For the aerobic samples, hydrogen peroxide was quantified in fresh supernatant solutions as described below.

Determination of hydrogen peroxide (H_2O_2)

Hydrogen peroxide was determined in supernatants of cultures grown under semi-aerobic and aerobic conditions and with pH set to 6.5. Culture samples of 1-ml were harvested at different time-points of the growth curves, centrifuged (16,000 × *g*, 2 min, 4ºC) and filtered (Millex-GN 0.22 µm filters). The Amplex® Red Hydrogen Peroxide/Peroxidase assay kit (Invitrogen) was used to quantify H_2O_2 contents below 10 µM. Determinations of H_2O_2 up to 300 µM were performed as described elsewhere (Meiattini, 1988). Briefly, 1.25 ml of peroxide reagent (192 mM phosphate, 14.8 mM azide, 0.96 ml l^{-1} Triton X-100, 2 KU l^{-1} horseradish peroxidase (Roche), 0.48 mM 4-aminophenazone and 9.6 mM chromotropic acid) was added to 50 µl of supernatant, mixed and allowed to stand for 5 minutes at room temperature. In the presence of H_2O_2, the chromotropic acid was converted by the peroxidase into a blue coloured compound with maximal absorbance at 600 nm. Absorbance was read at 600 nm. Water was used as the blank and standard curves were performed with fresh dilutions of a stabilized

solution of 30% (wt/vol) H_2O_2. The absorbance of the samples was compared to that of the standard solutions.

Enzymatic activities

(i) Pyruvate oxidase activity. Cell lysates and pyruvate oxidase activity were performed as described in (Belanger *et al*., 2004) with minor modifications. Cells grown aerobically with pH control were harvested in late-exponential phase of growth (R6, OD_{600} 0.16 ± 0.00; D39, OD_{600} 0.29 ± 0.06), centrifuged (5750 × *g*, 5 min, 4ºC), and the pellets washed twice in one volume of 50 mM KP_i, pH 7.4. Cells were re-suspended in 0.1 volume of the same buffer containing 0.1% Triton X-100, and incubated for 10 min at 37ºC. Reactions for determination of pyruvate oxidase activity contained 50 mM potassium phosphate (pH 6.0), 5 mM $MgSO_4$, 0.5 mM thiamine pyrophosphate, 0.1 mM FAD, 15 mM sodium pyruvate, 0.2 U ml^{-1} horseradish peroxidase, 100 µM Amplex® Red Reagent (Invitrogen) and 10 µl of cell lysate. Standard curves were performed with fresh dilutions of a stabilized solution of 30% (wt/vol) of H_2O_2. The assays were incubated at 37ºC and the absorbance of the reaction was read in a SmartSpec^{TM}Plus spectrophotometer (BioRad) at 563 nm every 5 min for 1h.

(ii) NADH oxidase activity. NADH oxidase activity was determined in cells grown without pH control under semi-aerobic and aerobic conditions. Cells were harvested in late-exponential phase of growth (Fig. 2.1), and cell lysates prepared as above. NADH oxidase activity was assayed spectrophotometrically (Beckman DU70) at 37ºC in a total volume of 1 ml containing 100 mM Tris-HCl buffer, pH 7.2, 5 mM $MgCl_2$, and 0.29 mM NADH. The reaction was initiated by the addition of an adequate amount of cell lysate and monitored by the decrease in absorbance at 340 nm. One unit of enzyme activity was defined as the amount

of enzyme catalyzing the conversion of 1 µmol of substrate per minute under the experimental conditions used.

(iii) Lactate dehydrogenase activity. Lactate dehydrogenase (LDH) activity was determined in cells grown without pH control under semi-aerobic conditions. Cells were grown until late-exponential phase, centrifuged (5750 × *g*, 5 min, 4ºC), washed with KP_i 10 mM (pH 7.0) and suspended in the same buffer. The cell suspensions were disrupted in a French Press (SLM Aminco Instruments, Golden Valley, MN, USA) at 36 MPa. LDH activity was assayed spectrophotometrically by NADH measurement, as described elsewhere (Gaspar *et al.*, 2007), except that the temperature was kept at 37ºC.

In vivo ^{13}C-NMR experiments

S. pneumoniae R6 cells (2l) were grown under anaerobic conditions with pH control as described above, harvested in the late-exponential phase of growth (OD_{600} 1.9), centrifuged (5750 × *g*, 7 min, 4ºC), washed twice with 5 mM KP_i buffer with 2% (wt/vol) choline, pH 6.5 (5750 × *g*, 5 min, 4ºC) and suspended to a protein concentration of 13-14 mg ml^{-1} in 50 mM KP_i with 2% (wt/vol) choline, pH 6.5. Deuterium oxide (^2H_2O) was added to a final concentration of 6% (vol/vol) to provide a lock signal. NMR experiments were performed using the on-line system described elsewhere, which consists of a mini-bioreactor (50 ml working volume) coupled to NMR detection with a circulating system that allows for non-invasive studies of metabolism under controlled conditions of pH, gas atmosphere and temperature (Neves *et al.*, 1999). Glc specifically labeled with ^{13}C on carbon one (20 mM) was added to the cell suspension at time-point zero and spectra (30 s) acquired sequentially after its addition. The time course of Glc consumption, product formation, and changes in the pools of intracellular metabolites were monitored *in vivo*. At the end of the *in vivo* NMR experiment the cell suspension

was passed through a French press: the resulting cell extract was incubated at 80-90°C (10 min) in a stoppered tube, cooled down on ice and cell debris and denatured macromolecules were removed by centrifugation. The supernatant (NMR-extract) was used for quantification of end-products and minor metabolites as below. Due to the fast pulsing conditions used for acquiring *in vivo* ^{13}C-spectra, correction factors for resonances due to C1 and C6 of FBP (0.73 ± 0.02) were determined to convert peak intensities into concentrations as described by Neves *et al.* (2002a), except that the temperature was kept at 37ºC. The quantitative kinetic data for intracellular metabolites were calculated as described elsewhere (Neves *et al.*, 1999). The lower limit for *in vivo* NMR detection of intracellular metabolites under these conditions was 3-4 mM. Intracellular metabolite concentrations were calculated using a value of 3.0 µl (mg of protein)$^{-1}$ determined for the intracellular volume of *S. pneumoniae* as in Ramos-Montañez *et al.* (2010). Although individual experiments are illustrated in each figure, each type of *in vivo* NMR experiment was repeated at least twice and the results were highly reproducible. The values reported are averages of two experiments and the accuracy varied from 5% to 15% in the case of metabolites with concentrations below 5 mM.

In vivo ^{31}P-NMR experiments

Cell suspensions were prepared as above, except that 50 mM MES buffer, pH 6.5, was used. Glc (20 mM) was added to the cell suspension at time-point zero and spectra (2 min 6 s) acquired sequentially after its addition. Pools of NTP and inorganic phosphate (P_i) were obtained in real time non-invasively.

Quantification of products by NMR

Lactate and acetate were quantified in NMR-extracts by ^{1}H-NMR (Neves *et al.*, 1999). Formic acid (sodium salt) was added to the samples and used as an internal concentration standard. The concentration of minor products (glycerol, glycerate, alanine, aspartate, ethanol) and metabolic intermediates that remained inside the cells (3-phosphoglycerate, 3-PGA) was determined from the analysis of ^{13}C spectra of NMR-extracts as described by Neves *et al.* (1999). The concentration of labeled lactate determined by ^{1}H-NMR was used as a standard to calculate the concentration of the other metabolites in the sample.

NMR Spectroscopy

Carbon-13 and phosphorus-31 spectra were acquired at 125.77 MHz and 202.48 MHz, respectively on a Bruker AVANCE II 500 MHz spectrometer (Bruker BioSpin GmbH). All *in vivo* experiments were run using a quadruple nuclei probe head at 37ºC as described elsewhere (Neves *et al.*, 1999). Acquisition of ^{31}P-NMR and ^{13}C-NMR spectra was performed as described by Neves *et al.* (1999). For calculation of the correction factors ^{13}C-NMR spectra were acquired with a 60º flip angle and a recycle delay of 1.5 s (saturating conditions) or 60.5 s (relaxed conditions). Carbon and phosphorus chemical shifts are referenced to the resonance of external methanol and H_3PO_4 (85% vol/vol) designated at 49.3 and 0.0 ppm, respectively.

Results and Discussion

Chemically defined medium for high yield streptococcal growth

The study of metabolic complexity is largely facilitated by the application of well defined environmental and nutritional conditions. In this respect, bacterial growth in media for which the exact component concentrations are known (chemically defined media) is preferred. A number of CDM formulations have been described before for *S. pneumoniae* (Tomasz, 1964; Sicard, 1964; Kloosterman *et al.*, 2006a). However, these CDM were not suitable to obtain enough biomass for *in vivo* NMR experiments due to the presence of high concentrations of paramagnetic ions and to the low biomass yields obtained during growth. Paramagnetic ions broaden the line width of NMR spectra, decreasing significantly the spectral quality and hampering detection of intracellular metabolites. Thus, we sought for a CDM formulation devoid of paramagnetic ions that could be used routinely in the laboratory to grow *S. pneumoniae* with high biomass production. A CDM enabling the acquisition of high quality NMR data has been described for the closely related bacterium *Lactococcus lactis* (Neves *et al.*, 1999). We used the lactococcal medium as starting point to develop a CDM intended for all physiological studies performed in our laboratory. However, a simplification and optimization of the medium was not carried out, since our aim was not to design a minimal medium containing only essential nutrients. Conversely, our goal was to obtain a CDM for high yield streptococcal growth. Thus, initial growth tests, in which the lactococcal CDM was supplemented with additional nutrients, were performed with *S. pneumoniae* strain R6 in standing rubber-stoppered bottles using 60 mM of Glc as carbon source. Choline-HCl and pyruvate (Table 2.1) are chemicals generally used in CDM for *S. pneumoniae* growth (Tomasz, 1964; Sicard, 1964; Kloosterman *et al.*,

2006a). The growth dependency of *S. pneumoniae* on exogenous choline, which is used to decorate its unusual teichoic acids, is well known (Tomasz, 1967), and was confirmed in our conditions (data not shown). Furthermore, we verified that increasing the choline-HCl concentration from 5 to 10 mg l^{-1} increased the final biomass by 30%.

Table 2.1. Composition of CDM used for growth of *S. pneumoniae* in pH-controlled batch cultures

Components	**Concentration (g l^{-1})**	**Components**	**Concentration (g l^{-1})**
Buffers/Salts		**Aminoacids (10^{-3})**	
KH_2PO_4	3.0	Alanine	0.24
K_2HPO_4[a]	2.5	Arginine	0.13
Na - acetate	1.0	Asparagine	0.35
$(NH_4)_3$ - citrate	0.6	Aspartate	0.40
Na- pyruvate	0.1	Cysteine-HCl	0.40
Vitamins (10^{-3})		Glutamate	0.50
Choline-HCl	0.01	Glutamine	0.39
Na-p-Aminobenzoate	5.0	Glycine	0.18
D-biotin	2.5	Histidine	0.15
Folic acid	1.0	Isoleucine	0.21
Nicotinic acid	1.0	Leucine	0.46
Ca (D^+) Pantothenate	1.0	Lysine	0.44
Pyridoxamine-HCL	2.5	Methionine	0.13
Pyridoxine-HCl	2.0	Phenylalanine	0.28
Riboflavin	1.0	Proline	0.68
Thiamine-HCl	1.0	Serine	0.34
DL-6,8-Thioctic acid	1.5	Threonine	0.22
Vitamin B_{12}	1.0	Tryptophane	0.05
Nucleobases (10^{-2})		Valine	0.33
Adenine	1.0	**Micronutrients (10^{-1})**	
Uracil	1.0	$MgCl_2$	2.0
Guanine	1.0	$CaCl_2$	0.4
Xanthine	1.0	$ZnSO_4$	0.05

[a]K_2HPO_4 is replaced by disodium β-glycerophosphate (21 g l^{-1}) for growth without pH control

Sodium pyruvate (0.1 g l^{-1}, Table 2.1) is an ingredient of our CDM, but a 10-fold concentration reduction or even its omission had no effect on biomass or growth rate of strains (data not shown). Possibly, the acetate present in our CDM (Table 2.1) masks the effect arising from pyruvate depletion (Ramos-Montañez *et al.*, 2010). Moreover, individual addition of $CuSO_4$, $FeCl_3$, $CoCl_2$, or $MnSO_4$ to a final concentration of 0.05 mg l^{-1} in the medium had no effect on the growth profile of *S. pneumoniae* R6 (data not shown). Also, supplementation with tyrosine (0.025 g l^{-1}) or inositol (0.5 mg l^{-1}) showed no effect, while ascorbate (0.5 g l^{-1}) affected the growth negatively and complex nitrogenous sources (soytone and casein EH) improved the final biomass by about 50%. The latter result might indicate a preference of *S. pneumoniae* for oligopeptides over single amino acids. Oligopeptide transporters have been identified in *S. pneumoniae* (Alloing *et al.*, 1994; Hoskins *et al.*, 2001). The undefined composition of the complex nitrogenous sources hinders, however, their inclusion in our CDM. Thus, the final composition of the medium was set as in Table 2.1, and typical growth curves for precultures and cultures obtained under semi-aerobic conditions (standing rubber-stoppered bottles, cultivation conditions as in Materials and Methods) for strains R6 and D39 are shown in Fig. 2.1.

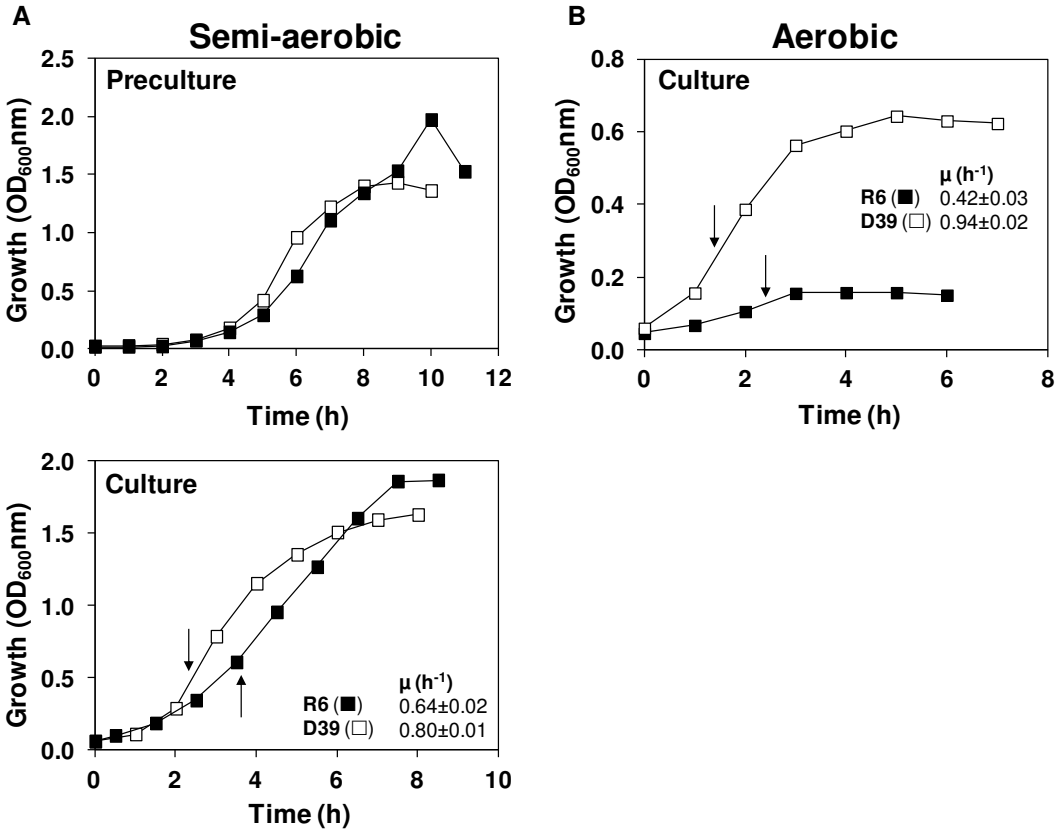

Fig. 2.1. Growth profiles of strains D39 and R6 without pH control. Growth of strains D39 (□) and R6 (■) in CDM containing 60 mM Glc, without pH control (initial pH of 6.5), at 37ºC, under different oxygen atmospheres. (A) precultures (graph above) and cultures (graph below) were grown under semi-aerobic conditions in static rubber-stoppered bottles (B) cultures were grown aerobically in shake flasks at 150 rpm. OD_{600} was measured at 1-h intervals. Cultures were inoculated with a preculture in late-exponential phase (6-7 hours incubation at 37ºC, OD_{600} 0.8-1.0). The arrows indicate the time-points at which cells were harvested for measurement of NADH oxidase and LDH activities. The growth rates for each culture grown semi-aerobically and aerobically are also indicated and the values are averages ± SD.

Batch cultivations under controlled environmental conditions

S. pneumoniae is a strictly fermentative organism that relies on the energy obtained during the conversion of sugars into pyruvate for growth. To fulfill the redox balance, the NAD^+ consumed in glycolysis is primarily recycled through reduction of pyruvate to lactate, causing acidification of the medium and ultimately growth arrest. It is well established that increasing acidities progressively inhibit growth of *Streptococcaceae* (Béal *et al*., 1989; Mercade *et al*., 2000). Thus, we hypothesized that biomass production could be improved by maintaining the medium pH at 6.5, a value determined in independent experiments to be beneficial for growth of *S. pneumoniae* (data not shown). To circumvent medium acidification we resorted to high performance bioreactors to perform batch cultivations of *S. pneumoniae*. Bioreactors allow for the tight control of pH, as well as other growth parameters, such as gas atmosphere and temperature, and provide increased working volumes. Hence, strain R6 was grown in a 2-l fermentor vessel under controlled conditions of pH (6.5), temperature (37ºC) and gas atmosphere (anaerobiosis), and the effects of pH control and preculture age examined in CDM supplemented with 60 mM Glc.

(i) Effect of pH control and preculture age on growth of *S. pneumoniae* R6. Preliminary results pinpointed the age of the starting preculture as a determinant factor in the physiology of growth. This observation was confirmed in batch cultivations in which all other parameters were kept constant, except for the age of the preculture used to initiate growth (Fig. 2.2 and Table 2.2).

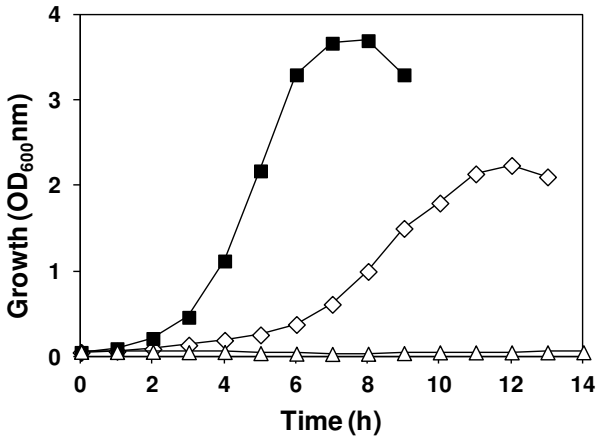

Fig. 2.2. Effect of preculture age. Growth of strain R6 in CDM containing 60 mM Glc, under controlled conditions of pH (6.5), temperature (37ºC) and atmosphere (anaerobiosis with argon atmosphere), in a 2-l bioreactor. OD_{600} was measured at 1-h intervals. Symbols: (■), inoculation with a preculture in late-exponential phase (LExp, 6-7 hours of incubation at 37ºC); (◇), inoculation with a preculture in early-stationary phase (EStat, 8-9 hours of incubation at 37ºC); (△), inoculation with a preculture in late-stationary phase (LStat, 18 hours of incubation at 37ºC).

Table 2.2. Growth parameters (length of lag, maximal growth rate and biomass) obtained for strain R6 cultures started with precultures harvested in different phases of growth, as in Fig. 2.2. The values for maximal growth rate and maximal biomass are averages of at least two independent experiments and the errors are reported as ± SD.

Preculture			**Culture (as in Fig. 2.2)**		
Growth phase	**Time (h)**	**OD_{600}**	**Lag**	**μ_{max} (h^{-1})**	**OD_{Max}**
LExp	6-7	0.8-1.0	No	0.78 ± 0.03	3.7 ± 0.0
EStat	8-9	1.4-1.6	No	0.37 ± 0.00	2.0 ± 0.3
LStat	18	~1.0	No growth[a]	-	-

LExp, late-exponential, EStat, early-stationary, LStat, late-stationary phases of growth; [a]No growth observed during the 14 h of monitoring.

Indeed, both the growth rate (μ, h^{-1}) and the maximal cell mass (OD_{Max}) were considerably higher when late-exponentially phase precultures (6-7 hours at 37ºC) rather than early-stationary precultures (8-9 hours at 37ºC) were used for inoculation. Moreover, no growth was detected during the 14 h of monitoring when precultures in late-stationary phase (18 h) were used for inoculation. Although a full explanation cannot be put forward, it is likely that with ageing larger fractions of the cell population switch to the lytic phase and are thereby unable to divide (Tomasz *et al.*, 1970; López and García, 2004; Regev-Yochay *et al.*, 2007). Cell viability was not determined under these conditions, but a repeatedly observed decrease in the maximal OD_{600} after 10-11 hours of incubation at 37ºC is indicative of cell death/lysis. The initial growth retardation can be understood in this basis, but the reason as to why the maximal biomass is much lower remains unclear. It is well documented that both the metabolic status and gene expression are dramatically affected in cells entering stationary phase (Kolter *et al.*, 1993; Regev-Yochay *et al.*, 2007; Navarro Llorens *et al.*, 2010), and consequently the observed dissimilar behaviors can lie in complex mechanisms, which study is out of the scope of this work. Considering the results, the utilization of exponentially harvested *S. pneumoniae* cells to initiate cultures was applied and is routinely used in our laboratory. Implementation of this procedure circumvented an array of growth defects, such as long lag phases, inability to enter exponential phase or low biomass production.

As for pH control, in accordance to our hypothesis R6 cultures grown at constant pH of 6.5, under semi-aerobic conditions (Fig. 2.3-A), showed a 2-fold increase in maximal biomass (OD_{Max} 3.6 as compared to 1.7-1.9 in cultures without pH control) and identical growth rate (Table 2.3 and Fig. 2.1-A). Thus, pH is a key parameter to control when high biomass yields are to be obtained.

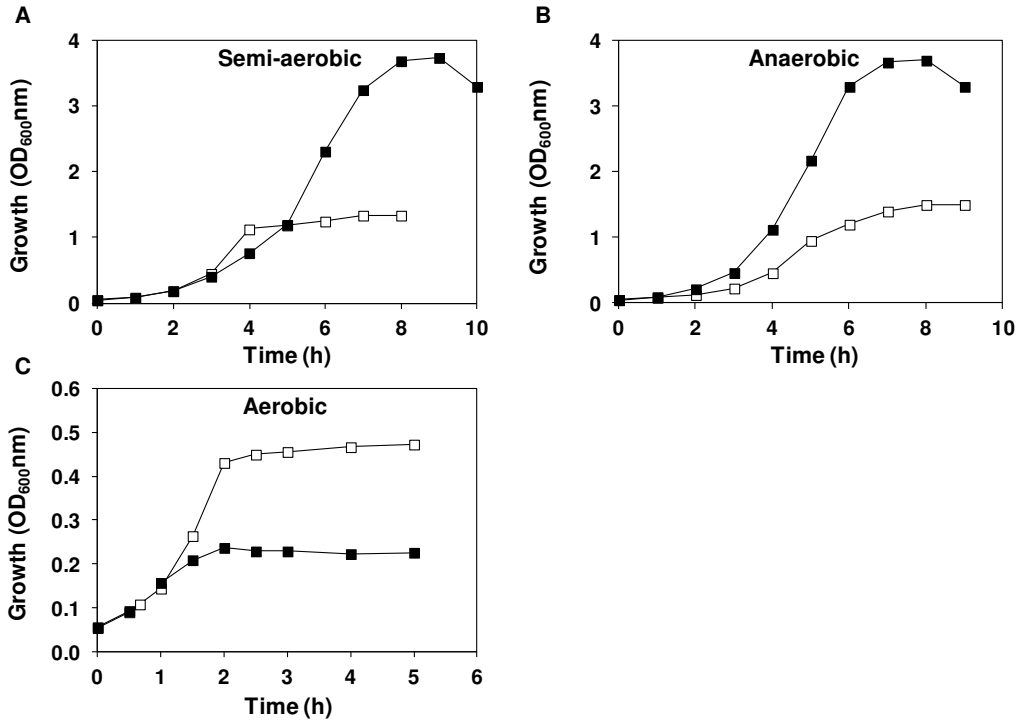

Fig. 2.3. Effect of oxygen on growth profiles. Growth of strains D39 (□) and R6 (■) in CDM containing 61 ± 1 mM Glc, under controlled conditions of pH (6.5), temperature (37ºC) and atmosphere (A) semi-aerobiosis (initial specific air tension of 50-60%) (B) anaerobiosis with argon atmosphere (C) aerobiosis (continuous specific air tension of 40%), in a 2-l bioreactor. OD_{600} was measured at 1-h intervals or less for aerobic growths. All cultures were inoculated with a preculture in late-exponential phase (6-7 hours incubation at 37ºC, OD_{600} 0.8-1.0).

Table 2.3. Growth parameters (length of lag, maximal growth rate and biomass) obtained for strains R6 and D39 cultured in CDM containing 61 ± 1 mM Glc, with pH-controlled at 6.5, at 37ºC and semi-aerobic (initial air tension 50-60%), anaerobic (argon atmosphere) or aerobic (constant air tension 40%) conditions, as in Fig. 2.3. The values for maximal growth rate and maximal biomass are averages of at least two independent experiments and the errors are reported as ± SD.

	Semi-aerobic		**Anaerobic**		**Aerobic**	
	D39	**R6**	**D39**	**R6**	**D39**	**R6**
Lag	No	No	No	No	No	No
μ_{max} (h^{-1})	0.80 ± 0.00	0.69 ± 0.03	0.55 ± 0.04	0.78 ± 0.03	1.00 ± 0.05	1.07 ± 0.04
OD_{Max}	1.3 ± 0.1	3.6 ± 0.2	1.4 ± 0.2	3.7 ± 0.0	0.49 ± 0.03	0.23 ± 0.02

(ii) Growth and fermentation profiles of *S. pneumoniae* D39 at constant pH of 6.5. pH control was shown to positively affect the performance in terms of OD_{Max} of the unencapsulated D39 derivative strain R6 (Fig. 2.3-A, Fig. 2.1-A and Table 2.3). Considering the genomic relatedness of strain R6 and its progenitor strain D39 (Lanie *et al.*, 2007), we expected the latter to perform similarly when grown under the same conditions (CDM with 60 mM Glc, semi-aerobiosis, pH 6.5, and 37ºC). To our surprise, strain D39 reached an OD_{Max} value of 1.3 ± 0.1, slightly lower than that under non-controlled pH conditions (1.6 ± 0.2), and reduced by 64% when compared to OD_{Max} value of strain R6 (3.6 ± 0.2). The growth rate was independent of pH control, and higher than that of strain R6 by 15%. Intrigued by these results we questioned to whether the dissimilar growth profiles could be due to altered central metabolism. Accordingly, we examined substrate consumption and the pattern of end-products resulting from the fermentation of Glc (for a metabolic scheme see Fig. 2.4).

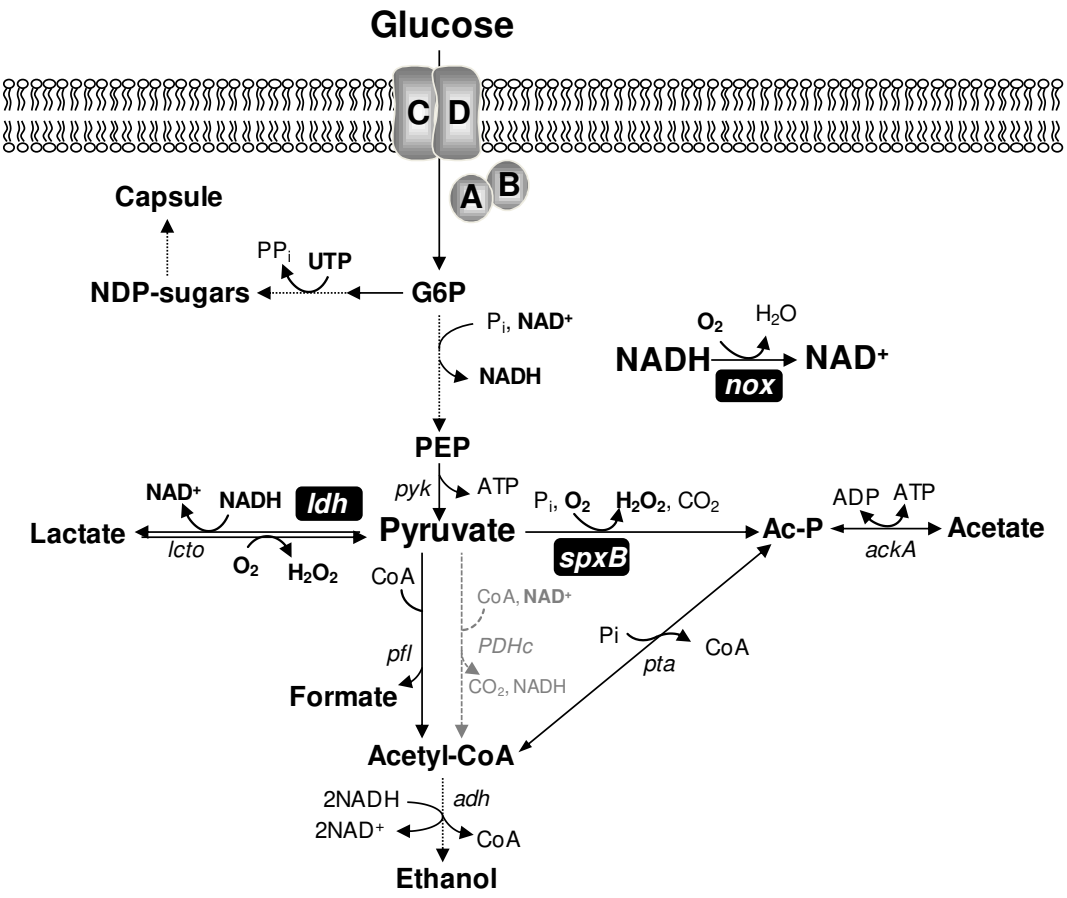

Fig. 2.4. Schematic overview of the pathways for Glc metabolism and capsule production in *S. pneumoniae*. Glc is oxidized to pyruvate via the Embden-Meyerhof-Parnas pathway (glycolysis); a common metabolic intermediate in glycolysis is glucose 6-phosphate (G6P), which is also a precursor for the biosynthesis of capsule NDP-sugars; NDP-sugars are synthesized at the expense of UTP. Pyruvate is the substrate of three competing enzymes: lactate dehydrogenase, pyruvate formate-lyase and pyruvate oxidase. Homolactic fermentation reduces pyruvate into lactate, through lactate dehydrogenase (LDH), whereas mixed-acid fermentation leads to formate, acetate and ethanol. Oxygen might be consumed at the level of lactate oxidase (LOX coded by *lcto*), pyruvate oxidase (SpxB) or H_2O-NADH oxidase (NOX). The occurrence of the pyruvate dehydrogenase complex (PDHc) depicted in grey remains to be proved. Proposed

pathways were reconstructed based on genome information (http://www.ncbi.nlm.nih.gov/genomes/lproks.cgi), literature and database surveys (KEGG, MetaCyc). Gene annotation downloaded from NCBI: *nox*, NADH oxidase; *pyk,* pyruvate kinase; *ldh*, L-lactate dehydrogenase; *lcto*, lactate oxidase; *spxB*, pyruvate oxidase; *ackA*, acetate kinase; *pfl*, pyruvate formate-lyase; *pta*, phosphotransacetylase; *adh*, bifunctional acetaldehyde-CoA/alcohol dehydrogenase; *PDHc*, putative pyruvate dehydrogenase complex.

Under controlled pH conditions, strain R6 stopped growing due to Glc limitation (Glc was totally consumed in the early-stationary phase after 9 h of growth, Fig. 2.3-A and Table 2.4). A similar behavior had previously been reported for *L. lactis* grown under constant pH in the CDM improved for NMR (Neves *et al.*, 1999), and is common among the *Streptococcaceae*. In contrast, growth arrest in D39 cultures occurred at time-point 5 h while Glc was still abundant in the medium (Fig. 2.3-A and Table 2.4), suggesting that a factor (nutritional or environmental) other than the carbon substrate is limiting growth. Both strains showed, however, typical homolactic fermentation, lactate being by far the major end-product. Minor amounts of mixed-acid fermentation products were also detected in supernatants of both strains, but pyruvate accumulation was only observed for strain D39 (Table 2.4). To our knowledge, in *S. pneumoniae* three competing enzymes, lactate dehydrogenase, pyruvate formate-lyase and pyruvate oxidase, might catalyze the conversion of pyruvate to end-products (Fig. 2.4). The pyruvate dehydrogenase complex has been postulated (grey lines in scheme portrayed in Fig. 2.4), but its occurrence remains to be proved (Taniai *et al.*, 2008; Ramos-Montañez *et al.*, 2010). The distribution of end-products is thereby dependent on the specific activities and the affinities of each enzyme for pyruvate as well as the presence or not of oxygen (Fig. 2.4). Production of formate (3.4 ± 0.4 mM), ethanol (1.3 ± 0.3 mM) and acetate (2.2 ± 0.5 mM) in strain R6 is consistent with

pyruvate formate-lyase activity, since formate is produced in an equimolar amount to the sum of acetate and ethanol (Chapter 5). Formate (1.1 ± 0.1 mM) was also detected in the culture medium of strain D39, but ethanol and acetate were most likely below the detection limit (0.4 - 0.5 mM) of the HPLC technique. Considering this end-product distribution, the mixed-acid products accounted only for 3% of the Glc used in each strain. Accumulation of pyruvate in the medium suggests impairment of the activities at the pyruvate node in strain D39. In view of the fermentation type exhibited by *S. pneumoniae*, the most obvious candidate to be affected is LDH.

Table 2.4. Product yields, substrate consumption rate, total substrate consumed, carbon and redox balances and growth and energetic parameters as determined from substrate and fermentation product analysis at the time-point of maximal biomass achieved by D39 and R6 strains cultured in CDM containing 61 ± 1 mM Glc, with pH-controlled at 6.5, at 37ºC, under semi-aerobic (initial air tension 50-60%) and anaerobic (argon atmosphere) conditions. Values of at least two independent experiments were averaged and errors are reported as ± SD.

	Semi-aerobic		**Anaerobic**	
	D39	**R6**	**D39**	**R6**
Product yields[a]				
Lactate	1.63 ± 0.01	1.81 ± 0.10	1.77 ± 0.01	1.86 ± 0.04
Pyruvate[b]	0.04 ± 0.01		0.01 ± 0.00	
Formate	0.06 ± 0.01	0.06 ± 0.01	0.07 ± 0.01	0.06 ± 0.01
Acetate	BDL	0.04 ± 0.02	BDL	0.05 ± 0.00
Ethanol	BDL	0.02 ± 0.01	BDL	0.02 ± 0.00
H_2O_2 (µM)	10 ± 0	ND	ND	ND
q_s^{max} (µmol min^{-1} mg^{-1} prot)[c]	0.92 ± 0.04	0.76 ± 0.16	0.60 ± 0.16	0.94 ± 0.05
Consumed substrate (%)	28 ± 0	100 ± 0	34 ± 5	98 ± 1
Carbon balance[d]	87 ± 1	93 ± 5	93 ± 1	96 ± 2
Redox balance	85 ± 1	93 ± 6	89 ± 1	94 ± 2
Biomass yield (g mol^{-1} Glc)	26.2 ± 1.0	23.1 ± 1.2	24.5 ± 0.1	24.6 ± 1.9
ATP yield (mol mol^{-1} Glc)	1.7 ± 0.0	1.9 ± 0.1	1.8 ± 0.0	2.0 ± 0.0
Y_{ATP} (g biomass mol^{-1} ATP)	15.0 ± 0.7	19.3 ± 0.6	13.8 ± 0.0	12.6 ± 0.8

[a]Product yields, [End-product] / [Glc consumed]; [b]Blank cells, negative yields were found for these conditions (cells used pyruvate from the medium); [c]q_s^{max} was estimated from a first-order derivative of a polynomial fit of the measured substrate consumption time series. [d]Carbon balance is the percentage of carbon in metabolized Glc that is recovered in the fermentation products (lactate, formate, acetate and ethanol) and pyruvate. Dry weight (DW) was used as a measure of cell mass. BDL, below detection limit; ND, not determined.

However, the activity values determined for LDH in cell extracts of strains D39 and R6 (Table 2.5) were in the same range, indicating similar expression of LDH in both strains. The *in vivo* activity could, however, be directly influenced by metabolic regulation. In view of the higher Glc consumption rate of strain D39 relative to strain R6, it is reasonable to hypothesize dissimilar accumulation of intracellular metabolites, potentially involved in metabolic regulation (Table 2.4). Considering that LDH activity does not seem to be in great excess, since a lactate flux of 1.5 µmol min^{-1} mg^{-1} prot. can be estimated from a maximal Glc consumption rate of 0.92 µmol min^{-1} mg^{-1} prot. and a lactate yield of 1.63, direct modulation could easily explain the pyruvate accumulation. To the best of our knowledge a thorough biochemical characterization of the pneumococcal LDH is not available and, hence, potential activity inhibitors and/or activators unknown.

Table 2.5. Enzyme specific activities determined in late-exponential fresh cell lysates or cell-free extracts of the D39 and R6 strains grown in CDM containing 60 mM Glc under semi-aerobic (rubber-stoppered bottles) or aerobic conditions (constant air tension 40%).

	Semi-aerobic		**Aerobic**	
Enzyme[a]	**D39**	**R6**	**D39**	**R6**
NADH oxidase	1.34 ± 0.00	1.02 ± 0.05	0.99 ± 0.13	0.42 ± 0.01
Pyruvate oxidase	ND	ND	0.04 ± 0.00	0.15 ± 0.00
Lactate dehydrogenase	4.75 ± 0.24	3.98 ± 0.40	ND	ND

[a]Enzyme activities are expressed in micromoles per minute per milligram of protein and are means of at least two independent experiments. Errors are reported as ± SD. ND, not determined.

The gene encoding pyruvate oxidase, *spxB*, is among the 81 allelic variants in strain R6 and D39 (Lanie *et al.*, 2007). A major consequence of this genetic variation is the different pyruvate oxidase activity values reported in the literature for D39 and R6 strains (Belanger *et al.*, 2004; Ramos-Montañez *et al.*, 2008), and fully corroborated by our own activity measurements in fresh lysates of cells grown aerobically (Table 2.5). Furthermore, the detection of H_2O_2 in the cultivation medium of strain D39 grown semi-aerobically is indicative of *in vivo* activity under the conditions studied. Thus, the lower pyruvate oxidase activity of strain D39 could in part explain the higher accumulation of pyruvate in the growth medium. In addition, this metabolic trait is likely reinforced in strain D39 by the higher NADH oxidase activity (Table 2.5), which overcomes the need to regenerate NAD^+ through pyruvate reduction (Fig. 2.4). However, these mechanisms cannot account for the total pyruvate accumulation (0.78 ± 0.08 mM), mainly because under semi-aerobic conditions the oxidase activities are limited by the oxygen in the medium (initial concentration of *circa* 0.13-0.14 mM), which decreased to undetectable levels in about 60 min for strain D39 (Fig. 2.5). The rate of oxygen consumption was lower in strain D39 than in R6 (Fig. 2.5), which is consistent with the lower pyruvate oxidase activity, but not the higher NADH oxidase activity. Considering that the specific pyruvate oxidase activity is lower than that of NADH oxidase, the latter results can only be explained assuming a higher affinity of the pyruvate oxidase for oxygen.

The carbon and redox recoveries were consistently lower for strain D39 (Table 2.4). Based on this observation it is tempting to speculate that in the capsulated strain carbon is being re-directed from merely catabolic processes to biosynthesis.

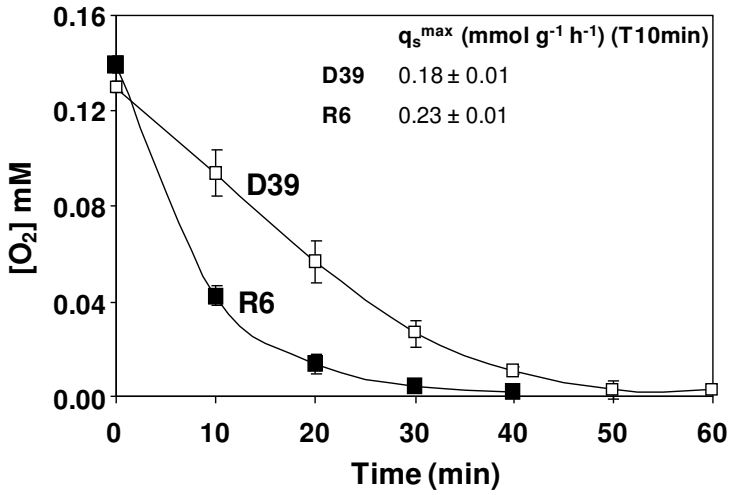

Fig. 2.5. Kinetics of oxygen consumption. Strains D39 (□) and R6 (■) were grown under semi-aerobic conditions (initial specific air tension of 50-60%) as in Fig. 2.3-A. The oxygen consumption rates (q_s^{max}) are also shown. The plotted curves are averages of two independent experiments ± SD.

Effect of oxygen on growth and metabolism of *S. pneumoniae* D39 and R6

Our data under semi-aerobic conditions establishes substantial differences in the growth profiles of strains D39 and R6. The level of oxygenation influences a number of cellular processes in *S. pneumoniae*, including central metabolism and competence (Echenique *et al.*, 2000; Taniai *et al.*, 2008). Thus, we deemed important to examine the effect of oxygen availability on the growth of strains D39 and R6.

(i) Growth and fermentation profiles of *S. pneumoniae* D39 and R6 under anaerobic conditions (argon atmosphere). The growth profile of strains D39 and R6 under strictly anaerobic conditions is depicted in Fig. 2.3-B. The values of OD_{Max} obtained, 1.4 ± 0.2 and 3.7 ± 0.0 for strains D39 and R6,

respectively, were similar to those observed in semi-aerobic conditions (Table 2.3). Under anoxic conditions, while the growth rate of strain D39 was decreased by 30%, that of strain R6 was slightly higher as compared to semi-aerobic conditions (Table 2.3). Likewise under semi-aerobiosis, Glc was still abundant when growth of strain D39 ceased (66% of the initial Glc remained in the culture medium at the time-point of maximal biomass, 8h, Table 2.4), whereas strain R6 consumed all the Glc present in the medium (time-point 7h, Table 2.4). The distribution of end-products was comparable to that observed under semi-aerobic conditions, except for the accumulation of pyruvate, lactate and formate in strain D39. In D39, at the time-point of growth arrest (maximal biomass, 8h), pyruvate, lactate and formate reached concentrations of 0.12 ± 0.01 mM, 38 ± 6 mM and 1.5 ± 0.1 mM, respectively. The concentrations of these end-products under semi-aerobic conditions at the time-point of growth arrest were 0.78 ± 0.08 mM, 28 ± 0 mM and 1.1 ± 0.2 mM, respectively. Considering that pyruvate reduction under O_2 nil conditions is only dependent on the activities of LDH and PFL (Fig. 2.4), most likely the lower accumulation of pyruvate results from the higher pressure to regenerate NAD^+ via the dehydrogenases downstream of pyruvate. In strain R6, lactate reached a concentration of 107 ± 6 mM, accounting for 89% of the Glc consumed and formate (3.7 ± 0.7 mM), acetate (2.8 ± 0.5 mM) and ethanol (0.86 ± 0.16 mM) were produced in a 2:1:1 ratio, denoting activity of PFL. Assuming that all ATP is formed by substrate level phosphorylation the higher ATP yield (mol ATP mol^{-1} Glc) in strain R6 (Table 2.4) is consistent with higher acetate production.

Considering the fermentation profiles exhibited by strains D39 and R6, the differences in the growth rates between semi-aerobic and anaerobic conditions can tentatively be explained on the basis of pneumococcal metabolic activities. The 30% decline in D39´s growth rate when switching the atmosphere from semi-

aerobiosis to anaerobiosis can partly be due to the decreased Glc consumption rate (0.92 ± 0.04 in semi-aerobiosis as compared to 0.60 ± 0.16 µmol min^{-1} mg^{-1} prot. in anaerobiosis) (Table 2.4), which in turn can be attributed to a lower NAD^+ recycling capacity under anoxic conditions, as NADH oxidases are inoperative. Under semi-aerobic conditions, while oxygen is available (60 min), activity of NADH oxidase presumably enables a faster NAD^+ regeneration, and consequently a higher Glc consumption rate (Table 2.4). It is worth noting that the activity of NADH oxidase measured in cell extracts of strains R6 and D39 (Table 2.5) was considerably higher than that found for other related bacteria (Higuchi *et al.*, 1993, Neves *et al.*, 2002a). The lower growth rate of R6 under semi-aerobic conditions can be a direct consequence of the activity of pyruvate oxidase (Table 2.5). The involvement of its product, H_2O_2, in oxidative stress and genetic instability in *S. pneumoniae* is documented (Pericone *et al.*, 2000; Pericone *et al.*, 2003).

(ii) Growth and fermentation profiles of *S. pneumoniae* D39 in aerobic conditions (continuous supply of 40% air). We then examined the effect of supplying a constant oxygen tension on the growth of strains D39 and R6. Under aerobic conditions the maximal biomass (OD_{Max}) reached for strains D39 (0.49 ± 0.03) and R6 (0.23 ± 0.02) were, respectively, 3-fold and 16-fold lower than those observed under semi-aerobic conditions (Fig. 2.3-C and Table 2.3). This drastic decrease in the OD_{Max} contrasts with the higher growth rates obtained for both strains (around 1 h^{-1}) (Table 2.3). Noteworthy, at the time-point of transition to stationary phase of growth (time-point 2h), strains D39 and R6 consumed only 3.7 % and 2.8 % of the Glc supplied, respectively (Fig. 2.6 and Table 2.6).

Table 2.6. Product yields, total substrate consumed, carbon and redox balances and growth and energetic parameters as determined from substrate and fermentation product analysis, at the time-points 2h (transition phase) and 3h (stationary), in D39 and R6 strains cultured in CDM containing 61 ± 1 mM Glc, with pH-controlled at 6.5, at 37ºC, under aerobic conditions (constant air tension of 40%). Values of at least two independent experiments were averaged and errors are reported as ± SD.

	Aerobic			
	Transition phase		**Stationary**	
	D39	**R6**	**D39**	**R6**
Product yields[a]				
Lactate	1.06 ± 0.07	0.67 ± 0.09	0.47 ± 0.09	0.34 ± 0.02
Pyruvate[b]				
Formate	BDL	BDL	BDL	BDL
Acetate	0.92 ± 0.11	1.32 ± 0.08	1.53 ± 0.09	1.64 ± 0.01
Ethanol	BDL	BDL	BDL	BDL
H_2O_2	0.37 ± 0.01	0.60 ± 0.01	0.82 ± 0.01	0.91 ± 0.01
Consumed substrate (%)	3.7 ± 0.5	2.8 ± 0.2	4.4 ± 0.1	2.8 ± 0.4
Carbon balance[c]	100 ± 0	100 ± 0	100 ± 0	99 ± 1
Redox balance	ND	ND	ND	ND
Biomass yield (g mol^{-1} Glc)	64.6 ± 0.4	52.6 ± 4.0	68.1 ± 2.4	50.9 ± 6.6
ATP yield (mol mol^{-1} Glc)	2.9 ± 0.2	3.3 ± 0.1	3.5 ± 0.1	3.6 ± 0.0
Y_{ATP} (g biomass mol^{-1} ATP)	22.2 ± 1.2	15.8 ± 1.6	19.3 ± 1.1	14.1 ± 1.8

[a]Product yields, [End-product] / [Glc consumed]; [b]Blank cells, negative yields were found for these conditions (cells used pyruvate from the medium); [c]Carbon balance is the percentage of carbon in metabolized Glc that is recovered in the fermentation products (lactate and acetate). Dry weight (DW) was used as a measure of cell mass. BDL, below detection limit; ND, not determined.

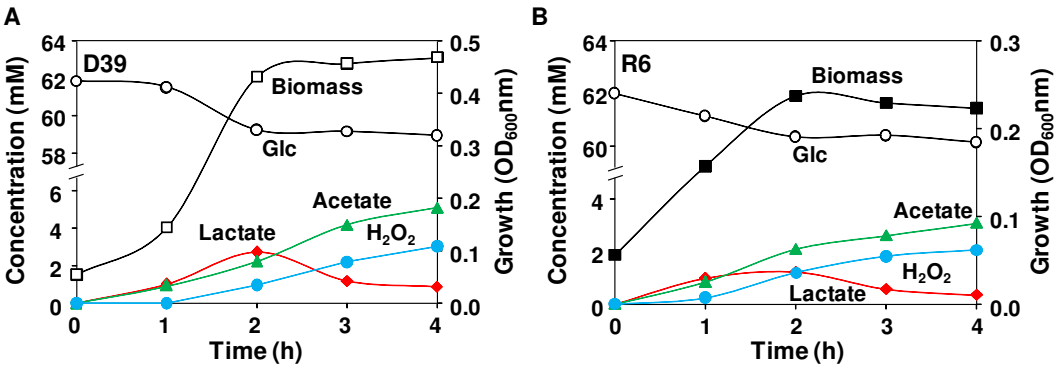

Fig. 2.6. Fermentation profiles of strains D39 and R6 under aerobic conditions. Growth curves, substrate consumption and end-products formed by the D39 (A) and R6 (B) strains growing aerobically (continuous specific air tension of 40%) as in Fig. 2.3-C. Culture supernatant samples for end-product analysis by HPLC and/or ^{1}H-NMR were harvested during growth. Symbols: (○), Glc consumption; (□), growth curve of D39; (■), growth curve of R6; (◆), lactate; (▲), acetate; (●), H_2O_2. The error was below 7% for major products (>2 mM) and 25% for minor products (<2 mM).

In both strains, the presence of oxygen (at a concentration of 0.09 mM) shifted the metabolism from lactate to acetate and H_2O_2 production, denoting high activity of pyruvate oxidase (SpxB) (Fig. 2.4 and Fig. 2.6). In strain R6 this shift was more pronounced, as indicated by the higher yields of acetate and H_2O_2 (Table 2.6). This observation is in good agreement with the higher activity of pyruvate oxidase measured for this strain and, possibly, with lower activity of the competing enzyme, NADH oxidase (Table 2.5 and Fig. 2.4). In contrast to work by others, in our study, a considerable reduction of NADH oxidase activity was observed in cells grown aerobically relative to semi-aerobically grown cells (Table 2.5) (Auzat *et al.*, 1999; Yu *et al.*, 2001). Under these aeration conditions, formate was not detected in the culture medium, indicating total inhibition of PFL (Fig. 2.6 and Table 2.6). Interestingly, growth arrest was observed when the levels of acetate

and H_2O_2 in the medium reached the values of about 2 and 1 mM, respectively, independently of the strain (Fig. 2.6). After the transition to stationary phase of growth (time-point 2h) no Glc was significantly consumed (Fig. 2.6 and Table 2.6) and the levels of acetate and H_2O_2 increased at the expense of lactate, showing lactate oxidase (LOX coded by *lcto*) activity (Fig. 2.4 and Fig. 2.6). In accordance, in the early-stationary phase of growth (time-point 3h) the yields of lactate decreased and the yields of acetate and H_2O_2 increased (Table 2.6). *S. pneumoniae* strain GTC13809, when grown aerobically, displayed similar metabolic features (Taniai *et al.*, 2008). This, however, is not a general mechanism among lactic acid bacteria (Neves *et al.*, 2002a; Seki *et al.*, 2004; Quatravaux *et al.*, 2006). Most commonly, activity of lactate and/or pyruvate oxidase is only apparent after Glc depletion, a phenomenon that allows additional metabolism after Glc starvation (Seki *et al.*, 2004; Quatravaux *et al.*, 2006). The advantage of pyruvate recycling via lactate oxidase is extra generation of ATP in the ensuing conversion to acetate (Fig. 2.4). Therefore, in accordance with higher acetate production, the higher ATP yields (mol ATP mol^{-1} Glc) determined for strains D39 and R6 under aerobic conditions were expected (Table 2.6).

In aerobic conditions, the surplus of ATP produced by *S. pneumoniae* D39 and R6 strains most likely enhanced their growth rates, leading to increased biomass yields (g mol^{-1} Glc), but did not impact on the maximal biomass (OD_{Max}) achieved (Table 2.3 and Table 2.6). This observation suggests a re-direction of ATP away from biosynthetic purposes into the maintenance of cellular processes, an event that can be triggered by a stressful condition, like high accumulation of H_2O_2. Considering the excess of nutrients and substrate present in the medium at the time-point of growth arrest and the control of pH to 6.5, the most plausible candidate affecting biomass production is H_2O_2. In accordance, studies have shown induction of pneumococcal death by H_2O_2 (Regev-Yochay *et al.*, 2007;

Ramos-Montañez *et al.*, 2008). Moreover, the concentration of H_2O_2 accumulated at the time-point of growth arrest (Fig. 2.6), about 1 mM, is in good agreements with the reported minimal inhibitory concentration (MIC) necessary to prevent growth of strain D39 (Pericone *et al.*, 2003). Therefore, the higher maximal biomass achieved by strain D39 can be explained by the 3-fold lower H_2O_2 to biomass ratio in this strain as compared to R6 (compare 5.7 ± 0.1 in D39 to 15.5 ± 0.1 nmol H_2O_2 mg DW^{-1} in R6 at time-point 2h). A major drawback in the aerobic metabolism of sugars by *S. pneumoniae* is its poor capacity to break down H_2O_2. Indeed, the pneumococcus does not possess the typical defense mechanisms against oxidative stress, such as catalase activity or expression of homologues of the OxyR/PerR transcriptional regulators (Tettelin *et al.*, 2001; Hoskins *et al.*, 2001; Lanie *et al.*, 2007). However, production of H_2O_2 in the mM range is also a competitive advantage used by *S. pneumoniae* to kill or inhibit other potential nasopharyngeal flora members, including *H. influenzae* and *N. meningitidis* (Pericone *et al.*, 2000; Pericone *et al.*, 2003). In this context, metabolic activities downstream of pyruvate in *S. pneumoniae* could have arisen from an evolutionary adaptation to the oxygen-rich environment of the nasopharynx, which is abundantly populated by other competitor microorganisms.

Manipulation of the concentration of nutrients in culture medium

Our data showed that both growth and metabolic profiles of strains D39 and R6 are differently affected by oxygen. Semi-aerobiosis (50-60% initial air tension) supported the highest growth parameters (growth rate and biomass) in strain D39. Therefore, this condition was chosen for further studies.

Recently Hathaway and co-workers showed that capsule is a cost in energetic terms and probably competes for energy with the other metabolic processes (Hathaway *et al.*, 2012). We showed that growth arrest of strain D39

occurred well before Glc depletion, independently of the parameters tested. Conversely, total consumption of Glc was detected for strain R6 under anaerobic and semi-aerobic conditions. Considering that capsule is a major difference between the two strains, it is plausible to assume that its production is an additional cost in nutritional terms at the expense of biomass (Fig. 2.4). This hypothesis was investigated by varying the amounts of medium components presumably required for capsule synthesis. In *S. pneumoniae* strain D39, serotype 2 capsule is a major virulence factor formed by repeating units of glucose, glucuronic acid and rhamnose in the proportion of 1:2:3 (Iannelli *et al.*, 1999). The precursors of these sugar monomers (UDP-glucose, UDP-glucuronic acid and dTDP-rhamnose) require UTP and dTTP for their synthesis (Iannelli *et al.*, 1999). The sugar moiety in the NDP-sugars derives from the glycolytic intermediate glucose 6-phosphate (Fig. 2.4). Hence, in addition to ATP generation, Glc is also used for capsule biosynthesis. In our conditions, Glc (~1% wt/vol) is apparently in excess in D39 cultivations, and thereby the nucleobases are the most promising candidates as growth-limiting nutrients. Thus, the effect of varying the nucleobases in the culture medium was assessed. To completely rule out Glc as the limiting nutrient, fermentations at a lower and a higher initial Glc concentration were also performed.

(i) Effect of glucose concentration on growth of *S. pneumoniae* D39 and R6. Fig. 2.7 shows the growth profiles of strains D39 and R6 in the presence of different Glc concentrations. The growth profile of strain D39 was not significantly changed when 0.5% rather than 1% (wt/vol) Glc was used as carbon source (Fig. 2.7-A). The growth parameters, growth rate (0.80 ± 0.06) and OD_{max} (1.5 ± 0.0), were identical to those observed on 1% Glc (Table 2.7). This behavior was not unexpected considering that, D39 had consumed only 28% of the Glc in medium containing 1% (wt/vol) of the sugar. On the other hand, strain R6 showed

a decrease in maximal biomass of about 40% when grown on 0.5% as compared to 1% Glc (Fig. 2.7-B and Table 2.7). Interestingly, triplicating the Glc in the culture medium led to an initial 2-fold decrease in the growth rate of strain D39 (from time-point 0 to time-point 2h, Fig. 2.7-A), when comparing with the growth on 1% Glc, and a lag of 1h in strain R6 (Fig. 2.7-B). However, after the time-point 2h, strain D39 recovered to 88% of the growth rate on 1% Glc. The growth rate of strain R6 on 3% Glc was 1.5-fold lower than that on 1% Glc. Unexpectedly, the maximal biomass achieved by strain R6 on 3% Glc was slightly lower than that on 1% Glc (Fig. 2.7-B and Table 2.7).

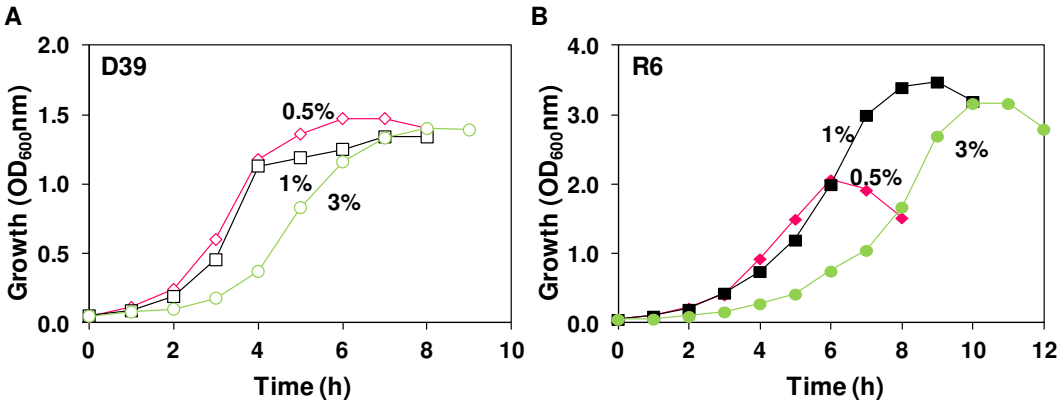

Fig. 2.7. Growth profiles at different glucose concentrations. Growth of strains D39 (A) and R6 (B) in CDM containing (◇,◆) 0.5%, (□,■) 1% or (○,●) 3% (wt/vol) Glc, under controlled conditions of pH (6.5), temperature (37ºC) and atmosphere (initial specific air tension of 50-60%), in a 2-l bioreactor. OD_{600} was measured at 1-h intervals. All cultures were inoculated with a preculture in late-exponential phase (6-7 hours incubation at 37ºC, OD_{600} 0.8-1.0).

Table 2.7. Growth parameters (length of lag, maximal growth rate and biomass) obtained for strains R6 and D39 cultured in CDM containing 0.5, 1 or 3% (wt/vol) Glc, with pH-controlled at 6.5, at 37ºC, and under semi-aerobic conditions (initial air tension 50-60%). The values for maximal growth rate and maximal biomass are averages of at least two independent experiments and the errors are reported as ± SD.

	0.5% Glc		**1% Glc**		**3% Glc**	
	D39	**R6**	**D39**	**R6**	**D39**	**R6**
Lag	No	No	No	No	No	Yes (1h)
μ_{max} (h^{-1})	0.80 ± 0.06	0.68 ± 0.01	0.80 ± 0.00	0.69 ± 0.03	0.70 ± 0.01	0.47 ± 0.01
OD_{Max}	1.5 ± 0.0	2.2 ± 0.2	1.3 ± 0.1	3.6 ± 0.2	1.4 ± 0.0	3.1 ± 0.1

In the dairy *L. lactis*, a positive correlation between biomass and sugar concentration has been reported up to concentrations of 2.5% (wt/vol); at an external concentration of 5%, a slight decrease (about 10%) in maximal biomass was observed (Papagianni *et al.*, 2007). Thus, *S. pneumoniae* seems to be more sensitive to high Glc concentrations than the dairy *L. lactis*. A complete explanation for the different behaviors is difficult to put forward, but it might be related to the environments sensed by these microorganisms in their natural habitats: while the dairy *L. lactis* is continuously exposed to a high sugar concentration in milk (~150 mM lactose), *S. pneumoniae* thrives in the nasopharynx where free sugars, and in particular Glc (< 1 mM), are low (Shelburne *et al.*, 2008a). Lipid bilayers are impermeable to Glc, thus the inhibitory effect of Glc (3% wt/vol) most likely occurs in the cellular membrane. Since the growth of strains D39 and R6 was not limited or inhibited by 1% (wt/vol) of Glc, this concentration was used in subsequent studies. Furthermore, our data clearly shows that Glc is not the limiting-nutrient in pH-controlled batch cultures of strain D39.

(ii) Effect of nucleobases concentration on growth of *S. pneumoniae* D39 and R6. The nucleobases present in our CDM (Table 2.1) are the purines adenine, guanine and xanthine and the pyrimidine uracil. To investigate the effect of this group of nucleobases on the growth of strains D39 and R6, their concentrations were raised simultaneously from 10 to 30 mg l^{-1} in the culture medium. This increase had a marked positive effect on the maximal biomass reached by strain D39 but did not improve growth of strain R6 (Fig. 2.8).

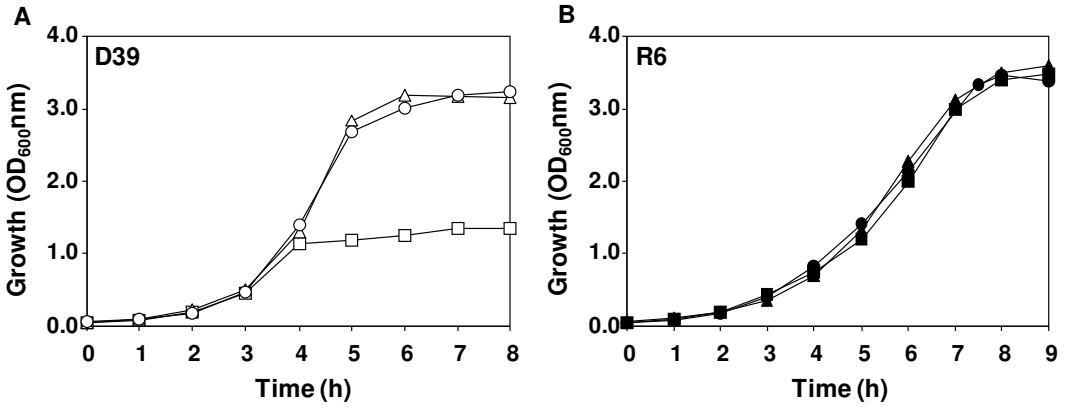

Fig. 2.8. Effect of nucleobases concentration on growth profiles. Growth of strains D39 (A) and R6 (B) in CDM containing 1% (wt/vol) Glc, under controlled conditions of pH (6.5), temperature (37ºC), and atmosphere (initial specific air tension of 50-60%), in a 2-l bioreactor. The nucleobases were added to the medium as follows: (□,■), G, A, X, U 10 mg l^{-1} each; (△,▲), G, A, X, U 30 mg l^{-1} each; (○,●), G, A, X 10 mg l^{-1} each plus 30 mg l^{-1} U. G= guanine; A= Adenine; X= Xanthine; U= Uracil. OD_{600} was measured at 1-h intervals. All cultures were inoculated with a preculture in late-exponential phase (6-7 hours incubation at 37ºC, OD_{600} 0.8-1.0).

The OD_{Max} reached by strain D39 in CDM containing 30 mg l^{-1} of nucleobases was 3.2 ± 0.0, a value 2.5-fold higher than that obtained in CDM with 10 mg l^{-1} of

nucleobases (1.3 ± 0.1) (Fig. 2.8-A). The growth rate and the growth profile of strains D39 and R6, respectively, were not affected by increasing the concentration of nucleobases (Fig. 2.8). The data indicate that capsule biosynthesis demands a group of nucleobases or a particular nucleobase. In line, dissimilar behaviors were also expected between strains D39 and R6 grown in CDM without nucleobases. Growth of strain D39 in the absence of nucleobases was characterized by a long lag-phase and an OD_{Max} of about 3 at time-point 27h (data not shown). On the other hand, strain R6 exhibited no lag-phase, a growth rate of about 0.54 h^{-1}, and an OD_{Max} of approximately 2.3, in CDM without nucleobases (data not shown). Our data indicate that strains D39 and R6 are able to synthesize nucleobases. The presence of genes encoding their biosynthetic pathways in the genome sequences of strains R6 and D39 fully corroborates our results (Hoskins *et al.*, 2001; Lanie *et al.*, 2007). Furthermore, the maximal biomass obtained for strain D39 grown without nucleobases (OD_{Max} 3), was 2.3-fold higher than that achieved by the same strain on 10 mg l^{-1} of nucleobases (OD_{Max} 1.3), implying that the pathways for their synthesis were repressed when the nucleobases were present in the medium. Thus, growth was limited by concentration.

(iii) Effect of uracil on growth and glucose fermentation in *S. pneumoniae* D39 and R6. Given the results above, we deemed important to determine if the positive effect of the nucleobases on growth of strain D39 was due to a particular base or the ensemble. Of the four nucleobases present in our CDM (Table 2.1), uracil is a constituent of UDP-Glc and UDP-glucuronic acid, precursors of D39 serotype 2 capsule repeating units (Fig. 2.4) (Iannelli *et al.*, 1999). Transporters for uracil are predicted in the genome sequence of strain D39 (Lanie *et al.*, 2007). Thus, we hypothesize uracil to be the limiting nutrient. Thymine nucleosides are formed from uracil nucleosides in the salvage pathway

of pyrimidine biosynthesis, (reviewed in Kilstrup *et al.*, 2005), and to our knowledge transporters for thymine in *Streptococcaceae* have not been described (reviewed in Kilstrup *et al.*, 2005). To test our hypothesis, strain D39 was grown in microtiter plates in CDM containing 0.25% (wt/vol) Glc (initial pH 6.5), and each nucleobase was added individually to a final concentration of 30 mg l^{-1}. Among the nucleobases tested, only an increase in uracil concentration led to improved growth of strain D39 (Fig. 2.9). Therefore, the effect of uracil *per se* was investigated.

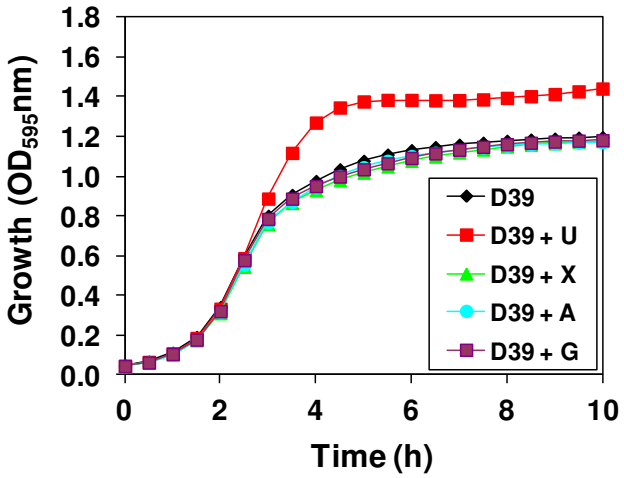

Fig. 2.9. Effect on growth of increasing a single nucleobase. Growth profile of strain D39 in CDM containing 0.25% (wt/vol) Glc with 30 mg l^{-1} of the specified nucleobase. Cultures were prepared in 250 µl in 96-well microtiter plates and growth monitored at 595 nm and 37ºC. Symbols: (◆),G, A, X, U 10 mg l^{-1} each; (■), G, A, X 10 mg l^{-1} each plus 30 mg l^{-1} U; (▲), G, A, U 10 mg l^{-1} each plus 30 mg l^{-1} X; (●), G, X, U 10 mg l^{-1} each plus 30 mg l^{-1} A; (■), A, X, U 10 mg l^{-1} each plus 30 mg l^{-1} G. G= guanine; A= Adenine; X= Xanthine; U= Uracil.

D39 was grown in static rubber-stoppered bottles in CDM containing 1% (wt/vol) Glc, without pH control (initial pH 6.5), and uracil was added to final concentrations of 40, 30, 10, 5, 3.3, 1, 0.67 and 0 mg l^{-1}. Interestingly, incrementing the final concentration of uracil in the culture medium from 0.67 mg l^{-1} to 30 mg l^{-1}, led to an increase in maximal biomass from about 0.2 to 2.2 of OD_{Max} (Fig. 2.10-A). Notably, this increase was linear from 0.67 mg l^{-1} to 10 mg l^{-1} uracil (Fig. 2.10-B). The maximum growth rate (approximately 0.8 h^{-1}) was not significantly affected, except for the lower concentrations of 3.3, 1 and 0.67 mg l^{-1}, which exhibited a rate of about 0.74, 0.53 and 0.48 h^{-1}, respectively.

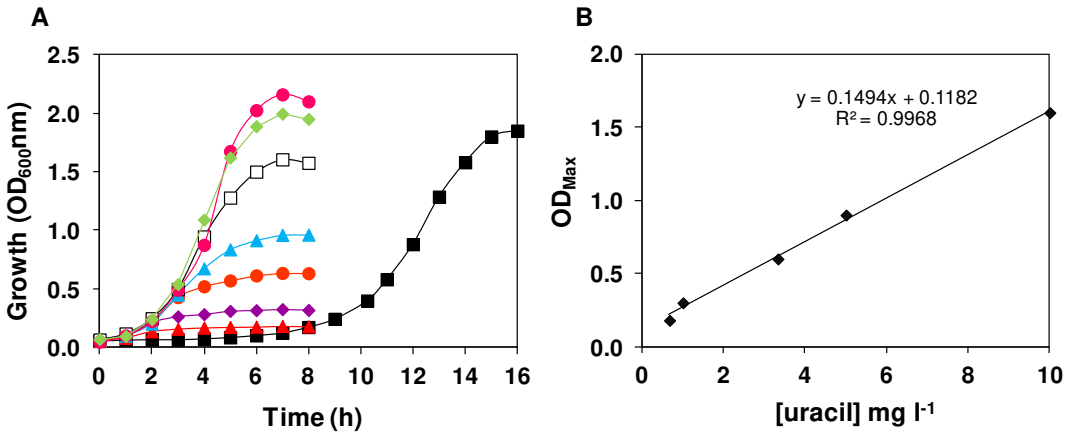

Fig. 2.10. Effect of varying uracil concentration on growth of strain D39. (A) Growth of strain D39 in CDM containing 1% (wt/vol) Glc with different concentrations of uracil (U), as specified below. Growth was performed at 37ºC, without pH control (initial pH 6.5), in static rubber-stoppered bottles, after inoculation with a preculture in late-exponential phase (6-7 hours incubation at 37ºC, OD_{600} 0.8-1.0). OD_{600} was measured at 1-h intervals. Uracil concentrations in mg l^{-1}: (■), 0; (▲), 0.67; (◆), 1; (●), 3.3; (▲), 5; (□), 10; (●), 30; (◆), 40. The other three nucleobases (G, X, A) were always present in the medium at a concentration of 10 mg l^{-1}. G=guanine; X, xanthine; A, adenine. (B) Linear correlation between the maximal D39 biomass (OD_{Max}) and the medium uracil concentration (from 0.67 to 10 mg l^{-1}).

A saturation at around 30 mg l^{-1} of uracil was found, as increasing the concentration even further, *i.e.* to 40 mg l^{-1}, did not improve growth (Fig. 2.10). Strain D39 was able to grow in uracil-free medium, as expected from genome analysis (Lanie *et al.*, 2007), and the growth profile displayed a lag of 6h, a growth rate of 0.42 h^{-1} and 1.8 of $OD_{Max.}$ In lactic acid bacteria, pyrimidine nucleobases are synthesized *de novo* using bicarbonate (HCO_3^-) or CO_2 and amino acids as substrates (reviewed in Kilstrup *et al.*, 2005).

In pH-controlled batch cultivations, a 3-fold increase in the concentration of uracil had a similar effect on growth (μ, 0.80 ± 0.02 h^{-1} and OD_{Max} of 3.2 ± 0.1) as that produced when all the four nucleobases were 3 times increased (Fig. 2.8-A). This result unequivocally shows that uracil is the sole base stimulating biomass production in the capsulated strain D39. Indeed, the increment of uracil concentration did not affect the growth rate of strain R6. Curiously, strain D39 showed a more pronounced shift to mixed-acid fermentation in Glc-CDM containing 30 mg l^{-1} uracil (Fig. 2.11). Lactate was the major end-product, accounting for 76% of the Glc consumed (Table 2.8), and formate (6.3 ± 1.3 mM) was produced in a ratio of 2:1:1 relative to ethanol (2.8 ± 1.1 mM) and acetate (3.1 ± 0.4 mM), which is ascribed to PFL activity. The pyruvate accumulated in this condition (*circa* 0.44 mM) was 2-fold lower than in medium containing 10 mg l^{-1} uracil (Table 2.4 and Table 2.8). This represents a shift to mixed-acid products 3-fold higher than that when uracil was limiting (Fig. 2.11-A and C). The levels of acetate accumulated by strain D39 in uracil-enriched medium were at least 2-fold higher than those accumulated in normal CDM. However, the ATP yields (mol ATP mol^{-1} Glc) were similar between both conditions (*circa* 1.8 and 1.7 in 30 and 10 mg l^{-1} uracil, respectively) and relative to strain R6 (Table 2.4 and Table 2.8).

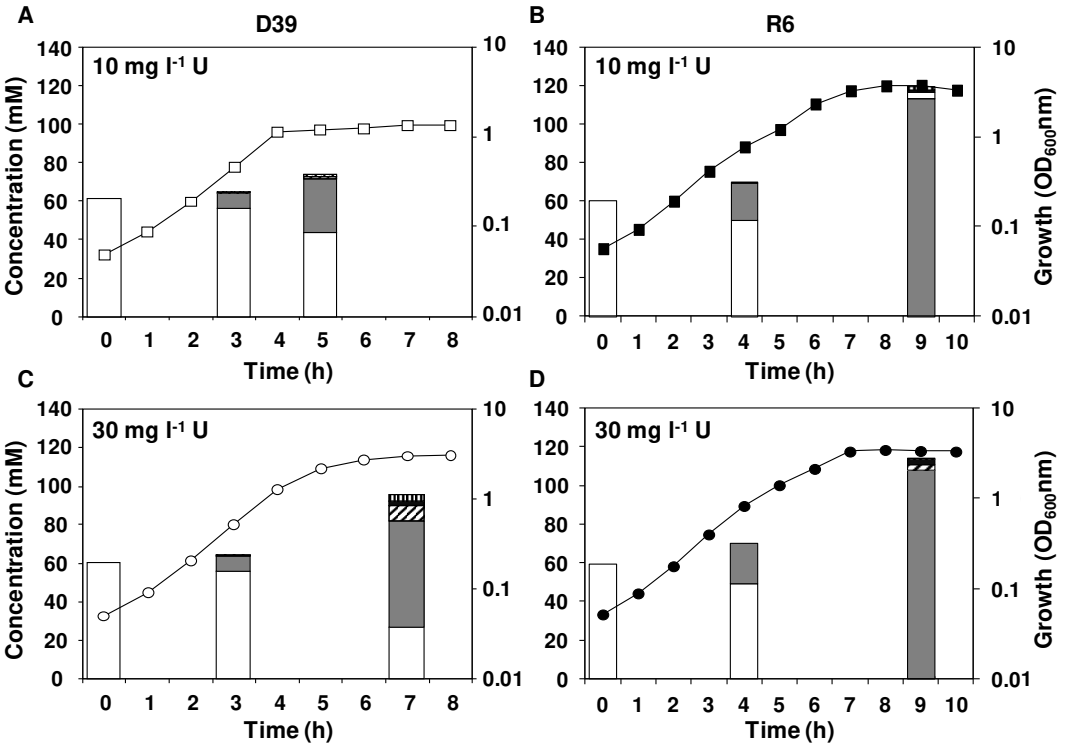

Fig. 2.11. Growth and fermentation products as a function of uracil concentration in pH-controlled batch cultures. Growth curves, substrate consumption and end-products formed by the D39 (A and C) and R6 (B and D) strains in CDM containing 10 mg l^{-1} uracil (A and C) or 30 mg l^{-1} uracil (B and D) under controlled conditions of pH (6.5), temperature (37ºC) and gas atmosphere (initial specific air tension of 50-60%) in a 2-l bioreactor after inoculation with a preculture in late-exponential phase (6-7 hours incubation at 37ºC, OD_{600} 0.8-1.0). Initial concentrations of Glc were for both strains 60 ± 1 mM. At 1-h time intervals OD_{600} was measured. Culture supernatant samples for end-product analysis by HPLC and/or ^{1}H-NMR were harvested for each of the conditions at time-points zero, exponential and growth arrest (maximal biomass) (bars in the plots). Symbols: (□,■), growth curves in 10 mg l^{-1} uracil; (○,●), growth curves in 30 mg l^{-1} uracil; (white bars), Glc; (grey bars), lactate; (hatched bars), formate; (black bars), acetate; (stripped bars), ethanol. D39 and R6 growth curves in 10 and 30 mg l^{-1} uracil as in Fig. 2.8, except that OD_{600} scale (y-axis) is logarithmic.

Table 2.8. Product yields, total substrate consumed, carbon and redox balances and growth and energetic parameters as determined from substrate and fermentation product analysis, at the time-point of maximal biomass achieved by D39 and R6 strains cultured in CDM containing 61 ± 1 mM Glc and supplemented with 30 mg l^{-1} uracil, with pH-controlled at 6.5, at 37ºC, under semi-aerobic conditions (initial air tension 50-60%). Values of at least two independent experiments were averaged and errors are reported as ± SD.

	Semi-aerobic	
	30 mg l^{-1} uracil	
	D39	**R6**
Product yields[a]		
Lactate	1.62 ± 0.04	1.82 ± 0.01
Pyruvate[b]	0.01 ± 0.00	
Formate	0.20 ± 0.02	0.05 ± 0.00
Acetate	0.10 ± 0.02	0.04 ± 0.00
Ethanol	0.09 ± 0.03	0.01 ± 0.00
Consumed substrate (%)	55 ± 0.4	100 ± 0
Carbon balance[c]	91 ± 1	93 ± 1
Redox balance	90 ± 1	92 ± 1
Biomass yield (g mol^{-1} Glc)	34.7 ± 0.1	22.9 ± 0.2
ATP yield (mol mol^{-1} Glc)	1.8 ± 0.1	1.9 ± 0.1
Y_{ATP} (g biomass mol^{-1} ATP)	19.3 ± 0.6	12.1 ± 0.2

[a]Product yields, [End-product] / [Glc consumed]; [b]Blank cells, negative yields were found for these conditions (cells used pyruvate from the medium); [c]Carbon balance is the percentage of carbon in metabolized Glc that is recovered in the fermentation products (lactate, formate, acetate and ethanol) and pyruvate; Dry weight (DW) was used as a measure of cell mass.

Our data establish a positive correlation between uracil supply and production of capsule in *S. pneumoniae* serotype 2. Under the conditions studied, we showed that uracil is the factor limiting growth of strain D39, while the acapsular strain R6 is irresponsive to the uracil concentration in the medium. The bioenergetic parameters fully support this view. In summary, we developed a CDM and growth

conditions that support high yield of strains D39 and R6. For strain D39, a better growth performance was observed in CDM (Table 2.1) containing 1% (wt/vol) Glc and supplemented with uracil to a final concentration of 30 mg l^{-1}, under controlled conditions of temperature (37ºC), pH (6.5) and gas atmosphere (semi-aerobic, initial air tension of 50-60%). For strain R6, the best growth was observed in CDM containing 1% (wt/vol) Glc, under controlled conditions of temperature (37ºC), pH (6.5) and gas atmosphere (strictly anaerobic). The optimized conditions were used to perform *in vivo* NMR studies.

Glucose metabolism monitored by *in vivo* NMR

The use of the *in vivo* NMR technique to study bacterial metabolism has been reported before (Neves *et al.*, 1999). However, due to the low sensitivity of this technique, dense cell suspensions are usually required. Thus, we sought to prepare dense cell suspensions of strains D39 and R6. However, and despite several attempts and condition variations we were unable to pellet strain D39 by centrifugation. This is most likely a consequence of electrostatic repulsion due to its heavily negative charged capsule. In contrast, compact pellets were obtained upon centrifugation of R6 cultures, which enabled the preparation of dense cell suspensions and the application of *in vivo* NMR techniques to study sugar metabolism. For *in vivo* NMR studies, strain R6 was grown in CDM containing 1% (wt/vol) Glc, at 37ºC, pH 6.5 and under strictly anaerobic conditions (argon atmosphere). Cells were harvested in the late-exponential phase of growth (OD_{600} = 1.9, as in Fig. 2.3-B), washed twice in 5 mM KP_i or MES buffer with 2% (wt/vol) choline and then suspended in 50 mM KP_i or MES buffer with 2% (wt/vol) choline to a protein concentration of 13-14 mg ml^{-1}. Choline was added to prevent cell lysis (Giudicelli and Tomasz, 1984; Balachandran *et al.*, 2001; Steinmoen *et al.*, 2002). In buffer containing choline, lysis was marginal during the time span of

^{13}C-NMR experiments (30 min). The OD_{600} value of the suspension decreased by less than 3% in 30 min and 6.5% in 1h, while in the absence of choline the optical density values had decreased by 40% and 85% after 30 and 60 min, respectively (Fig. 2.12). Glc metabolism of R6 resting cells was monitored under controlled conditions of pH (6.5), temperature (37ºC) and gas atmosphere (anaerobic) using the on-line NMR system developed by Neves *et al.* (1999).

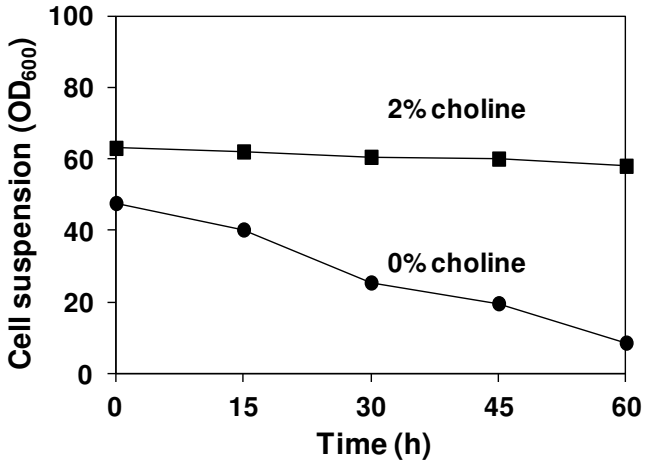

Fig. 2.12. Pneumococcal lysis in resting cell suspensions. Optical density variation during Glc (20 mM) metabolism of resting cells of strain R6, grown as for *in vivo* NMR, suspended in 50 mM KP_i with (■) 2% or (●) 0% (wt/vol) choline. OD_{600} was measured with intervals of 15 minutes.

(i) Pools of metabolites by *in vivo* ^{13}C-NMR. The time course for Glc consumption and product formation under anaerobic conditions is shown in Fig. 2.13. The end-products of [1-^{13}C]Glc (20 mM) metabolism were lactate (35.8 ± 0.4) mM), acetate (2.6 ± 0.4 mM) and glycerol (0.36 ± 0.04 mM). As expected lactate was the major end-product accounting for 89% of the Glc consumed.

Interestingly, a 2 min delay for Glc consumption was observed after the pulse of Glc, which was then consumed at a maximal rate of 0.32 µmol min^{-1} mg^{-1} of protein (Fig. 2.13). The pool of fructose 1,6-bisphosphate (FBP) increased to a steady concentration of about 30 mM, and declined to undetectable levels at the onset of Glc exhaustion (Fig. 2.13). FBP was the only glycolytic metabolite detected. The glycolytic dynamics in *S. pneumoniae* are considerably different from those reported for the closely related organism *L. lactis* (reviewed in Neves *et al.*, 2005). In *L. lactis*, at the onset of Glc depletion the pool of FBP declines to an intermediate level, and thereafter decreases slowly to undetectable concentrations (reviewed in Neves *et al.*, 2005). Moreover, in *L. lactis*, 3-phosphoglycerate (3-PGA) and phospho*enol*pyruvate (PEP) accumulate after Glc depletion (reviewed in Neves *et al.*, 2005). In the dairy bacterium, slow depletion of FBP and accumulation of 3-PGA and PEP were rationalized as resulting from progressive obstruction at the level of pyruvate kinase (PK), a glycolytic enzyme regulated at the metabolic level by FBP (activator) and inorganic phosphate (inhibitor) (reviewed in Neves *et al.*, 2005). Based on the established differences between the metabolic profiles in *L. lactis* and *S. pneumoniae*, a different regulatory mechanism at the level of pyruvate kinase can be hypothesized for the pathogen.

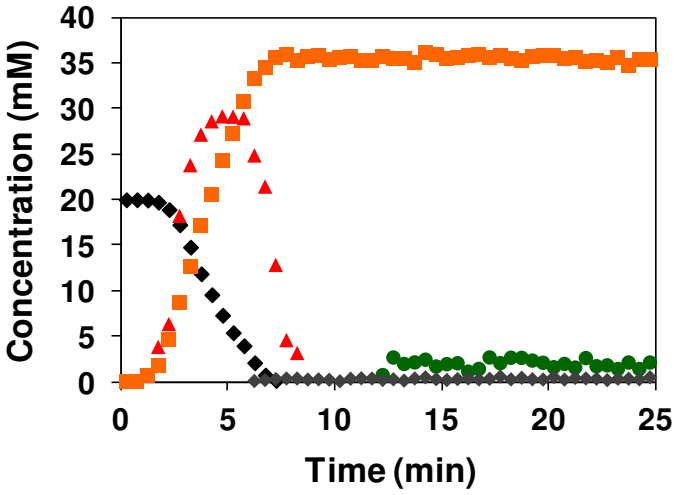

Fig. 2.13. Glucose metabolism in resting cell suspensions of *S. pneumoniae* R6 monitored by *in vivo* ^{13}C-NMR. Kinetics of 20 mM [1-^{13}C]glucose consumption, end-products formation and build-up of glycolytic intermediate pools by a cell suspension (50 ml) of resting cells of *S. pneumoniae* R6 under anaerobic conditions as monitored *in vivo* by ^{13}C-NMR. R6 cells, grown anaerobically as in Fig. 2.3-B until late-exponential phase (OD_{600} 1.9), were suspended in 50 mM KP_i with 2% (wt/vol) choline (pH 6.5) at a concentration of 13-14 mg protein ml^{-1}. [1-^{13}C]glucose was added at time zero and 30 s spectra were acquired sequentially after its addition. The extracellular pH was maintained at 6.5 during the experiment by automatic addition of NaOH. Symbols: (◆), glucose; (■), lactic acid; (●), acetate; (◆), glycerol; (▲), fructose 1,6-bisphosphate.

(ii) Pools of NTP and P_i by *in vivo* ^{31}P-NMR. To obtain information on the energetic status of the cells, *in vivo* ^{31}P-NMR spectra were obtained during the metabolism of Glc by resting cells of strain R6. Glc (20 mM) was supplied at a time designated zero (0 min) and the time course for formation of NTP and total P_i is shown in Fig. 2.14. Upon Glc addition, the pool of inorganic phosphate (P_i) decreased from about 60 to 2 mM, in 7 min, consistent with glycolytic usage. In accordance, this was also the time required for total consumption of Glc in the *in*

vivo ^{13}C-NMR experiment of strain R6. During Glc consumption the NTP pools reached values of about 2.2 mM, which were maintained until the time-point 10 min, and disappeared afterwards. The pool of P_i became visible well after NTP depletion (after Glc disappearance) reaching values of approximately 60 mM. The build-up of the P_i pool in *S. pneumoniae* differs from that in *L. lactis*, for which P_i accumulates much earlier. Moreover, the NTP pools in *L. lactis* are 3-fold higher than in *S. pneumoniae* R6, and remain high beyond Glc depletion (Neves *et al*., 1999; Neves *et al*., 2005). The levels of NTP detected *in vivo* in *S. pneumoniae* are similar to the concentrations measured *in vitro* (Chapter 6). In *S. pneumoniae*, the dynamics of glycolytic intermediates at the onset of Glc exhaustion (Fig. 2.13) could in part be explained by the delay in P_i accumulation, and thus lack of inhibition of PK. However, our own preliminary results indicate that the pneumococcal PK is less sensitive to P_i than its lactococcal homologue (data not shown). The effects of FBP and P_i on PK activity are currently under investigation in our laboratory.

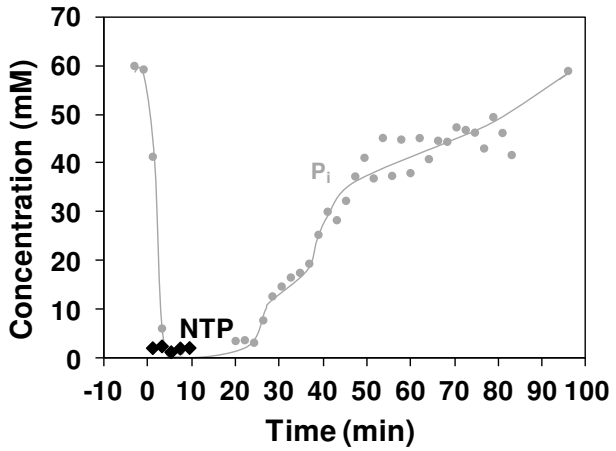

Fig. 2.14. Determination of the pools of NTP and P_i by *in vivo* ^{31}P-NMR. Time course for the concentration of NTP (◆) and total inorganic phosphate, P_i (●) in resting cells of *S. pneumoniae* R6 under anaerobic conditions as monitored *in vivo* by ^{31}P-NMR. R6 cells, grown anaerobically as in Fig. 2.3-B until late-exponential phase (OD_{600} 1.9), were suspended in 50 mM MES buffer with 2% (wt/vol) choline (pH 6.5) at a concentration of 13-14 mg protein ml^{-1}. Glc was added at time zero and spectra (126 s) were acquired sequentially after its addition. The extracellular pH was maintained at 6.5 during the experiment by automatic addition of NaOH.

Conclusion

A chemically defined medium and growth conditions supporting high biomass yield of *S. pneumoniae* strains D39 and R6 have been developed. Importantly, during this process an extensive comparative metabolic characterization between these strains under controlled conditions of pH, temperature and gas atmosphere has been accomplished. The results of these studies showed that strains D39 and R6 display a better growth performance under different environmental and nutritional conditions. In strain D39 the growth

rate was stimulated under semi-aerobic conditions, while in strain R6 strictly anaerobic conditions rendered optimal growth. The better performance of D39 in semi-aerobic conditions was attributed to the lower activity of pyruvate oxidase and higher activity of NADH oxidase as compared to R6. Furthermore, the maximal biomass achieved by strain D39 was substantially enhanced when a supplement of uracil was added to the culture medium, whereas R6 was irresponsive to the nucleobase. Our metabolic data showed that more than an energetic burden capsule is a cost in nutritional terms and uracil is the limiting nutrient. This view indicates a direct link between capsule production and the requirement for uracil. The surprising marked physiological differences between strains D39 and R6, showed in our studies substantiate the view that findings in strain R6 cannot be generalized to D39, at least in what growth physiology is concerned (Lanie *et al*., 2007). Finally, the chemically defined medium optimized in this study was suitable for the application of *in vivo* NMR to study sugar metabolism. We were the first to obtain time series data on concentrations of metabolite pools online and non-invasively for *S. pneumoniae*. Our data suggest unique regulation of glycolysis in *S. pneumoniae* as compared to other *Streptococcaceae*.

Acknowledgements

SM Carvalho helds a fellowship SFRH/BD/35947/2007 from Fundação para a Ciência e a Tecnologia (FCT). The NMR spectrometers are part of the National NMR Network (REDE/1517/RMN/2005), supported by "Programa Operacional Ciência e Inovação (POCTI) 2010" and FCT. This work was funded by FCT and FEDER, projects PDCT/BIA-MIC/56235/2004, PTDC/BIA-MIC/099963/2008 and PTDC/SAU-MII/100964/2008 and through grant PEst-OE/EQB/LA0004/2011. SM Carvalho and AR Neves would like to thank Prof. Helena Santos for all the support provided during the course of this work.

Author's Contribution

All the experiments were performed by Sandra Carvalho. Conceived and designed the experiments: SM Carvalho and AR Neves. Analyzed the data: SM Carvalho, OP kuipers and AR Neves.

Chapter 3

Interplay between capsule expression and uracil metabolism in *Streptococcus pneumoniae*

The results of this chapter will be submitted for publication:

SM Carvalho, T Kloosterman, J Caldas, S Vinga, OP Kuipers, AR Neves (2012) "Interplay between capsule expression and uracil metabolism in *Streptococcus pneumoniae*". Manuscript in preparation.

Chapter 3 – Contents

Summary

Pyrimidine nucleotides play an important role in the biosynthesis of NDP-sugars, the precursors of structural polysaccharides in bacteria. The precursors for the biosynthesis of capsule, a major virulence factor of the human pathogen *S. pneumoniae*, are activated by pyrimidine nucleotides. *S. pneumoniae* is known to switch between opaque and transparent phenotypes, which are among other factors characterized by different capsule amounts. We identified a spontaneous non-reversible mutant of strain D39 that displayed characteristics of underproducing capsule similar to a transparent variant. Sequencing analysis of the *dexB-cps2A* intergenic region containing the capsule operon promoter revealed a point mutation in the -10 box of P*cps*. By directed mutagenesis we showed that this mutation was solely responsible for the drastic decrease in capsule expression and production. Transcriptome analysis comparing the spontaneous mutant with its progenitor resulted in altered expression of several genes, including the capsule operon, a gene involved in uracil transport (*spd_0267*) and *pyrC* (*spd_1030*), coding for a protein of *de novo* pathway for pyrimidine biosynthesis. These data suggested a link between pyrimidine metabolism and capsule production. In medium lacking uracil, D39 showed increased lag phase, decreased growth rate and higher biomass, as compared to growth in uracil-containing medium. Moreover, the activity of the capsule promoter and the amounts of capsule were lower in uracil-deprived conditions. In contrast, uracil had no effect on the spontaneous mutant strain. Co-cultivation of both strains indicated a competitive advantage of the spontaneous mutant (transparent phenotype) in medium devoid of uracil. Taken together, our data suggest that uracil may act as a signal in the molecular switch between the distinct capsular phenotypes in *S. pneumoniae*.

Introduction

Streptococcus pneumoniae is a deadly human pathogen. This bacterium that resides in the human nasopharynx can, when the host immune system is debilitated, migrate to and infect normally sterile niches, such as the lower respiratory tract (bronchi and lungs), middle ear, meninges and blood (reviewed in Mitchell, 2003). The fluctuating environments in the host elicit different gene expression patterns in *S. pneumoniae*, leading to different phenotypes (Orihuela *et al.*, 2004b; LeMessurier *et al.*, 2006; Oggioni *et al.*, 2006). One of the most remarkable examples of pneumococcal adaptation to the microenvironments of the human host is the so-called ON and OFF switch of phase variation (Kim and Weiser, 1998; Hammerschmidt *et al.*, 2005). In this process, the switch occurs between two phenotypic variants of *S. pneumoniae*, the opaque and the transparent (Kim and Weiser, 1998; Kim *et al.*, 1999). Opaque pneumococci are less efficient colonizers of the nasopharynx, produce more capsule and are more virulent than transparent variants (Kim and Weiser, 1998; Kim *et al.*, 1999; Magee and Yother, 2001; Ogunniyi *et al.*, 2002; Morona *et al.*, 2004; Hammerschmidt *et al.*, 2005; Nelson *et al.*, 2007). This specific phase variation (opaque *versus* transparent phenotype), which differs in capsule amounts, is generally reversible (Saluja and Weiser, 1995; Weiser *et al.*, 2001; Waite *et al.*, 2001; Waite *et al.*, 2003). However, irreversible phase transitions have also been reported (Hammerschmidt *et al.*, 2005; McEllistrem *et al.*, 2007; Allegrucci and Sauer, 2008). Adaptation mechanisms leading to pneumococcal irreversible mutations and thereof to readjustment of regulatory networks have been described (Claverys *et al.*, 2000; Hakenbeck *et al.*, 2001; Pericone *et al.*, 2002; Stevens and Sebert, 2011). These mechanisms include horizontal gene transfer and homologous recombination, transposition of insertion sequences (ISs), gene

duplication, rearrangement of short-sequence DNA repeats (namely RUP and BOX elements), and oxidative damage-mediated responses (Claverys *et al.*, 2000; Hakenbeck *et al.*, 2001; Hoskins *et al.*, 2001; Tettelin *et al.*, 2001; Pericone *et al.*, 2002; Lanie *et al.*, 2007; Stevens and Sebert, 2011; Hakenbeck *et al.*, 2012). The aptitude to acquire new mutations is further corroborated by the recent findings showing that *S. pneumoniae* accumulates beneficial mutations at a rate of 4.8×10^{-4} per genome per generation time, during single-colony serial transfer (Stevens and Sebert, 2011), a value similar to that obtained for *E. coli* by Perfeito and co-workers (Perfeito *et al.*, 2007).

The present study started with the identification of a non-reversible D39 spontaneous mutant displaying characteristics of underproducing capsule, similar to a transparent phenotypic variant. This isolate arose together in solid cultures with D39 opaque colonies. Capsule has been recognized as a condition *sine qua non* of virulence in *S. pneumoniae*. Hence, regulation of its synthesis and of phase variation is central to the ability of the pneumococcus to cause invasive disease (Kim and Weiser, 1998; Llull *et al.*, 2001). The involvement of the global regulator CcpA, pyruvate oxidase (SpxB), and the tyrosine phosphoregulatory system (CpsBCD) in the control of pneumococcal capsule production has been postulated (Chapters 4 and 6) (Weiser *et al.*, 2001; Giammarinaro and Paton, 2002; Bender *et al.*, 2003; Morona *et al.*, 2006; Ramos-Montañez *et al.*, 2008; Yother, 2011). Despite recent advances, a true understanding of the mechanisms connecting capsule production and central metabolism in *S. pneumoniae* remains unclear (reviewed in Yother, 2011).

In Chapter 2, a link between the pyrimidine uracil metabolism and capsule production in strain D39 is surmised. The capsule of strain D39 is formed by repeating units of glucose, glucuronic acid and rhamnose in the proportion of 1:2:3 (Iannelli *et al.*, 1999). The sugar constituents are activated by UTP, yielding

UDP-glucose and UDP-glucuronic acid, and dTTP, yielding dTDP-rhamnose (Iannelli *et al.*, 1999). In several Gram positive microorganisms, UTP is produced from UMP in the salvage pathway of pyrimidine biosynthesis (reviewed in Kilstrup *et al.*, 2005). However, the precursors for UMP production may be synthesized endogenously in the pathway of *de novo* synthesis of pyrimidines or from uracil or uridine supplied exogenously (reviewed in Kilstrup *et al.*, 2005).

In this work, we show that the underproducing capsule phenotype of the D39 spontaneous mutant (D39SM) can be ascribed to a point mutation in the -10 box element of the capsule (*cps*) promoter. Reconstitution of the single mutation in D39 rendered a strain defective in capsule production, but in other aspects phenotipically distinct from D39SM. This finding indicates the occurrence of additional mutations in D39SM, which are currently being investigated by whole genome sequencing. Resorting to growth characterization and transcriptome analysis of D39 and its derivative strains in the presence or absence of uracil, a link between pyrimidine metabolism and capsule was unveiled. In light of these results, we speculate that the stressful condition triggering the mutations in D39 changed UMP/UTP availability, leading to the underproducing capsule phenotype. Considering this assumption, we analyzed the growth profiles of D39 and D39SM in co-cultivation in medium with or without uracil and observed that in uracil-deprived conditions the transparent phenotype is a competitive advantage. In addition, we investigated how capsule production and growth of *S. pneumoniae* responded to the presence and absence of uracil. Based on our findings we propose that sensing of uracil is one mean by which *S. pneumoniae* alters capsule production, and thus, virulence.

Materials and Methods

Bacterial strains and growth conditions for strain isolation

Strains and plasmids used in this study are shown in Table 3.1. *S. pneumoniae* strains were routinely grown in M17 agar containing 0.5 % (wt/vol) Glc and 1% (vol/vol) defibrinated sheep blood (Probiológica, Portugal) or as standing cultures without aeration in M17 broth (DifcoTM) supplemented with 0.5% (wt/vol) Glc, at 37ºC. Stocks and working stocks of isolated strains were prepared as described in Chapter 2. When appropriate, 0.25 µg ml^{-1} erythromycin or 2.5 µg ml^{-1} tetracycline were added to the medium. *E. coli* EC1000 was grown in TY broth in a shaking incubator at 37ºC; erythromycin was used in a concentration of 120 µg ml^{-1}.

Growth conditions for physiological studies

S. pneumoniae was grown in the CDM described in Chapter 2, except when stated otherwise. *S. pneumoniae* cultures were started at an initial optical density at 600 nm (OD_{600}) of 0.05-0.06 by addition of preculture cells harvested in exponential phase (OD_{600} 0.8 - 1.0), centrifuged and suspended in fresh CDM without uracil. Cultivations were performed in static rubber-stoppered bottles at 37ºC without pH control (initial pH 6.5). Glc (1% wt/vol) was used as the carbon source. Growth was monitored by measuring OD_{600} every hour. Maximum specific growth rates (μ_{max}) were calculated through linear regressions of the plots of ln (OD_{600}) *versus* time during the exponential growth phase.

The effect of uracil deprivation on growth of the pneumococcus strains was assessed by cultivating cells as above, except that uracil was omitted from the medium.

Table 3.1. Bacterial strains and plasmids used in this work

Strains	Description	Source/Reference
S. pneumoniae		
D39	Serotype 2 strain	Avery *et al*., 1944; Lanie *et al*., 2007
D39SM	Spontaneous mutant derived from serotype 2 strain D39 with characteristics of underproducing capsule. Colony phenotype on plate: small and transparent.	This work
D39P$cps_{T\rightarrow C}$	D39 containing a point mutation (T→C, 30 nucleotides upstream of the starting codon (ATG) of the *cps2A* gene) in the -10 region of the *cps* promoter (P*cps*)	This work
D39pPP2[P$cps_{T\rightarrow C}$]	D39 Δ*bgaA*::P$cps_{T\rightarrow C}$-*lacZ*; Tet^R	This work
D39pPP2[P*cps*]	D39 Δ*bgaA*::P*cps-lacZ*; Tet^R	This work
D39SMpPP2[P$cps_{T\rightarrow C}$]	D39SM Δ*bgaA*::P$cps_{T\rightarrow C}$-*lacZ*; Tet^R	This work
D39SMpPP2[P*cps*]	D39SM Δ*bgaA*::P*cps-lacZ*; Tet^R	This work
E. coli		
EC1000	MC1000 derivative carrying a single copy of the pWV01 *repA* gene in *glgB*; km^R	Leenhouts *et al*., 1996
Plasmids		
pPP2	Promoter-less *lacZ*. For replacement of *bgaA* with promoter-*lacZ* fusions. Derivative of pPP1; Amp^R, Tet^R.	Halfmann *et al*., 2007
pORI280	*ori*$^+$ repA$^-$, deletion derivative of pWV01; constitutive *lacZ* expression from P32 promoter; Em^R	Leenhouts *et al*., 1996
pORI[P$cps_{T\rightarrow C}$]	pORI280 carrying a 1268-bp fragment, which contains a point mutation (T→C, 30 nucleotides upstream of the starting codon (ATG) of the *cps2A* gene) in the -10 region of the *cps* promoter (P*cps*); Em^R	This work
pPP2[P*cps*]	pPP2 carrying a 1268-bp fragment, which contains the native *cps* promoter (P*cps*), in front of *lacZ*; Tet^R.	This work
pPP2[P$cps_{T\rightarrow C}$]	pPP2 carrying a 1268-bp fragment, which contains a point mutation (T→C, 30 nucleotides upstream of the starting codon (ATG) of the *cps2A* gene) in the -10 region of the *cps* promoter (P*cps*), in front of *lacZ*; Tet^R	This work

Abbreviations: Tet^R, tetracycline resistance; Amp^R, ampicillin resistance; Em^R, erythromycin resistance; Km^R, kanamycin resistance.

Intraspecies competition growth experiments

D39 and D39SM were grown in CDM supplemented or not with uracil (10 mg l^{-1}) in monoculture or co-culture. Both monocultures and co-cultures were started at an initial OD_{600} of 0.06 ± 0.03 by addition of exponentially growing precultures suspended in fresh CDM without uracil, as described above. In the co-culture experiments, in which uracil is present, D39 and D39SM were inoculated at a cell ratio of 4:1, 1:1 and 1:4. For experiments in the absence of uracil D39 and D39SM were inoculated at a cell ratio of 3:1, 1:1 and 1:4. Colony forming units per ml (CFUs ml^{-1}) of D39 and D39SM were determined at time-point zero of inoculation (OD_{600} of 0.06 ± 0.03) as follows: suspensions were diluted 1000 times in CDM without uracil and plated (2 µl) in M17 blood agar containing 0.5% (wt/vol) Glc. For the determination of strain relative abundance, samples in mid-exponential phase (OD_{600} of 0.48 ± 0.05) were collected, diluted 100 times and plated (100 µl) in M17 blood agar containing 0.5% (wt/vol) Glc. Plated cells were always grown at 37ºC in a 5% (vol/vol) CO_2 incubator. The estimation of the relative abundances of the D39 and D39SM populations was determined by cell counting (CFUs ml^{-1}). All the plates were scanned with white light epi-illumination and stored as digitized image files with a Molecular Imager® ChemiDocTM XRS+ Imaging System (Bio-Rad). The Quantity one software package was used to adjust the contrast, thus enhancing the visualization of the colonies on the plates.

Molecular techniques

Chromosomal DNA isolation was performed according to the procedure of Johansen and Kibenich (1992). Plasmid isolation was carried out using the plasmid isolation kit from Roche. Pwo DNA polymerase (Roche), T4 DNA ligase (Biolabs, New England) and restriction enzymes (Biolabs, New England) were used according to the supplier's recommendations. Purification of the PCR

products was performed using the High pure PCR product purification kit from Roche. Purified PCR products or recombinant plasmids were introduced into *S. pneumoniae* by transformation as described in Kloosterman *et al.* (2006a). Positive transformants were selected in M17 blood agar containing 0.5% (wt/vol) Glc with the appropriate antibiotic and confirmed by PCR and sequencing.

Sequencing of the *dexB-cps2A* genomic region

The genomic region comprising 1453-bp before and 396-bp after the starting codon (ATG) of the *cps2A* gene was PCR amplified with primers P1_capsule to P5_capsule and sent for sequencing (Service XS, Leiden, The Netherlands).

Construction of a point mutation in the -10 box of the capsule *locus* (P*cps*)

The oligonucleotide primers used in this study are listed in Table 3.2. Thymine, located 30 nucleotides upstream of the initiation codon (ATG) of the *cps2A* gene, was replaced in the TATAAT binding box of the *cps locus* with a cytosine, thereby leading to TATAAC (Fig. 3.3-A), as follows. Up- and downstream DNA fragments of 659- and 625-bp, respectively, comprising the desired mutation were obtained by PCR amplification with the primer pairs Pcapsule-1/ Pcapsule-mut2 and Pcapsule-2/ Pcapsule-mut1, using D39 wild-type DNA as a template. The internal primers, Pcapsule-mut2 and Pcapsule-mut1, comprise the point mutation leading to the TATAA(T→C) change. The resulting PCR products were fused by means of overlap extension PCR (Song *et al.*, 2005) using the primers Pcapsule-1 and Pcapsule-2, leading to the formation of a DNA fragment (1263-bp) containing the altered -10 binding box (TATAAC). This fragment was cloned into the EcoRI/BamHI sites of pORI280, forming the pORI[P$cps_{T\rightarrow C}$] construct. *E. coli* EC1000 was used as cloning host. This

construct was used to introduce the point mutation in the -10 promoter region of the *cps locus* of the chromosome of strain D39 following the procedure described previously by Kloosterman *et al.* (2006a). The resulting strain was designated D39P*cps*$_{T\rightarrow C}$.

Table 3.2. Oligonucleotide primers used in this study

Primers	Sequence (from 5' to 3' end)	REnz
Spec_Fp	CTAATCAAAATAGTGAGGAGG	-
Spec_Rp	ACTAAACGAAATAAACGC	-
Pcapsule-1[a]	CGGAATTCAGTATCGAATCCTGTTTCGTC	*EcoRI*
Pcapsule-2[a]	CGGGATCCGTCTGGATACTCTAACTCGATG	*BamHI*
Pcapsule-mut1[b]	**AACCGTAAGATGTTCAATGTA**TAG	-
Pcapsule-mut2[b]	**TACATTGAACATCTTACGGTT**ATA	-
P1_capsule	CCATGGGATGCTTTCTGTG	-
P2_capsule	GAGGTGCTTTTTGATATGAG	-
P3_capsule	AGCCCATAGCTTTGAGCGC	-
P4_capsule	AGGTGTAGACATTACCG	-
P5_capsule	GTTACGCAACTGACGAGTG	-

REnz, restriction enzyme; [a]Restriction enzyme sites are underlined. [b]Point mutations are underlined. Overlap of primers Pcapsule-mut1 and Pcapsule-mut2 is indicated in bold.

Construction of ectopic P*cps-lacZ* and P*cps*$_{T\rightarrow C}$-*lacZ* fusions

An ectopic transcriptional fusion of the capsule *locus* promoter (P*cps*) with the *lacZ* reporter gene was constructed using the pPP2 plasmid (Halfmann *et al.*, 2007). A DNA fragment comprising P*cps* was PCR-amplified from D39 chromosomal DNA using the primer pair Pcapsule-1/Pcapsule-2. This fragment (1284-bp) was cloned into the EcoRI/BamHI sites of pPP2 and the resulting plasmid (pPP2[P*cps*]) was integrated via double cross-over into the *bgaA locus* of

strains D39 and D39SM, yielding strains D39pPP2[P*cps*] and D39SMpPP2[P*cps*], respectively. To construct a *lacZ* fusion with the mutated *cps locus* promoter (P$cps_{T\rightarrow C}$), the PCR fragment containing P$cps_{T\rightarrow C}$, generated as described above, was cloned into the EcoRI/BamHI sites of pPP2. The resulting plasmid (pPP2[P$cps_{T\rightarrow C}$]) was integrated via a double cross-over event into the *bgaA locus* of strains D39 and D39SM, leading to the formation of strains D39pPP2[P$cps_{T\rightarrow C}$] and D39SMpPP2[P$cps_{T\rightarrow C}$], respectively.

β-galactosidase activity measurements

Cells containing the promoter-*lacZ* fusions were grown in CDM containing 1% (wt/vol) Glc, with or without uracil, as described above. Culture samples of 2 ml were harvested during mid-exponential phases of growth and the activity of the promoters was assayed by measuring β-galactosidase activities as described before by Kloosterman *et al.* (2006a).

Transcriptome analysis

Strains D39SM and D39P$cps_{T\rightarrow C}$ were compared to *S. pneumoniae* D39 by transcriptome analysis using whole-genome *S. pneumoniae* DNA microarrays, representing all TIGR4 ORFs, as well as R6 and D39 ORFs that are not in TIGR4 (Kloosterman *et al.*, 2006b). A complete description of amplicons and oligonucleotides is provided at http://www.ncbi.nlm.nih.gov/geo/query/acc.cgi?acc=GPL11484. Each strain was grown in triplicate in CDM containing 1% (wt/vol) Glc and with or without uracil as described above. Cells for RNA isolation were harvested in mid-exponential phase of growth (see time-points indicated by arrows in Fig. 3.2-A and Fig. 3.4-A). mRNA isolation, synthesis of cDNA and labelling of cDNA was performed as described in Chapter 6. All samples were hybridized in duplicate in the spotted DNA microarrays. Scanning

of the slides and the processing and analysis of the data was carried out as described in Chapter 6. Genes were considered to have significantly altered expression when the bayesian *p*-value was <0.0001 and the ratio (signal D39SM /signal D39 or signal D39P*cps*$_{T\rightarrow C}$ /signal D39) was >3 and <-3. An *in silico* comparison was done between conditions with and without uracil in both D39 wild-type as well as D39SM. To this end, raw signals (*i.e.* slide images) of the experiments with uracil were compared with the corresponding signals of the experiments without uracil and analyzed as described above. The microarray data will be deposited at GEO.

Quantification of the glucuronic acid content of capsular polysaccharide

Samples for the determination of the capsular glucuronic acid amounts were grown in CDM supplemented with 1% (wt/vol) Glc, with or without uracil, as described above, harvested during mid-exponential phases of growth (see time-points indicated by arrows in Fig. 3.2-A and 3.4-A) and treated as in Chapter 6. Capsule measurements were performed in duplicate using samples from two independent cultures.

Results

Isolation of a D39 mutant with underproducing capsule phenotype

Unexpectedly, streaking a single working stock of strain D39 on GM17-agar plates resulted in the appearance of two colony phenotypes. One colony type displayed the typical characteristics of the D39 Lilly isolate (Lanie *et al.*, 2007), *i.e.* large and opaque colonies. The other colony type, hereafter denominated D39SM (D39 spontaneous mutant), exhibited a substantially smaller

colony size and higher transparency than D39 (Fig. 3.1-A). The phenotype of D39SM colonies, resembling that of strain R6 (data not shown), could be due to a considerably lower growth rate or to a decreased capsule production (Kim and Weiser, 1998).

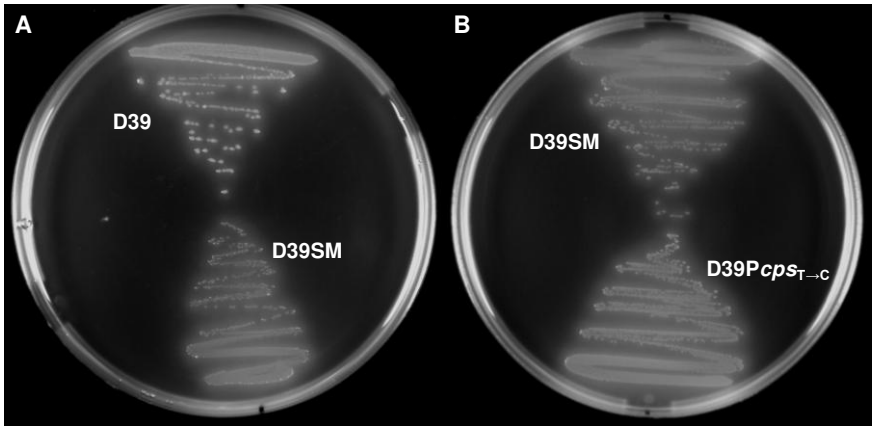

Fig. 3.1. Colony phenotype of D39 and derivative strains in Glc-M17 blood agar. Phenotypic appearance of D39 and D39SM (A) and D39SM and D39P*cps*$_{T\rightarrow C}$ (B) strains in Glc-M17 blood agar. Pictures of the plate were taken using the Molecular Imager® ChemiDoc™ XRS+ Imaging System (Bio-Rad) and the Quantity one software package.

A single colony isolate of the phenotypic variant was selected for further characterization. Both wild-type and D39SM strains were grown in CDM containing 1% (wt/vol) Glc, as described in Material and Methods, and the amount of capsule was determined in the mid-exponential phase of growth (D39, OD_{600} of 0.40 ± 0.00; D39SM, OD_{600} of 0.48 ± 0.02) (see time-points indicated by the arrows in Fig. 3.2-A). The maximal growth rate of strain D39SM was 1.4-fold lower than that of strain D39 (Fig. 3.2-A). Interestingly, this decrease in the growth

rate is in contrast with the 1.4-fold increase in the final biomass reached by D39SM strain relative to the parent strain (Fig. 3.2-A). Moreover, the amount of capsule in D39SM was 12.4-fold lower relative to D39 levels (Fig. 3.2-B).

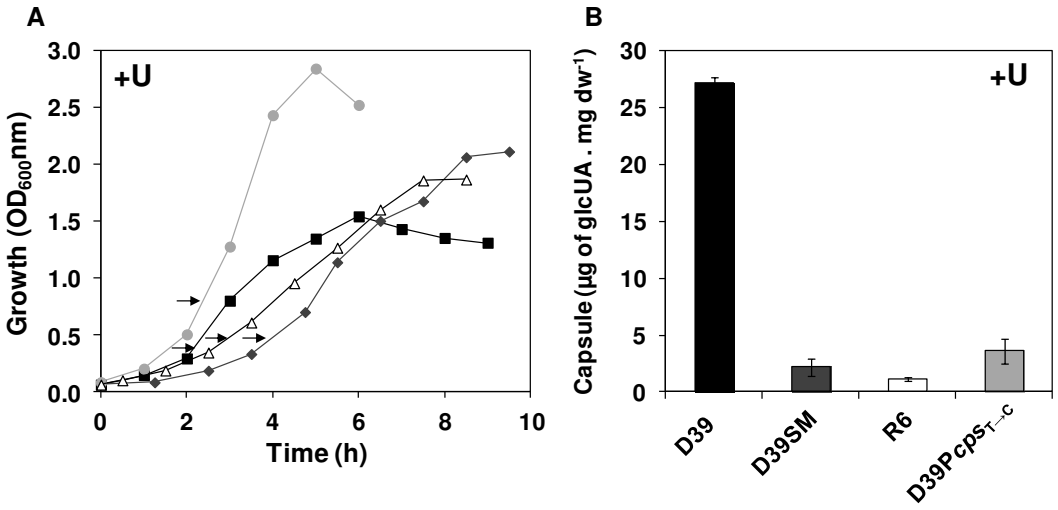

	Uracil (+U)
Strain	**μ_{max} (h^{-1})**
D39 (■)	0.82 ± 0.03
D39SM (◆)	0.57 ± 0.04
D39P*cps*$_{T\rightarrow C}$ (●)	0.86 ± 0.01
R6 (△)	0.68 ± 0.01

Fig. 3.2. Growth profile and capsule production in D39 and its derivative strains. (A) Growth of strains D39 (■), D39SM (◆), D39P*cps*$_{T\rightarrow C}$ (●) and R6 (△) in CDM with 1% (wt/vol) Glc, at 37ºC, without pH control (initial pH 6.5), in static rubber-stoppered bottles, after inoculation with precultures in late-exponential phase (OD_{600} 0.8-1.0). The arrows indicate time of sampling for measurement of capsule amounts and for transcriptome analysis. The growth rates for each strain are indicated in the table and the values shown are averages ± SD. For each growth at least three independent experiments were performed. The plotted growth curves are from a representative experiment and the error in each point was in all cases below 15%. (B) Estimation of capsule was performed based

on the determination of its glucuronic acid content in strains D39 (black bars), D39SM (dark grey bars), D39P*cps*$_{T\rightarrow C}$ (light grey bars) and R6 (white bars) in mid-exponential phases of growth. All the determinations were done twice in two independent cultures and the values are means ± SD. +U, with uracil.

Considering these data, the small colony and high transparency phenotype most likely reflects the substantial reduction in capsule amount, rather than the slight decrease in growth rate. Interestingly, the amounts of glucuronic acid (GlcUA) in D39SM were similar to those of R6, the non-encapsulated derivative of strain D39, showing that D39SM is almost or entirely devoid of capsule as well (Fig. 3.2-B).

Further analysis of the original culture from which D39SM was isolated revealed a frequency of D39SM colonies approximately 100-fold lower than that of the wild-type colonies. The scarce number of mutant colonies suggests that their appearance was an exceptional event that occurred exclusively during the preparation of this working stock. Supporting this notion, the only phenotype recovered upon growth of any other of our working stocks in Glc-M17 agar was that of the progenitor D39 strain.

A point mutation in D39 P*cps locus* leads to decreased capsule production

To explain the diminished capsule production in strain D39SM we hypothesized two possible scenarios: a deletion within the *cps* locus or point-mutations in the *cps* operon, particularly in the initial five genes *cps2A*-*E* and/or in the promoter region of the capsule cluster (P*cps*). A correlation between decreased *cps* expression and polymorphisms in the promoter of the *cps* gene cluster or in the *cps2A* gene in *S. pneumoniae* is not unprecedented (Moscoso and Garcia, 2009; Hanson *et al*., 2011; Yother, 2011). Sequencing of the *dexB*-

cps2A genomic region was performed and its analysis revealed a single point mutation in the -10 promoter region localized 30 nucleotides upstream of the starting codon of *cps2A*, and leading to the transition of the consensus sequence TATAAT to TATAAC (P*cps*$_{T\rightarrow C}$) (Fig. 3.3-A).

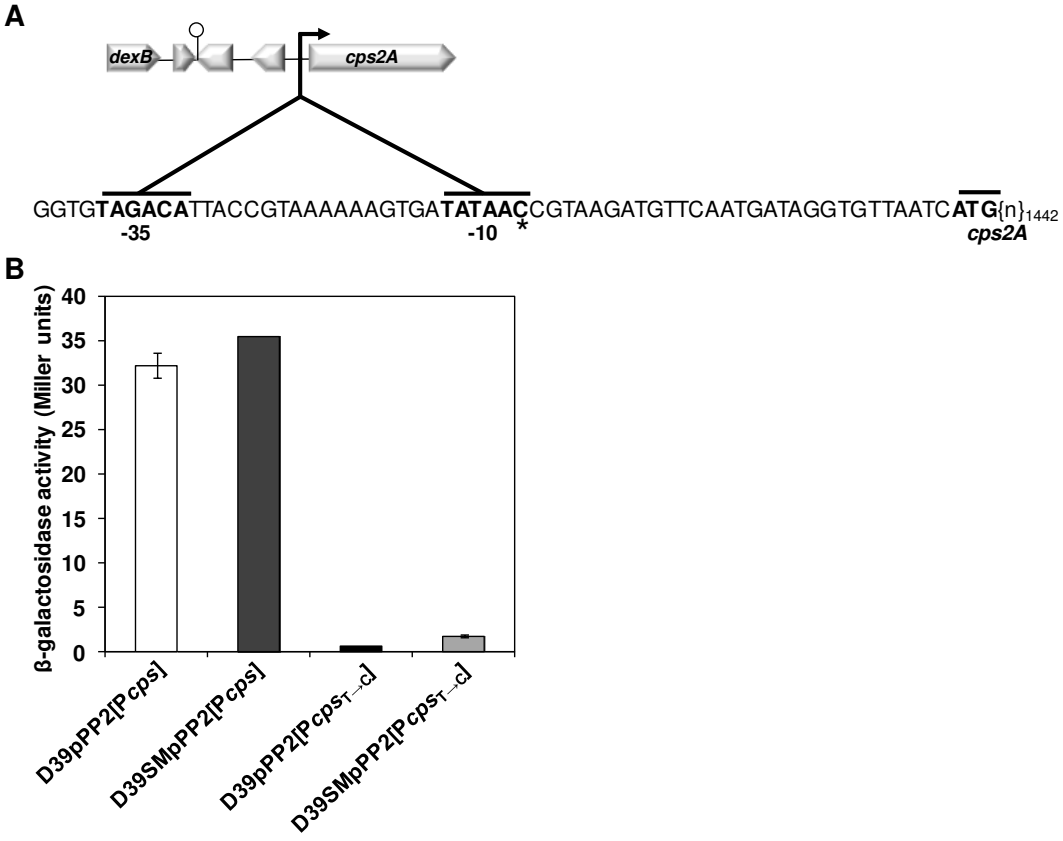

Fig. 3.3. Expression of P*cps* and P*cps*$_{T\rightarrow C}$ in *S. pneumoniae* D39 and D39SM. (A) Schematic overview of the *dexB-cps2A* region and magnification of the *cps* promoter area of D39SM. Hooked arrow, *cps* promoter; lollipop, putative terminator; zoomed area (inset), promoter region of the *cps* gene cluster; -35 and -10 binding box, and the starting codon of the *cps2A* gene are indicated in bold; the number of bp of the *cps2A* gene next to the starting codon is subscripted after {n}; *, point mutation (T→C) in -10 binding box of

D39SM strain. (B) Transcription of *cps* and $cps_{T\rightarrow C}$ promoters was estimated by measuring β-galactosidase activity in strains D39 (white and black bars) and D39SM (dark and light grey bars) carrying the pPP2 integrative *lacZ* reporter plasmid (see Table 3.1). Cultures were grown in CDM with 1% (wt/vol) Glc, at 37ºC, without pH control (initial pH 6.5), in static rubber-stoppered bottles, and samples for activity measurement were harvested in mid-exponential phase of growth (for details see Materials and Methods). All the determinations were done in duplicate in two independent experiments and the values are means ± SD. β-galactosidase activities are expressed as Miller units.

Interestingly, the same base substitution is present in the P*cps* of the non-encapsulated D39 derivative strain R6 (Lanie *et al*., 2007; Moscoso and Garcia, 2009). In addition, strain R6 harbors a large deletion (7.5 kbp) in the *cps* locus comprising genes *cps2A* to *cps2H*. Using PCR we verified that *cps2A* and the downstream *cps2B-D* genes are present in D39SM (data not shown), suggesting that the events leading to arousal of the two strains were distinct. To investigate whether the decreased capsule production was mediated at the transcriptional level by P$cps_{T\rightarrow C}$ mutation, the activity of *cps* and $cps_{T\rightarrow C}$ promoters was measured. Fusions of these promoters with the *lacZ* reporter gene were generated in the pPP2 plasmid (Halfmann *et al*., 2006) and introduced into D39 and D39SM backgrounds. The D39pPP2[P*cps*], D39pPP2[P$cps_{T\rightarrow C}$], D39SMpPP2[P*cps*] and D39SMpPP2[P$cps_{T\rightarrow C}$] strains generated in this way were grown in CDM containing 1% (wt/vol) Glc, harvested in exponential phase and β-galactosidase activities were determined. The activity of the $cps_{T\rightarrow C}$ promoter was decreased by 18-fold relative to the activity of the P*cps* in D39 and D39SM strains (Fig. 3.3-B). Even though data are only shown for mid-exponential phase of growth (Fig. 3.3-B), low promoter activity was observed throughout growth (data not shown). This suggests that the reduction in capsule production is caused solely by the P$cps_{T\rightarrow C}$ mutation. To strengthen our hypothesis, the

P*cps*$_{T\rightarrow C}$ point mutation was generated in the chromosome of strain D39 by using the pORI280 plasmid as described in Material and Methods. The amount of capsule in the D39P*cps*$_{T\rightarrow C}$ mutant, as estimated from the GlcUA method, was similar to that in D39SM and 8-fold lower than that of the parent strain D39 (Fig. 3.2-B). Furthermore, in Glc-M17 blood agar plates the morphology of D39P*cps*$_{T\rightarrow C}$ colonies totally resembled that of D39SM (Fig. 3.1-B). These data provides conclusive evidence that the P*cps*$_{T\rightarrow C}$ mutation is responsible for reduction of capsule synthesis. Differences in maximal growth rate and final biomass between strains D39P*cps*$_{T\rightarrow C}$ and D39SM (Fig. 3.2-A) are perhaps indicative of additional mutations in the latter strain. Moreover, the growth profile of strain D39SM, closer to that of strain R6, and altered relative to the progenitor strain D39 (Fig. 3.2-A), further supports the assumption of the occurrence of other mutations in D39SM. This possibility is currently being investigated by whole genome sequencing of strains D39SM and its progenitor D39.

Genomic changes in strain D39SM influence greatly the transcriptome

Clearly, strains D39SM and D39P*cps*$_{T\rightarrow C}$ presented disparate growth profiles, which were also distinct from that of the parent D39. Based on these results and considering the systemic character of growth we hypothesized distinct transcriptional responses in the spontaneous and engineered mutant. To investigate this assumption we performed whole-genome transcriptome analysis comparing mRNA levels in the mutant strains to those in strain D39. This type of approach proved useful in providing clues to genomic mutations in strain variants (Caymaris *et al.*, 2010; Linares *et al.*, 2010). Thus, we expected to obtain clues possibly leading to the identification of other mutations in D39SM. The D39P*cps*$_{T\rightarrow C}$ *versus* D39 transcriptional response was 5.8-fold lower than that of D39SM *versus* D39 (please see Table S.3.1 and Table S.3.2 provided in digital

format on the included CD), showing that the engineered strain was more similar to the parent than D39SM. This could imply a larger number of genomic differences between D39SM and D39 or the alteration of one major or several regulatory mechanisms. As expected from our targeted analysis, the *cps* genes (*spd_315-18, spd_321-2*) were strongly downregulated in the mutant strains.

In D39P*cps*$_{T\rightarrow C}$ the transcriptional response was modest and besides capsule repression, the most significant alterations were the upregulation of the *spd_0277-83* operon, coding for a 6-phospho-beta-glucosidase, a lactose-type PTS- transporter and a multidomain transcriptional regulator, presumably involved in the transport of beta-glucosides (Bidossi *et al.*, 2012), and the downregulation of three hypothetical proteins (*spd_0486*, *spd_2001*, *spd_2038*) and of the *spd_0514-6* operon, which includes an ABC transporter and two hypothetical proteins (Table S.3.2 on the CD).

The transcriptional response of strain D39SM affected about 5% of the whole genome, *i.e.* about 100 genes. Most of the genes (35 genes) showing altered expression belonged to the carbohydrate transport and metabolism category. In addition, many genes with unknown (7 genes) or unpredicted (21 genes) function, as well as a number of genes (9 genes) with general function prediction only, were among the differentially expressed genes (Table S.3.1, on the CD). Noteworthy, eight PTS uptake systems (*spd_0066-9*, *spd_0502*, *spd_0559-61*, *spd_0661*, *spd_1047-8*, *spd_1057*, *spd_1959* and *spd_1992-89*), and the enzymes involved in the metabolism of the PTS-incoming sugars (*spd_0063*, *spd_0065*, *spd_0070-1*, *spd_0503*, *spd_0562*, *spd_1046*, *spd_1958-7* and *spd_1995-4*) were all strongly induced in the mutant strain (Table S.3.1, on the CD). The *spd_0277-83* operon induced in the D39P*cps*$_{T\rightarrow C}$ mutant was, however, not among the upregulated genes in strain D39SM. The PTS transporters upregulated in D39SM are hypothetically involved in the uptake of

sugars (galactose, beta-glucosides, lactose, galactitol, maltose, tagatose, fucose, L-arabinose) other than glucose (Table S.3.1 on the CD) (Bidossi *et al.*, 2012). RegR, a global regulator of the family LacI/LacR, involved in carbohydrate metabolism, was upregulated in D39SM. In addition to the PTS transporters, the catabolic enzymes, and RegR, the altered expression of two other genes called our attention in strain D39SM. The first gene (*spd_0267*) encodes a permease that putatively transports xanthine/uracil and the second gene encodes a putative dihydroorotase (*pyrC*, *spd_1030*), which is known in other species to dehydrate carbamoyl aspartate (CAA) forming dihydroorotate (DHO) in the *de novo* pathway for pyrimidine synthesis (reviewed in Kilstrup *et al.*, 2005). *pyrC* is part of a transcriptional unit comprising two other genes, *ung* and *mutT*, also induced in the mutant strain, and encoding functions unrelated to the *de novo* synthesis of pyrimidines (Table S.3.1 on the CD). Dihydroorotate is an early precursor for the synthesis of UMP, which is subsequently converted to UTP via the salvage pathway for pyrimidine biosynthesis (reviewed in Kilstrup *et al.*, 2005). In Chapter 2 we showed that growth of *S. pneumoniae* D39 is limited by the nucleobase uracil. Since the unencapsulated strain R6 was rather insensitive to uracil and only marginally affected when the nucleobase was omitted from the cultivation medium, we speculated that the effects on D39 were related to capsule synthesis, a process that consumes UTP. In this context, the differential regulation of genes involved in the pyrimidine biosynthetic pathways, a putative uracil transporter and *pyrC*, in D39SM, a strain impaired in capsule synthesis, when uracil was present in the medium was intriguing. Furthermore, repression of the xanthine/uracil permease gene or induction of the *pyrC* gene was not observed in D39P*cps*$_{T\rightarrow C}$ strain, also deficient in capsule production.

Our genome-wide transcriptome analysis confirmed our hypothesis of larger transcriptional response in the spontaneous mutant as compared to that of

the strain with a single point-mutation. The altered expression of genes involved in pyrimidine biosynthetic pathways further reinforces the assumption of a tight connection between uracil metabolism and capsule production.

D39 mutants impaired in capsule production are largely unresponsive to the presence of uracil

Strains D39SM and D39P*cps*$_{T\rightarrow C}$ are "*quasi*" non-encapsulated (Fig. 3.2-B), and consequently should have a lower requirement for uracil/UTP as shown for strain R6 in Chapter 2. The influence of uracil on capsule production was evaluated by cultivating strains D39, D39SM and D39P*cps*$_{T\rightarrow C}$ in the absence of the nucleobase (Fig. 3.4) and comparing with the results obtained in complete medium (Fig. 3.2). In the absence of uracil, strains D39SM and D39P*cps*$_{T\rightarrow C}$ presented growth profiles and capsule amounts similar to those in medium with uracil (compare Fig. 3.4 with Fig. 3.2). In contrast, strain D39 was profoundly affected by the omission of uracil: growth was characterized by a lag of about 6 hours, a growth rate of 0.42 ± 0.01 h^{-1}, 2-fold lower than in medium containing uracil, and a maximal biomass 1.8 ± 0.0, which represented a 20% increase as compared to the standard conditions (uracil 10 mg l^{-1}) (Fig. 3.4-A). Furthermore, strain D39 exhibited a significant 22% decrease (unpaired *t*-test, P=0.0002) in capsule amount relative to that produced in medium containing uracil (Fig. 3.4-B). Our data show a subtle coupling between uracil metabolism, capsule production and growth of strain D39. In agreement, the growth dependency on uracil is lost in unencapsulated strains.

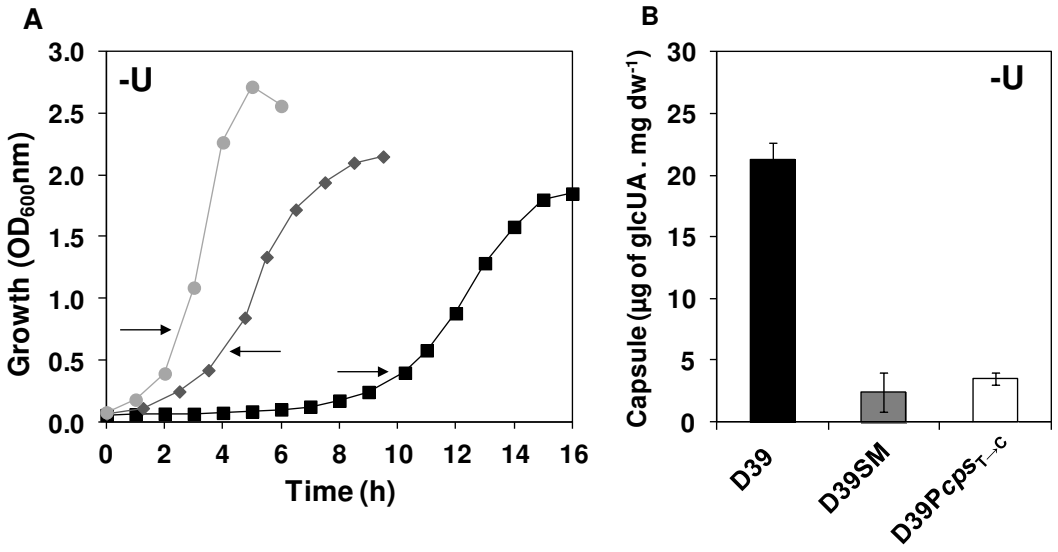

	No uracil (-U)
Strain	**μ_{max} (h^{-1})**
D39 (■)	0.42 ± 0.01
D39SM (◆)	0.59 ± 0.09
D39P$cps_{T\rightarrow C}$ (●)	0.85 ± 0.01

Fig. 3.4. Growth profile and amount of capsule in the absence of uracil. (A) Growth of strains D39 (■), D39SM (◆) and D39P$cps_{T\rightarrow C}$ (●) in CDM without uracil containing 1% (wt/vol) Glc, at 37ºC, without pH control (initial pH 6.5), in static rubber-stoppered bottles. Cultures were inoculated with late-exponential phase (OD_{600} 0.8-1.0) precultures suspended in fresh CDM without uracil. The arrows indicate time of sampling for measurement of capsule amounts and for transcriptome analysis. The growth rates for each strain are indicated in the table and the values shown are averages ± SD. For each growth at least three independent experiments were performed. The plotted growth curves are from a representative experiment and the error in each point was in all cases below 15%. (B) Estimation of capsule was performed based on the determination of its glucuronic acid content in strains D39 (black bars), D39SM (dark grey bars) and D39P$cps_{T\rightarrow C}$ (light grey bars) in mid-exponential phases of growth. All the determinations were done twice in two independent cultures and the values are means ± SD. –U, without uracil.

Uracil affects the transcriptome of strain D39

In other microorganisms the genes of the *de novo* synthesis of pyrimidines are exclusively induced in the absence of pyrimidines (O'Donovan and Neuhard, 1970; Potvin *et al*., 1975; Nicoloff *et al*., 2005; Kilstrup *et al*., 2005; Turnbough and Switzer, 2008). Therefore, the 5-fold induction of *pyrC* in D39SM in medium containing uracil was a complete surprise (Table S.3.1 on the CD). Intrigued by this effect we questioned to whether induction of the *pyrC* gene in strain D39SM would also occur in the absence of uracil. Therefore, we grew strains D39SM and D39 as in Fig. 3.4-A, and harvested samples at the time-points indicated by the arrows for transcriptome analysis (Fig. 3.4-A). In the absence of uracil, the D39SM *versus* D39 transcriptional response affected 4.2% of the whole genome (2069 genes). Of the genes showing altered transcript levels, 87% were common in medium with and without uracil, including *pyrC* (Table S.3.3 on the CD). This gene showed increased expression in D39SM, in a uracil-independent manner (Table S.3.1 and S.3.3 on the CD). Considering the low requirement of D39SM for uracil, the data suggest different or no regulation of *pyrC* by pyrimidines in D39SM. An *in silico* DNA microarray analysis comparing D39 grown in CDM with and without uracil revealed a strong derepression of genes involved in *de novo* synthesis of pyrimidines (*spd_0608-9* (*pyrFE*) and *spd_0851-2* (*pyrKDb*)) in the absence of uracil (Table S.3.4 on the CD); *pyrC* was not significantly changed. Consistent with activation of the genes of the *de novo* synthesis of pyrimidines, the gene encoding a putative PyrR regulatory protein (*spd_1134)*, an homologue of the lactococcal PyrR protein known to activate the expression of pyrimidine biosynthetic genes (reviewed in Kilstrup *et al*., 2005), was also upregulated in *S. pneumoniae* strain D39 when uracil was omitted (Table S.3.4 on the CD). Our *in silico* data are in good agreement with the accepted view for other *Streptococcaeae* (reviewed in Kilstrup *et al*., 2005).

The *in silico* DNA microarray analysis comparing D39SM grown in CDM with and without uracil showed no significant altered expression of genes (a cut-off of >3 or <-3 was used for the fold change and a Bayesian *p*-value ≤0.0001 to consider fold change statistically significant). Similarly, the absence of uracil did not induce major changes in the transcriptome profile of strain D39P$cps_{T\rightarrow C}$ when compared with its parent strain D39, exceptions being the operon *spd_1514-6* and gene *spd_0109* (Table S.3.5 compared to Table S.3.2 on the CD). Overall, these results show that uracil (or pyrimidines) has no major effect on the transcriptome of strains D39SM and D39P$cps_{T\rightarrow C}$, while inducing a considerable transcriptional response in the capsulated strain D39.

The activity of the *cps* promoter is lower in the absence of uracil

In strain D39 the amounts of capsule decreased in medium lacking uracil. To investigate whether this effect was mediated at the transcriptional level we measured the activity of the native and mutated *cps* promoters in cells grown without uracil (Fig. 3.5). Interestingly, in the absence of uracil the activity of the native *cps* promoter was 25% lower, a decrease similar to that observed for the reduction of capsule in strain D39 in uracil depleted conditions (Fig. 3.5). As expected, uracil had no effect on the activity of the $cps_{T\rightarrow C}$ promoter, independently of the strain genetic background (Fig. 3.5, compare with Fig. 3.3). In this light, the observed reduction in capsule production is controlled at the transcriptional level through modulation of the *cps* promoter activity by uracil or a product of its intracellular metabolism, such as UMP or UTP. In the capsulated strain D39, the UTP pool was higher in medium containing uracil (data not shown). The same pattern was observed for strain D39SM (data not shown), but since this variant produced little or no capsule, its requirements for UTP are lower, and thus growth is not affected.

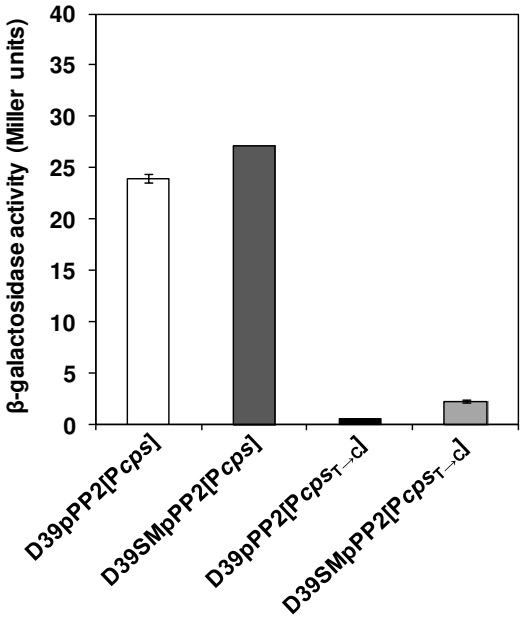

Fig. 3.5. Effect of uracil depletion on the expression of P*cps* and P*cps*$_{T\rightarrow C}$. Transcription of *cps* and *cps*$_{T\rightarrow C}$ promoters was estimated by measuring β-galactosidase activities of strains D39 (white and black bars) and D39SM (dark and light grey bars) carrying the pPP2 integrative *lacZ* reporter plasmid (see Table 3.1) in the exponential phase of growth. Cultures were grown in CDM without uracil with 1% (wt/vol) Glc, at 37ºC, without pH control (initial pH 6.5), in static rubber-stoppered bottles (for details see Materials and Methods). All the determinations were done in duplicate in two independent experiments and the values are means ± SD. β-galactosidase activities are expressed as Miller units.

In uracil-free medium D39SM performs better than the parent D39

Bacterial spontaneous mutations generally occur during adaptation to a stressful environment. In this context, it is likely that loss of the ability to produce capsule conferred the resulting phenotype with a competitive advantage. Considering the established interplay between uracil metabolism and capsule

production we surmised that the mutant strain would perform better in uracil-devoid environments. To verify our hypothesis D39SM and its parent D39 were grown in co-cultivation in medium with and without uracil (Fig. 3.6).

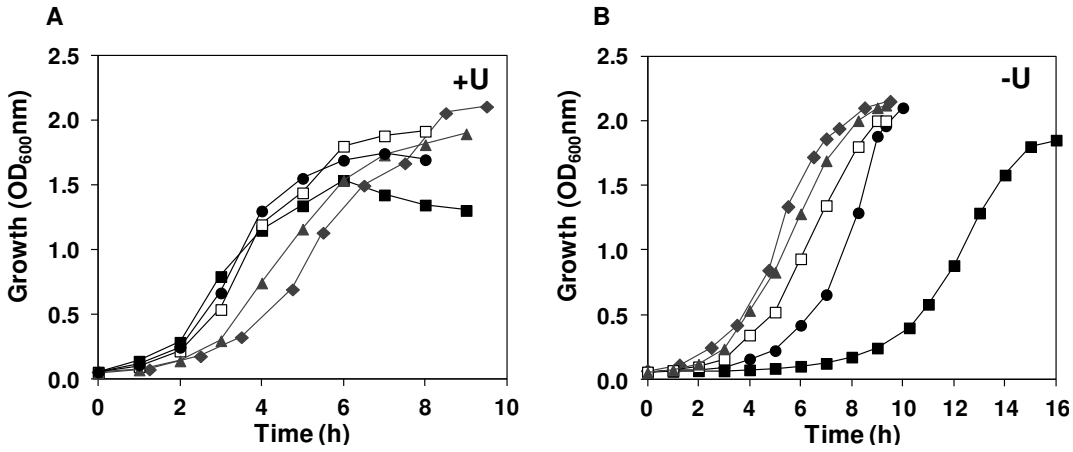

	Uracil (+U)	No uracil (-U)
D39:D39SM ratio	**μ_{max} (h^{-1})**	**μ_{max} (h^{-1})**
1:0 (■)	0.82±0.03	0.42±0.01
0:1 (◆)	0.57±0.04	0.59±0.09
1:1 (□)	0.79±0.00	0.53±0.01
1:4 (▲)	0.68±0.01	0.58±0.03
3.5:1 (●)	0.80±0.00	0.50±0.01

Fig. 3.6. Growth profiles of strains D39 wild-type and D39SM in co-cultivation. D39 and D39SM strains were inoculated at a cell ratio of 1:1 (□), 1:4 (▲), and 3.5:1 (●) in (A) CDM or (B) CDM without uracil, containing 1% (wt/vol) Glc, with precultures in late-exponential phase (OD_{600} 0.8-1.0) suspended in fresh CDM without uracil and grown at 37ºC, without pH control (initial pH 6.5), in static rubber-stoppered bottles. The growth rates of the co-cultures are presented in the table. The values are averages ± SD. For comparison the growth curves and growth rates of monocultures of D39 (■) and D39SM (◆) are also shown. For each condition at least three independent growth experiments were performed. The plotted growth curves are from a representative experiment and the error in each point was in all cases below 15%. +U, with uracil; -U, without uracil.

Strain abundance in the co-cultures was assessed by the CFU counts of samples harvested in mid-exponential phase of growth (Table 3.3 and Fig. 3.7). In medium containing uracil, in mid-exponential growth the most abundant species was the one predominating at the time of inoculation (Table 3.3 and Fig. 3.7-A and 3.7-B).

Table 3.3. D39 to D39SM ratios of viable cell counts (CFU ml^{-1}) in co-culture at the time of inoculation (T_0) and in mid-exponential phase of growth (T_MExp). Co-cultures of D39 wild-type and D39SM were grown as in Fig. 3.6 and plated as in Fig. 3.7.

D39:D39SM ratio	**Uracil (+U)**			**No uracil (-U)**		
T_0	0.94±0.19 (1/1)	0.28±0.04 (1/4)	4.09±0.38 (4/1)	0.99±0.42 (1/1)	0.23±0.03 (1/4)	2.83±0.25 (3/1)
T_MExp	1.34±0.45 (1/1)	0.43±0.11 (1/2)	4.87±0.39 (5/1)	0.09±0.02 (1/11)	0.04±0.01 (1/25)	0.40±0.12 (1/3)

Moreover, the dominant strain in the co-culture dictated to a great extent the growth profile of the mixture (Fig. 3.6-A). Curiously, a D39:D39SM ratio of 1 at the beginning of growth resulted in a very slight prevalence of strain D39 at mid-exponential phase (ratio D39:D39SM of 1.34, Table 3.3); the growth rate of the co-culture was more similar to that of D39, but the maximal biomass reached values similar to those achieved by D39SM (Fig. 3.6-A and Fig. 3.7-A and 3.7-B). A possible explanation resides on the ability of D39SM to grow well in the absence uracil, which at 10 mg l^{-1} is limiting for strain D39. Notably, in uracil-free medium at mid-exponential growth strain D39SM prevailed over D39, independently of the inoculation ratio (Table 3.3 and Fig. 3.7-C and 3.7-D). The predominance of strain D39SM in uracil-deprived medium resulted in maximal biomass of about 2.1 (OD_{Max}) in the different co-cultures, values similar to those reached by strain D39SM alone (Fig. 3.6-B). In uracil-free medium, the average

growth rate of the co-cultures also reflected the predominance of strain D39SM (Fig. 3.6).

Our data show that D39SM presents competitive fitness over strain D39 in uracil-free conditions. This advantage most likely derives from the low requirement of the mutant strain for uracil due to impairment in capsule production. In conclusion, our data indicate that in uracil poor media capsule production is a tremendous nutritional burden.

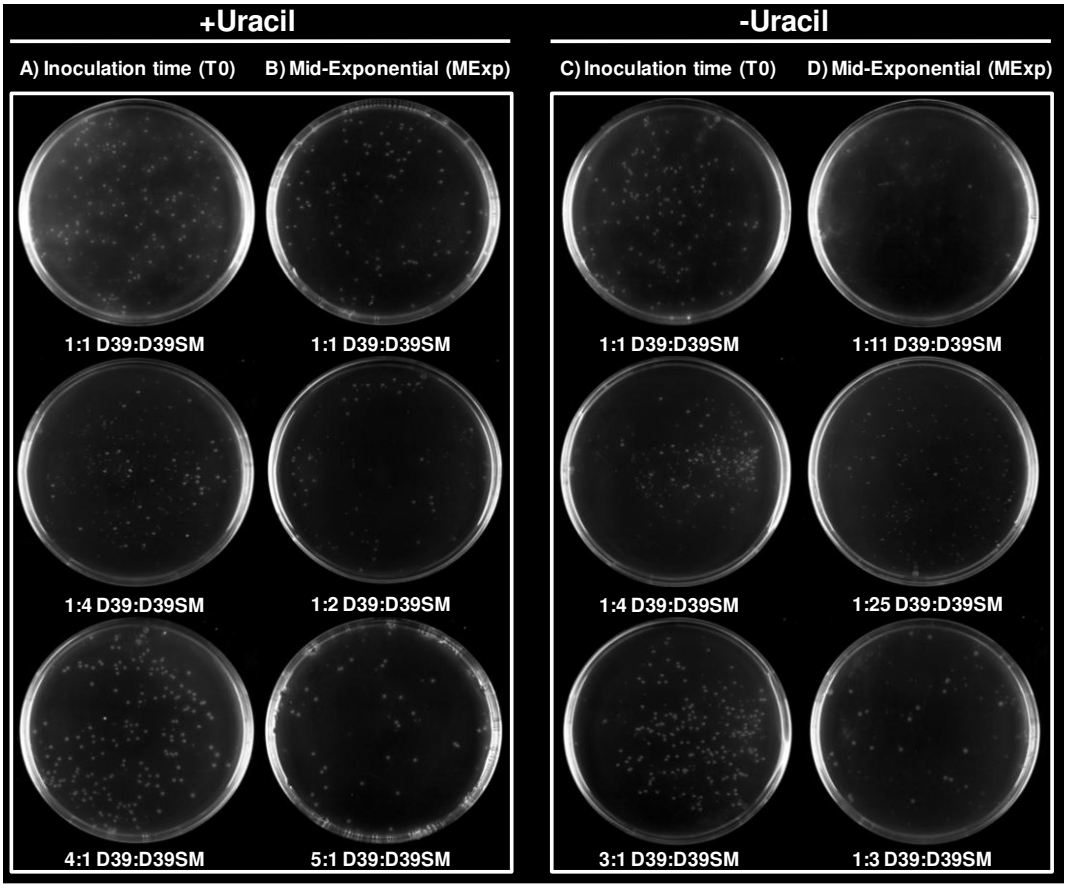

Fig. 3.7. Colony morphology in co-cultures of strains D39 and D39SM. D39 and D39SM colony-forming units formed from D39 and D39SM co-cultures, grown with uracil as in Fig. 3.6-A (A and B) or without uracil as in Fig. 3.6-B (C and D). Samples harvested at the time of inoculation (T0, A and C) or at the mid-exponential phase of growth (MExp, B and D) were streaked on Glc-M17 blood agar plates and incubated at 37ºC for 24 h in a CO_2 chamber. For the sake of clarity, D39:D39SM CFU ratios are also shown. Plating was performed in triplicate for each independent growth. The error in each count was always below 30%.

Discussion

Capsule is the major virulence factor of *S. pneumoniae,* and conditions affecting its synthesis are of great interest for the scientific community. Pneumococcal phase variants commonly isolated from the human host are, among other traits, differentiated by high and low capsule expression (reviewed in Weiser, 2010). Transparent variants show less capsule and are found predominantly in the nasopharynx, due to their ability to adhere. In contrast, the opaque phenotype prevails in the blood, an environment in which a thicker capsule is an absolute requirement to escape the immune system of the host. The involvement of oxygen in the regulation of the phase switch event has been postulated, however, the factors controlling capsule production remain at large unknown (Weiser *et al.*, 2001; Hammerschmidt *et al.*, 2005).

In Chapter 2, we proposed a link between pyrimidine metabolism and capsule biosynthesis in *S. pneumoniae* D39. In this Chapter, we show that uracil affects capsule promoter expression and capsule production in *S. pneumoniae* strain D39. Uracil is a pyrimidine nucleobase involved in the production of sugar-precursors for the synthesis of exopolysaccharides and peptidoglycan in lactic acid bacteria (De Vuyst and Degeest, 1999; Delcour *et al.*, 1999). In *S. pneumoniae* strain D39, formation of the activated sugar precursors, UDP-Glc, UDP-GlcUA, and dTDP-Rha, for capsule production, requires the pyrimidine nucleotides, UTP and dTTP. Generally, UTP is synthesized via the salvage pathway for pyrimidine biosynthesis, but it can as well be synthesized *de novo* from glutamine, aspartate and CO_2 (Fig. 3.8). The routes for pyrimidine biosynthesis in this bacterium are not biochemically characterized, but the complete salvage and *de novo* pathways can be deduced from genome information (http://www.ncbi.nlm.nih.gov/genomes/lproks.cgi) and database

surveys (KEGG, MetaCyc) (Fig. 3.8). Moreover, transporters for uracil are predicted in the genome sequence of strain D39 (Lanie *et al.*, 2007). In light of our results we propose that in *S. pneumoniae* strain D39 the operative pathway for pyrimidine biosynthesis in uracil-containing media is the salvage, whereas in the absence of uracil the *de novo* route is activated. In agreement is the long lag phase displayed by D39 in medium devoid of uracil that most likely reflects the time required for significant expression of the genes of *de novo* synthesis of pyrimidines (Fig. 3.8). This idea is further corroborated by the strong induction of the *de novo* pathway genes in medium without uracil. Induction of the pathways of *de novo* synthesis of pyrimidines in the absence of pyrimidines is not unprecedented (O'Donovan and Neuhard *et al.*, 1970; Potvin *et al.*, 1975; Nicoloff *et al.*, 2005; Kilstrup *et al.*, 2005; Turnbough and Switzer, 2008). The lower growth rate observed for strain D39 in uracil-free medium could derive from a less efficient *de novo* pyrimidine production.

We also hypothesized that capsule expression of strain D39 is influenced by the levels of intracellular pyrimidine(s). The lower UTP concentrations and capsule amounts determined for strain D39 in medium lacking uracil is in good agreement with this assumption. Changes in pyrimidine concentrations have been reported to affect polysaccharide expression in *E. coli* (Garavaglia *et al.*, 2012). Limitation of the *de novo* pyrimidine pathway by its own substrates (aspartate, glutamine and bicarbonate/CO_2) cannot be ruled out, but is improbable under our conditions: the initial concentrations of aspartate and glutamine in the growth medium are relatively high (*circa* 3 mM), thus depletion is not expected. Furthermore, the growth profile of strain D39 in CDM without uracil is not affected by addition of bicarbonate up to 50 mM (data not shown).

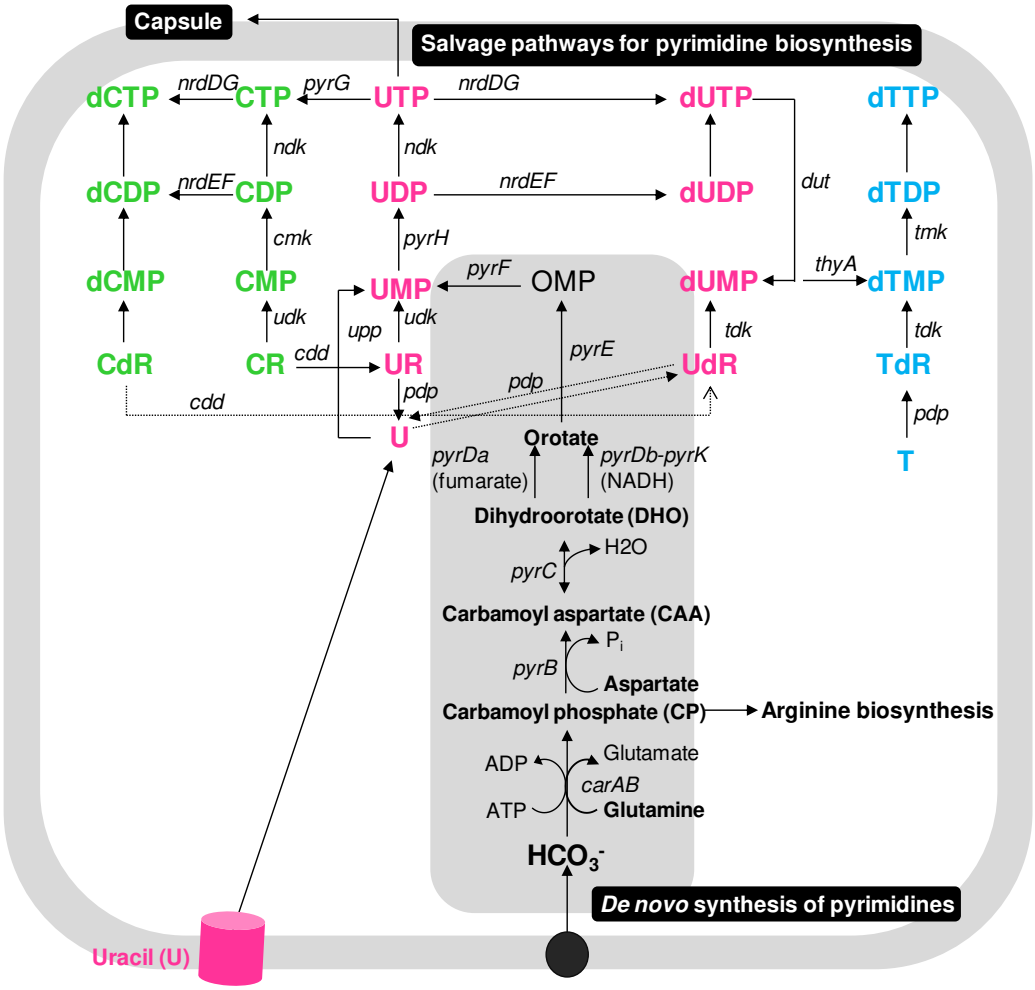

Fig. 3.8. Putative routes for the metabolism of pyrimidines in *S. pneumoniae*. The intracellular reactions depicted are catalyzed by the following enzymes (the genes that code for the enzymes are in parenthesis): carbamoyl-phosphate synthase, small and large subunit (*carAB*), aspartate carbamoyltransferase (*pyrB*), dihydroorotase (*pyrC*), dihydroorotate dehydrogenase A (*pyrDa*), dihydroorotate dehydrogenases (*pyrDb-pyrK*), orotate phosphoribosyltransferase (*pyrE*), orotidine 5-phosphate decarboxylase (*pyrF*), uridylate kinase (*pyrH*), pyrimidine-nucleoside phosphorylase (*pdp*), uridine kinase (*udk*), cytidine deaminase (*cdd*), uracil phosphoribosyltransferase (*upp*), cytidylate kinase (*cmk*),

nucleoside-diphosphate kinase (*ndk*), ribonucleoside-diphosphate reductases, alpha and beta subunits (*nrdEF*), ribonucleoside-triphosphate reductases (*nrdDG*), CTP synthase (*pyrG*), deoxyuridine 5'-triphosphate nucleotidodehydrolase (*dut*), thymidine kinase (*tdk*), thymidylate synthase (*thyA*), thymidylate kinase (*tmk*).

In the absence of uracil, D39 produces less capsule, but more biomass. Even though a full explanation cannot be put forward, we can speculate that the coupling between uracil metabolism and capsule production is somewhat lost in the absence of external uracil. Very recently capsule was indicated as an enormous energetic burden, and its production was suggested to compete directly with central metabolism for energy (Hathaway *et al.*, 2012). In this light, in uracil-free medium the lower production of capsule is accompanied by a lesser energy demand, and consequently the energy surplus can be redirected for growth and cell division. This energy can be in the form of ATP, but also UTP, as herein we demonstrate that capsule is also a nutritional burden that imposes a high demand for uracil to support fast growth.

We have shown that a point mutation in the -10 box of the *cps* promoter region is responsible for the remarkable decrease in promoter activity leading to reduced capsule production in strain D39. This point mutation was identified in the D39 spontaneous mutant, D39SM, exhibiting phenotypic characteristics of a transparent phase variant. Unexpectedly, this mutant arose in a rich/complex medium from D39 opaque colonies. Even though a chronology of the events leading to the mutant is available, a mechanistic explanation is difficult to put forward. This view is exacerbated by the considerable transcriptional changes (about 5% of genome) in the mutant when compared to its parent D39. The desensitization to uracil of the mutant strain and the differential expression of genes involved in its metabolism could indicate a batch-specific deficiency of the

nucleobase in the M17 powder used. However, a deficiency of other components, such as sugars, cannot be discarded. Importantly, reconstitution of the *cps* promoter single mutation in D39 rendered a strain D39P$cps_{T\rightarrow C}$ phenotipically different from D39SM, except for the deficiency in capsule synthesis. These findings strongly point towards the occurrence of additional mutations in strain D39SM. Comparative transcript levels analysis of D39SM *versus* D39 and D39P$cps_{T\rightarrow C}$ *versus* D39 further supports our assumption. To establish additional genomic differences, genomes of strain D39SM and its parent D39 are currently being sequenced.

A number of carbohydrate PTS transporters and associated sugar catabolic enzymes were induced in the mutant strain as compared to the parent D39 in the microarray analysis. In several Gram-positive microorganisms, including *S. pneumoniae*, CcpA is a global regulator of carbon metabolism affecting a high number of sugar transporters and catabolic enzymes (Chapter 6) (Abranches *et al.*, 2008; Shelburne *et al.*, 2008b; Singh *et al.*, 2008). In our conditions, *ccpA* was not altered. On the other hand, the gene encoding RegR, a regulator of the LacI/LacR, was strongly induced in the mutant strain. It is tempting to suggest the involvement of RegR in the regulation of the PTS transporters and sugar-specific enzymes. It should be noted however, that the role of RegR in the metabolism of sugars has been minimized (Chapuy-Regaud *et al.*, 2003).

The differential expression of genes involved in the metabolism of pyrimidines in the spontaneous mutant D39SM was a positive surprise. In Chapter 2 we inferred a connection between capsule synthesis and demand for uracil. In this work, we identified a mutant deficient in capsule production that shows downregulation of a putative uracil transporter (*spd_0267*) and upregulation of *pyrC* (*spd_1030*) (Fig. 3.8). In *S. pneumoniae*, *pyrC* is in an

operon containing two other genes, *spd_1032* (*ung*, uracil DNA-glycosylase) and *spd_1031* (mutT protein), encoding functions involved in DNA repair and trapping/removing of uracil residues from dUTP precursors during replication (Chen and Lacks, 1991). The transcriptome analysis might shed some light on the event leading to the spontaneous generation of strain D39SM. A plausible explanation could entail the induction of the *ung-mutT-pyrC* operon by a stressful condition, followed by changed pyrimidine availability, which would ultimately lead to a suppressor *cps* promoter mutation. In accordance, the spontaneous mutant D39SM exhibited lower accumulation of UTP pools (data not shown) and uracil showed no effect on growth and capsule expression and production of this strain. The *cps* promoter point mutation and thus, the underproducing capsule phenotype, should improve the bacterium fitness under a particular stressful condition. We showed that the underproducing capsule phenotype confers a competitive advantage to strain D39SM when co-cultivated with its parent D39 in uracil-free medium. In this light, in host niches poor in uracil a predominance of transparent phenotypes could be expected, suggesting that uracil would provide a selective pressure. Pyrimidine bases and nucleosides are often unavailable as exogenous nutrients, which most likely explain the conservation of the genes of the *de novo* pathways for pyrimidine biosynthesis in extracellular microorganisms (reviewed in Turnbough and Switzer, 2008). Curiously, pyrimidines, in particular uridine, were detected in blood, where capsule is an absolute requirement for the survival of *S. pneumoniae*. In healthy men, the homeostatic concentration of uridine is about 3-4 µmol l^{-1} (Simmonds and Harkness, 1981). This concentration is substantially lower than the standard initial uracil concentration in our medium (89 µmol l^{-1}). However, it might not be limiting for growth since in the blood the uridine is *quasi* constantly available. Replacement of uracil by uridine showed no effect on batch cultures of strains D39 and D39SM (data not shown).

In this work, we ascertained that expression of the capsule operon and production of the polysaccharide in *S. pneumoniae* is altered in response to uracil. A subtle interplay between uracil metabolism, the pathways for pyrimidine synthesis and the production of capsule is unveiled. In light of our results, we propose that the sensing of pyrimidines by *S. pneumoniae* triggers changes in capsule production. Exploring the mechanisms integrating pyrimidine metabolism and capsule synthesis will certainly contribute to an improved understanding of the regulatory phenomena underlying the control of capsule synthesis, and ultimately virulence in the human pathogen *S. pneumoniae*.

Acknowledgements

SM Carvalho helds a fellowship SFRH/BD/35947/2007 from Fundação para a Ciência e a Tecnologia (FCT). This work was funded by FCT and FEDER, projects PTDC/BIA-MIC/099963/2008 and PTDC/SAU-MII/100964/2008 and through grant PEst-OE/EQB/LA0004/2011.

Author's Contribution

Performed the experiments: SM Carvalho and T Kloosterman. mRNA isolation and microarray experiments, construction of PP2 derivative plasmids and of strain D39P*cps*$_{T\rightarrow C}$, and β-galactosidase assays were performed by T Kloosterman. Conceived and designed the experiments: SM Carvalho, T Kloosterman and AR Neves. Analyzed the data: SM Carvalho, T Kloosterman, Jan Martinussen, J Caldas, S Vinga, OP kuipers and AR Neves. J. Martinussen is acknowledged for supervising SM Carvalho during a stay at DTU, Lyngby, Denmark, and for the determination of pyrimidine nucleotides. We thank J Caldas and S Vinga for microarray analysis.

Chapter 4

Pyruvate oxidase influences the sugar utilization pattern and capsule production in *Streptococcus pneumoniae*

Part of the results of this chapter will be submitted for publication:
SM Carvalho, VF Andisi, H Gradsted, OP Kuipers, AR Neves, JJE Bijlsma (2012) "Pyruvate oxidase influences the sugar utilization pattern and capsule production in *Streptococcus pneumoniae*". To be submitted.

Chapter 4 – Contents

Summary

Pyruvate oxidase is a key function in the metabolism and lifestyle of many lactic acid bacteria and its activity depends on the presence of environmental oxygen. In *S. pneumoniae* the protein has been suggested to play a major role in metabolism and has been implicated in virulence, oxidative stress survival and death in stationary phase. Under semi-aerobic conditions, transcriptomic and metabolite profiling analysis of a *spxB* mutant showed minor changes compared to the wild-type, indicating that the role of the enzyme in metabolism is most likely milieu-dependent. More importantly, we show that mutation of *spxB* results in the production of increased amounts of capsule, the major virulence factor of *S. pneumoniae*. Part of this increase might be due to induction of *cps2A* transcription. Additionally, mutation of *spxB* results in an increase of the expression of two putative operons involved in carbohydrate uptake and processing. A combination of metabolic analysis and growth experiments showed that this increase leads to a change in the sugar utilization capabilities of the bacterium. Therefore, we propose that *S. pneumoniae* utilizes pyruvate oxidase as an indirect sensor of the oxygenation of the environment, resulting in the adaption of its nutritional capability and the amount of capsule to survive in the host.

Introduction

Streptococcus pneumoniae is an important human pathogen as it is a common cause of respiratory pathologies and serious invasive diseases such as pneumonia, sepsis and meningitis; especially infants, the elderly and immuno-compromised individuals are at risk. Annually, over 1 million children die of pneumonia and meningitis and in the US alone 40.000 deaths each year are caused by pneumococcal pneumonia or meningitis (Obaro and Adegbola, 2002). Capsule, an extracellular structure of polysaccharide nature attached to the cell wall, is one of the main virulence factors of *S. pneumoniae*; its main purpose is to inhibit complement-mediated opsonophagocytosis and acapsular mutants are avirulent (Paton *et al.*, 1993; Hardy *et al.*, 2001; Magee and Yother, 2001). The composition of the capsule varies from strain to strain and up to 93 different capsular serotypes have been identified (Song *et al.*, 2012). Capsular polysaccharide synthesis is intimately connected with central carbon metabolism as it requires activated carbohydrates; a number of these NDP-sugars derive from the glycolytic intermediates glucose 6-phosphate and fructose 6-phosphate (Iannelli *et al.*, 1999; Hardy *et al.*, 2000; Bentley *et al.*, 2006). A direct correlation between capsule thickness and virulence has been reported (Magee and Yother, 2001; Morona *et al.*, 2004). The amount of capsule varies throughout infection and decreases dramatically in the proximity of, and while invading, eukaryotic cells (Ogunniyi *et al.*, 2002; Hammerschmidt *et al.*, 2005). In addition, *S. pneumoniae* displays at least two phenotypic variants, transparent and opaque, that are to a large extent determined by the quantity of capsule and have differences in virulence properties (Kim and Weiser, 1998; Kim *et al.*, 1999). Transparent pneumococci are more efficient colonizers of the nasopharynx, produce less capsule, but more cell-wall associated teichoic acids than opaque

variants (Kim and Weiser, 1998; Kim *et al.*, 1999; Nelson *et al.*, 2007). Additionally, the two variants show differential production of various proteins, one of which is the pneumococcal pyruvate oxidase enzyme SpxB (Overweg *et al.*, 2000). However, the factors determining the occurrence of phase variation and the regulation of the amount of capsule are still not entirely clear, nor the connections that exist between central carbon metabolism and capsule production.

SpxB is reported to play a central role in fermentation and in particular in the generation of the phosphoryl donor metabolite acetyl-phosphate (Ac-P) (Spellerberg *et al.*, 1996). The enzyme decarboxylates pyruvate into Ac-P by reducing oxygen (O_2) to hydrogen peroxide (H_2O_2) and consuming inorganic phosphate (P_i). SpxB activity in *S. pneumoniae* might produce H_2O_2 in the mM range (Spellerberg *et al.*, 1996; Pericone *et al.*, 2002), concentrations higher than those generated by many other species (Pericone *et al.*, 2002; Pericone *et al.*, 2003), and sufficient to kill or inhibit other nasopharyngeal flora members, such as *H. influenzae* and *N. meningitidis* (Pericone *et al.*, 2000). Furthermore, these amounts have cytotoxic effects on human cells (Duane *et al.*, 1993; Hirst *et al.*, 2000; Braun *et al.*, 2002). The *spxB* gene has also been designated as a suicide gene since the H_2O_2 induces pneumococcal death and reduces survival in stationary phase in the presence of oxygen (Regev-Yochay *et al.*, 2007). In addition, the H_2O_2 produced endogenously influences the membrane composition through modulation of fatty-acid biosynthesis F (FabF) protein activity (Pesakhov *et al.*, 2007; Benisty *et al.*, 2010). Interestingly, and despite the potential deleterious effect of its product, SpxB has also been associated with streptococcal resistance to H_2O_2 (Pericone *et al.*, 2003). Besides its function in central metabolism, a prominent role of SpxB in the virulence of the bacterium, especially in colonization and pneumonia, is corroborated by a number of studies

(Spellerberg *et al.*, 1996; Orihuela *et al.*, 2004b; Regev-Yochay *et al.*, 2007; Ramos-Montañez *et al.*, 2008). Here, we studied the role of SpxB under semi-aerobic conditions as this is likely to reflect the atmospheric conditions encountered by *S. pneumoniae* in the deeper layers of the mucus, close to the epithelial cells. We describe that the inactivation of *spxB* results in the overproduction of capsule under semi-aerobic conditions, which is partially mediated by increased transcription of the capsule *locus*. Furthermore, we characterized the transcriptomic and metabolic consequences of *spxB* inactivation, which consist of a change in sugar utilization capacities and hypothesize that these effects also contribute to its role in virulence.

Materials and Methods

Bacterial strains and growth conditions

Strains used in this study are listed in Table 4.1 and were stored in glycerol at -80ºC. *S. pneumoniae* was routinely grown as standing cultures in M17 broth (Oxoid) containing 0.5% (wt/vol) Glc (Glc-M17) at 37ºC. *L. lactis* NZ9000 was grown in the same medium at 30ºC and *E. coli* was grown in LB broth in shaken cultures at 37ºC. Chloramphenicol and erythromycin were used at concentrations of 2.5 and 0.25 µg ml^{-1} for *S. pneumoniae* and 5 and 4 µg ml^{-1} for *L. lactis*. Trimethoprim was used at a concentration of 15 µg ml^{-1}, and ampicillin was used at 100 µg ml^{-1} for *E. coli*. For *S. pneumoniae* growth on plates, 3% (vol/vol) defibrinated sheep blood (Johnny Rottier, Kloosterzande, the Netherlands) was added to Glc-M17 agar.

Table 4.1. Strains and plasmids used in this study

Strains/Plasmid	Description	Reference/Source
S. pneumoniae		
D39	Serotype 2 strain	Avery *et al.*, 1944
TIGR4	Serotype 4 strain	Tettelin *et al.*, 2001
D39 pGh9 T7	D39 *spxB::* pGh9:ISS1T7; Em^R	This study
TIGR4 pGh9 T7	TIGR4 *spxB::* pGh9:ISS1T7; Em^R	This study
D39*spxB*$^-$	D39 *spxB*::ISS1	This study
D39*nisRK*	D39 Δ*bgaA*::*nisRK*; Tm^R	Kloosterman *et al.*, 2006a
D39*nisRK*pNZ8048	D39 Δ*bgaA*::*nisRK* harbouring pNZ8048; Tm^R, Cm^R	Neef *et al.*, 2011
D39*nisRKspxB*$^-$	D39 Δ*bgaA*::*nisRK spxB*::ISS1; Tm^R	This study
D39*nisRKspxB*$^-$pNZ8048	D39 Δ*bgaA*::*nisRK spxB*::ISS1 harbouring pNZ8048; Tm^R, Cm^R	This study
D39*nisRK*pNZ *spd_0637*	D39 Δ*bgaA*::*nisRK* harbouring pNZ *spd_0637*; Tm^R, Cm^R	This study
D39*nisRKspxB*$^-$pNZ *spd_0637*	D39 Δ*bgaA*::*nisRK spxB*::ISS1 harbouring pNZ *spd_0637*; Tm^R, Cm^R	This study
D39pORI P*cps2A*	D39 harbouring pORI P*cps2A-lacZ*; Em^R	Kloosterman *et al.*, 2006a
D39pORI P*cps2A spxB*$^-$	D39 *spxB*::ISS1 harbouring pORI[P*cpsA-lacZ*]; Em^R	This study
L. lactis		
NZ9000	MG1363 Δ*pepN*::*nisRK*	Kuipers *et al.*, 1998
Plasmids		
pGh9:ISS1T7	Insertion mutagenesis plasmid with T7 RNA polymerase promoter	Bijlsma *et al.*, 2007
pNZ8048	Nisin-inducible P*nisA*; Cm^R	de Ruyter *et al.*, 1996
pNZ *spd_0637*	pNZ8048 carrying *spd_0637* under nisin-inducible P*nisA*; Cm^R	This study
pORI13	*ori*$^+$ *repA*$^-$; promoterless *lacZ*; Em^R	Sanders *et al.*, 1998
pORI P*cps2A*	pORI13 carrying *cps2A* promoter in front of the promoterless *lacZ* ; Em^R	Kloosterman *et al.*, 2006a

Abbreviations: Em^R, erythromycin resistance; Tm^R, trimethoprim resistance; Tet^R, tetracycline resistance; Cm^R, chloramphenicol resistance; Amp^R, ampicillin resistance.

Generation of mutants in *S. pneumoniae*

S. pneumoniae D39 was transformed with pGh9 T7 as described before (Bijlsma *et al.*, 2007). To excise the plasmid from the genome of *S. pneumoniae*, which leaves behind one copy of the ISS1 element (Maguin *et al.*, 1996), the strain containing the pGh9 T7 plasmid was grown overnight at 28ºC after which serial dilutions were plated on Glc-M17 agar without antibiotics. Erythromycin sensitive colonies were selected for further study. The site of insertion into the genome was determined using a PCR based method as described in Karlyshev *et al.* (2000).

Transmission electron microscopy of *S. pneumoniae*

Aliquots of *S. pneumoniae* were quickly thawed at 37ºC and diluted 1:40 in Glc-M17 and grown under semi-aerobic conditions at 37ºC. Bacteria were harvested by centrifugation for 10 minutes at 3000 x *g* at 4ºC and subsequently stained with lysine ruthenium red (LRR) and treated as described before (Hammerschmidt *et al.*, 2005). For visualization a Philips EM201 (maximum resolution of ~ 0.5 nm) electron microscope was used.

Construction of a pNZ8048 derivative that expresses *spd_0637*

A pNZ8048 derivative containing the *spd_0637* gene under the control of a nisin inducible promoter was constructed. The gene was amplified from the chromosome of D39 using the primers pair Spd0637.fw (CATGCCATGGATGAATTTAAATCAATTAGATATTATCG) and Spd0637.rev (CTAGTCTAGACTATTTCATACGATAAAAATCAAGC) that contained an NcoI and XbaI site, respectively. The resulting 350-bp PCR fragment was cloned into the pNZ8048 plasmid using NcoI and XbaI, transformed into *L. lactis* NZ9000, sequenced and transferred to the D39*nisRK* and D39*nisRKspxB*$^{-}$ strains.

Determination of transcription using *lacZ*

To measure transcription of the *cpsA* gene, a pORI13 derivative containing the D39 *cpsA* promoter was used in the D39 and D39*spxB*$^-$ backgrounds (Kloosterman *et al.*, 2006a). Strains were grown standing in CDM containing 1% Glc and harvested at mid-exponential (~OD_{600} 0.2) or late-exponential (~OD_{600} 0.4) phase. Activity of the *cps2A* promoter was assayed by measuring β-galactosidase activity as described before (Kloosterman *et al.*, 2006a).

Transcriptome analysis

For DNA microarray analysis, D39 wild-type and two independently obtained D39*spxB*$^-$ mutants were grown as four, two and two biological replicates, respectively, in Glc-M17 under semi-aerobic conditions and harvested at an OD_{595} of approximately 0.25. The RNA of both D39*spxB*$^-$ strains was compared to D39 and the combined data was analyzed. All other procedures regarding microarray analyses were done as described before (Neef *et al.*, 2011). A gene was considered differentially expressed when the fold change was ≥ 2, ≤ 0.5, with a Bayes $p \leq 0.00001$ and when at least 7 measurements were available. The microarray data is now being submitted to the GEO database.

Growth conditions for metabolic analysis

Cells were grown at 37ºC in static rubber-stoppered bottles (500-ml) in complex medium M17 (Difco^{TM}), supplemented with Glc 1% (wt/vol) and without pH control (initial pH 6.5). Prior to inoculation sterile air was bubbled through the medium for 20 min. Alternatively cells were grown in 2-l bioreactors in the CDM described in Chapter 2 with the pH controlled at 6.5, and under initial specific air tension of 50-60% (semi-aerobic, maximum dissolved O_2 concentration of 130

µM) or aerobic (continuous specific air tension of 40%, constant dissolved oxygen concentration of 90 µM) conditions. In the bioreactors, dissolved oxygen was monitored with a polarographic oxygen electrode (Mettler-Toledo International). The electrode was calibrated to zero or 100% by bubbling sterile argon or air through the medium, respectively. A specific air tension of 40% was maintained by automatic control of the airflow and agitation. Irrespectively of the growth conditions, Glc (1% wt/vol) was used as carbon source. Cultures were inoculated to an initial optical density at 600 nm (OD_{600}) of 0.05 with cells growing exponentially in the same medium. Growth was monitored by measuring the OD_{600}. Specific growth rates (μ) were calculated through linear regressions of the plots of $\ln(OD_{600})$ *versus* time during the exponential growth phase. A factor of 0.39, determined from a DW (mg ml^{-1}) *versus* OD_{600} curve, was used to convert OD_{600} into dry weight (mg biomass ml^{-1}).

Quantification of fermentation products during growth on glucose

Strains were grown in Glc-M17 or Glc-CDM as described above. Culture samples (2 ml) were taken at different time-points of the growth curves, centrifuged (16,000 × *g*, 2 min, 4ºC), filtered (Millex-GN 0.22 µm filters), and the supernatant solutions were stored at 20ºC until analysis by high performance liquid chromatography (HPLC). Substrates and end-products were quantified in an HPLC apparatus equipped with a refractive index detector (Shodex RI-101, Showa Denko K. K., Japan) using an HPX-87H anion exchange column (Bio-Rad Laboratories Inc., California, USA) at 60ºC, with 5 mM H_2SO_4 as the elution fluid and a flow rate of 0.5 ml min^1. Alternatively, quantification of metabolites in supernatants was performed by ^{1}H-NMR in a Bruker AMX300 spectrometer (Bruker BioSpin GmbH). Formic acid (sodium salt) was added to the samples and used as an internal concentration standard. The ATP yield was calculated as the

ratio of ATP produced to glucose consumed. The global yields of ATP were calculated from the fermentation products determined at the time-point of growth arrest assuming that all ATP was synthesized by substrate-level phosphorylation.

Determination of hydrogen peroxide (H_2O_2)

Strains were grown in Glc-CDM as described above. Culture samples of 1-ml were harvested at different time-points of the growth curves, centrifuged (16,000 × *g*, 2 min, 4ºC) and filtered (Millex-GN 0.22 µm filters). The Amplex® Red Hydrogen Peroxide/Peroxidase assay kit (Invitrogen) was used to quantify hydrogen peroxide contents below 10 µM. Determinations of H_2O_2 up to 300 µM were performed as described elsewhere (Meiattini, 1988). Briefly, 1.25 ml of peroxide reagent (192 mM phosphate, 14.8 mM azide, 0.96 ml l^{-1} Triton X-100, 2 KU l^{-1} horseradish peroxidase (Roche), 0.48 mM 4-aminophenazone and 9.6 mM chromotropic acid) was added to 50 µl of supernatant, mixed and allowed to stand for 5 minutes at room temperature. In the presence of H_2O_2, the chromotropic acid was converted by the peroxidase into a blue coloured compound with maximal absorbance at 600 nm. Absorbance was read at 600 nm. Water was used as the blank and standard curves were performed with fresh dilutions of a stabilized solution of 30% (wt/vol) H_2O_2. The absorbance of the samples was compared to that of the standard solutions.

Determination of intracellular metabolites during growth on glucose

Strains were grown in Glc-CDM under semi-aerobic as described above. Ethanol extracts for analysis by ^{31}P-NMR and quantification of phosphorylated metabolites in D39*spxB*$^-$ and control strain D39 at late-exponential (LExp) and early-stationary (EStat) phases of growth (time-points indicated by the arrows in Fig. 4.4-B) were prepared as described in Chapter 6. In brief, a volume of culture

was withdrawn from the fermentor, adjusted to obtain approximately 16-18 mg of cell protein for extract, and centrifuged (21,000 x *g*, 15 min, 4ºC). The pellet was suspended in 28 ml of 5 mM 3-(N-morpholino) propanesulfonic acid (MOPS) buffer, pH 7.2 (Sigma-Aldrich), transferred to 70 ml of cold ethanol (final concentration 70% vol/vol) in an ice bath, and extraction was performed for 30 min with vigorous agitation. Cell debris was removed by centrifugation (35,000 x *g*, 30 min, 4°C), the ethanol was evaporated and the residue lyophilized. The dried extracts were dissolved in 1 ml $^{2}H_2O$ containing 5 mM EDTA (final pH approximately 6.5) and stored at -20ºC. Assignment of resonances was based on previous studies (Ramos *et al.*, 2001; Neves *et al.*, 2006), work presented in Chapter 6 or by spiking the sample extracts with the suspected, pure compounds. The concentrations of intracellular metabolites were calculated from the areas of their resonances in ^{31}P-spectra by comparison with the area of the resonance due to methylphosphonic acid (Sigma-Aldrich), added as an internal standard, and after application of an appropriate factor for correcting saturation of resonances. The reported values for intracellular phosphorylated compounds are averages of two to four independent growth experiments. The accuracy was around 15-20%. Phosphorus-31 spectra were acquired on a Bruker AVANCE II 500 spectrometer (Bruker BioSpin GmbH) with a phosphorus selective 5-mm-diameter probe head at 30°C with a pulse width of 6.5 µs (flip angle, 70°) and a recycle delay of 1s. Saturation of resonances due to fast pulsing conditions was calculated by comparison with spectra acquired under fully relaxed conditions (recycle delay, 20s). Phosphorus chemical shifts were referenced to the resonances of external 85% H_3PO_4 designated at 0.0 ppm.

Quantification of the glucuronic acid content of the capsular polysaccharide

Samples for the determination of the capsular glucuronic acid amounts were prepared as follows: cells grown in Glc-CDM under semi-aerobic conditions as above and harvested during the late-exponential (LExp) and early-stationary (EStat) phases of growth (time-points indicated by the arrows in Fig. 4.4-B) were centrifuged (6,000 x *g*, 3-7 min, 4ºC), resuspended in PBS and pelleted at 3000 x *g*, 4ºC, for 20 min. The pellet was resuspended in 500 µl of 150 mM Tris-HCl (pH 7.0) and 1 mM $MgSO_4$ and treated as described elsewhere (Morona *et al.*, 2006). The supernatants derived from the two centrifugations referred before were pooled and treated with 20% (wt/vol) trichloroacetic acid for protein precipitation. After 2 h of incubation in an ice bath proteins were pelleted and the exopolysaccharides were precipitated with cold ethanol as in Ramos *et al.* (2001). The glucuronic acid of capsule attached or loosely attached (lost in centrifugations to the supernatants) to the cell wall was quantified by the method for quantitative determination of uronic acids as described in Blumenkrantz and Asboe-Hansen, 1973. Capsule measurements were performed in duplicate using samples from two independent cultures.

Growth of D39*spxB*$^-$ and D39 strains on specified sugars

To test the ability of specific sugars to support growth of *S. pneumoniae* strains D39 and D39*spxB*$^-$ cultures of 250 µl were prepared in CDM containing 0.25% (wt/vol) of glucose (Glc), glucuronic acid (GlcUA), rhamnose (Rha), gluconic acid (GlcA), N-acetylglucosamine (GlcNAc) or a 1:2:3 mixture of GlcUA, Glc and Rha, respectively. Cultures were started at an initial OD_{595} of 0.25-0.3 by addition of a preculture, grown on Glc-M17 (0.5% Glc wt/vol), suspended in fresh CDM without sugar. Cultures were grown for 24 h at 37°C in 96-well microtiter plates. Cell density was monitored at 595 nm with a ELx808 microplate

spectrophotometer (BioTek Instruments, Inc.) and the growth curves were generated using Gen5^{TM} (BioTek Instruments, Inc.) with readings taken every 30 min. Each growth condition was done in triplicate using two independent precultures. Growth rates and other growth parameters were generated as above and the results were analyzed using the Instat software (GraphPad Software).

Results

Inactivation of *spxB* leads to an increase in capsule production

While generating a transposon library in strain D39 using the pGh9:ISS1 T7 plasmid (Bijlsma *et al.*, 2007), a colony displaying characteristics of overproducing capsule was isolated; on solid medium this isolate yielded large, opaque and slimy colonies (Fig. 4.1-A). To ensure that the observed phenotype was genetically linked to the transposon insertion, the chromosomal DNA of this mutant was back-crossed into strain D39 which gave rise to the same phenotype. Transformation into strain TIGR4 also resulted in the same phenotype, indicating that the phenotype was serotype-independent (Fig. 4.1-B). Comparison of the TIGR4 strain containing the insertion with an opaque and transparent variant of the same strain indicated that the phenotype of the mutant was dissimilar to the opaque phase variant as it seemed to produce even more capsule (Fig. 4.1-B). Introduction of the chromosomal DNA into strain R6 and an unencapsulated mutant of D39 did not result in this phenotype (data not shown), indicating that the observed phenotype is exclusively capsule-dependent. Excision of the pGh9:ISS1 T7 plasmid did not alter the phenotype and sequencing showed that the ISS1 element was inserted into the 3' end of the *spxB* gene. This gene encodes the *S. pneumoniae* pyruvate oxidase, which generates Ac-P and H_2O_2 and whose

activity plays a key role in pneumococcal colonization and pathogenesis (Spellerberg *et al.*, 1996; Orihuela *et al.*, 2003; Regev-Yochay *et al.*, 2007; Ramos-Montañez *et al.*, 2008). The amount of H_2O_2 produced by the mutant was reduced about 80% compared to the wild-type and PCR analysis showed the insertion of approximately 600-bp into the *spxB* gene (data not shown), confirming that the insertion of ISS1 disrupted *spxB* and its function. The observed phenotype of the colonies (large, opaque and slimy) could be due to the reported absence of death in stationary phase of *spxB* mutants and the ensuing increase in biomass production over time (Regev-Yochay *et al.*, 2007) or due to increased capsule production. Therefore the amount of capsule was determined in both the wild-type and the *spxB* mutant (from here on denominated D39*spxB*$^-$) in late-exponential (Fig. 4.2-A) and early-stationary phases of growth (Fig. 4.2-B) in liquid medium. The data showed that the amount of capsule in the D39*spxB*$^-$ mutant was significantly increased compared to that of the wild-type levels (students t-test $P \leq 0.01$), meaning that the observed larger colonies are to a large extent due to increased capsule amounts rather than differences in survival. Furthermore, TEM pictures of bacteria grown to exponential phase in liquid medium, also indicated an increased amount of capsule in the mutant (Fig. 4.1-C and 4.1-D) as well as some subtle changes in the cell membrane (Fig. 4.1-E and 4.1-F). Thus, we showed that inactivation of *spxB* increased the amount of capsule in *S. pneumoniae*.

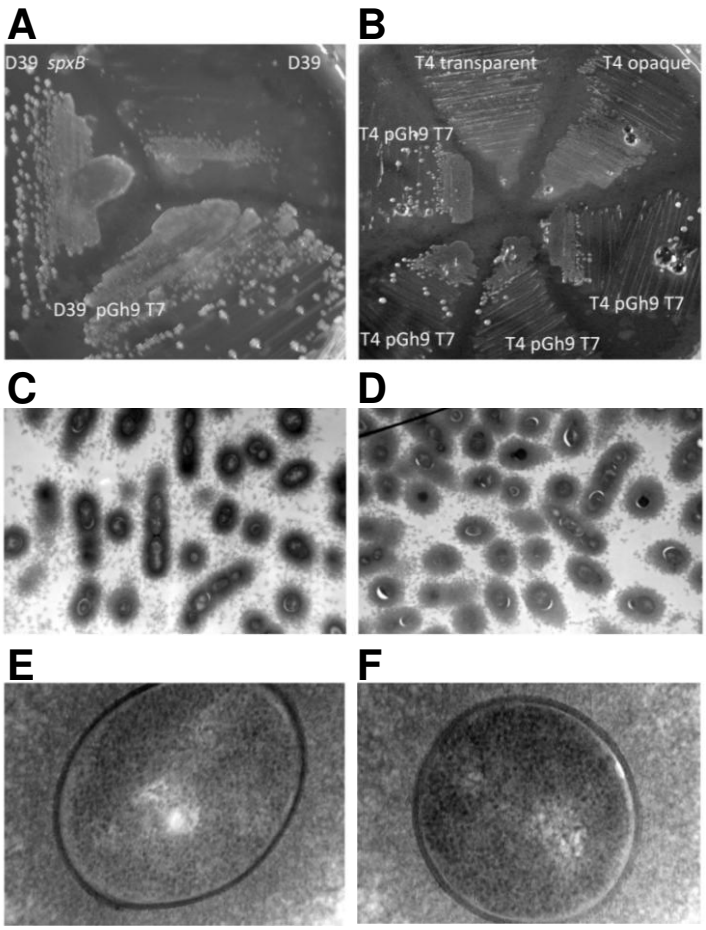

Fig. 4.1. Inactivation of *spxB* led to an increase in capsule production. (A) Phenotype on Glc-M17 agar plate of D39 (D39), D39 containing the pGh9 T7 plasmid (D39pGh9 T7) and D39 in which the plasmid is excised leaving the ISS1 element in *spxB* (D39*spxB*$^-$). (B) Phenotype on Glc-M17 agar plate of TIGR4 transparent variant (T4 transparent), TIGR4 opaque variant (T4 opaque) and TIGR4 in which the pGh9 T7 plasmid is inserted into the genome (T4 pGh9 T7). (C-F) TEM pictures of *S. pneumoniae* grown in broth to exponential phase and stained with LRR. (C) D39, 9700 times magnified, (D) D39*spxB*$^-$, 9700 times magnified, (E) D39, 135.000 times magnified, (F) D39*spxB*$^-$, 135.000 times magnified.

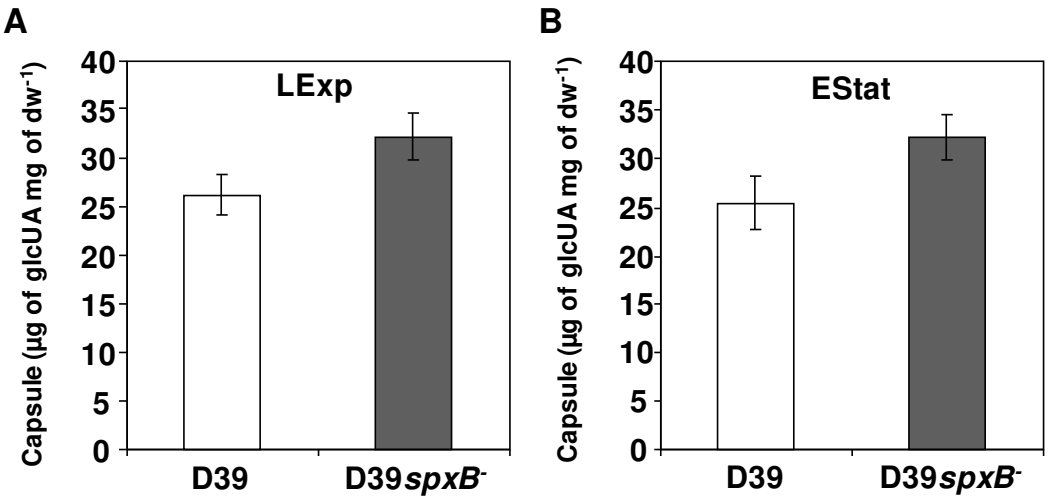

Fig. 4.2. Effect of *spxB* mutation on capsule production. Estimation of capsule was performed based on the determination of its glucuronic acid content in strains D39 (white bars) and D39*spxB*⁻ (grey bars) in late-exponential (LExp) (A) and early-stationary (EStat) (B) phases of growth. Cultures were grown in CDM containing 1% (wt/vol) Glc at 37ºC, with pH control (6.5), and under semi-aerobic conditions (for details see Materials & Methods). All the determinations were done twice in two independent cultures and the values are means ± SD.

Transcription of *cps2A* is increased in the *spxB* mutant

Next we determined whether the increase in capsule production was mediated by changes in transcription of the capsule *locus* by determining the activity of the promoter of the first gene of the capsule *locus*, *cpsA*. A fusion with a promoterless *lacZ* was generated in pORI13 (Kloosterman *et al*., 2006a) and introduced into D39 and the D39*spxB*⁻ mutant. Both in mid-exponential phase as well as late-exponential phase, transcription of the *cpsA* promoter was increased approximately 1.5-fold in the D39*spxB*⁻ mutant (Fig. 4.3). Thus, the increased

capsule production is at least partially mediated by a change in transcription of the capsule *locus*.

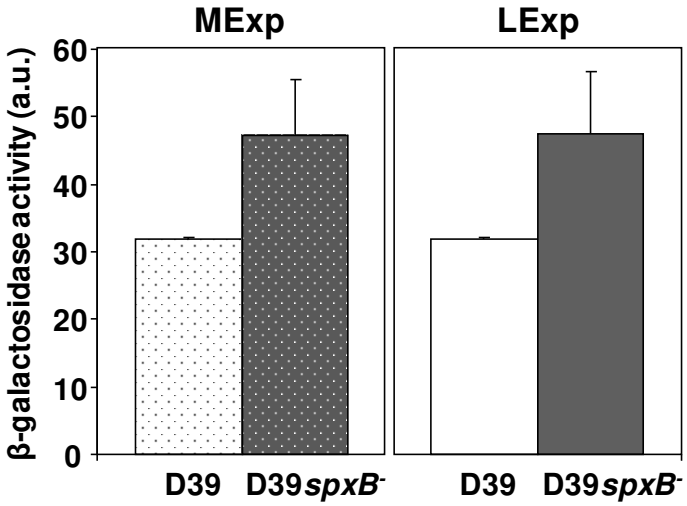

Fig. 4.3. Effect of *spxB* mutation on *cpsA* transcription. Transcription of the *cpsA* promoter was estimated by measuring the β-galactosidase activities of strains D39 (bars with white background) and D39*spxB*$^-$ (bars with grey background) harbouring pORI P*cps2A* (see table 4.1) in mid-exponential (MExp) (left panel) and late-exponential (LExp) (right panel) phases of growth. Cultures were grown in CDM containing 1% (wt/vol) Glc at 37ºC, and under semi-aerobic conditions. All the determinations were done at least in triplicate and the values are means ± SD. a.u. = arbitrary units.

Deletion of *spxB* has only a minor influence on the transcriptome of D39

To obtain a better insight into why inactivation of *spxB* resulted in an increase in capsule production, the transcriptome of the *spxB* mutant was compared to that of the wild-type strain (Table 4.2). As the insertion of the ISS1 element was at the 3' end of the *spxB* gene, no changes in its transcription level were observed. Furthermore, due to technical problems with the R6 specific

amplicons on the array, which include the genes of the capsule *locus* except *cps2A to G*, no reliable signals were obtained for the capsule *locus*. Although *spxB* and its downstream gene s*pd_0637* do not appear to be located in an operon, expression of s*pd_0637* was significantly reduced in the mutant. Theoretically, this could also be the cause of the observed effects of the ISS1 insertion into *spxB*. However, overexpression of this gene in the D39*spxB*$^-$ mutant did not revert the phenotype of the colonies back to wild-type appearance (data not shown), indicating that s*pd_0637* repression played no role in the increase in capsule production. Interestingly, despite the reported major influence of SpxB activity on the metabolism of *S. pneumoniae* (Pericone *et al.*, 2003; Taniai *et al.*, 2008; Ramos-Montañez *et al.*, 2010), the transcriptional response was modest (Table 4.2). Strikingly, two divergent putative operons were (highly) induced in the D39*spxB*$^-$ mutant (Table 4.2). The first one (*spd_0289* to *spd_0292*) contains genes whose homology indicates involvement in the catabolism of ketogluconate (Yum *et al.*, 1999). The second putative operon encodes four genes (*spd_0293, spd_0295-7*) showing homology to a mannose-family PTS system that is predicted, based on homology of the IIC and IID components, to use as substrate N-acetylglucosamine (TransportDB, www.membranetransport.org), and one gene, *spd_0294* encoding a glucuronyl hydrolase (Maruyama *et al.*, 2009). A recent report provided evidence for the involvement of the Man-family PTS in the utilization of hyaluronic acid, a glycosaminoglycan consisting of repeating disaccharides, which are composed of D-glucuronic acid and D-N-acetylglucosamine (Marion *et al.*, 2012). Thus, in line with its role in metabolism and the observed increase in capsule production, two putative operons that are likely involved in carbohydrate metabolism were highly induced.

Table 4.2. Genes differentially regulated in the D39*spxB*⁻ mutant grown in Glc-M17

SP number	*SPD number*	*TIGR annotation*	*Fold change*	*Bayes. p*
SP0095	SPD0091	conserved hypothetical protein	0.4	8.38E-08
SP0317	SPD0289	4-hydroxy-2-oxoglutarate aldolase/2-deydro-3-deoxyphosphogluconate aldolase	7.4	3.00E-15
SP0318	SPD0290	carbohydrate kinase, PfkB family	9.5	0
SP0319	SPD0291	conserved domain protein	9.6	0
SP0320	SPD0292	oxidoreductase, short chain dehydrogenase /reductase	8.6	0
SP0321	SPD0293	PTS system, IIA component	2.3	7.08E-07
SP0322	SPD0294	glucuronyl hydrolase	3.5	4.66E-12
SP0323	SPD0295	PTS system, IIB component	2.6	4.30E-07
SP0324	SPD0296	PTS system, IIC component	4.6	4.54E-09
SP0325	SPD0297	PTS system, IID component	10.2	0
SP0506	SPD0452	integrase/recombinase, phage integrase family	2.4	1.67E-06
SP0626	SPD0546	branched-chain amino acid transport system II carrier	0.3	3.61E-11
SP0731	SPD0637	conserved domain protein	0.3	2.22E-16

Genes were considered differentially expressed when the fold change was ≥ 2, ≤ 0.5 with a Bayesian $p \leq 0.00001$

Growth and fermentation profiles are not affected by *spxB* inactivation under semi-aerobic conditions

Given the metabolic function of SpxB and in order to explore a potential connection between carbohydrate metabolism and capsule production, growth properties of D39*spxB*⁻ and its parent strain D39 were determined in Glc-M17. Under these conditions, the *spxB* mutation had no significant effect on the growth profile or fermentation type of *S. pneumoniae* D39 (Fig. 4.4-A and Table 4.3). Both the D39 and it *spxB* derivative grew to maximal OD_{600} of about 1.5 in 6 h at similar specific growth rates (Table 4.3), showing a typical homolactic

fermentation pattern (Table 4.3), with lactate accounting for about 90% of the Glc consumed.

Considering the minor differences in growth characteristics of strain D39 and its D39*spxB*$^-$ mutant in the complex medium M17, we asked whether in a chemically defined medium the loss of the metabolic enzyme SpxB would have a more pronounced effect. Furthermore, the use of CDM not only facilitates the interpretation of results, but also allows the use of NMR techniques for metabolic characterization. Strains D39 and D39*spxB*$^-$ were grown in Glc-CDM as described in Materials & Methods (Fig. 4.4-B, Table 4.3). The specific growth rates and maximal OD_{600} were lower in Glc-CDM than in the complex medium (Glc-M17). In the defined medium D39 and D39*spxB*$^-$ displayed identical growth properties, namely, the biomass yield, lactate and formate yields, and bioenergetic parameters (Table 4.3). Strain D39 presented, however, a maximal growth rate significantly higher (P value of 0.002) than D39*spxB*$^-$. Consistent with inactivation of pyruvate oxidase, the pyruvate yield was 2-fold higher in the D39*spxB*$^-$ mutant (Table 4.3). Also in agreement, H_2O_2 (about 10 µM) was detected in the extracellular medium during the growth of the parent strain, but not in D39*spxB*$^-$. We were surprised with the low amount produced by D39, since the maximal dissolved oxygen concentration was at least 10-fold higher. Nevertheless, we are not the first to report lower H_2O_2 production in *S. pneumoniae* than the expected from stoichiometry (Taniai *et al.*, 2008). Thus, it is plausible to assume that the low H_2O_2 observed under semi-aerobic conditions arose from a combination of factors: the low dissolved oxygen and H_2O_2 decomposition by the action of protection mechanisms against its toxicity.

As in Chapter 2, Glc was still abundant when growth ceased (70% of the initial Glc remained in the culture medium, Table 4.3). Strains D39 and D39*spxB*$^-$

were grown under controlled neutral pH, thus growth arrest was likely due to uracil limitation (Chapter 2).

Overall, *spxB* mutation decreases slightly the growth rate of D39 under semi-aerobic conditions and pyruvate accumulation during Glc metabolism. Lower accumulation of pyruvate and H_2O_2 production in strain D39 are indicative of SpxB activity.

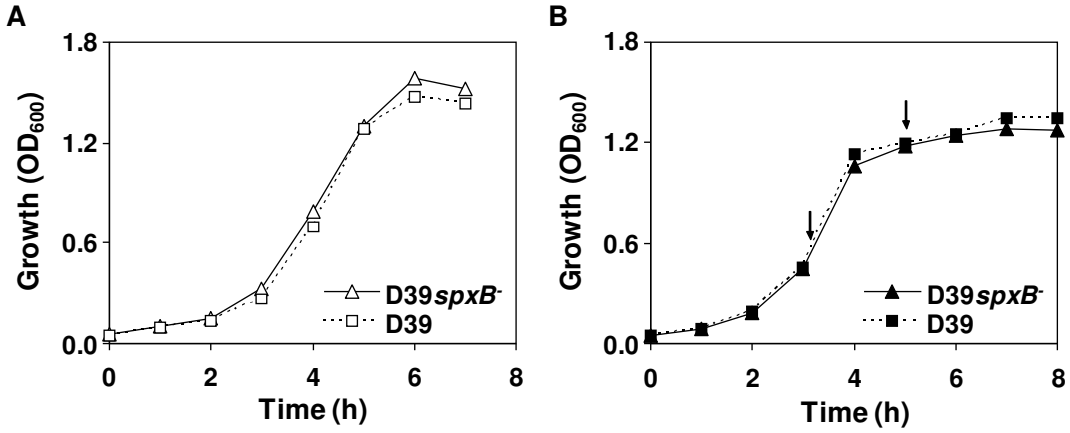

Fig. 4.4. Growth profiles of *S. pneumoniae* D39*spxB*⁻ and its parent strain D39 under semi-aerobic conditions. (A) Cultures were grown in M17 (open symbols) or in (B) CDM supplemented with 1% (wt/vol) Glc at 37ºC, with pH control (6.5), and under semi-aerobic conditions (closed symbols) (for details see Materials & Methods). The plotted growth curves are from a representative experiment. For each condition at least three independent experiments were performed and the error was below 15%. Symbols: (△,▲), D39*spxB*⁻; (□,■), D39. Arrows indicate sampling time for capsule determination and intracellular metabolite analysis (Figs. 4.2 and 4.5).

Table 4.3. Product yields, total substrate consumed, carbon and redox balances, growth and energetic parameters as determined from substrate and fermentation product analysis at the time-point of maximal biomass achieved by D39*spxB*$^-$ and D39 strains cultured in complex medium (M17) or CDM supplemented with Glc (1% wt/vol), under semi-aerobic conditions as described in Material and Methods. The specific growth rates are also shown. Values of at least two independent experiments were averaged and errors are reported as ± SD.

	Semi-aerobic			
	Glc-M17		**Glc-CDM**	
	D39*spxB*$^-$	**D39**	**D39*spxB*$^-$**	**D39**
Product yields[a]				
Lactate	1.75 ± 0.06	1.78 ± 0.02	1.69 ± 0.03	1.63 ± 0.01
Formate	0.05 ± 0.05	0.10 ± 0.03	0.08 ± 0.01	0.06 ± 0.01
Pyruvate[b]			0.09 ± 0.02	0.04 ± 0.01
Acetate	BDL	BDL	BDL	BDL
H_2O_2 (µM)	ND	ND	BDL	10 ± 0
Consumed substrate (%)	36 ± 2	35 ± 1	28 ± 1	28 ± 0
Carbon balance[c]	88 ± 1	89 ± 1	93 ± 1	87 ± 1
Redox balance	84 ± 3	83 ± 1	88 ± 1	85 ± 1
Biomass yield (g mol^{-1} of Glc)	24.8 ± 0.4	23.7 ± 0.2	24.9 ± 3.1	26.2 ± 1.0
ATP yield (mol mol^{-1} of Glc)	1.8 ± 0.0	1.8 ± 0.1	1.8 ± 0.1	1.7± 0.0
Y_{ATP} (g of biomass mol^{-1} of ATP)	14.1 ± 0.2	13.3 ± 0.1	14.2 ± 1.3	15.0 ± 0.7
μ_{max} (h^{-1})	0.85 ± 0.01	0.87 ± 0.06	0.70 ± 0.05	0.83 ± 0.04

[a]Product yields, [End-product] / [Glc consumed]; [b]Blank cells, negative yields were found for these conditions (cells used pyruvate from the medium); [c]Carbon balance is the percentage of carbon in metabolized Glc that is recovered in the fermentation products (lactate and formate) and pyruvate; Dry weight (DW) was used as a measure of cell mass; BDL, below detection limit; ND, not determined.

spxB deletion has an effect on the pools of intracellular metabolites

Our data showed that the *spxB* mutation had a modest impact on growth and fermentation products in cultures under semi-aerobic conditions, but clearly affected the production of the polysaccharide capsule (Fig. 4.2). The disparate capsule production could suggest an altered intracellular metabolism. In line, the specific growth rate of D39*spxB*$^-$ was slightly, but consistently, lower than that of D39. To verify this hypothesis we measured the intracellular metabolites at the partitioning node between glycolysis and the polysaccharide 2 biosynthetic pathway, as well as several NDP-sugars, including the capsule precursors UDP-Glc and UDP-GlcUA (Fig. 4.5). Metabolite concentrations were determined in ethanol extracts obtained during late-exponential and early-stationary phases of growth by ^{31}P-NMR (see the time-points indicated by the arrows in Fig. 4.4-B). Interestingly, the loss of *spxB* led to a considerable reduction in the levels of the upper glycolytic metabolites glucose 6-phosphate (G6P) and fructose 1,6-bisphosphate (FBP) (Fig. 4.5-A). G6P is a key metabolite at the hub of glycolysis and several biosynthetic pathways, and its conversion to α-glucose 1-phosphate (α-G1P) is the first step that commits it to the synthesis of many structural polysaccharides, including type 2 polysaccharide (Fig. 4.8). The intracellular concentration of α-G1P was similar in D39 and its D39*spxB*$^-$ mutant. The same was true for the UDP-activated capsule precursors, UDP-Glc and UDP-GlcUA (Fig. 4.5). These data indicate a redirection of carbon away from glycolysis in the D39*spxB*$^-$, and is consistent with the higher capsule production. In addition, no major differences were detected between the levels of other NDP-activated metabolites in D39 and the D39*spxB*$^-$ mutant. As expected, the product of SpxB activity, the high energy phosphoryl donor acetyl-P (Ac-P), was reduced in the mutant by 65% of the parent strain (Fig. 4.5), which is in the same range as the values recently reported by Ramos-Montañez *et al.* (2010). The ATP levels in the

late-exponential phase of growth were not affected by the loss of *spxB* (2.3 ± 0.3 and 2.1 ± 0.2 nmol mg DW^{-1} in D39 and *spxB* mutant, respectively). In general, the intracellular concentrations of phosphorylated metabolites in both strains were lower in early-stationary phase, except for phospho*enol*pyruvate (PEP), which increased slightly.

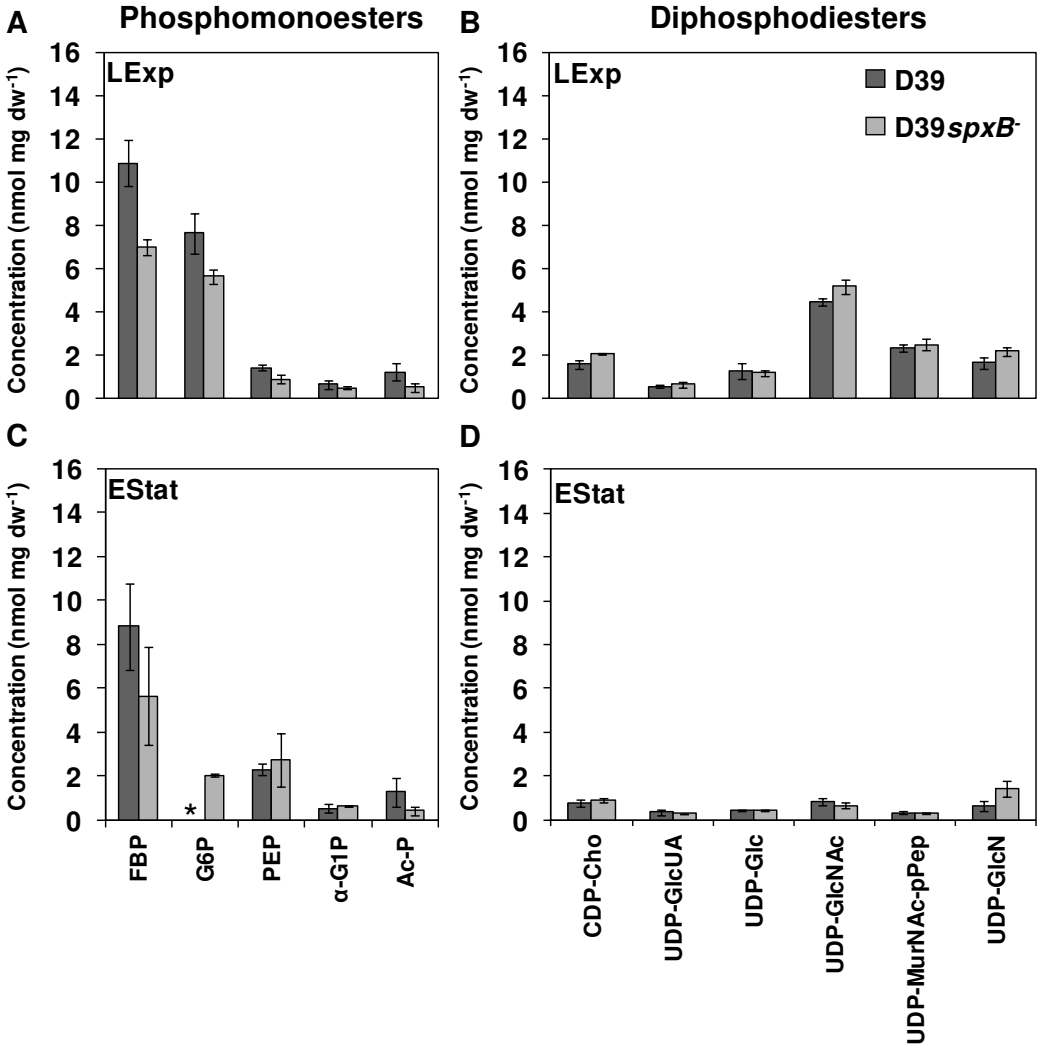

Fig. 4.5. Effect of *spxB* mutation on intracellular phosphorylated metabolites during growth in Glc-CDM under semi-aerobic conditions. Phosphorylated metabolites were measured by ^{31}P-NMR in ethanol extracts of D39 and D39*spxB*$^-$ cells grown to late-exponential (LExp) (A, B) and early-stationary (EStat) (C, D) phases of growth in CDM supplemented with 1% (wt/vol) Glc as in Fig. 4.4-B. The results are averages of four independent growths and the average accuracy was ± 15%. Symbols: (dark grey bars), D39, (light grey bars), D39*spxB*$^-$. FBP, fructose 1,6-bisphosphate; G6P, glucose 6-phosphate; PEP, phospho*enol*pyruvate; α-G1P, α-glucose 1-phosphate; Ac-P, acetyl-phosphate; CDP-Cho, CDP-choline; UDP-GlcUA, UDP-glucuronate; UDP-Glc, UDP-glucose; UDP-GlcNAc, UDP-N-acetylglucosamine; UDP-MurNAcp-Pep, UDP-N-acetyl-muramoyl-pentapeptide; UDP-GlcN, UDP-glucosamine; LExp, late-exponential phase of growth; EStat, early-stationary phase of growth; A and C, phosphomonoesters; B and D, diphosphodiesters; (*), quantification was impaired by overlapping resonances in NMR spectra.

SpxB skews the sugar utilization profile of *S. pneumoniae*

The fact that the majority of transcriptomic differences between D39 and D39*spxB*$^-$ were observed for genes potentially involved in central metabolism, and in particular sugar catabolic pathways, prompted us to analyze the growth of the two strains on selected sugars. Genome annotation and homology studies suggested that the genes differentially expressed might play roles in the catabolism of N-acetylglucosamine (GlcNAc), glucuronic acid (GlcUA) and/or gluconic acid (GlcU). Since loss of *spxB* leads to higher amount of capsule polysaccharide, and considering the higher expression of a putative glucuronyl hydrolase (*spd_0294*) and the PTS system needed to import its products (Marion *et al.*, 2012), we surmised an aptitude of the D39*spxB*$^-$ strain to utilize type 2 polysaccharide derived sugars (GlcUA, Glc, and rhamnose, Rha) as carbon sources. Thus, rhamnose and a sugar mixture mimicking the type 2 capsule (1 GlcUA: 2 Glc: 3 Rha) were also tested. Growth was performed in CDM supplemented with 0.25% (wt/vol) sugar in 96-well microtiter plates (Fig. 4.6). As

expected, on Glc, D39 showed a modest, but significant (P value < 0.05) higher specific growth rate than the D39*spxB*⁻ strain (1.18 ± 0.06 as compared to 0.91 ± 0.06 h^{-1}). The maximal OD_{595} was similar for both strains on Glc (about 1.1).

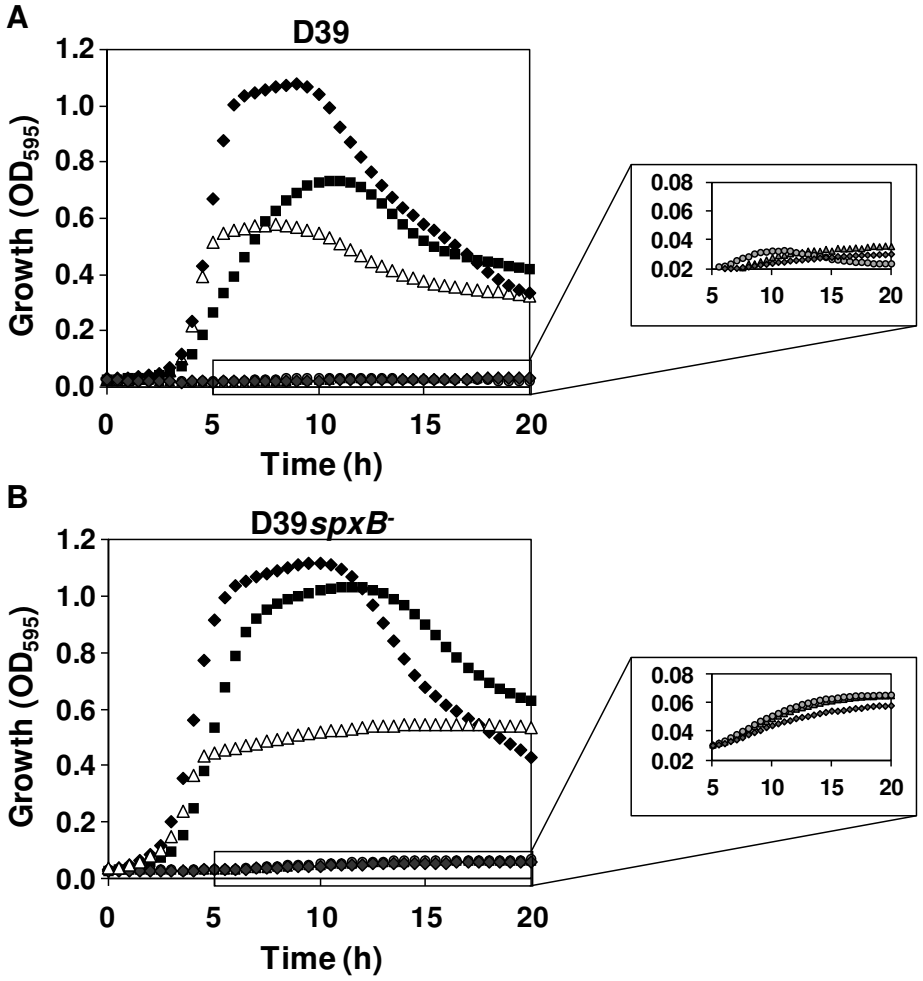

Fig. 4.6. Effect of s*pxB* mutation on the ability to grow on specified sugars. Growth profiles of *S. pneumoniae* D39 (A) and its derivative D39*spxB*⁻ (B) in CDM containing 0.25% (wt/vol) of the specified sugar. Cultures were prepared in 250 µl in 96-well

microtiter plates and growth monitored at 595 nm and 37ºC. Symbols: (◆), Glc; (■), GlcNAc; (△) 1 GlcUA : 2 Glc: 3 Rha; (◆), GlcUA; (▲), Rha; (●), GlcA. Zoomed areas: expansions of time-points 5 to 20 h for growths in rhamnose, gluconic acid and glucuronic acid. Each point of the growth curves is an average of triplicate experiments from two independent cultures, and the error was in all cases below 20%, except for rhamnose which was below 30%.

Growth on GlcNAc was characterized by identical specific growth rates (around 0.83 h^{-1}) for both strains, but lack of *spxB* resulted in 25% increase in the final biomass (from OD_{595} of 0.75 to 1.03). This result supports a role of the PTS system (*spd_0293-0297*), which is differentially expressed in our transcriptomic analysis, in the catabolism of GlcNAc. In the sugar mixture, both strains displayed identical specific growth rates and maximal biomass; however, while the OD_{595} values of D39 decreased upon growth arrest, the D39*spxB*$^-$ mutant showed a slow but steady increase of the OD_{595} values during the time of monitoring (24 h). Also, the D39*spxB*$^-$ strain showed residual growth on GlcUA, Rha and GlcU, while D39 was totally unable to use these sugars as sole carbon sources for growth. These data strongly indicate that *spxB* considerably influences the nutritional utilization capabilities of *S. pneumoniae*.

Oxygen affects differently end-product distribution in strain D39 and *spxB*$^-$ mutant under aerobic conditions

Molecular oxygen is the substrate for the SpxB reaction. Hence, to firmly assign the SpxB deficient phenotype, we grew strain D39 and its derivative *spxB* mutant under a continuous specific air tension of 40% (constant dissolved oxygen concentration of 90 µM at 37ºC). We expected visible changes in end-product profiles in strain D39 (SpxB$^+$), but minor or no changes in D39*spxB*$^-$. Indeed, the increase in oxygen availability was translated into a substantial raise in H_2O_2

production to about 2 mM in the parent strain D39. The concentration of hydrogen peroxide in supernatants of strain D39*spxB*⁻ was still in the micromolar range (2 µM), three order of magnitude lower than in D39 (Fig. 4.7 and Table 4.4). These data fully corroborate the loss of SpxB function in our mutant strain.

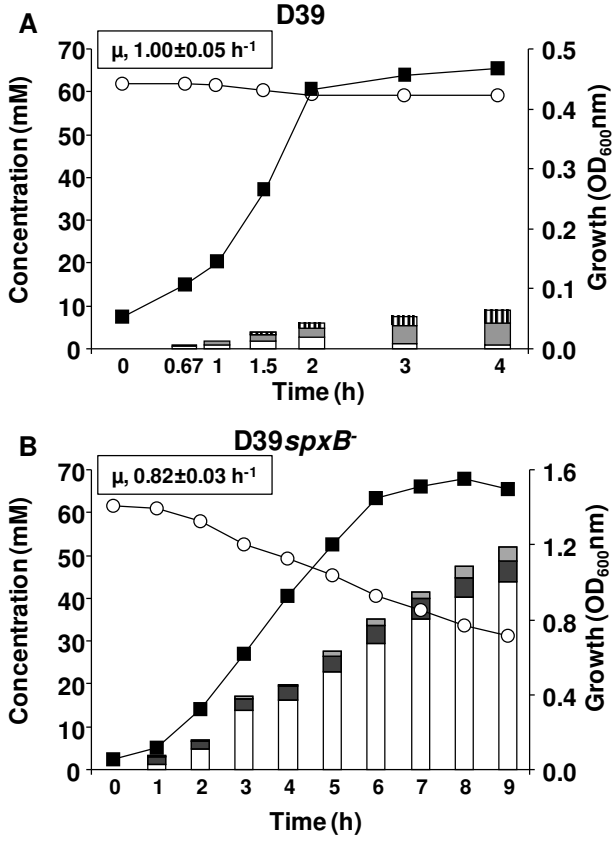

Fig. 4.7. Growth and fermentation profiles in *S. pneumoniae* D39*spxB*⁻ and its parent strain D39 under aerobic conditions. Growth curves, substrate consumption and end-products formed by D39 (A) and D39*spxB*⁻ (B) strains growing on Glc-CDM, at 37ºC, with pH control (6.5), and under aerobic conditions (for details see supplemental Materials & Methods). Culture supernatant samples for substrate and end-product

analysis by HPLC and/or ^{1}H-NMR were harvested at denominated time-points along growth (bars in the plots). The plotted growth curves, substrate consumption curves and end-products bars are from a representative experiment. For each condition at least two independent experiments were performed. For the growth and substrate consumption curves the error in each point was below 10%. For the end-products concentrations, the error was below 7% for major products (> 3.5 mM) and 30% for minor products (< 3.5 mM) Symbols: (○), substrate consumption; (■), growth curve; white bars, lactate; dark grey bars, pyruvate; light grey bars, acetate; stripped bars, hydrogen peroxide.

Under aerobic conditions, the maximal biomass reached for strains D39 and D39*spxB*$^{-}$ was 0.49 ± 0.03 (time-point 3h) and 1.64 ± 0.13 (time-point 8h), respectively (Fig. 4.7-A and 4.7-B). At these time-points the D39*spxB*$^{-}$ mutant consumed approximately 50% of the Glc supplied and the control strain only about 4% (Table 4.4). Under these conditions, the low biomass generated by D39 is most likely a consequence of high H_2O_2 accumulation due to SpxB activity. Loss of *spxB* caused a significant decrease (about 20%) in the maximal growth rate (Table 4.4), which suggests that when oxygen is available SpxB stimulates faster growth on Glc. In terms of end-products, D39 produced from Glc, acetate, H_2O_2 and lactate, which reached at the time-point of growth arrest (maximal biomass) concentrations of 4.2 ± 0.1 mM, 2.2 ± 0.1 mM and 1.3 ± 0.3 mM, respectively. Before entering the stationary phase of growth a continuous increment in the yields of lactate, acetate and H_2O_2 was observed for strain D39. Interestingly, in the stationary phase the levels of acetate and H_2O_2 increased at the expense of lactate, suggesting the occurrence of lactate oxidase activity in this strain (Fig. 4.7-A and 4.7-B). As expected, loss of *spxB* led to a typical homolactic behavior, with lactate as major end-product (maximal concentration 44 ± 0 mM), accounting for 75% of the Glc consumed (Table 4.4); acetate was also formed in minor amounts and the yield of pyruvate was 2-fold enhanced as compared to semi-aerobic conditions. No formate was observed, suggesting suppression of pyruvate

formate lyase (PFL) activity when the oxygen concentration is kept steady around 0.09 mM. In the D39*spxB*$^-$ mutant, the H_2O_2 detected was below 10 µM, confirming inactivation of pyruvate oxidase. Detection of acetate in the *spxB*$^-$ mutant while *spxB* is inactivated and PFL suppressed by O_2 indicates an alternative pathway for the formation of this organic acid.

In summary, the high accumulation of H_2O_2 exclusively in strain D39 fully confirms the absence of SpxB activity in the mutant strain. Furthermore, our data show that the metabolic response to oxygen is largely mediated by SpxB, since growth and fermentation profiles of strain D39*spxB*$^-$ were barely affected under aerobic conditions.

Table 4.4. Product yields, total substrate consumed, carbon and redox balances, growth and energetic parameters as determined from substrate and fermentation product analysis at the time-point of maximal biomass achieved by D39*spxB*$^-$ and D39 strains cultured in CDM supplemented with Glc (1% wt/vol) under aerobic conditions (constant air tension of 40%) (see Materials and Methods). The specific growth rates are also shown. Values of at least two independent experiments were averaged and errors are reported as ± SD.

	Aerobic	
	Glc-CDM	
	D39*spxB*$^-$	**D39**
Product yields[a]		
Lactate	1.47 ± 0.02	0.47 ± 0.09
Formate	BDL	BDL
Pyruvate[b]	0.16 ± 0.01	
Acetate	0.11 ± 0.00	1.53 ± 0.09
H_2O_2	BDL	0.82 ± 0.01
Consumed substrate (%)	49 ± 0	4.4 ± 0.6
Carbon balance[c]	87 ± 2	100 ± 0
Redox balance	ND	ND
Biomass yield (g mol^{-1} of Glc)	20.9 ± 2.6	68.1 ± 2.4
ATP yield (mol mol^{-1} of Glc)	1.9 ± 0.0	3.5 ± 0.1
Y_{ATP} (g of biomass mol^{-1} of ATP)	11.3 ± 1.1	19.3 ± 1.1
μ_{max} (h^{-1})	0.82 ± 0.03	1.00 ± 0.05

[a]Product yields, [End-product] / [Glc consumed]; [b]Blank cells, negative yields were found for these conditions (cells used pyruvate from the medium); [c]Carbon balance is the percentage of carbon in metabolized Glc that is recovered in the fermentation products (lactate and acetate) and pyruvate; Dry weight (DW) was used as a measure of cell mass. ND, not determined; BDL, below detection limit.

Discussion

The role of pyruvate oxidase (SpxB) in the aerobic metabolism of several Gram-positive bacteria is well established (Sedewitz *et al.*, 1984; Seki *et al.*, 2004; Lorquet *et al.*, 2004; Goffin *et al.*, 2006). In the human pathogen *S. pneumoniae*, a number of studies describe the involvement of SpxB in virulence (Spellerberg *et al.*, 1996; Pericone *et al.*, 2000), fermentation (Taniai *et al.*, 2008) and colony phenotypic variation (Overweg *et al.*, 2000; Belanger *et al.*, 2004; Ramos-Montañez *et al.*, 2008; Allegrucci and Sauer, 2008). However, in depth investigation of the molecular mechanisms underlying these modes of action is far from complete. In this study we show that inactivation of *spxB* leads to an increase in capsule production. High capsule amounts have been consistently associated with opaque phase variants, which are interestingly also characterized by low SpxB activity (Kim and Weiser, 1998; Kim *et al.*, 1999; Overweg *et al.*, 2000). However, a comparison of phenotypes on plate showed that, although displaying similar properties, the D39*spxB*$^-$ mutant is not an opaque variant. Nevertheless, the observation that deletion of *spxB* or a reduction in SpxB activity leads to an opaque-like or mucoid phenotype on plate is recurrent (Overweg *et al.*, 2000; Ramos-Montañez *et al.*, 2008; Allegrucci and Sauer, 2008).

Our data show for the first time, that the mucoid phenotype appearance of D39 colonies lacking SpxB activity is due to an increase in capsule biosynthesis, as indicated by the higher expression levels of the *cps* promoter and glucuronic acid amounts, and is independent of differences in growth or death rate. Capsule hinders the attachment of *S. pneumoniae* to host cells, a step that has been described as important for colonization and for the ability to cause invasive disease (Ring *et al.*, 1998; Magee and Yother, 2001; Morona *et al.*, 2004). On the other hand, it prevents opsonophagocytosis and is presumably essential for

growth in blood. Additionally, it prevents mucus-mediated clearance from the nasopharynx (Nelson *et al.*, 2007). Interestingly, most studies report that deletion of *spxB* leads to a defect in nasopharyngeal colonization (Spellerberg *et al.*, 1996; Orihuela *et al.*, 2003; Regev-Yochay *et al.*, 2007; Ramos-Montañez *et al.*, 2008). The data from our study show that this attenuation can partially be due to the increased amounts of capsule present in the D39*spxB*$^-$. Although capsule is needed for colonization (Magee and Yother, 2001), too much capsule is detrimental especially during the establishment phase of colonization as demonstrated by comparing opaque and transparent variants (Magee and Yother, 2001; Nelson *et al.*, 2007). In this light, it is expected that the capsule surplus of the *spxB* mutant will impair colonization, and subsequent invasive disease. On the other hand, *spxB* mutants are less attenuated in invasive disease and bacteremia models where capsule is an absolute requirement (Orihuela *et al.*, 2003). In concordance with this idea, *spxB* expression is higher in the nasopharynx than in the lungs and the blood (LeMessurier *et al.*, 2006) probably ensuring that not too much capsule is being produced. Conversely, in transparent variants thought to be better equipped for colonization, as they contain more teichoic acids and less capsule, *spxB* is higher expressed than in opaque variants which contain more capsule and are poor colonizers (Overweg *et al.*, 2000; Li-Korotky *et al.*, 2009). Thus, we would like to propose that SpxB activity in response to the oxygen concentration of its environment is an important signal for *S. pneumoniae* to determine the amount of capsule that needs to be produced. This hypothesis is strengthened by the observation that changes in oxygen seem to induce changes in capsule production. Furthermore, transparent variants were predominantly isolated from the nasopharynx and opaque variants from blood (Weiser *et al.*, 2001). Furthermore, growth of D39 under anaerobic conditions also led to a uniform mucoid appearance of the colonies on blood agar plates (data not

shown). How this signaling would occur is currently unclear, one possibility is that the changes in the membrane induced by SpxB activity (Benisty *et al.*, 2010) mediate alterations in the production and expression of the capsule *locus*.

Capsule synthesis is tightly interconnected with peptidoglycan synthesis and is partly regulated by membrane proteins (Yother, 2011), thus it is not unlikely that disturbances in the membrane or cell wall influence capsule synthesis and *vice versa*. The high magnification TEM pictures of the D39*spxB*$^{-}$ mutant also indicated changes in the membrane which could be mediated by *spxB* inactivation and thus result in a change in capsule production. In other streptococci, CcpA, the main regulator of carbon metabolism in *S. pneumoniae* (Chapter 6) and other Gram-positive bacteria, represses *spxB* (Zheng *et al.*, 2011a; Zheng *et al.*, 2011b). Although there is no *cre* site in the *S. pneumoniae spxB* promoter and the gene was also not found in extensive transcriptome analysis (Chapter 6), we did attempt to generate a *ΔccpA* mutant in the D39*spxB*$^{-}$ background. This failed unless the *ccpA* gene was already ectopically present in the D39*spxB*$^{-}$ mutant, indicating that this combination is lethal for *S. pneumoniae* (data not shown). Thus, in *S. pneumoniae* CcpA does not regulate *spxB* but repression (or activation) of a product of the CcpA regulon does seem necessary to counteract deleterious effects of *spxB* inactivation. Another alternative to mediate this regulation is SpxR, however no capsule genes were differentially regulated in the transcriptome analysis of this mutant, making it a less likely candidate (Ramos-Montañez *et al.*, 2008). It is worth mentioning that while Winkler and co-workers used D39 strain NCTC7466 as genetic background, in our work we have characterized a Lilly derivative strain and in a different medium (Lanie *et al.*, 2007). D39 NCTC and Lilly are allelic variants of thirteen genes, including a putative capsule regulator *cpsY* and *spxB*; in terms of the latter mutation the major consequence is a considerably lower SpxB activity in the Lilly D39 (Ramos-

Montañez *et al.*, 2008). Thus, a direct extrapolation from previous work performed with D39 NCTC might not be possible. Interestingly, transcriptome analysis of our D39*spxB*⁻ mutant did not show the same pattern as that of the *spxB* mutant in the NCTC isolate (Ramos-Montañez *et al.*, 2008). This could be due to the allelic variance between the two D39 isolates (NCTC and Lilly), differences in sampling time (phase of growth) and or in the composition of the medium used for growth. To our surprise, the transcriptome analysis of D39*spxB*⁻ showed only minor changes (13 altered transcripts) compared to the wild-type, despite the fact that the experiments were carried out under semi-aerobic conditions and harvest took place during early-exponential growth phase when we expect that oxygen is still present and SpxB activity can be detected. Loss of *spxB* did not affect the transcript levels of regulatory proteins. These findings reinforce the idea that neither SpxR nor CcpA play prominent roles in the signaling pathways mediating the SpxB phenotypes.

Of the genes that were differentially expressed, 77% encode functions involved in central metabolism (Table 4.2). Of these, 9 genes organized in two transcriptional units (*spd_0289-92*, *spd_0293-97*) were highly induced in the *spxB* mutant. *Spd_0293-97* encodes a Man-family PTS system and a glucuronyl hydrolase, which have recently been implicated in the metabolism of hyaluronic acid, and in particular in the uptake and degradation of GlcNAc-GlcUA disaccharides (Marion *et al.*, 2012; Bidossi *et al.*, 2012). The four genes in *spd_0289-92* are most likely involved in the degradation of ketogluconic acid, as judged by homology comparisons (Yum *et al.*, 1999). Thus, a role for SpxB was surmised on the utilization of carbon sources for growth, which was corroborated by the better growth on GlcNAc compared to the wild-type and the observed residual growth of the D39*spxB*⁻ strain on sugars potentially present in capsules or host glycans (Fig. 4.8). Growing evidence supports the utilization of host

glycans as nutritional sources for pneumococcal growth (Burnaugh *et al*., 2008; Yesilkaya *et al*., 2008; Marion *et al*., 2012). To our knowledge, we are the first to show a link between SpxB and carbohydrate utilization. Based on our results, it is tempting to hypothesize that in specific host microenvironments with oxygen where Glc becomes the major carbon source available, for instance during inflammation or hyperglycemia (*e.g.* lungs during infection) (Philips *et al*., 2003), SpxB activity minimizes the use of alternative sugar utilization pathways (repression of specific catabolic steps involved in the metabolism of sugars other than Glc) in a cost effective manner, which will allow for rapid proliferation and fast energy production, *i.e.* improved fitness.

We found that SpxB stimulated the pneumococcal rate of growth on Glc and inhibited capsule production (Fig. 4.2 and Fig. 4.3; Table 4.3 and Fig. 4.8). Importantly, the soluble activated precursors for serotype 2 capsule synthesis are all derivatives of α-glucose 1-phosphate, which originates from the action of α-phosphoglucomutase on the glycolytic intermediate glucose 6-phosphate. The lower accumulation of glucose 6-phosphate and fructose 1,6-bisphosphate in the D39*spxB*$^{-}$ mutant indicate a redirection of carbon towards biosynthetic pathways, in particular capsule (Fig. 4.8). The data on intracellular metabolites is therefore in full agreement with our findings in respect to capsule production and growth rate, and allows us to propose that the *spxB* mutation affects the intracellular fluxes of *S. pneumoniae*.

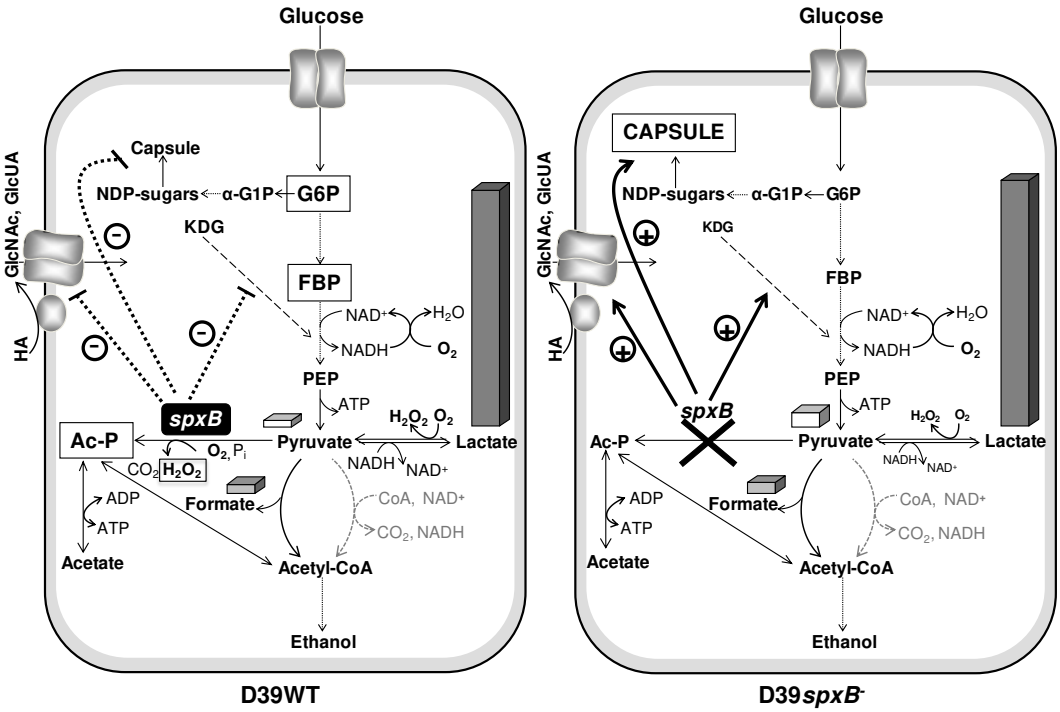

Fig. 4.8. Model of the *spxB* deletion effect on glucose metabolism and capsule production in *S. pneumoniae*. Glucose is converted by the conventional glycolytic pathway to pyruvate. Fermentation products result from the action of different competing enzymes (lactate dehydrogenase, pyruvate formate-lyase, pyruvate oxidase and hypothetically the pyruvate dehydrogenase complex). Overall, our data show that SpxB represses carbohydrate specific pathways (ketogluconate and hyaluronic acid utilization), capsule production, and stimulates formation of acetyl-P and acetate at the expense of pyruvate and lactate. Pyruvate and end-products are represented by three-dimensional bars and the height of the bar represents the relative amount; grey slashed arrows, function not experimentally verified; boxed metabolites indicate higher metabolite accumulation. Thick pointed-line, repression; Thick black arrow, activation. KDG, ketogluconate; HA, hyaluronic acid; GlcNAc, N-acetylglucosamine, GlcUA, glucuronic acid; Ac-P, acetyl-phosphate; α-G1P, α-glucose 1-phosphate; G6P, glucose 6-phosphate; FBP, fructose 1,6-bisphosphate; PEP, phospho*enol*pyruvate.

Curiously, under the imposed semi-aerobic conditions the fermentation pattern of the pneumococcus was only marginally affected by loss of *spxB*, the major difference being a higher accumulation of pyruvate in the mutant (Fig. 4.8). This effect was consistent with a decreased level of Ac-P in D39*spxB*$^-$. In bacteria, a role of the central metabolite Ac-P in linking the nutritional status to global signaling, namely by acting as a phosphoryl donor to two-component response regulators has been proposed (Wolfe, 2010). One could argue that similar molecular mechanisms are in effect in *S. pneumoniae*, *i.e.* Ac-P phosphorylation of response regulators. In fact, the cross talk between capsule synthesis and SpxB function could also be mediated by this high energy molecule acting directly on the phosphorylation of the auto-phosphorylating kinase CpsD. Although some controversy remains, a positive correlation between CpsD phosphorylation and capsule production is accepted (Yother 2011). The capsule production is, however, enhanced in the *spxB* mutant (Fig. 4.2), a phenomenon that is not in agreement with Ac-P acting as phosphoryl donor for CpsD, since the intracellular accumulation of this metabolite is smaller in D39*spxB*$^-$. It cannot be excluded that the lower Ac-P concentration results both from lack of SpxB activity and higher demand for biosynthetic purposes. In a recent work, Winkler and co-workers provided some evidence suggesting cross talk phosphorylation of a response regulator (VicR *aka* WalR) by Ac-P, but most their work did not support phosphorylation of regulators by Ac-P as a general signaling mechanism in *S. pneumoniae* (Ramos-Montañez *et al.*, 2010). This is in line with the minimal effect of *spxB* deletion on the transcriptome, inferred in our and other studies. Rather than relaying the metabolic state to regulatory pathways, Ac-P is a major energy reservoir for ATP synthesis. Likewise, in our study loss of *spxB* did not affect the steady-state ATP concentration (exponential cells). It has been suggested that maintenance of wild-type ATP levels is essential to cope with H_2O_2

imposed stress (Pericone *et al.*, 2003; Ramos-Montañez *et al.*, 2010). Our observation that the level of H_2O_2 produced under semi-aerobic conditions is 10-fold lower than that expected from a stoichiometry of one molecule of O_2 consumed per molecule of hydrogen peroxide formed attests to the presence of H_2O_2 scavenging mechanisms in strain D39. However, the presence of other O_2 consuming activities, such as NADH oxidase, cannot be ruled out, but the similarity of the carbon and redox balance values observed for strain D39 (Table 4.3) is in stark disagreement with the presence of high NADH-oxidase activity. When environmental oxygen is provided continuously (constant partial air tension of 40%), the yield of strain D39 was dramatically reduced to about 30% of the semi-aerobic level, while no significant difference in biomass was detected for strain D39*spxB*$^-$ (Fig. 4.4 and Fig. 4.7). In terms of fermentative products, oxygenation induced a mild shift to acetate production in the *spxB* mutant, denoting an alternative aerobic acetate producing pathway. The presence of a functional pyruvate dehydrogenase complex in the pneumococcus has been suggested, but is still to be proven (Taniai *et al.*, 2008; Ramos-Montañez *et al.*, 2010). On the other hand, lactate production was severely decreased and a switch to acetate and H_2O_2, which accumulated up to 2-3 mM, was observed in strain D39. This metabolic shift is in accordance with a higher cell demand for ATP, and is well known to occur in other *Streptococcaceae* as a response to stress conditions (aerobiosis, substrate limitation, poor substrates, etc.) (Neves *et al.*, 2005; Price *et al.*, 2011). Despite the substantially higher yields of acetate in strain D39, the biomass produced was much lower and the ATP concentration in exponential cells was comparable to that under semi-aerobic conditions (data not shown). An important implication from the combined results is that ATP is being redirected to other purposes, seemingly H_2O_2 detoxification. This view is further

corroborated by the growth properties of strain D39*spxB*$^{-}$ under the same conditions.

Despite the modest response of *spxB* deletion in the transcriptome of strain D39, we show in this study that SpxB affects the pattern of carbohydrate utilization in *S. pneumoniae*, and thereby is likely to contribute to the fitness of this microorganism in specific microenvironments. In line, it is reasonable to assume that the influence of environmental oxygen on capsule production and to a lesser extent on growth of *S. pneumoniae* is partially concurred by modulation of pyruvate oxidase activity. Interestingly, oxygen is one of the main environmental factors varying in host niches. In this light, the observed connection between capsule amount and oxygen-dependent SpxB activity is plausible. Based on our data we propose that in the nasopharynx, where the oxygen is high, improved SpxB activity restrains capsule production facilitating effective colonization. In contrast, in more internal host niches with no or very limited oxygen, SpxB activity is reduced which relieves the repressing effect on capsule production. This leads ultimately to a thicker capsule that allows *S. pneumoniae* to better evade the host immune system.

Acknowledgements

SM Carvalho was supported by Fundação para a Ciência e a Tecnologia (FCT), Ph.D. grant (SFRH/BD/35947/2007). The Portuguese team work was supported by FCT and FEDER, project PTDC/BIA-MIC/099963/2008 and through grant PEst-OE/EQB/LA0004/2011. The NMR spectrometers are part of The National NMR Network (REDE/1517/RMN/2005), supported by "Programa Operacional Ciência e Inovação (POCTI) 2010" and FCT. JJE Bijlsma is a Rosalind Franklin Fellow of the University Medical Center of Groningen (UMCG). H Gradstedt is funded by the Rosalind Franklin Fellowship of the UMCG.

Author's Contribution

Performed the experiments: SM Carvalho, VF Andisi, H Gradsted and JJE Bijlsma. Construction of mutants and plasmids, transcriptomics and β-galactosidase determination of *lacZ* reporter strains were performed by VF Andisi and JJE Bijslma. H Gradsted performed the TEM analysis of *S. pneumoniae*. Conceived and designed the experiments: SM Carvalho, VF Andisi, H Gradsted, OP Kuipers, AR Neves, JJE Bijlsma. Analyzed the data: SM Carvalho, VF Andisi, H Gradsted, OP Kuipers, AR Neves, JJE Bijlsma.

Chapter 5

The functional pyruvate formate-lyase (PFL) and PFL-activating enzymes of *Streptococcus pneumoniae*

The results of this chapter are published in:

H Yesilkaya, F Spissu, SM Carvalho, VS Terra, KA Homer, R Benisty, N Porath, AR Neves, PW Andrew (2009) "Pyruvate formate-lyase is required for pneumococcal fermentative metabolism and virulence". Infection and Immunity **77:** 5418-5427.

Chapter 5 – Contents

Summary

Knowledge of the *in vivo* physiology and metabolism of *S. pneumoniae* is limited, even though pneumococci rely on efficient acquisition and metabolism of the host nutrients for growth and survival. Under glucose excess conditions *S. pneumoniae* displays typical homolactic fermentation, but the nutrient-limited milieu of host tissues most likely favor mixed-acid fermentation. In fermentative Gram-positive bacteria, pyruvate formate-lyase (PFL), an enzyme that requires post-translational activation by pyruvate formate-lyase activating enzyme (PFL-AE), plays a key role in end-product distribution. Pneumococcal genomes possess two copies each of genes whose products show homology to PFL and PFL-AE. In this work, the functional PFL and PFL-AE enzymes were assigned. To this end, we generated by gene replacement loss-of-function mutants of the putative *pfl* genes, *spd_0235* and *spd_0420*, as well as the potential *pfl-ae* genes, *spd_0229* and *spd_1774*. End-product analysis showed that formate, the signature product of the reaction catalyzed by PFL, was still produced by *spd_0235* and *spd_0229* mutants, but not by *spd_0420* and *spd_1774*. These findings identify *spd_0420* and *spd_1774* as the genes encoding the pneumococcal PFL and PFL-AE, respectively.

Introduction

Energy metabolism is one of the most understudied fields of pneumococcal biology. The pneumococcus is strictly fermentative and sugars are the major sources of energy for biosynthesis and growth (Tettelin *et al.*, 2001; Hoskins *et al.*, 2001). Therefore *in vivo* fitness is to a large extent determined by the efficiency of sugar metabolism. Accumulating evidence suggests a direct link

between pneumococcal virulence and sugar metabolism (Spellerberg *et al.*, 1996; Auzat *et al.*, 1999; Giammarinaro and Paton, 2002; Iyer *et al.*, 2005; Iyer and Camilli, 2007). This connection is not limited to proteins involved in polysaccharide production/degradation, transport and regulation (Giammarinaro and Paton, 2002; Manco *et al.*, 2006), but also includes metabolic enzymes involved in redox metabolism, such as NADH oxidase (NOX) (Auzat *et al.*, 1999), and in pyruvate metabolism (Spellerberg *et al.*, 1996; Pericone *et al.*, 2003). For example, mutation of *nox* caused diminished virulence in a systemic infection model, and this was attributed to a probable change in the NADH/NAD^+ ratio or the increased sensitivity of *S. pneumoniae* to oxidative stress (Auzat *et al.*, 1999). Mutation of *spxB* (pyruvate oxidase) led to a reduction in virulence, in both pneumonia and sepsis models in mice, which was attributed to a decrease in the products of SpxB activity and downregulation of adhesive proteins (Spellerberg *et al.*, 1996; Regev-Yochay *et al.*, 2007; Ramos-Montañez *et al.*, 2008).

The pneumococcus is known to maintain a fermentative metabolism regardless of oxygen, since it lacks a complete set of genes required for respiration (Tettelin *et al.*, 2001; Hoskins *et al.*, 2001). Breakdown of carbohydrates by classical Embden-Meyerhof pathway results in generation of pyruvate, NADH and a net gain of two ATP per mole of substrate (Neves *et al.*, 2002a). In homolactic bacteria, NAD^+ regeneration is mainly accomplished via the lactate dehydrogenase (LDH) catalyzed conversion of pyruvate to lactate (Fig. 5.1) (Neijssel *et al.*, 1997). However, under certain conditions, such as aerobiosis, sugar limitation or the presence of sugars less preferred than Glc, such as Gal, there is a metabolic shift from homolactic (lactate production) to mixed-acid fermentation with the formation of products other than lactate (*e.g.* ethanol, acetate, and formate) (Fig. 5.1) (Neijssel *et al.*, 1997; Melchiorsen *et al.*, 2000; Neves *et al.*, 2002a). Mixed-acid fermentation is mediated in part by the activities

of the pyruvate dehydrogenase complex (PDHc), or pyruvate formate-lyase (PFL) (Neijssel *et al.*, 1997; Melchiorsen *et al.*, 2000; Neves *et al.*, 2002a). While PDHc catalyses the oxidative decarboxylation of pyruvate to form acetyl-CoA and CO_2 in aerobiosis, under microaerobic and anaerobic conditions, most of the pyruvate is converted to acetyl-CoA and formate by the oxygen-sensitive PFL (Neves *et al.*, 2002a; Zhu and Shimizu, 2004). Further metabolism of acetyl-CoA by phosphotransacetylase/acetate kinase, or by aldehyde and alcohol dehydrogenases leads to the generation of acetate or ethanol, respectively. While acetate formation generates an additional molecule of ATP, ethanol production from acetyl-CoA regenerates two molecules of NAD^+ (Melchiorsen *et al.*, 2000; Neves *et al.*, 2002a). Unlike other lactic acid bacteria (Yamada *et al.*, 1985; Arnau *et al.*, 1997), in *S. pneumoniae* no genes for PDHc activity have been predicted (Tettelin *et al.*, 2001; Hoskins *et al.*, 2001). The presence of a functional pyruvate dehydrogenase complex in the pneumococcus has been suggested, but is still to be proven (Taniai *et al.*, 2008; Ramos-Montañez *et al.*, 2010). Therefore, mixed-acid fermentation is expected to occur mainly by the action of PFL. The regulation of PFL activity in other bacteria has been reported to arise at three levels (Sauter and Sawers, 1990; Knappe and Sawers, 1990). PFL is synthesized as an inactive enzyme and then post-translationally converted to an active form by accepting an electron from the PFL-activating enzyme (PFL-AE) (Buis and Broderick, 2005). PFL may also be regulated transcriptionally, and allosterically (Asanuma *et al.*, 2004). In *L. lactis*, transcription of *pfl* was found to be significantly higher when the organism was grown in Gal as compared to Glc-containing media (Arnau *et al.*, 1997; Melchiorsen *et al.*, 2000). In addition, in other lactic acid bacteria, low pH and excess supplies of energy reduced *pfl*–mRNA levels, while the level of *ldh*-mRNA increased (Asanuma *et al.*, 1999). The regulation of PFL is allosterically controlled in *L. lactis* by the glycolytic intermediates fructose 1,6-bisphosphate

(FBP), glyceraldehydes 3-phosphate (GAP) and dihydroxyacetone phosphate (DHAP), which are strong inhibitors of PFL (Melchiorsen *et al.*, 2001).

The sequenced genome of *S. pneumoniae* D39 strain has two copies of both the *pfl,* annotated as *spd_0235* and *spd_0420*, and *pfl-ae* homologs, annotated as *spd_0229* and *spd_1774* (Tettelin *et al.*, 2001; Hoskins *et al.*, 2001; Lanie *et al.*, 2007). However, the role of the PFL/PFL-AE system in pneumococci is not known, despite the fact that *spd_0420* and *spd_1774* were predicted to be among the highest expressed genes based on codon usage (Karlin *et al.*, 2004). In addition, it is not clear why the pneumococcus has multiple copies of these genes. Given that host tissues are limited environments for free readily fermented sugars (Philips *et al.*, 2003), such as Glc, but are rich in glycoproteins with O- and N-linked glycans that contain monosaccharides including Gal (Sheehan *et al.*, 1995), and because deep tissue sites are hypoxic, both conditions that favor mixed-acid fermentation (reviewed in Neves *et al.*, 2005), we hypothesized that the PFL/PFL-AE system must be important for the *in vivo* fitness of the pneumococcus. In this Chapter, we identified the genes responsible for pneumococcal PFL activity by relying on a bioinformatic analysis and on the fermentation types of wild-type and putative mutant *pfl* and *pfl-ae* strains. A detailed description of the impact of the assigned *pfl* and *pfl-ae* genes on the expression of selected genes involved in glycolysis, on lipid composition of cell membrane and on virulence can be found on the published version of this Chapter (Yesilkaya *et al.*, 2009), which is provided in digital form on the included CD.

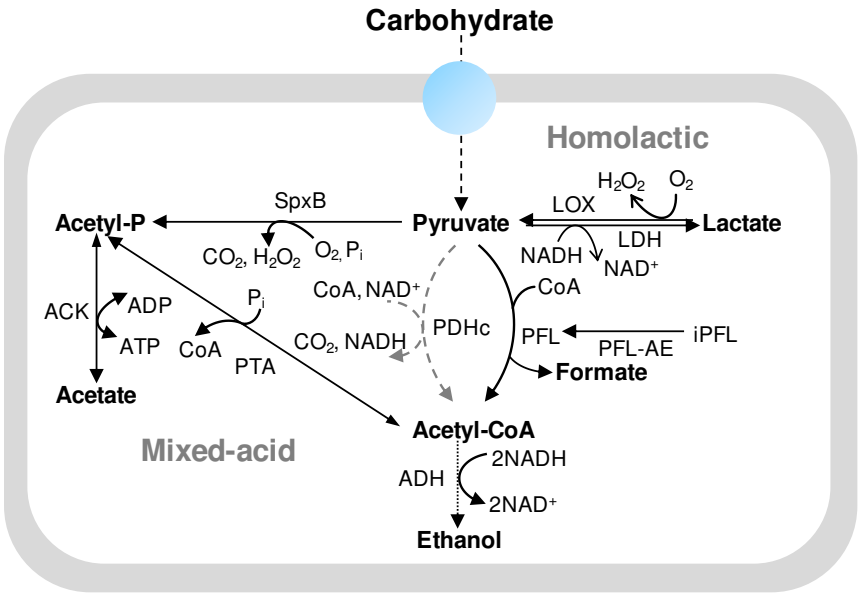

Fig. 5.1. Schematic representation of reactions downstream of pyruvate in lactic acid bacteria. Glc or Gal are converted to pyruvate which is then further catabolized by homolactic or mixed-acid fermentation pathways. LDH, lactate dehydrogenase; PFL, pyruvate formate-lyase; iPFL, inactive pyruvate formate-lyase; PFL-AE, pyruvate formate-lyase activating enzyme; PDHc, pyruvate dehydrogenase complex; SpxB, pyruvate oxidase; ADH, bifunctional acetaldehyde-CoA/alcohol dehydrogenase; ACK, acetate kinase; PTA, phosphotransacetylase. The occurrence of the pyruvate dehydrogenase complex (PDHc) depicted in grey remains to be proved.

Materials and Methods

Bacterial growth conditions

S. pneumoniae type 2 strain D39 and its isogenic mutants were used in this work. Routinely, pneumococci were grown at 37ºC in microaerophilic conditions either in brain heart infusion broth (BHI) (Oxoid, Basingstoke, UK) or

on Blood Agar Base (Oxoid) supplemented with 5% (vol/vol) horse blood. When appropriate the growth medium was supplemented with 100 µg ml^{-1} spectinomycin or 500 µg ml^{-1} kanamycin.

Bacteria were also grown in CDM (Chapter 2) at 37ºC without pH control (initial pH 6.5). Glc (1% wt/vol) or Gal (1% wt/vol) was used as the carbon source. *S. pneumoniae* was grown under anaerobic conditions in rubber-stoppered bottles (200 ml). Aerobic growth was established under low oxygen tension in Erlenmeyer flasks with an agitation of 50 rpm. Growth was monitored by measuring the optical density at 600 nm. Growth rates (µ) were calculated through linear regressions of the plots of $ln(OD_{600})$ *versus* time during the exponential growth phase.

Mariner mutagenesis

In vitro mariner mutagenesis was used to construct the mutants (Martin *et al.*, 2000). Approximately 2 kb genomic regions containing the target genes were amplified with the appropriate primers (Table 5.1). For transposition reactions approximately 200 ng of PCR fragments were mixed with 200-400 ng of donor mariner plasmid pR412, which contains a spectinomycin resistance cassette, and incubated in the presence of purified *Himar1* transposase, as described previously (Martin *et al.*, 2000). Gaps in transposition products were repaired with T4 DNA polymerase (New England Biolabs, Ipswick, USA) and subsequently by *E. coli* ligase (New England Biolabs). Repaired transposition products were transformed into *S. pneumoniae* D39 using synthetic competence-inducing peptide (Alloing *et al.*, 1996). Transformants isolated from selective medium were tested for the presence of mariner mini-transposons through PCR and sequencing. One of the transposon-specific primers, MP127 and MP128 (Table 5.1), was used in PCR, together with an appropriate chromosomal primer. In

addition, chromosomal primers were also used to confirm the absence of the intact copy of the gene that may result due to duplication. Typical PCR conditions consisted of 1 cycle of 95ºC denaturation, 35 cycles of amplification (30 s denaturation at 94ºC, 60 s annealing at 53-55ºC, and 3 min extension at 72ºC) with a final 3 min of final extension at 72ºC. The amplification products were analyzed by agarose (1% wt/vol) gel electrophoresis. In addition, the exact insertion sites and direction of the antibiotic cassette were also determined by sequencing. The amplicons for sequencing were prepared by three rounds of PCR using MP128 primer as described previously (Karlyshev *et al.*, 2000), and then the purified products were sequenced using the MP127 primer. Sequencing indicated that the spectinomycin cassette had been inserted in 608-bp, 833-bp, 650-bp and 116-bp away from the 5'-end of *spd_0229, spd_0235, spd_0420*, and *spd_1774*, respectively. SPD0229M, SPD0235M, SPD0420M, and SPD1774M (mutated in *spd_0229*, *spd_0235*, *spd_0420* and *spd_1774*, respectively) (Fig. 5.2), were selected for further study.

Table 5.1. Oligonucleotide primers used in this study

Primer ID	Primer Sequence (5'-3')	Target gene in D39
SPD0229F	ACCTCCTGATAAAGTTAAACC	*spd_0229*
SPD0229R	ACGACTAGCGAACCACCG	*spd_0229*
SPD0235F	CAGCCTTACTGAAAGGATG	*spd_0235*
SPD0232R	GGGTTGCCTTAGAAAGAAC	*spd_0235*
SPD0420F	GACAGTTGTTGAAGCACAAG	*spd_0420*
SPD0420R	CTCAATGCATCCAAGGCATC	*spd_0420*
SPD0420CF	GTCCATGGATGGTTGTTAAGACAGTTGTTGAAG	*spd_0420*
SPD0420CR	GTGGATCCTTAGCTCAATGCATCCAAGG	*spd_0420*
MalF	GCTTGAAAAGGAGTATACTT	NA*
PCEPR	AGGAGACATTCCTTCCGTATC	NA*
SPD1774F	AGACACTTGGGCTATGGA	*spd_1774*
SPD1774R	GTTCCTTAGCCTTGGTGA	*spd_1774*
MP 127	CCGGGGACTTATCAGCCAACC	pR412-specific (Martin *et al*., 2000)
MP 128	TACTAGCGACGCCATCTATGTG	pR412-specific (Martin *et al*., 2000)

The underlined sequenced in SPD0420F and SPD0420R complementation primers indicate NcoI and BamHI recognition sites, respectively. NA, not applicable. (*) The recognition sites for MalF and PCEPR are in pCEP (Guiral *et al*., 2006).

Complementation of SPD0420M

To eliminate the possibility of polar effect, SPD0420M was complemented by introduction of an intact copy of *spd_0420* using pCEP, which is a nonreplicative plasmid and allows controlled gene expression following ectopic integration into the chromosome (Guiral *et al*., 2006). The plasmid integrates immediately downstream of the well-studied *ami* operon (Alloing *et al*., 1996). This site is believed to be transcriptionally silent and, as far as it is known, does not affect any cellular functions (Guiral *et al*., 2006). The intact copy of *spd_0420* was

amplified with SPD0420CF and SPD0420CR primers, which incorporate, NcoI and BamHI sites to 5'- and 3'- end of the gene, respectively (Table 5.1). The amplicons were digested with NcoI and BamHI, and the digested products were ligated with NcoI/BamHI digested pCEP. An aliquot of ligation mixture was directly transformed into SPD0420M as described previously (Alloing *et al.*, 1996), and the transformants were selected in the presence of spectinomycin and kanamycin. The successful introduction of the intact copy of the gene was confirmed by PCR using malF and pCEPR primers (Table 5.1), whose recognition sites are localized in immediately up and downstream of the cloning site, respectively. One of the positive transformants, SPD0420Comp, was selected for further analysis.

Quantification of fermentation products during growth

Strains were grown as described above. Culture samples (2 ml) were taken at the beginning of the stationary phase of growth, centrifuged (16,000 x *g*, 2 min, 4ºC), and the supernatants were stored at -20ºC until analysis by high performance liquid chromatography (HPLC) or ^{1}H-NMR (Neves *et al.*, 2002a). End-products were quantified using a HPLC apparatus equipped with a HPX-87H anion exchange column (Bio-Rad Laboratories Inc., CA, USA) and a refractive index detector (Shodex RI-101, Showa Denko K. K., Japan) operating at 60ºC, with 5 mM H_2SO_4 as the eluent at a flow rate of 0.5 ml min^{-1} (Neves *et al.*, 2002a). Alternatively, quantification of metabolites in the supernatants was performed by ^{1}H-NMR using a Bruker Avance II 500 MHz spectrometer. ^{1}H-NMR spectra were acquired with water presaturation, a 5.5-µs pulse width corresponding to a 70º flip angle, and a repetition delay of 50 s. Spectra were referenced to the resonance of 3-(trimethylsilyl) propanesulfonic acid (sodium salt), designated as 0 ppm. Formic

acid (sodium salt) was added to the samples as an internal concentration standard.

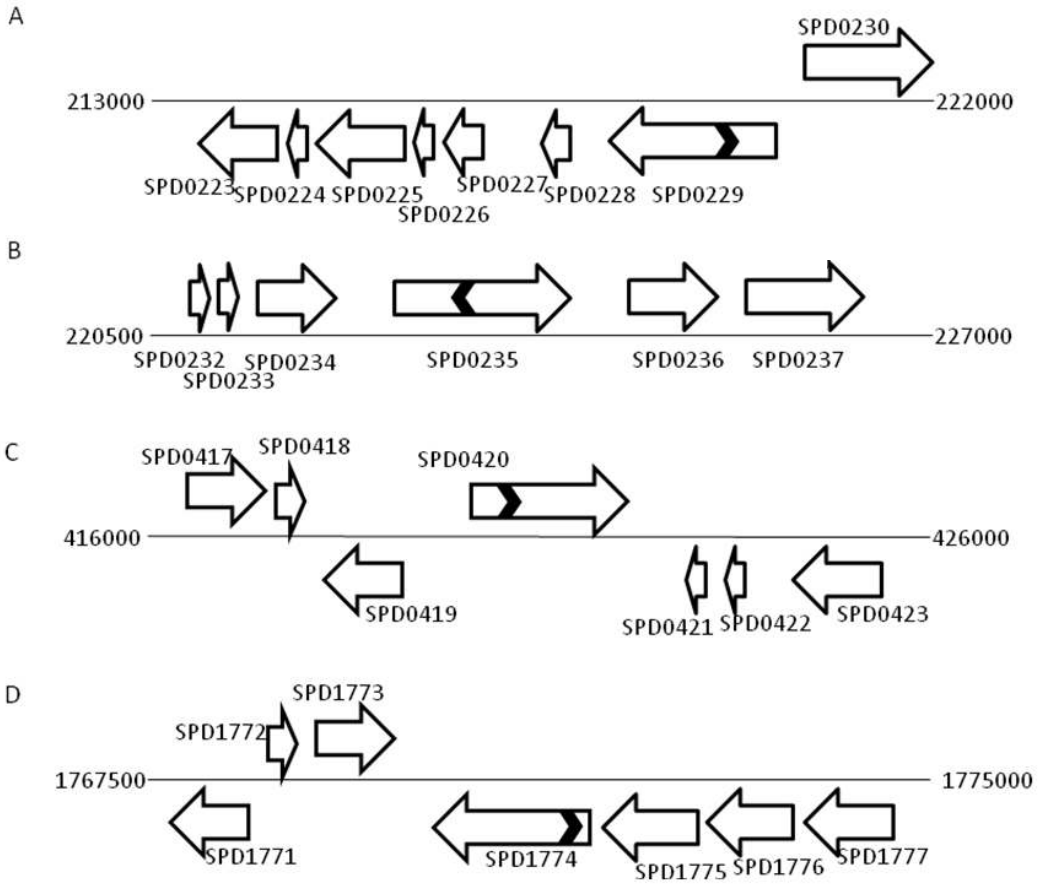

Fig. 5.2. Schematic representation of genomic regions containing putative *pfl* (*spd_0235* and *spd_0420*) (B and C) and *pfl-ae* (*spd_0229* and *spd_1774*) (A and D). The chromosome is represented with a thin solid line and genes are shown with a block arrow. The chevrons in *spd_0229*, *spd_0235*, *spd_0420* and *spd_1774*, represent approximate position of insertion (see text for details), and direction of chevrons represent the orientation of the spectinomycin cassette. Diagram is not drawn to scale.

Results

Bioinformatic analysis

The putative *pfl* genes, *spd_0235* and *spd_0420*, are found in all sequenced pneumococcal genomes (Tettelin *et al.*, 2001; Hoskins *et al.*, 2001; Lanie *et al.*, 2007). The predicted amino acid sequences of *spd_0235* and *spd_0420* exhibit 20% identity over 770 amino acids. While SPD0420 has conserved adjacent cysteinyl residues characteristic of a PFL active site (EMSCISCCVSPLD) (Sawers and Watson, 1998), as well as the highly conserved peptide sequence around the C-terminal glycyl residue (RISGY) (Sawers and Watson, 1998), SPD0235 does not have the conserved cysteine residues. This implies that *spd_0235* is unlikely to be encoding a PFL in spite of the annotation. However, it has a sequence motif containing the C-terminal glycyl residue (RVAGY), which is converted to a free radical in the PFL of *E. coli* (Weidner and Sawers, 1996; Vey *et al.*, 2008). Thus SPD0235 may be a member of a distinct class of glycyl radical enzymes with conserved pentapeptide region containing the C-terminal glycyl residue, albeit without PFL activity. This class of proteins is also found in *E. coli* but so far no function has been attributed to them (Sawers and Watson, 1998). In the vicinity of *spd_0235* there are cellobiose-specific sugar phosphotransferase (*spd_0234*) and fructose 6-phosphate aldolase (*spd_0236*) genes (Fig. 5.2) in all sequenced pneumococcal genomes, suggestive of a conserved nature of this *locus* (Tettelin *et al.*, 2001; Hoskins *et al.*, 2001; Lanie *et al.*, 2007). On the other hand, *spd_0420* is surrounded by a DNA-polymerase gene (*dinP*, *spd_0419*), and a hypothetical gene of unknown function (*spd_0421*) (Tettelin *et al.*, 2001; Hoskins *et al.*, 2001; Lanie *et al.*, 2007). The genes adjacent to *spd_0420* are transcribed in opposite directions (Fig. 5.2), implying that the mutation of *spd_0420* is unlikely to create a polar effect, and furthermore, a strong

rho-independent transcription terminator with an estimated ΔG_f of -12.3 kcal mol^{-1} is located 17-bp downstream of the *spd_0420* stop codon. While *dinP* is conserved universally in all sequenced pneumococcal genomes, the hypothetical gene (*spd_0421*) exhibits either sequence variation or is absent in certain pneumococcal genomes, such as in TIGR4 or Hungary19A_6, indicating that recent evolutionary genetic events have taken place in the region (www.ncbi.nlm.nih.gov). In contrast to *E. coli*, *H. influenzae* and *Clostridium pasteurianum* (Sauter and Sawers, 1990; Fleischmann *et al.*, 1995; Weidner and Sawers, 1996), in *S. pneumoniae* none of the putative *pfl* and *pfl-ae* are adjacently located, which is also a feature of the *pfl/pfl-ae* system in lactococci (Arnau *et al.*, 1997). The predicted amino acid sequence of the putative PFL-AE proteins, SPD0229 and SPD1774, share 32% identity over 236 amino acids, and they are found in all sequenced pneumococcal genomes (www.ncbi.nlm.nih.gov). Both of these proteins have a CXXXCXXC consensus sequence motif close to the N-terminus of the protein, which is reported to be the catalytic site in the *E. coli* enzyme (Buis and Broderick, 2005). *Spd_1774* is the last gene of a predicted operon (Ermolaeva *et al.*, 2001) and is surrounded by genes responsible for protein export (*spd_1773*) and pH homeostasis (*spd_1775*), while the *locus* encompassing *spd_0229* contains genes encoding for transcriptional regulators.

End-product analysis

The PFL enzyme can be measured directly (Yamamoto *et al.*, 2000) or indirectly (Arnau *et al.*, 1997). The indirect assay relies on formate detection in bacterial culture supernatants to indicate the presence of active enzyme. In this study we used the indirect method to assay PFL activity. The fermentation end-products of pneumococcal strains in aerobiosis and anaerobiosis, in CDM with Glc or Gal as sole carbon source, were analyzed using late-exponential culture

supernatants. Regardless of aeration, when Glc was used, the main fermentation product of D39 was lactate, with a small amount of acetate (Fig. 5.3-A). However, replacement of Glc with Gal led to the generation of mixed fermentation products, under both aerobic and anaerobic conditions, with formate being the most abundant metabolite in both cases (Fig. 5.3-A). Additionally, acetate and ethanol were also formed, and the ratio of products was approximately 2:1:1 for formate, acetate, and ethanol, both in aerobiosis and anaerobiosis. The end-product analysis of SPD0229M and SPD0235M was principally similar to D39 in the presence of Glc and Gal regardless of aeration, ruling out their involvement in active PFL synthesis (data not shown). On the other hand, in SPD0420M and SPD1774M culture supernatants the main end-product was lactate in all growth conditions, and no formate was detected under any of the conditions employed, indicating that these two genes are responsible for active PFL synthesis (Fig. 5.3-B and 5.3-D). Introduction of an intact copy of *spd_0420* to SPD0420M restored formate production (Fig. 5.3-C). In the light of sequence homology and end-product analysis, it is likely that *spd_0420* is responsible for PFL synthesis, and *spd_1774* is the putative PFL-AE.

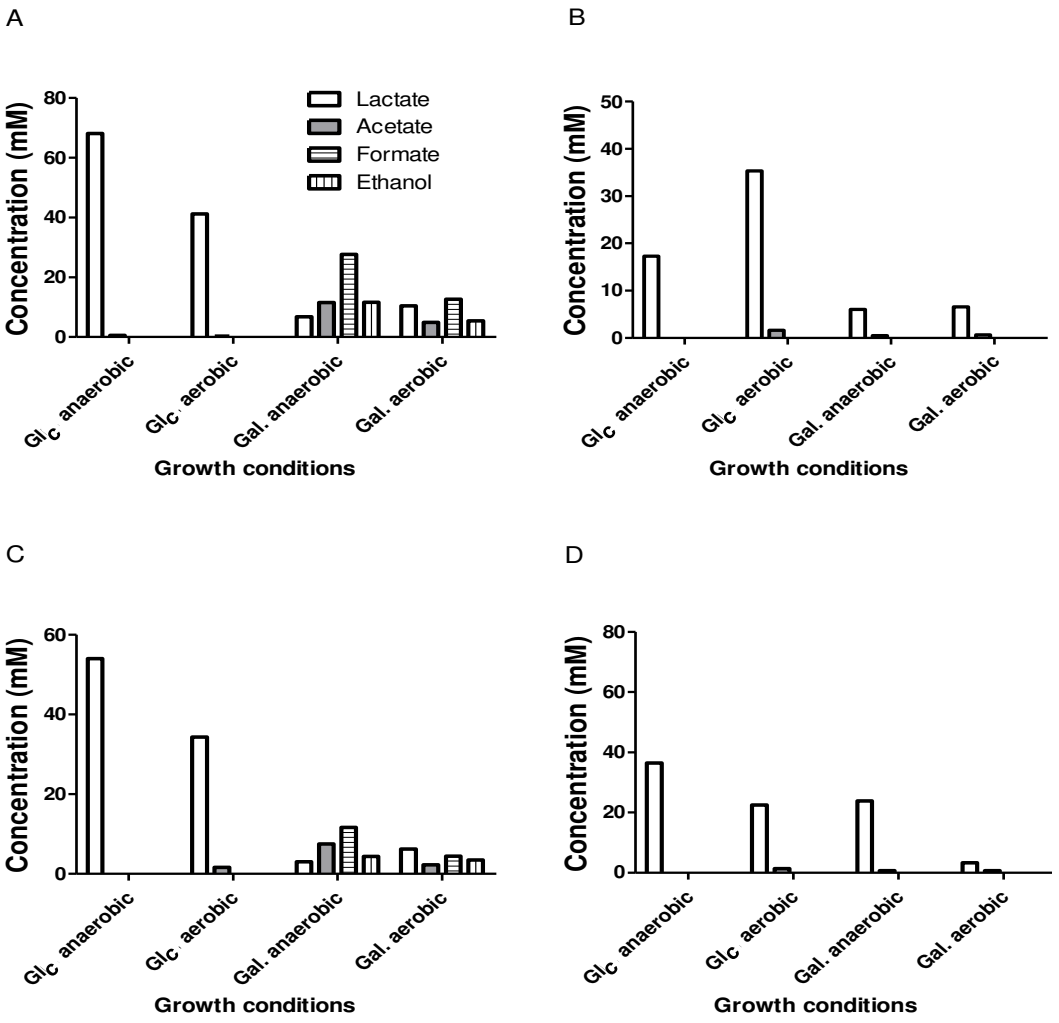

Fig. 5.3. Fermentation end-product analysis for strains D39 (A), SPD0420M (B), SPD0420Comp (C) and SPD1774M (D). The pneumococcal strains were grown in CDM containing glucose or galactose, aerobically or anaerobically. Glc, glucose; Gal, galactose. Each metabolite concentration was measured in duplicate in supernatants of three independently grown cultures.

Discussion

The transition from aerobiosis to an oxygen depleted environment signifies passage from mucosal surfaces to deep tissue sites for the pneumococcus, hence it is integral to pneumococcal virulence (reviewed in Kadioglu *et al.*, 2008). This move is expected to trigger a fundamental change in energy metabolism due to differences in nutrient availability and oxygen concentration (Philips *et al.*, 2003). We investigated biochemical aspects of these changes and the implication of this metabolic shift on pneumococcal virulence. In many microorganisms, PFL is one of the key enzymes for anaerobic energy metabolism, especially in the metabolic shift to mixed-acid fermentation (Arnau *et al.*, 1997; Melchiorsen *et al.*, 2000; Asanuma *et al.*, 2004; Derzelle *et al.*, 2005). We demonstrated that the pneumococcal *spd_0420* and *spd_1774* are responsible for active PFL protein, through mutational studies and subsequent metabolite analysis, and by an *in silico* approach. The mutant strains did not produce formate, which is generated only in the presence of active PFL, and a homology search indicated conserved residues that are found in other PFLs (Sawers and Watson, 1998). The mutation of *spd_0420* and *spd_1774* led to a reduction in virulence, as manifested by increased survival time of animals infected with SPD0420M and SPD1774M compared to the parental strain, and the bacteremia was developed later in cohorts infected with SPD0420M and SPD1774M than in D39 (manuscript by Yesilkaya *et al.*, 2009 provided on the CD). Moreover, growth of SPD0420M was attenuated in the nasopharynx and lungs, showing that PFL contributes to pneumococcal virulence in several tissue sites (Yesilkaya *et al.*, 2009, on the CD). Initially, we predicted that the main impact of PFL would be seen in the hypoxic environment of blood (Levy, 2005), and no role was envisaged during infection of the nasopharynx and lungs, because PFL was expected to be inactivated in these

oxygenated sites. Our results indicate that the pneumococcal PFL may not be as susceptible to oxygen as other bacterial PFLs (Knappe *et al.*, 1993). Indeed, it has been reported previously that PFL in *S. mutans* and *L. lactis* is relatively resistant to inactivation by oxygen compared to the *E. coli* enzyme (Yamada *et al.*, 1985; Arnau *et al.*, 1997). This could be due to the presence of a deactivation system that may protect the PFL (Melchiorsen *et al.*, 2000; Nnyepi *et al.*, 2007). PFL deactivation was suggested to occur through removal of the glycyl free radical, which is required for the active PFL, by alcohol dehydrogenase during the transition from anaerobic to aerobic growth (Sawers and Watson, 1998). Hence, future detailed structural and biochemical characterization is required to establish the mechanism of the oxygen resistant nature of the pneumococcal PFL. The second reason for attenuated virulence of strains lacking active PFL could be differences in overall sugar and oxygen composition in different tissue sites. For example the mucosal sites of nasopharynx and lungs are rich in Gal whereas blood is in Glc (Philips *et al.*, 2003). Hence, as Gal triggers mixed-acid fermentation mediated by PFL, it is expected that the lack of PFL will attenuate virulence in mucosal sites because of composition of sugars, and in blood because of low oxygen concentration.

The detailed analysis of reduction in SPD0420M and SPD1774M virulence was beyond the scope of this study. However, we speculate that the decreased virulence was due to reduction in ATP generation, which would have an adverse impact on diverse metabolic functions. Alternatively, the defect in PFL synthesis may affect purine synthesis, as was reported in *S. thermophilus* (Derzelle *et al.*, 2005). In addition, diminished synthesis of acetyl-CoA may influence virulence through its impact on choline and fatty-acid biosynthesis (Campbell and Cronan, 2001; Derzelle *et al.*, 2005). A small but significant change in membrane fatty-acid composition was detected in both SPD0420M and SPD1774M, due, most

probably, to shortage of acetyl-CoA in the mutant strains (Yesilkaya *et al.*, 2009, on the CD). Other studies have also shown that small changes in fatty-acid composition are meaningful, and account for membrane fatty-acid adaptation to stress conditions, such as temperature, H_2O_2, and pH (Guerzoni *et al.*, 2001; Di Pasqua *et al.*, 2006). Since the growth rate of bacteria depends on membrane fluidity (Zaritsky *et al.*, 1985), the lower fatty-acid unsaturation level is likely to explain the reduced growth rate in the mutant strains compared to the wild-type, thus affecting their virulence in mice (Yesilkaya *et al.*, 2009, on the CD).

PFL is post-translationally regulated by PFL-AE, which activates PFL by generation of a stable and catalytically essential glycyl radical at G734 of PFL (based on the *E. coli* PFL amino acid sequence). In *E. coli*, induction of *pfl* in anaerobiosis has been shown to involve both FNR and ArcA/ArcB regulators (Sawers and Watson, 1998; Melchiorsen *et al.*, 2000; Melchiorsen *et al.*, 2001). The global transcription factor FNR was reported to have a role in the expression of *pfl* via two recognition sequences located in the promoter region of this gene (Kaiser and Sawers, 1995). However, there is no *fnr* homolog in *S. pneumoniae* but the pneumococcal genomes contain homologs of ArcA/ArcB transcriptional regulators (data not shown).

In addition to *spd_0420* and *spd_1774*, *spd_0235* and *spd_0229* closely resemble *pfl* and *pfl-ae* genes, respectively. However, under the conditions tested these genes are not involved in the synthesis of an active PFL. Genomic analysis in *E. coli* indicated the presence of several *pfl-* and *pfl-ae*-like genes (Sauter and Sawers, 1990; Sawers and Watson, 1998). Many of these PFL-like enzymes are unlikely to have a role in the dissimilation of 2-keto acids, and therefore they may represent new classes of glycyl radical enzymes with novel enzymatic activities (Sauter and Sawers, 1990; Sawers and Watson, 1998).

In this study we identified the pneumococcal *pfl* and *pfl-ae* and demonstrated their involvement in mixed-acid fermentation. It was found that the mutation of *pfl* results in reduced pneumococcal virulence, indicating a strong link between the ability to have flexible fermentative metabolism and virulence (Yesilkaya *et al.*, 2009, on the CD). The reduced virulence was probably due to a defect in ATP and acetyl-CoA biosynthesis, which affects fitness and fatty-acid composition, respectively (Yesilkaya *et al.*, 2009, on the CD). At mucosal surfaces the concentration of Glc is low, but the pneumococcus is exposed to mucin at these sites and mucin is rich in Gal-containing glycosides (Sheehan *et al.*, 1995; Yesilkaya *et al.*, 2008). Recently it was demonstrated that the pneumococcus has the ability to utilize mucin (Yesilkaya *et al.*, 2008). In light of the available data, we conclude that the pneumococcus maintains mixed-acid fermentation in the nutrient limited niches of the host, and an active PFL plays a vital role in this metabolic event. Thus, future studies investigating pneumococcal virulence should not define virulence solely from the host perspective, but the intricacies of the environmental settings surrounding the microorganism should also be considered.

Acknowledgements

SM Carvalho was supported by Fundação para a Ciência e a Tecnologia (FCT), Ph.D. grant (SFRH/BD/35947/2007). This work was supported by The Wellcome Trust (078763/Z/05/Z) and by FCT, project PDCT/BIA-MIC/56235/2004. We thank Dr Marc Prudhomme for kindly providing pCEP and pR412.

Author's Contribution

Performed the experiments: H Yesilkaya, F Spissu, SM Carvalho, VS Terra, KA Homer, R Benisty. SM Carvalho performed the metabolic analysis of *pfl* and *pfl-ae* mutants. Conceived and designed the experiments: H Yesilkaya, F Spissu, SM Carvalho, VS Terra, KA Homer, R Benisty, N Porath, AR Neves, PW Andrew. Analyzed the data: H Yesilkaya, F Spissu, SM Carvalho, VS Terra, KA Homer, R Benisty, N Porath, AR Neves, PW Andrew.

Chapter 6

CcpA ensures optimal metabolic fitness of *Streptococcus pneumoniae*

The results of this chapter are published in:
SM Carvalho, T Kloosterman, OP Kuipers, AR Neves (2011) "CcpA ensures optimal metabolic fitness of *Streptococcus pneumoniae*". PLoS ONE. **6:** e26707

Chapter 6 – Contents

Summary

In Gram-positive bacteria, the transcriptional regulator CcpA is at the core of catabolite control mechanisms. In the human pathogen *S. pneumoniae*, links between CcpA and virulence have been established, but its role as a master regulator in different nutritional environments remains to be elucidated. Thus, we performed whole-transcriptome and metabolic analyses of *S. pneumoniae* D39 and its isogenic *ccpA* mutant during growth on Glc or Gal, rapidly and slowly metabolized carbohydrates presumably encountered by the bacterium in different host niches. CcpA affected the expression of up to 19% of the genome covering multiple cellular processes, including virulence, regulatory networks and central metabolism. Its prevalent function as a repressor was observed on Glc, but unexpectedly also on Gal. Carbohydrate-dependent CcpA regulation was also observed, as for the tagatose 6-phosphate pathway genes, which were activated by Gal and repressed by Glc. Metabolite analyses revealed that two pathways for Gal catabolism are functionally active, despite repression of the Leloir genes by CcpA. Surprisingly, Gal-induced mixed-acid fermentation apparently required CcpA, since genes involved in this type of metabolism were mostly under CcpA-repression. These findings indicate that the role of CcpA extends beyond transcriptional regulation, which seemingly is overlaid by other regulatory mechanisms. In agreement, CcpA influenced the level of many intracellular metabolites potentially involved in metabolic regulation. Our data strengthen the view that a true understanding of cell physiology demands thorough analyses at different cellular levels. Moreover, integration of transcriptional and metabolic data uncovered a link between CcpA and the association of surface molecules (*e.g.* capsule) to the cell wall. Hence, CcpA may play a key role in mediating the interaction of *S. pneumoniae* with its host. Overall, our results support the

hypothesis that *S. pneumoniae* optimizes basic metabolic processes, likely enhancing *in vivo* fitness, in a CcpA-mediated manner.

Introduction

The survival of bacterial pathogens in different host environments depends largely on the expression of specific virulence factors (reviewed in Mitchell, 2003; Kadioglu *et al.*, 2008), but also on recognition of nutrients and rapid adaptation to their availability in fluctuating environments. Human bacterial pathogens are heterotrophs that depend on carbon sources to generate energy and catabolic intermediates for growth. In many bacteria, adaptation to changing carbon sources is accomplished through a regulatory mechanism called carbon catabolite control (for reviews see Deutscher *et al.*, 2006; Görke and Stülke, 2008). At the molecular level, carbon catabolite control can be achieved through different regulatory mechanisms, namely transcription activation and repression of genes by global regulators, control of translation by RNA-binding proteins, and allosteric regulation, in response to a preferred carbon source. Overall, these phenomena ensure that carbon sources yielding a maximum profit for growth are utilized first.

In low-GC Gram-positive organisms, such as *B. subtilis* and *L. lactis,* Glc is generally the preferred carbohydrate and the catabolite control protein A (CcpA) is the main transcriptional regulator functioning at the core of carbon catabolite control (Zomer *et al.*, 2007; Lulko *et al.*, 2007). CcpA binds to DNA at catabolite-responsive element (*cre*) sites, the location of which, relative to the promoter region, determines whether it acts as a transcriptional inhibitor or activator (Zomer *et al.*, 2007; Lulko *et al.*, 2007). The *cre*-binding activity of CcpA is enhanced by interaction with the phosphoprotein HPr, a component of the multi-protein phospho*enol*pyruvate: carbohydrate phosphotransferase system (PTS-system),

when phosphorylated at serine 46 ($HPr_{(Ser46)}$~P) by a fructose 1,6-bisphosphate (FBP) activated kinase (reviewed in Deutscher *et al.*, 2006).

Although the mechanisms by which catabolite control is exerted are among the most studied in model bacteria, a paucity of data hampers our understanding on how human pathogens adapt to different host environments. In the pathogenic streptococci, increasing evidence supports key roles of CcpA and $HPr_{(Ser46)}$~P (Iyer *et al.*, 2005; Abranches *et al.*, 2008; Shelburne *et al.*, 2008b; Zeng and Burne, 2010). Notably, CcpA was shown to influence a high percentage of genes in *S. mutans* (about 9%) and *S. pyogenes* (up to 20%), including the production of a number of virulence factors (Abranches *et al.*, 2008; Shelburne *et al.*, 2008b).

S. pneumoniae is a major cause of life threatening diseases including pneumonia, meningitis and septicaemia, as well as other less severe but highly prevalent infections (*e.g.* otitis media). Pneumococcal disease is preceded by colonization of the human nasopharynx, *S. pneumoniae*'s natural habitat. It is well established that progression from carriage to pneumococcal invasion is associated with changes in expression of virulence factors, such as capsule and surface proteins (reviewed in Mitchell, 2003; Kadioglu *et al.*, 2008), but the basic metabolic mechanisms underlying these adaptations remain elusive. Unrelated studies have clearly shown that CcpA influences the expression of genes involved in pneumococcal carbohydrate metabolism (Giammarinaro and Paton, 2002; Iyer *et al.*, 2005; Kaufman and Yother, 2007). Furthermore, CcpA has been implicated in the regulation of virulence factors, namely expression of genes in the capsule (*cps*) *locus* (Giammarinaro and Paton, 2002) and was proven necessary for colonization of the nasopharynx and survival in the lungs (Iyer *et al.*, 2005). Curiously, CcpA-independent catabolite repression of metabolic enzymes was a recurrent observation, leading to a view that minimized the role of CcpA as a

master regulator of catabolite control in *S. pneumoniae* (Giammarinaro and Paton, 2002; Iyer *et al.*, 2005).

In this work, the impact of CcpA on pneumococcal physiology was reappraised by combining genome-wide transcriptomics with metabolite analysis of *S. pneumoniae* D39 and its isogenic *ccpA* mutant. Our approach is in line with the current view that true understanding of a microbial metabolism requires quantitative analyses of system components at different cellular levels (Heinemann and Sauer, 2010). A major question was whether *S. pneumoniae* regulates expression of carbohydrate utilization genes and virulence factors in a carbohydrate-dependent, CcpA-mediated manner. Hitherto, the information available has largely been limited to the response of a few specific metabolic genes involved in carbohydrate utilization (Giammarinaro and Paton, 2002; Iyer *et al.*, 2005; Kaufman and Yother, 2007). For our global studies, Glc and Gal were used as carbon sources for the growth of *S. pneumoniae*. This choice was based on the following: Glc is the most common preferred carbohydrate, and is also found in considerable amounts in the bloodstream and during infection in the respiratory tract of the host (Philips *et al.*, 2003). Gal, generally a slowly metabolized non-preferred carbohydrate, was selected among other host-derived carbohydrates as this monosaccharide is one of the prevailing carbohydrates encountered by the pneumococcus in the human nasopharynx (colonization state) (Yesilkaya *et al.*, 2008; King, 2010). Our data show that CcpA influences the expression profile of central and carbohydrate-specific metabolic genes of *S. pneumoniae* as well as virulence factor-encoding genes in a carbohydrate-dependent and independent manner. These results enhance our understanding of how CcpA-mediated regulation can contribute to the metabolic fitness of *S. pneumoniae* in the host, which further supports the view that virulence and basic microbial physiology are closely intertwined.

Materials and Methods

Bacterial strains, media and growth conditions

Strains and plasmids used in this study are shown in Table 6.1. *S. pneumoniae* strains were grown as standing cultures without aeration in M17 broth (Difco^{TM}) containing Glc 0.5% (w/v) or on Glc-M17 (0.5% w/v) agar plates with 1% (v/v) defibrinated sheep blood (Johnny Rottier) at 37ºC. When appropriate 150 µg ml^{-1} spectinomycin, 2.5 µg ml^{-1} chloramphenicol, 0.25 µg ml^{-1} erythromycin or 15 µg ml^{-1} trimethoprim were added to the medium. Capsule quantification, transcriptomic and metabolic experiments were performed with cells grown in CDM (Chapter 2) in static flasks at 37ºC without pH control (initial pH 6.5). Glc (56 ± 1mM) or Gal (57 ± 1mM) was used as the carbon source. For complementation studies, nisin was added at time zero. Growth of the cultures was monitored by measuring optical density at 600 nm every hour. Maximum specific growth rates (μ_{max}) were calculated through linear regressions of the plots of ln (OD_{600}) *versus* time during the exponential growth phase.

Molecular techniques

Chromosomal DNA isolation was performed according to the procedure of Johansen and Kibenich (Johansen and Kibenich, 1992). Plasmid isolation was carried out using the plasmid isolation kit from Roche. *Phusion* DNA polymerase (Roche), T4 DNA ligase (Roche) and restriction enzymes (Fermentas) were used according to the recommendations described by the suppliers. Purification of the PCR products was performed using the High pure PCR product purification kit from Roche. Purified PCR products or recombinant plasmids were introduced into *S. pneumoniae* by transformation as described in Kloosterman *et al.* (2006a). Positive transformants were selected on Glc-M17 agar with the appropriate

antibiotic and confirmed by PCR and sequencing. *L. lactis* MG1363 was transformed with plasmid DNA by electroporation according to Holo and Nes (Holo and Nes, 1995).

Table 6.1. Bacterial strains and plasmids used in this study

Strain	**Description**	**Source**
S. pneumoniae		
D39	Serotype 2 strain, *cps2* (MolGen Laboratory collection)	Avery *et al.*, 1944
D39Δ*ccpA*	D39 Δ*ccpA::spc*; Spc^R	This work
D39*nisRK*	D39 Δ*bgaA::nisRK*; $Trim^R$	Kloosterman *et al.*, 2006a
D39Δ*ccpAnisRK*	D39 Δ*ccpA::spc* Δ*bgaA::nisRK*; Spc^R, $Trim^R$	This work
D39Δ*ccpAnisRK*pNZ[*ccpA*]	D39 Δ*ccpA::spc* Δ*bgaA::nisRK* harbouring pNZ[*ccpA*]; Spc^R, $Trim^R$, Cm^R	This work
D39Δ*ccpAnisRK*pNZ8048	D39 Δ*ccpA::spc* Δ*bgaA::nisRK* harbouring pNZ8048; Spc^R, $Trim^R$, Cm^R	This work
L. lactis		
MG1363	Plasmid-free *L. lactis* subsp. *cremoris* NCDO712	Gasson, 1983
Plasmids	**Description**	**Source**
pNZ[*ccpA*]	pNG8048E carrying *ccpA* downstream of the *nisA* promoter; Cm^R	This work
pNG8048e	Nisin-inducible P*nisA*, pNZ8048 derivative containing em^R to facilitate cloning; Cm^R, Em^R	Kloosterman et *al.*, 2006a
pNZ8048	Nisin-inducible P*nisA*; Cm^R	de Ruyter *et al.*, 1996
pORI38	ori^+ $repA^-$, deletion derivative of pWV01; Spc^R	Leenhouts *et al.*, 1996

Abbreviations: Spc^R, spectinomycin resistance; $Trim^R$, trimethoprim resistance; Cm^R, chloramphenicol resistance; Em^R, erythromycin resistance.

Construction of a *ccpA* mutant of *S. pneumoniae* D39

Oligonucleotide primers used in this study are listed in Table 6.2. In *S. pneumoniae* D39, *ccpA* forms a monocistronic operon, flanked upstream by a well defined promoter region and downstream by a strong terminator (predicted ΔG^{o} = -13.8 kcal mol^{-1}). The *ccpA* deletion was accomplished by allelic replacement mutagenesis as follows: the up- (547-bp) and downstream (517-bp) regions of the *ccpA* gene (1010-bp) were PCR-amplified from D39 chromosomal DNA using the primer pairs ccpA_D39_KO-1/ ccpA_D39_KO-2 (spec) and ccpA_D39_KO-3 (spec)/ ccpA_D39_KO-4, respectively. The resulting PCR products were, by means of overlap extension PCR (Song *et al.*, 2005), fused to a Spc^{R} gene (1032-bp, amplified with primers Spec_Fp and Spec_Rp from plasmid pORI38) using the primers ccpA_D39_KO-1 and ccpA_D39_KO-4. The Δ*ccpA::spc* PCR product (2096-bp) obtained in this way was transformed to *S. pneumoniae* D39, giving rise to the *ccpA* deletion mutant (D39Δ*ccpA* in Table 6.1). Replacement of the *ccpA* gene with the *spc* gene and correct integration of the insert were confirmed by PCR and sequencing (Service XS). To rule out the possibility of suppressor mutations arising with the deletion of *ccpA*, the transformation efficiency of the Δ*ccpA::spc* PCR product was compared with that of the *spd_0786::spc* (*spd_0786* insertion-deletion) PCR product. SPD_0786 is a non-essential transcription factor, which disruption does not affect growth of *S. pneumoniae* in CDM (Kloosterman *et al.*, unpublished results). A similar number of transformants per ng of DNA (CFU ng^{-1}) was obtained, strongly suggesting that our *ccpA* strain contains no suppressor mutations.

Table 6.2. Oligonucleotide primers used in this study

Primers	Sequence (from 5' to 3')	REnz
ccpA_D39_KO-1	CCAATATTCTTTCAAAACTGG	-
ccpA_D39_KO-2[a]	**TCCTCCTCACTATTTTGATTAG**GGTTACTGTATCATCTGCATTC	-
ccpA_D39_KO-3[a]	**CGTTTTAGCGTTTATTTCGTTTAGT**CATGGTTTGACAGAACGTA GCTC	-
ccpA_D39_KO-4	CCCAGTCGCTCTGGTATCAC	-
ccpA_D39-1[b]	GCCGGTCTCTCATGAATGCAGATGATACAGTAACC	BsaI
ccpA_D39-2[b]	GCTCTAGATCGATTCCCTGATTTTTTCTATTTACG	XbaI
PnisAL-fw	GTCGATAACGCGAGCATAATAAACG	-
PnisAL-rev	CGTGCTGTAATTTGTTTAATTGCC	-
ccpA_D39_KO-1_conf	GGAACTATTCGAAACTATGTCACCAATATTCTTTCAAAACTGG	-
ccpA_D39_KO-4_conf	CTTCTGCAAAAAGGAATCCCAGTCGCTCTGGTATCAC	-
SpecRev	TCTGTCAATGGTTCAGATACGACGACTA	-
SpecFw	GCGGGAAATGCAGTGGCTGAATCT	-
Spec_Fp	CTAATCAAAATAGTGAGGAGG	-
Spec_Rp	ACTAAACGAAATAAACGC	-
Spd_0420-qRT-1	TGGGAAGGCTTCAAAGG	-
Spd_0420-qRT-2	GGACGAGTGTCCATTGG	-
Spd_0667-qRT-1	TCCATATGCATACGACGC	-
Spd_0667-qRT-2	TGGGATAGATTCTACATCAGC	-
metG-D39-2	TTCTGCCAGCTGGCTTTC	-
metG_D39-1	ATCCGTACAACTGATGAC	-
Spd_0790-qRT-1	GGTGAGGACGGATACTGG	-
Spd_0790-qRT-2	TAACAGTTGCCATACGCTC	-
Spd_1053-qRT-1	GTGCAGATGCTGCAGG	-
Spd_1053-qRT-2	GGCCACGAGTCATATAAGC	-
Spd_1078-qRT-1	TTGACCTTAGTCACGCCC	-
Spd_1078-qRT-2	TTACCTACAAGGTCAAGACGAG	-
Spd_1504-qRT-1	ATGAAACTCAACTTTCGGG	-
Spd_1504-qRT-2	GACATTTTCCAAATCTCGTG	-
Spd_1634-qRT-1	CTGAAACTCTTCGCAAAGAC	-
Spd_1634-qRT-2	TGCGCCGTATGTTCC	-

Abbreviations: REnz, restriction enzyme. [a]Overlap with Spc^R gene is indicated in bold. [b]Restrictions enzyme sites are underlined.

Transformation frequency assay

For the transformation frequency assay the 2096-bp fragment comprising the Δ*ccpA::spc* region was PCR-amplified from the chromosomal DNA of the *ccpA* mutant strain using the primer pairs ccpA_D39_KO_1 and ccpA_D39_KO_4. Similarly, a fragment (2725-bp) encompassing the *spd_0786::spc* region of a D39 *spd_0786::spc* strain was amplified using appropriate primer pairs. An identical concentration of each product was used to transform strain D39 as described above. Spectinomycin resistant colonies were selected and counted for each transformation and the number of colonies was compared to evaluate the transformation frequency.

Construction of the *ccpA* complementation strain

A *ccpA* complementation strain was constructed using the NICE system improved for *S. pneumoniae* (Kloosterman *et al.*, 2006a). In this arrangement the NisRK two-component system, coded by the *nisRK* genes, activate the expression of the *nisA* promoter in the presence of nisin. The procedure to construct the *ccpA* complementation strain is described as follows. The *ccpA* mutant strain (D39Δ*ccpA*) was transformed with chromosomal DNA from D39*nisRK*, a stable derivative of *S. pneumoniae* D39 that harbours the *nisRK* genes and a $Trim^R$ gene in the *bgaA* locus. Trimethoprim resistant clones (D39Δ*ccpAnisRK* in Table 6.1) were selected and the presence of both the *ccpA* deletion and the *nisRK* genes was confirmed by PCR. For the construction of the plasmid harbouring *ccpA* under the control of the nisin-indusible promoter *nisA* (pNZ[*ccpA*] in Table 6.1), the *ccpA* gene was PCR-amplified from D39 chromosomal DNA using the primers ccpA_D39-1 and ccpA_D39-2 and cloned as a BsaI/XbaI fragment in NcoI/XbaI digested pNG8048e. *L. lactis* MG1363 was used as the cloning host. The *ccpA* complementation strain

(D39*ΔccpAnisRK*pNZ[*ccpA*] in Table 6.1) was constructed by transformation of the D39*ΔccpAnisRK* strain with plasmid pNZ[*ccpA*] selecting for chloramphenicol resistant clones. As a control D39Δ*ccpAnisRK* strain was also transformed with the empty plasmid pNZ8048 (Table 6.1). Strains were confirmed by PCR.

Transcriptome analysis

S. pneumoniae D39 and the isogenic *ccpA* mutant were compared by transcriptome analysis using whole-genome *S. pneumoniae* DNA microarrays, representing all TIGR4 ORFs, as well as R6 and D39 ORFs that are not in TIGR4 (Kloosterman *et al.*, 2006b). See http://www.ncbi.nlm.nih.gov/geo/query/acc.cgi?acc=GPL11484, for a description of all amplicons and oligo's present on the DNA microarray. The two strains were grown as described above in three biologically independent experiments and harvested at mid-exponential (OD_{600} of 0.35 ± 0.02) and transition-to-stationary (OD_{600} of 1.3 ± 0.1) phases of growth (Fig. 6.1). mRNA isolation, synthesis of cDNA, labelling of cDNA, hybridization, scanning of the slides and the processing and analysis of the data was carried out as described before (Kloosterman *et al.*, 2006b). Genes were considered to have significantly altered expression when the bayesian *p*-value was < 0.001, the false discovery rate (FDR) was < 0.01 and the ratio (signal Δ*ccpA* /signal D39) was > 1.5 or < 0.66, but > 2 or < 0.5 in at least one of the four conditions. For the Gal_TS comparison, data were derived from two independent hybridizations and a Bayesian *p*-value < 0.01, FDR < 0.08 was applied. To exploit the data obtained in this way, also an *in silico* comparison was done between Glc and Gal, both for the M and TS phases and also in both D39 wild-type as well as *ΔccpA*. To this end, raw signals (*i.e.* slide images) of the Glc experiments were compared with the corresponding signals of the Gal experiments and analyzed as described above.

The microarray data have been deposited at GEO under accession number GSE31819.

Cre site prediction

Using the *L. lactis* consensus sequence (WGWAARCGYTWWMA, a *cre* site prediction was performed in D39, using Genome2D (Baerends *et al*., 2004; Zomer *et al*., 2007). Subsequently, genes with a *cre* site in their promoter region that were differentially expressed in the DNA microarray analyses of the *ccpA* mutant were used to built a weight matrix, which was subsequently used to search the genome again using Genome2D (Baerends *et al*., 2004), using a cut-off score of 9.9. In a similar way, the weight matrix of the RegPrecise (http://regprecise.lbl.gov/RegPrecise/) prediction was used. The resulting predictions (Table S.6.6 on the CD) were compiled together with the original prediction of RegPrecise and a prediction done in a recent publication (van Opijnen *et al*., 2009). The resulting list of 340 genes with putative *cre* sites was compared with the genes that were differentially expressed in the arrays. Of these 340 genes with *cre* sites, 115 matched with the list of genes differentially expressed in the *ccpA* mutant in at least one condition. After reanalysis of these matches with an online *cre* site prediction tool (http://molgen51.biol.rug.nl/websoftware /ppp/ppp_start.php), 90 genes were left that contain a putative *cre* site in their promoter region, or downstream of the translational start.

Real-time quantitative RT-PCR

Cell samples obtained as described above for transcriptome analyses using DNA microarrays were treated with RNase-free DNase I (Fermentas, St. Leon-Rot, Germany) for 60 min at 37ºC in DNaseI buffer (10 mmol l^{-1} Tris-HCl, pH

7.5, 2.5 mmol l^{-1} $MgCl_2$, 0.1 mmol l^{-1} $CaCl_2$). Samples were purified with the Roche RNA isolation kit. Reverse transcription was performed on 5 µg of total RNA using the same method as used during the microarray procedure. Quantification of specific cDNA of *spd_0420* (*pfl*), *spd_0667* (*sodA*), *spd_0790* (*pyk*), *spd_1053* (*lacE*), *spd_1078* (*ldh*), *spd_1504* (*nanA*) and *spd_1634* (*galK*) was performed on an CFX96 Real-Time PCR System (BioRad, Hercules, CA) using Maxima SYBR Green qPCR Master Mix (Fermentas, St. Leon-Rot, Germany) on 5 ng cDNA template in a 20 µl reaction volume. Primers used are listed in Table 6.2. The qRT-PCR data were normalized to the level of *metG* (*spd_0689*) cDNA using the $2^{-\Delta\Delta C}{}_T$ method (Livak and Schmittgen, 2001). The data are averages of four repeats.

Quantification of fermentation products during growth

Strains were grown as described above. Culture samples (2 ml) were taken in mid-exponential and transition-to-stationary phases of growth, centrifuged (16,000 × *g*, 2 min, 4ºC), filtered (Millex-GN 0,22 µm filters) and the supernatant solutions were stored at -20ºC until analysis by high performance liquid chromatography (HPLC). Prior to analysis, samples were allowed to thaw at room temperature. Glc or Gal and end-products were quantified in an HPLC apparatus equipped with a refractive index detector (Shodex RI-101, Showa Denko K. K.) using an HPX-87H anion exchange column (Bio-Rad Laboratories Inc.) at 60ºC, with 5 mM H_2SO_4 as the elution fluid and a flow rate of 0.5 ml min^{-1}. Alternatively, quantification of metabolites in the supernatant solutions was performed by ^{1}H-NMR in a Bruker Avance II 500 MHz spectrometer (Bruker BioSpin GmbH). Formic acid (sodium salt) was added to the samples and used as an internal concentration standard. The ATP yield was calculated as the ratio of ATP produced to Glc or Gal consumed. The global yields of ATP were calculated

from the fermentation products determined at the time-point of growth arrest assuming that all ATP was synthesized by substrate-level phosphorylation. A factor of 0.39, determined from a DW (mg ml^{-1}) *versus* OD_{600} curve, was used to convert OD_{600} into dry weight (mg biomass ml^{-1}). Hydrogen peroxide was quantified in fresh supernatant solutions using the Amplex® Red Hydrogen Peroxide/Peroxidase assay kit from Invitrogen.

Determination of hydrogen peroxide (H_2O_2)

Strains were grown in CDM as described above. Culture samples of 1-ml were harvested in mid-exponential and transition-to-stationary phases of growth, centrifuged (16,000 × *g*, 2 min, 4ºC) and filtered (Millex-GN 0,2 µm filters). The Amplex® Red hydrogen Peroxide/Peroxidase assay kit from Invitrogen was used to quantify the hydrogen peroxide contents in the fresh supernatant solutions.

Cold ethanol extractions and determination of intracellular metabolites by ^{31}P-NMR

The ethanol extracts were prepared as described previously by Ramos *et al.* (2001). For each extract the volume of cells harvested from mid-exponential (OD_{600} of 0.35 ± 0.02) and transition-to-stationary (OD_{600} of 1.3 ± 0.1) cultures corresponded to approximately 14 mg of protein and the centrifugation was performed at 4ºC, 6,000 x *g*, during 3 min. The dried extract was dissolved in 1-ml of deuterated water (pH 6.5 or pH 5.5) containing 5 mM EDTA and stored at -20ºC for further analysis by ^{31}P-NMR. This methodology was successfully used to measure phosphorylated metabolites in *L. lactis* (Ramos *et al.*, 2001). In *S. pneumoniae* ethanol extracts the following phosphorylated metabolites were detected: G6P, FBP, 3-PGA, PEP, α-Gal1P, α-G1P, TBP, UDP-Glc, UDP-N-acetylmuramoyl-pentapeptide (UDP-MurNAc-pPep), UDP-N-acetylglucosamine

(UDP-GlcNAc), UDP-glucosamine (UDP-GlcN), CDP-choline (CDP-cho), NAD^+, CTP, ATP and ADP. A small peak due to fructose 6-phosphate was also detected, but its quantification was hampered by strong overlapping with a resonance due to the medium component β-glycerophosphate. A weak resonance due to dihydroxyacetone phosphate was present, but reliable integration was not possible. The concentration limit for detection/quantification of metabolites in ethanol extracts by ^{31}P-NMR was approximately 0.4-0.5 mM. Resonances were assigned by addition of pure compounds to the extracts or on the basis of comparison with a previous study (Ramos *et al.*, 2001). Concentrations were calculated from the areas of the resonances in ^{31}P-spectra by comparison with the area of a resonance due to methylphosphonic acid (Aldrich), added as an internal standard, and after application of an appropriate factor for correcting saturation of resonances. The reported concentration values for intracellular phosphorylated compounds are averages of three independent growth experiments.

^{31}P-NMR spectra were recorded using a selective probe head (^{31}P-SEX) at 37ºC on a Bruker AVANCE II 500 MHz spectrometer (Bruker BioSpin GmbH) by using standard Bruker pulse programs. Spectra were referenced to the resonance of external 85% H_3PO_4, designated at 0 ppm.

Quantification of the glucuronic acid content of capsular polysaccharide

Samples for the determination of the capsular glucuronic acid amounts were prepared as follows: cells grown in CDM and harvested in mid-exponential (OD_{600} of 0.35 ± 0.02) and transition-to-stationary (OD_{600} of 1.3 ± 0.1) phases of growth were centrifuged (6,000 x *g*, 3-7 min, 4ºC), resuspended in PBS and pelleted at 3000 x *g*, 4ºC, for 20min. The pellet was resuspended in 500 µl of 150 mM Tris-HCl (pH 7.0) and 1 mM $MgSO_4$ and treated as described elsewhere

(Morona *et al.*, 2006). The supernatants derived from the two centrifugations referred before were pooled and treated with 20% (w/v) trichloroacetic acid for protein precipitation. After 2 h of incubation in an ice bath proteins were pelleted and the exopolysaccharides were precipitated with cold ethanol as in Ramos *et al.* (2001). The glucuronic acid of capsule attached or loosely attached (lost in centrifugations to the supernatants) to the cell wall was quantified by the method for quantitative determination of uronic acids as described by Blumenkrantz and Asboe-Hansen, 1973.

Results

Growth rates on glucose and galactose are differently affected by CcpA

Hitherto, a systemic appraisal to the role of CcpA in the physiology of *S. pneumoniae* was missing. We constructed a *S. pneumoniae ccpA* deletion-insertion mutant (D39Δ*ccpA*, for details see Material & Methods and Fig. 6.1-A) in the D39 serotype 2 background (Table 6.1), and determined the growth profiles of the *ccpA* mutant and the wild-type D39 in chemically defined medium (CDM) containing Glc without pH control (Fig. 6.1-B). Under the conditions studied, the maximal biomass reached at time-points 8 h and 14 h for strains D39 and D39Δ*ccpA*, respectively, was consistently slightly higher in the absence of CcpA. Loss of CcpA caused a substantial decrease (about 55%, Table 6.3) of the growth rate in Glc-containing CDM. Importantly, this growth rate defect was fully restored by complementation of a *ccpA* strain (D39Δ*ccpAnisRK*, $\mu = 0.76 \pm 0.00\ h^{-1}$) with expression in *trans* of *ccpA* under the control of the nisin promoter (Fig. 6.1-B). It should be noted that the growth profile of strain D39Δ*ccpAnisRK* closely resembles that of D39Δ*ccpA* (data not shown).

To extend our knowledge on the role of CcpA in the physiology of *S. pneumoniae*, growth on Gal was also assessed in batch cultivations as described for Glc (Fig. 6.1-C). On Gal, the maximal biomass produced was also similar in both strains. However, in strong contrast to the effect in Glc-CDM, in Gal-CDM the growth rate of strain D39Δ*ccpA* was slightly higher than that of D39, although this difference was not statistically significant.

Our data show that the effect of CcpA on the growth rate of *S. pneumoniae* is carbohydrate-dependent; CcpA noticeably stimulates fast growth on Glc, but the effect on Gal, if any, is unclear.

Table 6.3. Product yields, total substrate consumption, carbon and redox balances, growth and energetic parameters, and pH values determined at the time-point of maximal biomass achieved by D39 and D39Δ*ccpA* strains cultured on Glc (56 ± 1 mM) or Gal (57 ± 1 mM). Substrate consumption rate and the specific growth rate are also shown. Values of two or three independent experiments were averaged and errors are reported as ± SD.

	Glc		**Gal**	
	D39	**D39Δ*ccpA***	**D39**	**D39Δ*ccpA***
Product yields[a]				
Lactate	1.86 ± 0.02	1.71 ± 0.01	1.01 ± 0.04	1.78 ± 0.06
Formate	0.04 ± 0.0	0.20 ± 0.01	0.89 ± 0.00	0.14 ± 0.02
Acetate	BDL	0.12 ± 0.01	0.49 ± 0.01	0.15 ± 0.02
Ethanol	BDL	0.05 ± 0.01	0.45 ± 0.02	0.03 ± 0.00
q_s^{max} (mmol g^{-1} h^{-1})	31.4 ± 2.8	9.6 ± 2.0	10.0 ± 2.0	9.8 ± 1.5
μ_{max} (h^{-1})	0.75 ± 0.03	0.35 ± 0.01	0.27 ± 0.03	0.31 ± 0.01
Carbon balance[b]	95 ± 1	95 ± 1	95 ± 2	96 ± 4
Redox balance	93 ± 1	90 ± 2	96 ± 1	92 ± 2
Biomass yield (g mol^{-1} of substrate)	23.1 ± 0.5	30.3 ± 1.1	38.0 ± 1.7	41.8 ± 1.9
ATP yield (mol mol^{-1} of substrate)	1.86 ± 0.02	2.00 ± 0.05	2.45 ± 0.00	2.10 ± 0.01
YATP (g of biomass mol^{-1} of ATP)	12.4 ± 0.3	15.1 ± 0.2	15.5 ± 0.7	19.8 ± 0.8
Consumed substrate (%)	50 ± 1	42 ± 2	26 ± 2	31 ± 0
pH (growth arrest)	5.4 ± 0.1	5.5 ± 0.0	5.3 ± 0.0	5.3 ± 0.1

[a]Product yields, [End-product] / [Glc consumed]; [b]Carbon balance is the percentage of carbon in metabolized Glc or Gal that is recovered in the fermentation products (lactate, formate, ethanol and acetate); q_s^{max} was estimated from a first-order derivative of a polynomial fit of the observed substrate consumption time series. Dry weight (DW) was used as a measure of cell mass. BDL, below detection limit.

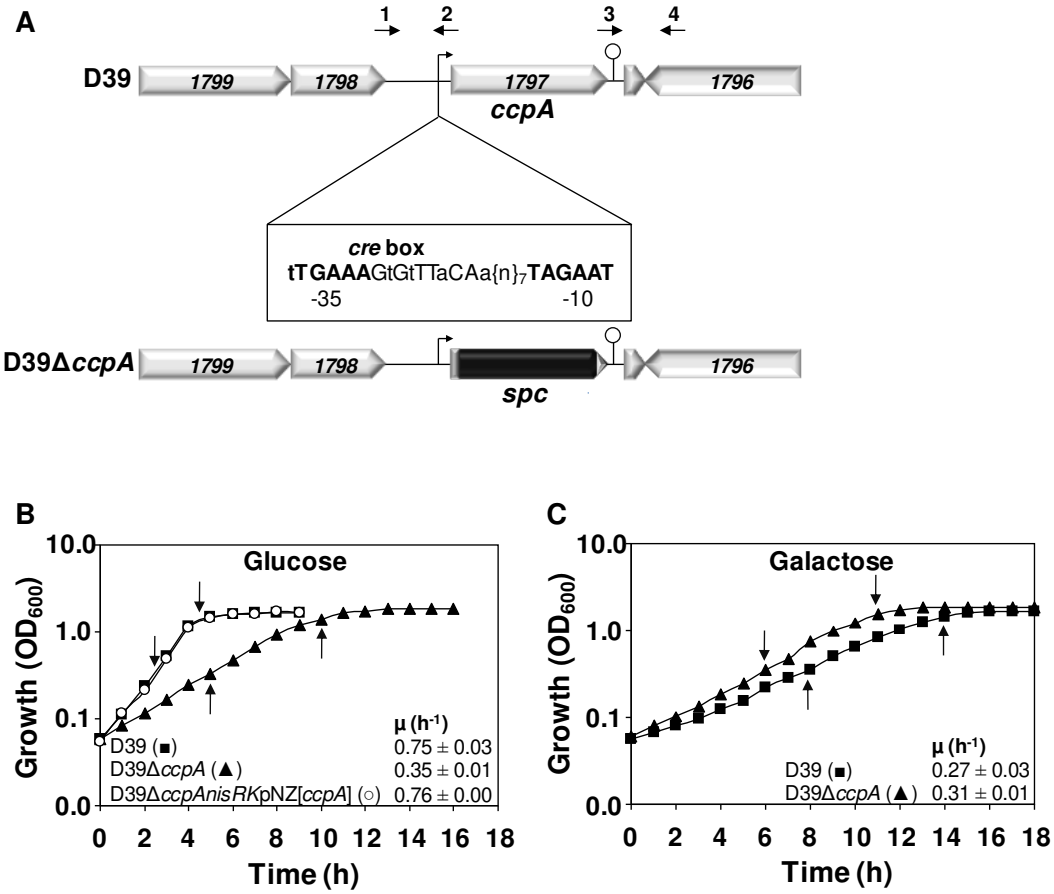

Fig. 6.1. Growth profiles of D39 wild-type and the isogenic *ccpA* mutant on Glc and Gal. (A) Schematic overview of the *ccpA* gene and its flanking genes and the genetic replacement of the *ccpA* gene with a spectinomycin marker in strain D39. Hooked arrow, putative promoter; lollipop, putative terminator; black area, *ccpA* gene replaced with a spectinomycin cassette; numbers inside the genes, D39 *spd* numbers; arrows and numbers above the figure indicate primers used to construct the D39Δ*ccpA* mutant; zoomed area (inset), putative *cre* box, -35 and -10 promoter regions; the number of bp spacing these regions are subscripted after {n}. (B and C) Growth of strains D39 (■), D39Δ*ccpA* (▲) and D39Δ*ccpAnisRK*pNZ[*ccpA*] (○) in CDM containing 1% Glc (B) or 1% Gal (C) at 37ºC in rubber-stoppered static bottles without pH control (initial pH 6.5); growth curves as in Fig. 6.4, except that logarithmic scale was used for the y-axis. The

growth of the complemented strain was performed without nisin in the medium. Optical densities at 600 nm (OD_{600}) were measured hourly. Each point of the growth curves is an average of at least three independent experiments and the error was in all cases below 15%. The growth rates for each strain are also indicated and the values shown are averages ± SD. The arrows indicate the mid-exponential and transition-to-stationary time-points at which D39 and D39Δ*ccpA* samples were withdrawn for transcriptomic and metabolic profiling analysis.

CcpA is a pleiotropic regulator in *S. pneumoniae*

To determine the effect of the *ccpA* deletion on the transcriptome of *S. pneumoniae*, the transcriptional profile of D39 wild-type was compared to that of its isogenic *ccpA* deletion mutant at mid-exponential (M) and transition-to-stationary (TS) phases of growth. In the four conditions tested, Glc_M, Gal_M, Glc_TS, Gal_TS, between 14 and 19% of the ORFs in the genome were significantly, differentially expressed in the *ccpA* deletion mutant, of which more genes upregulated than downregulated (Fig. 6.2; for an overview see also Table S.6.1 provided in digital format on the included CD). This is similar to *S. pyogenes* (up to 20% genes affected) (Shelburne *et al.*, 2008b), but higher than in *S. mutans*, *L. lactis*, and *B. subtilis* (less than 9% genes affected) (Zomer *et al.*, 2007; Lulko *et al.*, 2007; Abranches *et al.*, 2008). These findings confirm the role of CcpA as a global regulator with a prevalent repressor function. The COG category with the highest number of genes affected was carbohydrate transport and metabolism [G], which genes are mainly repressed by CcpA (Fig. 6.2-B).

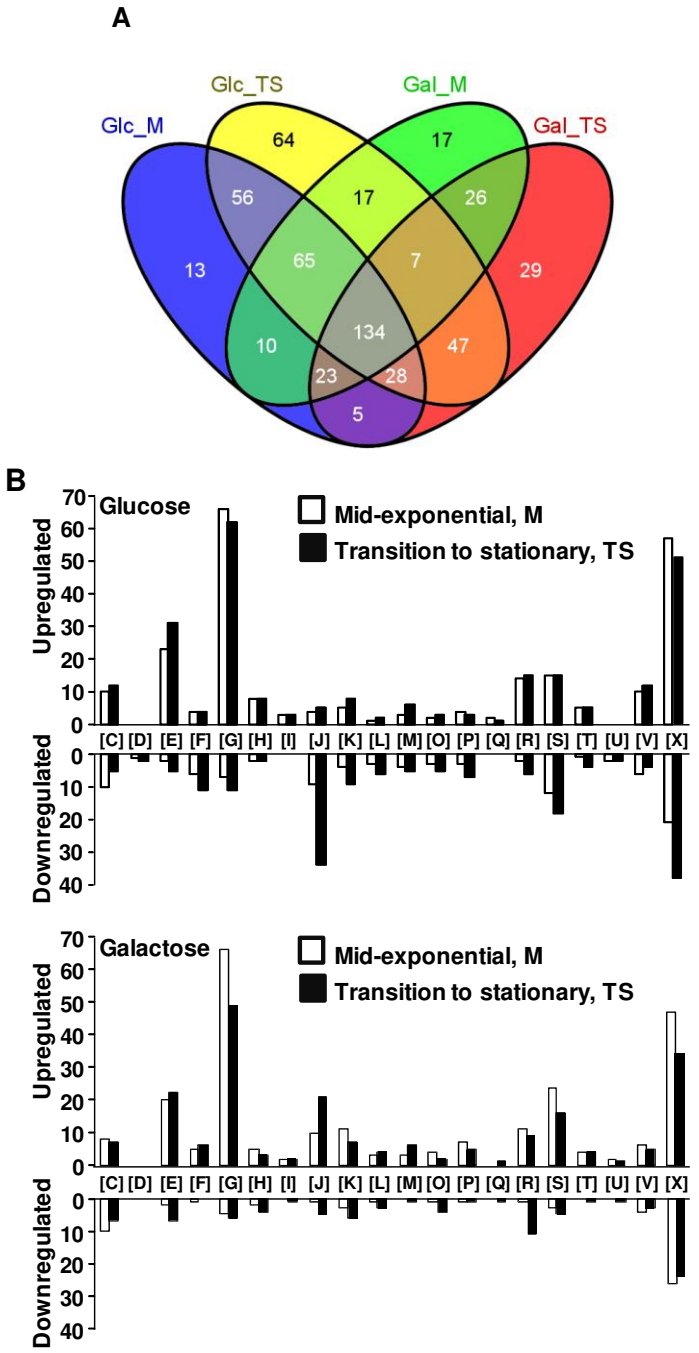
A
Glc_TS
Gal_M
Glc_M
Gal_TS
64
17
56
17
26
13
65
7
29
10
134
47
23
28
5
B
Glucose
Mid-exponential, M
Transition to stationary, TS
Upregulated
Downregulated
70
60
50
40
30
20
10
0
[C] [D] [E] [F] [G] [H] [I] [J] [K] [L] [M] [O] [P] [Q] [R] [S] [T] [U] [V] [X]
Galactose
Mid-exponential, M
Transition to stationary, TS
Upregulated
Downregulated

Fig. 6.2. Genes differentially expressed due to inactivation of *ccpA*. (A) Venn diagram of the genes significantly differentially transcribed due to loss of *ccpA*. Transcript levels in D39Δ*ccpA* were compared to D39 wild-type in Glc_M, Gal_M, Glc_TS, Gal_TS as generated by VENNY (*http://bioinfogp.cnb.csic.es/tools/venny/index.html*). For all intersections, which are not drawn to scale, the numbers of genes are indicated. The total number of genes influenced in each condition tested was: Glc_M, 334 (15.3%), Glc_TS, 418 (19.2%), Gal_M, 299 (13.7%), and Gal_TS 299 (13.7%) in a universe of 2177 genes in the genome of *S. pneumoniae*. (B) Numbers of genes significantly differently transcribed by the *ccpA* deletion in strain D39 ordered by COG categories. White bars represent M phase of growth, black bars TS phase of growth. [C] Energy production and conversion; [D] Cell cycle control, cell division; chromosome partitioning; [E] Amino acid transport and metabolism; [F] Nucleotide transport and metabolism; [G] Carbohydrate transport and metabolism; [H] Coenzyme transport and metabolism; [I] Lipid transport and metabolism; [J] Translation, ribosomal structure and biogenesis; [K] Transcription; [L] Replication, recombination and repair; [M] Cell wall/membrane/envelope biogenesis; [O] Posttranslational modification, protein turnover, chaperones; [P] Inorganic ion transport and metabolism; [Q] Secondary metabolites biosynthesis, transport and catabolism; [R] General function prediction only; [S] Function unknown; [T] Signal transduction mechanisms; [U] Intracellular trafficking, secretion, and vesicular transport; [V] Defense mechanisms; [X] No prediction. The ratio for each gene is > 1.5 or < 0.66, but > 2 or < 0.5 in at least one of the four conditions. The number 2177 represents the total number of amplicons analyzed, covering the entire genome of *S. pneumoniae* D39. This number is slightly higher than the number of genes in the genome of D39 (2069), since some amplicons were present in versions for different strains (*i.e.* TIGR4, R6, or D39) or in 2 copies.

Also, 21 genes encoding (putative) transcriptional regulatory proteins were affected, among which three two-component systems, indicating intertwinement of CcpA with other regulons. In addition, many genes with unknown or unpredicted function, as well as a number of genes within the amino acid transport and metabolism category [E], were among the differentially expressed genes (see also Table S.6.1 on the CD). Strikingly, roughly similar numbers of genes were regulated when Gal instead of Glc was used as the carbon source (Fig. 6.2 and

Table S.6.1). This means that during growth on the slowly metabolized Gal, carbon catabolite repression by CcpA still takes place. Furthermore, a large part of the genes (up to 44% per condition) differentially expressed were common to all 4 conditions, but carbohydrate and growth phase-specific CcpA-mediated regulation was also in effect (Fig. 6.2 and Table S.6.1 on the CD). To firmly confirm our microarray data, changes in transcript abundance of selected genes linked to metabolic and virulence pathways (*lacE*, *galK*, *pyk*, *ldh*, *pfl*, *sodA*, *nanA*), were assessed by qRT-PCR. For all genes tested, expression data obtained by qRT-PCR proved to correlate positively with transcript abundance as measured by microarray analysis (Table S.6.2 on the CD). In summary, the role of CcpA as a master regulator in *S. pneumoniae* is undoubtedly substantiated by our genome-wide transcriptome analyses. Curiously, not only Glc, but also Gal appears in this study as a repressing carbohydrate in *S. pneumoniae*.

CcpA influences carbohydrate-specific pathways in carbohydrate-dependent and independent manners

The first step in the metabolism of any carbohydrate is transport across the cell membrane. Genes in 17 out of 29 operons encoding carbohydrate uptake systems are affected in the *ccpA* arrays (Table S.6.3 on the CD). As for many other categories, several genes encoding carbohydrate transporters were not only strongly repressed by CcpA on Glc, but also on Gal. *ManLMN* (*spd_264-2*) codifying the mannose/glucose-PTS, a predominant Glc transporter in *Streptococcaceae* (reviewed in Deutscher *et al.*, 2006), was among them. Carbohydrate-specific CcpA-mediated regulation was also in effect: *spd_0661*, a Glc-family PTS system, was exclusively repressed in Gal-CDM. This gene is predicted to be a direct target of CcpA due to the presence of a *cre* site in its promoter region. Another PTS operon (*spd_0559-0562*), which also contains a

cre site in its promoter region, was strongly negatively regulated on Glc, but only mildly on Gal. Curiously, the latter PTS system has been previously postulated to transport Gal (Kaufman and Yother, 2007).

A genome survey of *S. pneumoniae* indicates that it possesses both the Leloir and tagatose 6-phosphate Gal catabolic pathways. Interestingly, the Leloir genes were repressed by CcpA independently of the carbohydrate, whereas the tagatose 6-phosphate pathway was weakly repressed by CcpA on Glc and strongly activated on Gal (Fig. 6.3). Also of note was the observed induction of the tagatose 6-phosphate pathway (10- to 12-fold higher) and the Leloir genes *galK* and *galT-2* (25 times higher) by Gal, regardless of CcpA (Table S.6.4 on the CD). As for the *lac* genes, other intracellular carbohydrate-specific metabolic steps were subjected to CcpA-mediated regulation in a carbohydrate dependent manner (Table S.6.1 on the CD). For example, a putative 1-*pfk* (*spd_0772*) and an upstream *lacR* were upregulated in the *ccpA* mutant only on Gal.

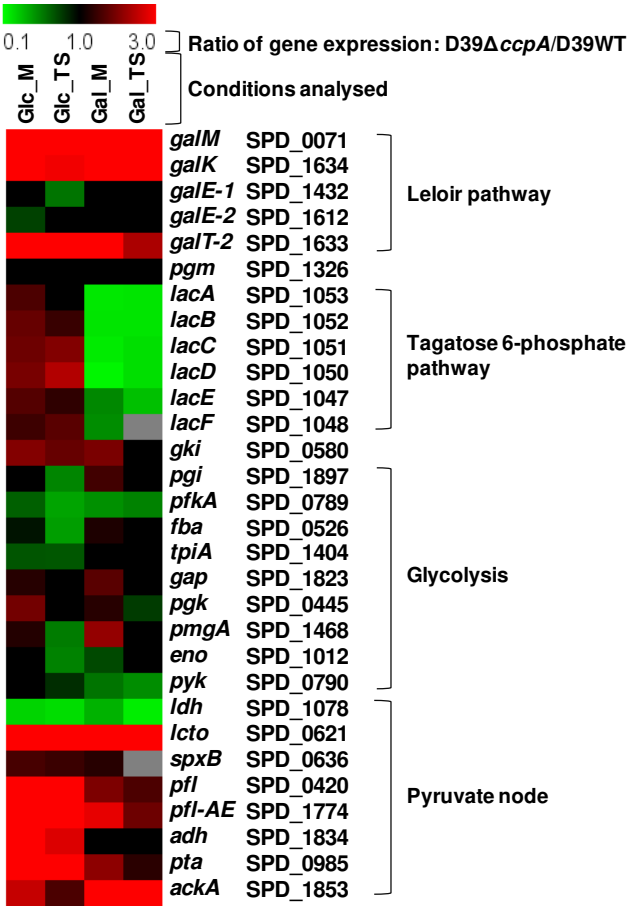

Fig. 6.3. Visual representation of the effect of CcpA on the transcription of genes involved in key basic metabolic processes. Ratio's of genes in glycolysis, the Leloir and tagatose 6-phosphate pathways, and the pyruvate node, in all four conditions analysed in this study (Glc_M, Gal_M, Glc_TS, Gal_TS) are depicted. On top of the figure, a colour scale is given for the ratio of the expression in the *ccpA* mutant over that in the wild-type strain. Thus, red means repression by CcpA (upregulation in the microarray analysis) and green means activation by CcpA (downregulation in the microarray analysis). For each gene the D39 *locus tag* and the gene name is given on the right. No cut-off value was applied for the expression ratios of the genes given in the figure. Genes were considered significantly changed when having a Bayesian *p*-value and FDR meeting

the criteria as outlined in the Materials & Methods. Genes that did not meet these criteria were given a ratio of 1.0 (black colour), meaning no significant change in expression. See Fig. 6.6 for an overview of these pathways in *S. pneumoniae* D39.

Cre site prediction in the genome of *S. pneumoniae*

To discern between direct and indirect CcpA dependent effects, an *in silico cre* site prediction was performed in the genome sequence of D39 (for details see Materials & Methods), yielding 90 predicted *cre* sites that match with the genes differentially expressed in the *ccpA* DNA microarray data in at least one condition (Tables S.6.1, S.6.5 and S.6.6 on the CD). A consensus *cre* is shown in Fig. 6.1. A rough estimation of operons in *S. pneumoniae* using Genome2D (Baerends *et al.*, 2004), based on sizes of intergenic regions and gene orientation, resulted in the division of the differentially expressed genes in 215 transcriptional units. This means that approximately 42% of the promoters regulated in the arrays have a *cre* site and may therefore be directly regulated by CcpA. When considering only the genes with a *cre* site in their promoter region, 68 genes (76%) have a *cre* site in a position that agrees with the observed regulation in the DNA microarray analysis (Table S.6.1 on the CD). For the remaining genes, either the promoter could not be predicted or regulation was weak and opposite when comparing the different conditions. Notably, there were many genes with a *cre* site in their promoter region that were not affected by the *ccpA* deletion (Table S.6.6 on the CD). On the other hand, the expression of some genes was highly changed, although a *cre* site was not found. This suggests indirect regulation of these genes, possibly by regulators that are influenced by CcpA.

CcpA is by large an activator of glycolysis and influences genes involved in fermentation

The role of CcpA in controlling expression of genes involved in central carbon metabolism is well established (Zomer *et al.*, 2007; Lulko *et al.*, 2007; Shelburne *et al.*, 2008b). Despite its prevalent repressor function, in *S. pneumoniae* CcpA was shown to activate several glycolytic genes (Fig. 6.3). The larger positive effects were observed for the key glycolytic gene *pfkA* (6-phosphofructokinase) and in *ldh* (lactate dehydrogenase), but activation of *pyk* (pyruvate kinase) was also considerable, which strongly suggests a predominant role of CcpA in assuring the efficient conversion of carbohydrates to lactate in this bacterium. In line, CcpA was in all instances a repressor of *pfl* (SPD_0420, pyruvate formate-lyase), which encodes a key activity that directly competes with lactate dehydrogenase for pyruvate, as well as of *pfl-ae* (SPD_1774, pyruvate formate-lyase activating enzyme) (Fig. 6.3 and Table S.6.1 on the CD). Carbohydrate-independent CcpA-dependent regulation of genes linked to the pyruvate node has been previously reported (Zheng *et al.*, 2011b). Moreover, the genes in the pathway leading to acetate, *pta* (SPD_0985, phosphotransacetylase) and *ackA,* (SPD_1853, acetate kinase) were upregulated in the mutant. Curiously, *adh* (SPD_1834, alcohol dehydrogenase) was also repressed by CcpA, but only in Glc-containing medium. Moreover, in the parent strain D39 the expression of *pfl*, *pfl-ae* and *adh* was induced by Gal, as denoted by the decimal fold change ratio Glc/Gal (Table S.6.4 on the CD). Overall, the expression pattern of genes involved in fermentative steps (activation of *ldh* and repression of mixed-acid fermentation genes) (Fig. 6.3) strengthens the view that the pneumococcal CcpA promotes homolactic fermentation.

Loss of CcpA changes the fermentation profiles of D39 on glucose and galactose

The dissimilar growth of D39 and D39Δ*ccpA* and the resulting expression profiles prompted us to perform an in-depth characterization of the fermentation patterns on Glc and Gal.

Substrate consumption and end-products. The pneumococcal strains were grown as above. Substrate consumption and concentrations of end-products are shown in Fig. 6.4. During growth on Glc strain D39 showed a typical homolactic behavior, the major end-product being lactate, which reached a concentration of 52 ± 1 mM at the time of growth arrest (maximal biomass), accounting for 93% of the Glc consumed (Table 6.3); formate was also formed in minor amounts (Fig. 6.4-A and Table 6.3). Loss of CcpA caused a shift towards a more mixed-acid fermentation: a 5-fold increase in the yields of formate, as well as formation of acetate and ethanol, were accompanied by a decrease on lactate production, which accounted for 85% of the Glc consumed as compared to 93% in D39 (Fig. 6.4-B and Table 6.3). Hydrogen peroxide (H_2O_2), a known minor end-product of streptococcal aerobic metabolism, was also detected. In the wild-type, the maximal concentration reached was about 0.04 ± 0.002 mM, while in the mutant this concentration was *circa* 7-fold enhanced. The low concentrations measured most likely reflect a limitation in oxygen availability due to the nearly anaerobic conditions used for growth. At the time-point of growth arrest, the *ccpA* mutant had consumed 8% less Glc, and the maximal consumption rate was about 30% of the wild-type level (Table 6.3). The observed decrease in Glc consumption was paralleled by the reduction in growth rate, which was 53% lower in D39Δ*ccpA*.

In Gal-containing medium strain D39 displayed a mixed-acid fermentation pattern with lactate, formate, acetate and ethanol as end-products (Fig. 6.4-C). At the time of growth arrest, lactate and formate accounted each for about 50% of

the Gal consumed (Table 6.3). Formate, acetate and ethanol were produced in a 2:1:1 ratio, denoting pyruvate formate-lyase activity. This pronounced shift to mixed-acid fermentation in strain D39 might be partially explained by alleviation of the CcpA-mediated repression of *adh, pfl* and *pfl-AE* during growth on Gal (Table S.6.1 on the CD). The molecular mechanism underlying the partial derepression of the mixed-acid fermentation genes by CcpA on Gal is not understood. Unexpectedly, in this carbohydrate, inactivation of *ccpA* resulted in a more homolactic profile: the yields of formate, acetate and ethanol decreased, whereas the yield of lactate increased (Fig. 6.4-D and Table 6.3). As opposed to Glc-CDM, on Gal the H_2O_2 produced was slightly higher in the wild-type (0.31 ± 0.02 mM) than in the *ccpA* mutant (0.23 ± 0.01 mM). At the time-point of maximal biomass, the *ccpA* mutant had consumed 31% of the initial Gal, 5% more than that consumed by D39. Loss of *ccpA* did not affect the maximal Gal consumption rate (Table 6.3).

Growth and bioenergetic parameters. On Glc, the amount of biomass (g) formed per mol of substrate consumed or per mol of ATP (Y_{ATP}) was higher in the CcpA-deficient strain. The same trend was observed for cultures growing on Gal: loss of *ccpA* resulted in higher biomass yields relative to substrate or ATP. The lower biomass yields in D39 indicate that, independently of the carbohydrate, CcpA directs the carbon source for catabolic processes. Assuming that all ATP is formed by substrate-level phosphorylation, the higher ATP yields in conditions with higher acetate production were expected (Table 6.3). However, the parameters biomass yield and yield on biomass relative to ATP were lower on Glc than on Gal for both D39 and the *ccpA* mutant. These data indicate that Glc is a poorer substrate than Gal in bioenergetic terms, as more Glc is necessary to produce similar amounts of pneumococcal biomass.

In brief, when Glc was used as carbon source transcriptome and metabolic information correlated positively, but on Gal the fermentation end-products deviated from the predictions based on transcript levels suggesting regulation at other cellular levels.

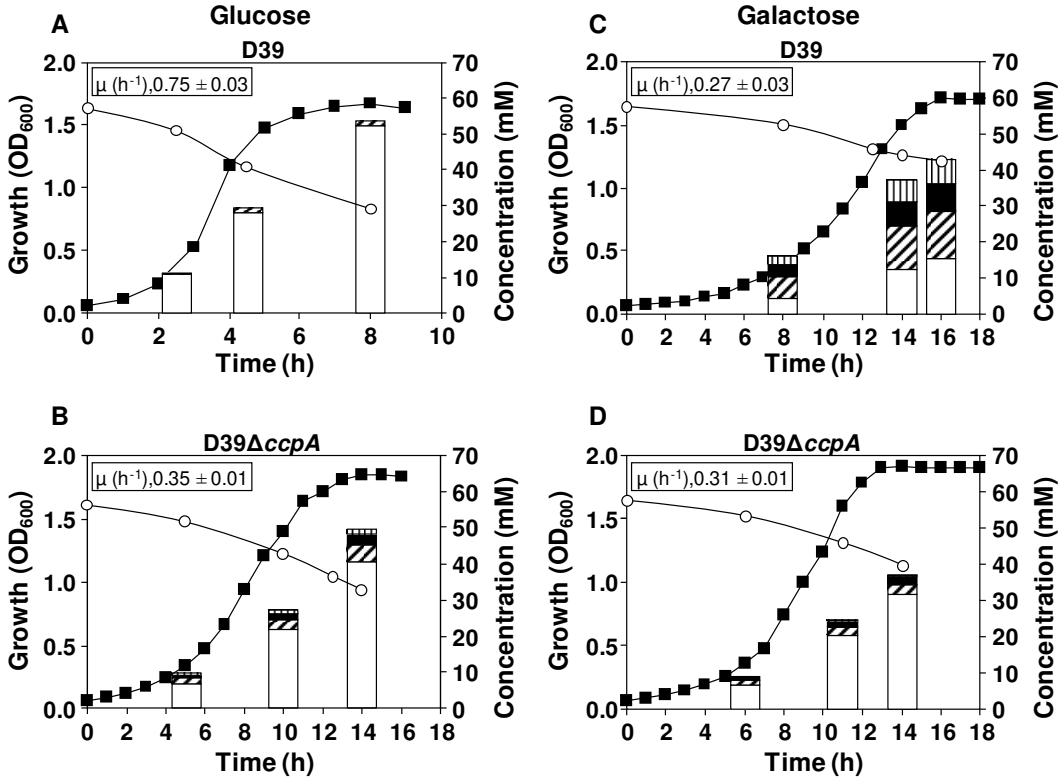

Fig. 6.4. Fermentation profiles of D39 and D39Δ*ccpA* on glucose and galactose. Growth curves, substrate consumption and end-products formed by the D39 (A and C) and D39Δ*ccpA* (B and D) strains growing on Glc (A and B) or Gal (C and D). Culture supernatant samples for substrate and end-product analysis by HPLC and/or ^{1}H-NMR were harvested for each of the conditions in the mid-exponential, transition-to-stationary and growth arrest (maximal biomass) time-points of the respective growth curves (bars in the plots). To calculate end-product concentrations, values of at least two independent

experiments were averaged and the error was below 7% for major products (> 2 mM) and 25% for minor products (< 2 mM). Initial concentrations of Glc and Gal were 56 ± 1 mM and 57 ± 1 mM, respectively. Time-points in substrate consumption curves are averages of at least two independent experiments and the error is below 5%. Symbols: (○), substrate consumption; (■), growth curve; white bars, lactate; hatched bars, formate; black bars, acetate; stripped bars, ethanol. Growth curves as in Fig. 6.1, except that OD_{600} scale (y-axis) is decimal.

CcpA influences the intracellular levels of phosphorylated metabolites

Inactivation of *ccpA* renders a strain with altered growth and fermentation profiles both on Glc and on Gal. In particular, the disparate substrate consumption rates and the fermentation end-product patterns, led us to surmise that levels of intracellular metabolites are also under the influence of CcpA. Intracellular metabolites were determined in ethanol extracts obtained as for transcriptome analyses (M and TS phases of growth) by targeted metabolomics using ^{31}P-NMR (Fig. 6.5). In this way we were able to quantify intracellular concentrations of metabolites in central carbon utilization pathways (carbohydrate-specific pathways, glycolysis), catabolic precursors in the synthesis of surface structures (cell wall, capsule), and co-factors, detailed below (see Fig. 6.6 for an overview of the pathways).

Glycolytic and carbohydrate-specific pathway intermediates. During growth on Glc the levels of the upper glycolytic metabolites glucose 6-phosphate (G6P) and FBP were higher in the *ccpA* mutant, independently of the phase of growth. Likewise, the lower glycolytic metabolites 3-phosphoglycerate (3-PGA) and phospho*enol*pyruvate (PEP) accumulated to higher concentrations in strain D39Δ*ccpA*. The size of the glycolytic pools showed a growth phase dependency: the concentrations of G6P, FBP, 3-PGA and PEP, were smaller in the TS phase. The decrease in the level of the lower glycolytic metabolites from M to TS phases

of growth was unexpected and is contrary to the accumulation profile of 3-PGA and PEP in other *Streptococcaceae* species (Iwami and Yamada, 1985; Neves *et al.*, 2002a), suggesting different regulation at the level of pyruvate kinase in *S. pneumoniae*. The concentrations of the glycolytic intermediates were also lower in the TS phase of growth when Gal was used as sole carbon source. In contrast to Glc, loss of CcpA on Gal resulted in slightly lower glycolytic pool levels. Furthermore, D39 and D39Δ*ccpA* cells growing on Gal accumulated tagatose 1,6-bisphosphate (TBP), α-galactose 1-phosphate (α-Gal1P) and α-glucose 1-phosphate (α-G1P), denoting simultaneous dissimilation of Gal via the tagatose 6-phosphate and Leloir pathways (Figs. 6.5 and 6.6). While deletion of *ccpA* had only a moderate negative effect on the accumulation of the Leloir intermediates (α-Gal1P and α-G1P), the concentration of TBP was 10-fold lower in D39Δ*ccpA*. This striking difference might be a direct consequence of the higher *lac* transcript levels in D39 (Tables S.6.1 and S.6.4 on the CD), since the overall Gal consumption flux was identical in both strains (Table 6.3). It should be noted that TBP and α-Gal1P are not detected during growth on Glc, whereas α-G1P, which is also the key precursor of structural polysaccharides (*e.g.* capsule, teichoic acids) accumulated exclusively in the *ccpA* mutant.

NDP-activated intermediates in the synthesis of surface structures. NDP-activated intermediates are soluble precursors in the synthesis of several cell surface structures of utmost importance for virulence and pathogenesis (reviewed in Mitchell, 2003; Kadioglu *et al.*, 2008). During growth on Glc, UDP-glucose, a precursor in the biosynthesis of the serotype 2 capsule and other structural polysaccharides, showed growth-dependent accumulation in both strains, but the reduction from M to TS was more pronounced in the *ccpA* mutant. Furthermore, the accumulation profile of the soluble cell wall precursor UDP-N-acetylglucosamine was not changed due to inactivation of *ccpA*, whereas the

concentration of UDP-N-acetylmuramoyl-pentapeptide was higher in D39Δ*ccpA*. Curiously, on Gal the soluble cell wall components were below detection limits (< 0.5 mM), except for UDP-N-acetylglucosamine, which accumulated in *S. pneumoniae* D39 in MS growth. Accumulation of CDP-choline, the phosphorylcholine donor in the synthesis of teichoic acids, was higher in the *ccpA* mutant, decreasing in both strains from M to TS phases during growth on Glc. The growth dependent behavior was also observed on Gal, but in this carbohydrate the levels of CDP-choline were approximately the same in D39 and D39Δ*ccpA*.

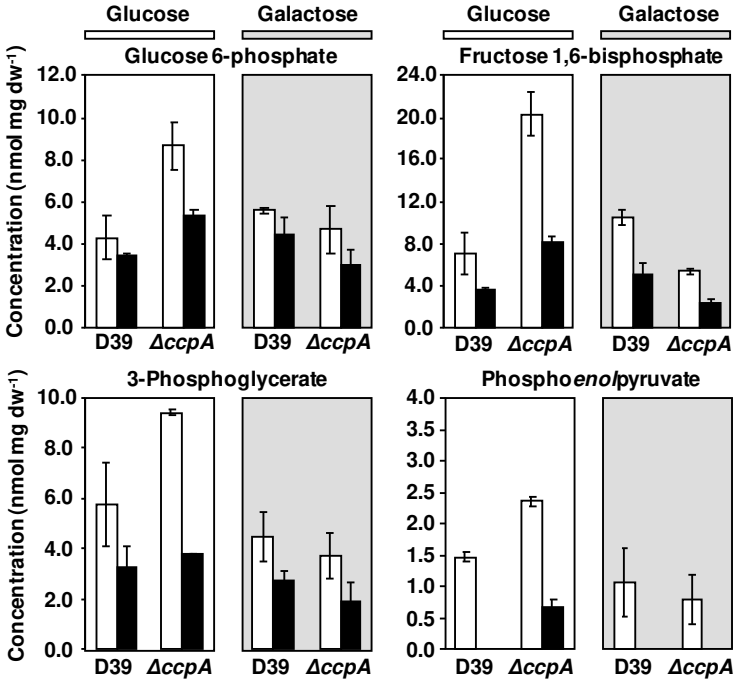

Fig. 6.5. Effect of *ccpA* deletion on intracellular concentrations of phosphorylated metabolites during growth on glucose or galactose. Phosphorylated metabolites were measured by ^{31}P-NMR in ethanol extracts of *S. pneumoniae* D39 and *ΔccpA* strains

grown to mid-exponential (M, white bars, OD_{600} of 0.35 ± 0.02) or transition-to-stationary phases (TS, black bars, OD_{600} of 1.3 ± 0.1) of growth in CDM supplemented with 56 ± 1 mM Glc (white background) or 57 ± 1 mM Gal (light grey background). Phosphorylated metabolites measured in extracts comprised glycolytic metabolites, phosphorylated carbohydrate-specific metabolites, UDP-activated metabolites, and co-factors. The values are the mean of three independent experiments ± SD.

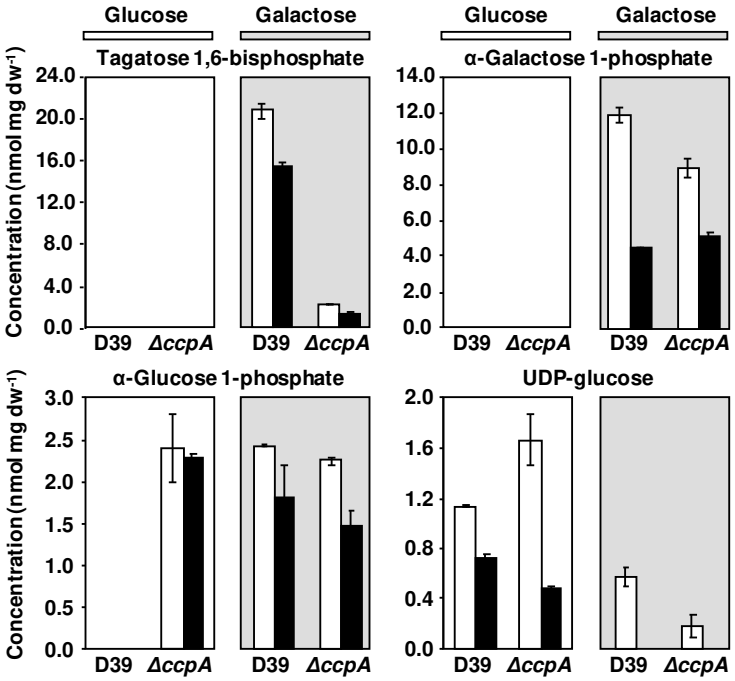

Fig. 6.5. ***continued***

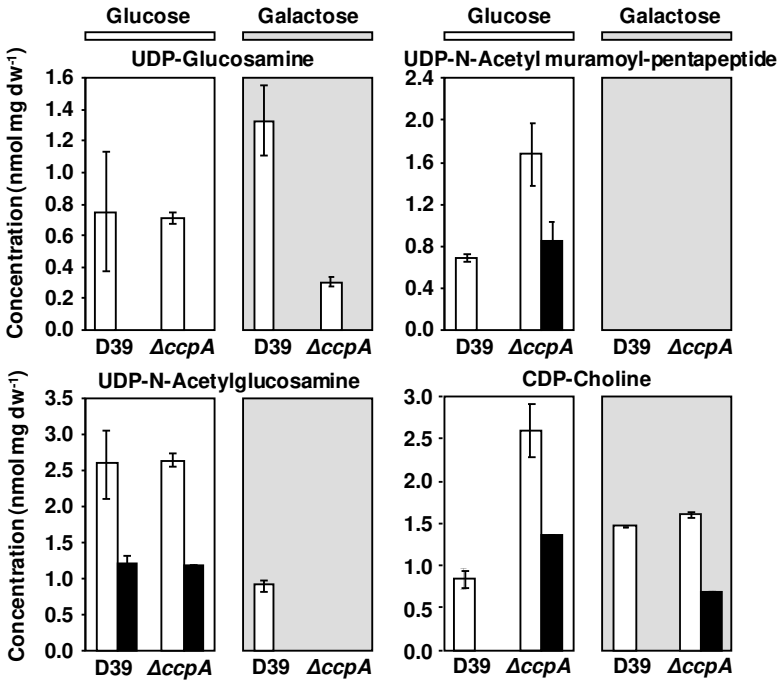

Fig. 6.5. ***continued***

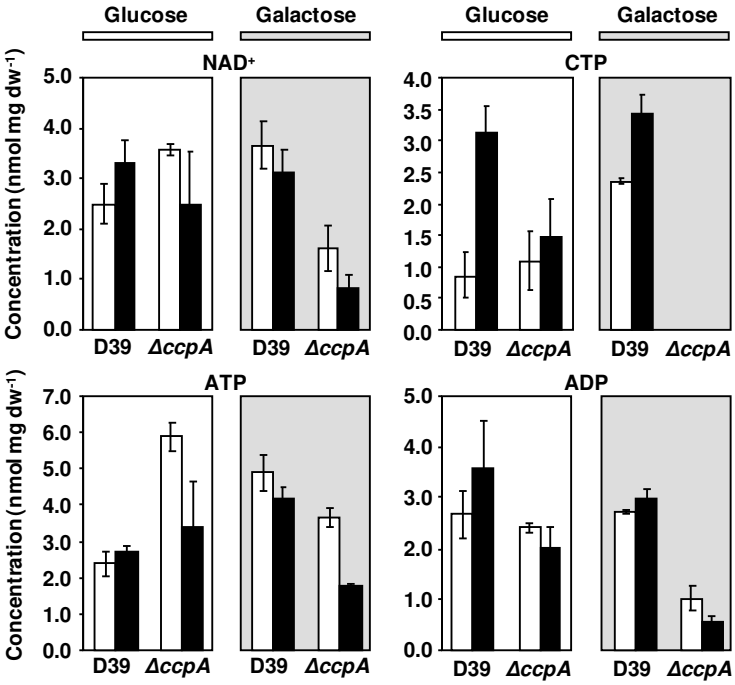

Fig. 6.5 ***continued***

Concentrations of metabolic cofactors. CcpA-defective cells growing on Glc accumulated slightly higher amounts of NAD^+, identical levels of CTP and ADP, and *circa* 2-fold higher amounts of ATP in MS growth (Fig. 6.5). In the TS phase of growth, NAD^+ and ATP were not significantly affected, ADP was slightly lower, and CTP was about half the concentration in the *ccpA* mutant. When Gal was used as substrate, the accumulated levels of NAD^+, CTP, ATP and ADP were lower in the *ccpA* mutant both in M and TS phases of growth.

The metabolite profiles herein presented clearly support the operation of two routes for Gal catabolism and suggest a unique mechanism underlying the regulation of glycolysis in *S. pneumoniae*. CcpA influences the level of key

phosphorylated metabolites (glycolytic metabolites, co-factors, etc.) potentially involved in metabolic regulation. These findings extend beyond transcriptional regulation the role of CcpA in controlling cellular network properties. Furthermore, CcpA-dependent changes in cell wall and capsule UDP-activated precursors indicates a role of CcpA in the modulation of cell surface properties, known to be critical in virulence and pathogenesis.

CcpA inactivation loosens capsule attachment to the cell wall

It has previously been reported that CcpA-deficient mutants show attenuated virulence, and this behavior was associated with lower expression of genes committed to the synthesis of the pneumococcal capsule (Giammarinaro and Paton, 2002). Our metabolome data showed significant differences in the pools of the capsule cytoplasmic precursors UDP-glucose and α-G1P. Therefore, we deemed it important to measure the amounts of capsule produced in D39 and its *ccpA* mutant (Fig. 6.7).

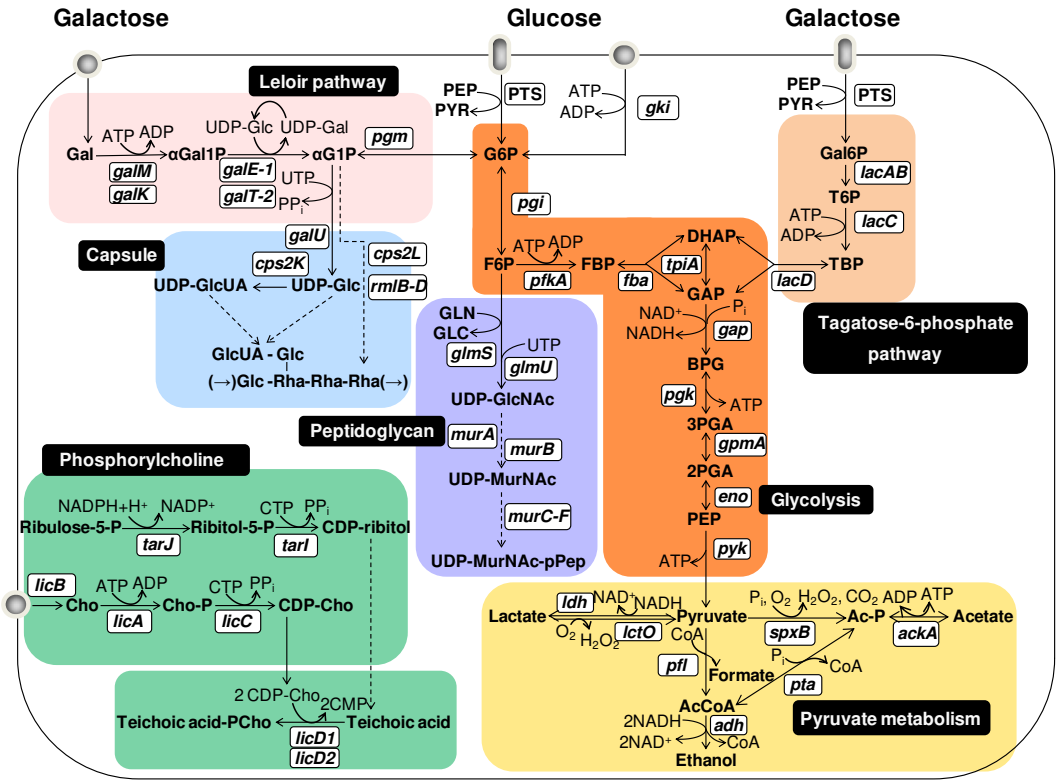

Fig. 6.6. Schematic representation of central metabolic pathways in *S. pneumoniae* D39. Glc is oxidized to pyruvate via the Embden-Meyerhof-Parnas pathway (Glycolysis, orange box). Homolactic fermentation reduces pyruvate into lactate, whereas mixed-acid fermentation leads to other products, such as formate, acetate and ethanol (Pyruvate metabolism, yellow box). Gal is converted to G6P by the Leloir pathway (light pink box) and to dihydroxyacetone phosphate (DHAP) or glyceraldehyde 3-phosphate (GAP) by the tagatose 6-phosphate pathway (light orange box). Pathways for capsule, peptidoglycan and phosphorylcholine biosynthesis are shown in light blue, light purple and light green boxes, respectively. Putative and functional characterized genes encoding depicted metabolic steps are shown in white boxes. Proposed pathways were reconstructed based on genome information (http://www.ncbi.nlm.nih.gov/genomes/lproks.cgi), literature and database surveys (KEGG, MetaCyc). Gene annotation downloaded from NCBI: *galM*, aldose 1-epimerase; *galK*, galactokinase; *galE-1*, UDP-glucose 4-epimerase; *galT-2*, galactose 1-phosphate uridylyltransferase; *pgm*, α-phosphoglucomutase; *galU*, glucose 1-

phosphate uridylyltransferase; *cps2L*, glucose 1-phosphate thymidylyltransferase; *cps2K*, UDP-glucose 6-dehydrogenase, putative; *rmlC*, dTDP-4-keto-6-deoxy-D-glucose 3,5-epimerase Cps2M; *rmlB*, dTDP-glc 4,6-dehydratase Cps2N; *rmlD*, dTDP-4-keto-L-rhamnose reductase Cps2O; *gki*, glucokinase; *pgi*, glucose 6-phosphate isomerase; *pfkA*, 6-phosphofructokinase; *fba*, fructose bisphosphate aldolase; *tpiA*, triosephosphate isomerase; *gap*, glyceraldehyde-3-phosphate dehydrogenase; *pgk*, phosphoglycerate kinase; *gpmA*, phosphoglyceromutase; *eno*, enolase; *pyk*, pyruvate kinase; *lacA*, galactose 6-phosphate isomerase subunit LacA; *lacB*, galactose 6-phosphate isomerase subunit LacB; *lacC*, tagatose 6-phosphate kinase; *lacD*, tagatose 1,6-diphosphate aldolase; *ldh*, L-lactate dehydrogenase; *lctO*, lactate oxidase; *spxB*, pyruvate oxidase; *ackA*, acetate kinase; *pta*, phosphotransacetylase; *pfl*, pyruvate formate-lyase; *adh* (*spd_1834*), bifunctional acetaldehyde-CoA/alcohol dehydrogenase; *glmS*, D-fructose 6-phosphate amidotransferase; *glmU*, UDP-N-acetylglucosamine pyrophosphorylase; *murA-1 and murA-2*, UDP-N-acetylglucosamine 1-carboxyvinyltransferase; *murB*, UDP-N-acetyl*enol*pyruvoylglucosamine reductase; *murC*, UDP-N-acetylmuramate-L-alanine ligase; *murD*, UDP-N-acetylmuramoyl-L-alanyl-D-glutamate synthetase; *murE*, UDP-N-acetylmuramoylalanyl-D-glutamate-2,6-diaminopimelate ligase; *murF*, UDP-N-acetylmuramoylalanyl-D-glutamyl-2, 6-diaminopimelate--D-alanyl-D-alanyl ligase; *tarJ* (*spd_1126*), alcohol dehydrogenase, zinc-containing or TarJ; *tarI* (*spd_1127*), 2-C-methyl-D-erythritol 4-phosphate cytidylyltransferase or TarI; *licB*, protein LicB; *pck*, choline kinase or LicA; *licC*, CTP:phosphocholine cytidylyltransferase; *licD1*, phosphotransferase LicD1; *licD2*, phosphotransferase LicD2.

Curiously, inactivation of *ccpA* did not affect the total amount of capsule either on Glc- or Gal-CDM. However, in Gal-containing medium the amount of capsule produced was higher for both strains. Furthermore, a major difference in Gal-CDM was the amount of loose capsule (not attached to the cell wall), which accounted for about 94% of the total polysaccharide in D39Δ*ccpA* (Fig. 6.7). In the parent strain, only a small fraction (~13%) of loose capsule was detected, exclusively in the TS phase of growth. Although the role of CcpA in the regulation of capsule production was not confirmed, our data show a function of CcpA in the association of capsule to the cell wall, at least during growth on Gal.

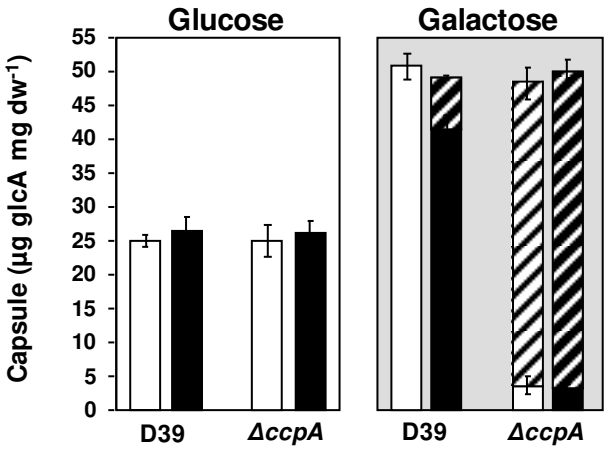

Fig. 6.7. Amount of capsule polysaccharide in D39 and its isogenic *ccpA* mutant. Estimation of capsule was performed based on the determination of its glucuronic acid content in strains D39 and D39Δ*ccpA* in mid-exponential (white bars, OD_{600} of 0.35 ± 0.02) and transition-to-stationary (black bars, OD_{600} of 1.3 ± 0.1) cultures grown in CDM containing 56 ± 1 mM Glc (white background) or 57 ± 1 mM Gal (light grey background). Hatched bars indicate loose capsule polysaccharide. All the determinations were done twice in two independent cultures and the values are means ± SD.

CcpA affects the expression of many virulence genes

To further identify links between CcpA and virulence we compared all genes that have been linked to the virulence of this pathogen with our list of genes influenced by deletion of *ccpA* (Table S.6.7 on the CD). In addition, the *ccpA* microarray data were compared to the list of genes identified in the STM screen performed by Hava and Camilli, 2002. Virulence genes affected by CcpA included classical virulence factors as well as many genes involved in amino acid and carbohydrate metabolism, transcriptional regulators, and genes with unknown function (Table S.6.7 on the CD). Of the classical virulence factors, the Mn^{2+}-dependent superoxide dismutase gene *sodA*, involved in virulence and protection

against oxidative stress (Yesilkaya *et al.*, 2000), was upregulated in the *ccpA* mutant, which fits well with higher H_2O_2 concentrations observed in this strain. Interestingly, two of the three neuraminidase genes, namely *nanA* and *nanB*, which have been extensively studied regarding their important role in pneumococcal virulence (King, 2010), were strongly upregulated in the *ccpA* mutant in all four conditions as well. Recently, NanA had been shown to, in conjunction with BgaA and StrH, two other exoglycosidases, protect *S. pneumoniae* from phagocytic killing through prevention of complement deposition (Dalia *et al.*, 2010). *StrH* was affected only slightly in Glc_TS and Gal_TS, but *bgaA* was, like *nanA* and *nanB*, upregulated in the *ccpA* mutant in all four conditions, most strongly on Glc; importantly, *bgaA* was repressed in Glc compared to Gal (Table S.6.4 on the CD) only in the wild-type, which further supports its role in nasopharyngeal colonization. All these three genes, as well as *nanB*, might be directly affected by CcpA, since there is a predicted *cre* site in their upstream region or in the upstream region of a gene with which they seem to be co-regulated in the array analyses. Of a total of 79 virulence genes of which transcription is affected in the *ccpA* mutant, 35 are possibly regulated directly by CcpA (Table S.6.7 on the CD). The *pcpA* gene, implicated in colonization/infection of the airways (Johnston *et al.*, 2006), showed Glc-dependent CcpA-mediated repression in D39. The *pcpA* gene is also regulated depending on the extracellular concentration of Mn^{2+} and Zn^{2+} through the action of PsaR (Kloosterman *et al.*, 2008), and activated by the nutritional regulator CodY (Hendriksen *et al.*, 2008). It therefore seems to be regulated in a complex way in response to various different environmental stimuli. Interestingly, genes involved in choline metabolism, namely the *tarIJlicABC* (*lic1*) operon, were upregulated in the *ccpA* mutant especially in Glc_TS. In agreement, the levels of CDP-choline were higher in the *ccpA* mutant (Fig. 6.5). Together the data suggest that *ccpA*

could affect the level of choline in the pneumococcal cell wall and as a result the decoration of the pneumococcal cell wall with choline-binding proteins, a class of virulence factors. An interesting observation, which might be associated with virulence, was the strong activation by CcpA of two genes involved in cell wall synthesis (*glmS* and *murF*) only during growth on Glc. Moreover, the increased transcript level of *glmS* and *murF* in D39 on Glc might correlate with the high demand for synthesis of biomass as denoted by the high growth rate in this condition. Of the transcriptional regulators identified as virulence genes, *comDE* was downregulated on Glc, whereas *TCS07* was upregulated in all conditions, which suggests that their regulons and their respective stimuli are connected to that of CcpA.

With a few exceptions, CcpA acts as a repressor of virulence gene expression in *S. pneumoniae*. Based on our data it is reasonable to assume that CcpA is one of the factors controlling the interaction of *S. pneumoniae* with its host during colonization and infection of the airways through regulation of the above mentioned key virulence genes.

Discussion

It is well established that bacteria adapt to fluctuating environments by altering expression of genes involved in basic metabolic processes. In the Firmicutes, the pleiotropic transcriptional regulator CcpA is recognized as a key player in carbon catabolite control, *i.e.* the regulatory phenomena that allow bacteria to selectively use substrates for growth (for reviews see Deutscher *et al*., 2006; Görke and Stülke, 2008). Importantly, in the last decade an increasing number of studies have exposed the role of CcpA in the regulation of virulence in

Gram-positive pathogens (Giammarinaro and Paton, 2002; Iyer *et al*., 2005; Seidl *et al*., 2006; Abranches *et al*., 2008; Shelburne *et al*., 2010; Chiang *et al*., 2011). In the human pathogen *S. pneumoniae*, regulation of carbohydrate-specific catabolic pathways as well as modulation of virulence factors by CcpA has been reported (Giammarinaro and Paton, 2002; Iyer *et al*., 2005; Kaufman and Yother, 2007). However, a comprehensive study of the role of CcpA in the physiology of *S. pneumoniae* was not undertaken so far. In a recent study, *ccpA* was found to interact with 64 other genes by Tn-seq transposon mutagenesis; based on the high number of genetic interactions these authors suggested that CcpA appears to be a master regulator in *S. pneumoniae* (van Opijnen *et al*., 2009). In this work, we used genome-wide transcriptome analyses and metabolite profiling to study in depth the impact of CcpA on pneumococcal metabolism and virulence. Our data show that beyond controlling carbohydrate transport and metabolic genes, CcpA is involved in various other cellular processes, including traits connected to virulence and pathogenesis (Fig. 6.8). Therefore, the role of CcpA as a master regulator in *S. pneumoniae* is undoubtedly demonstrated by the results in this study.

The CcpA regulon was substantial on Glc, the “preferred” carbohydrate of many Firmicutes, which supports high pneumococcal growth rate (Fig. 6.4), but remarkably this was also the case in the slowly metabolized Gal, a carbohydrate generally recognized as non-repressing. In *B. subtilis*, besides Glc several other PTS-transported carbohydrates are capable of eliciting CcpA-mediated catabolite repression (Singh *et al*., 2008). In *S. mutans*, the transport of Gal is exclusively mediated via PTS systems (Zeng *et al*., 2010), but curiously the CcpA regulon on Gal was markedly smaller than on Glc (Abranches *et al*., 2008), which is in contrast to our observations in *S. pneumoniae*. Also noticeable is the pronounced difference in the amount of genes influenced by CcpA in *S. mutans* (up to 9%)

and *S. pneumoniae* (up to 19%), which despite their genetic relatedness apparently have evolved distinct regulatory networks. In *S. mutants*, catabolite repression can be independent of CcpA and requires specific components of carbohydrate-PTS permeases (Zeng and Burne, 2010). A reasonable explanation lies in the nutritional diversity encountered by the two streptococci in their respective ecological niches.

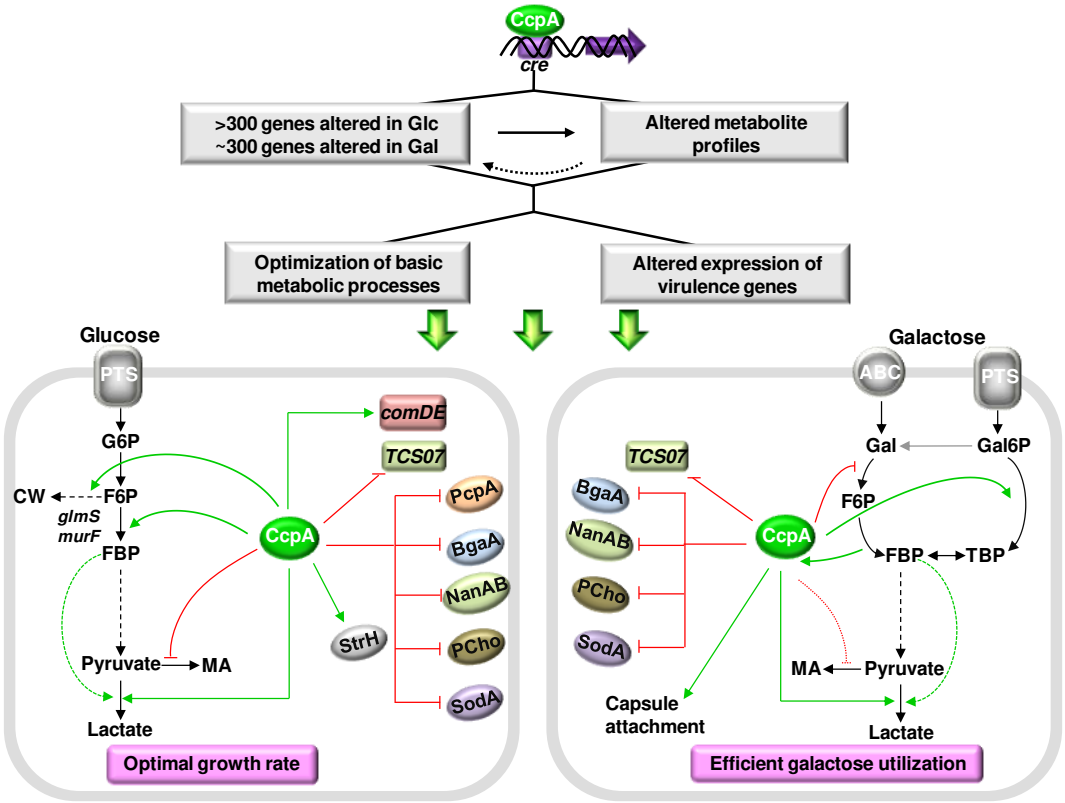

Fig. 6.8. Model for CcpA regulation of basic metabolic processes and virulence factor expression in the presence of glucose or galactose in *S. pneumoniae*. Transport of carbohydrates through the multi-protein phospho*enol*pyruvate: carbohydrate phosphotransferase system (PTS) ensures a typical PTS-mediated signal transduction

pathway for CcpA regulation. CcpA-mediated regulation results in altered expression of genes involved in carbohydrate metabolism and classical virulence factors, including cell wall associated proteins, transcriptional regulators and phosphorylcholine. Repression and activation are represented by red and green arrows, respectively. Dashed lines indicate metabolic regulation. G6P, Glucose 6-phosphate; F6P, fructose 6-phosphate; CW, cell wall; MA, mixed-acid fermentation; PcpA, choline-binding protein PcpA; BgaA, beta-galactosidase A; NanAB, neuraminidases A and B; *P*Cho, phosphorylcholine; SodA, superoxide dismutase, manganese-dependent; StrH, β-N-acetylhexosaminidase; TCS07 and ComDE, two-component systems.

In this study, CcpA ensures fast growth on Glc, but not on Gal, as the growth rate on the latter carbohydrate is basically independent of this pleiotropic regulator. In *S. pneumoniae* the routes for Gal catabolism have not been biochemically characterized, but complete Leloir and tagatose 6-phosphate pathways can be deduced from pneumococcal genome sequence data (http://www.ncbi.nlm.nih.gov/genome/lproks.cgi). We propose that both pathways are operative during growth on Gal. The presence of the intermediates α-Gal1P (Leloir) and TBP (tagatose 6-phosphate), as well as the elevated expression levels of the genes *galM, galKT-2* (Leloir), and *lacABCD* (tagatose 6-phosphate), fully support this claim. Interestingly, *lacFE* are also induced by Gal, suggesting a role of the pneumococcal lactose-PTS in Gal uptake as reported for *S. mutans* and *L. lactis* (Zeng and Burne, 2010; Neves *et al.*, 2010). The uptake of Gal via a PTS system would ensure a typical PTS-mediated signal transduction pathway for CcpA regulation and is in agreement with the large CcpA regulon determined during growth on Gal. On this carbohydrate, CcpA regulation seems to comply with the essence of catabolite control, which is to coordinate metabolic operation ensuring a maximum profit for growth. Activation by CcpA of the PTS-dependent route (tagatose 6-phosphate pathway) for Gal degradation, while repressing the

Leloir genes, is in agreement with that principle. Furthermore, activation of the glycolytic genes *pfk* and *pyk*, and *ldh* indicate that CcpA's role is to enable maximal Gal catabolism. In light of our results, an answer to the question as to why substrate consumption and growth rates on Gal are not stimulated by CcpA is difficult to put forward. Of note in Gal-grown D39 cells, is the elevated concentration of TBP (10-fold higher than in D39Δ*ccpA*), which might be toxic for the cells. Indeed, unrestricted accumulation of phosphorylated metabolites has previously been evoked to explain negative effects on growth rate (Thevelein and Hohmann, 1995; Andersen *et al*., 2001). Also surprising was the pronounced shift to mixed-acid fermentation in strain D39, since CcpA represses genes involved in that type of metabolism. However, Gal-induced alleviation of the CcpA-mediated repression might partially explain the observed behavior (Table S.6.1 on the CD). Indeed, higher expression of *pfl* and *pfl-ae* allow a more efficient competition with lactate dehydrogenase for the common substrate pyruvate, consequently increasing the flux to mixed-acid products, including acetate. Production of this organic acid is accompanied by ATP formation, which is certainly an advantage during the fermentation of Gal, as the glycolytic ATP generation is limited by the substrate consumption rate (three times lower than that of Glc). Shifts to mixed-acid fermentation as a means to counteract for ATP production during growth on slowly metabolized carbon sources or limiting carbohydrate concentrations carbohydrates are well documented in *Streptococacceae* (Yamada and Carlsson, 1975b; Garrigues *et al*., 1997). In view of the data it is reasonable to assume that Gal-dependent regulatory mechanisms at the translational, post-translational and/or metabolic levels overlay the transcriptional direct control by CcpA. A good example is the Gal-dependent activation of the Leloir pathway, which genes are in all instances under CcpA repression. The lack of correlation between phenotypic behaviors and changes in transcription levels is not unprecedented (Griffin *et al*.,

2002; Daran-Lapujade *et al.*, 2007) and most likely derives from the feedback regulation of metabolism on all regulatory layers (Heinemann and Sauer, 2010).

In this work we show that CcpA is crucial in the control of central physiological processes in *S. pneumoniae*, and thus most likely influences the ability to persist and proliferate in the host. Considering our data showing Glc- and Gal-dependent regulation it is tempting to hypothesize that in the specific host microenvironments basic metabolic processes are tuned by CcpA to maximize cellular profit (Fig. 6.8). In this light, the attenuated virulence shown by *ccpA* mutants in mouse models of pneumococcal colonization and infection (Giammarinaro and Paton, 2002; Iyer *et al.*, 2005) can plausibly be attributed to decreased fitness. However, this hypothesis might not depict the full picture, as we discovered that CcpA directly or indirectly influences the transcript level of a number of canonical virulence factors (Fig. 6.8). It is interesting to note that among the influenced genes several encode moonlighting proteins, with roles in host-pathogen interaction and basic metabolic processes. A good example is provided by BgaA, an exoglycosidase involved in adherence to epithelial cells (King, 2010), and recently found to be important in basal growth (van Opijnen *et al.*, 2009), which is repressed by CcpA as determined by us and others (Iyer *et al.*, 2005; Kaufman and Yother, 2007). Such findings certainly reinforce the subtle link between basic physiology and virulence in *S. pneumoniae*.

Involvement of CcpA in the control of classical virulence factors is a recurrent observation in *Streptococcaceae* (Giammarinaro and Paton, 2002; Iyer *et al.*, 2005; Abranches *et al.*, 2008; Shelburne *et al.*, 2008b; van Opijnen *et al.*, 2009). In a previous report, significant repression of the capsular polysaccharide biosynthesis *locus* (*cps*) was observed in a pneumococcal *ccpA* mutant (Giammarinaro and Paton, 2002). Except for a negligible effect on *rfbCBD* genes in the transition-to-stationary phase of Glc-grown cells, we have not found

significantly differentially expressed *cps* genes in any other tested conditions. Furthermore, the amount of capsule produced was not influenced by CcpA (Fig. 6.7). Accordingly, Camilli and co-workers did not observe a connection between CcpA and *cps* expression (Iyer *et al.*, 2005; van Opijnen *et al.*, 2009). Our data unequivocally show that the production of capsule is influenced by the carbon source, since the amount of polysaccharide was doubled in Gal-grown cells in a CcpA-independent manner. In view that Gal is a prevailing carbohydrate in nasopharyngeal secretions (Yesilkaya *et al.*, 2009 on the CD; King, 2010), this finding is relevant in terms of host-pathogen interactions, since a relatively thick capsule is essential to evade the immune system, and thus, for the pneumococcus to persist in the host (Magee and Yother, 2001). Curiously, on this carbohydrate the attachment of the capsular polysaccharide to the pneumococcal cell wall was substantially altered in the presence of CcpA.

Our transcriptome analyses revealed that genes involved in the synthesis of phosphorylcholine are under the control of CcpA. At the metabolic level, the lower concentration of CDP-choline (activated choline precursor) is in full agreement with the transcript levels of the biosynthetic genes. The tight control exerted by CcpA on the availability of CDP-choline might provide a means to influence the association of capsule, proteins and other molecules to the cell wall. Indeed, binding of macromolecules to the cell wall is conditioned by the decoration of the wall polysaccharides (teichoic acids and lipoteichoic acids) (Neuhaus and Baddiley, 2003; Bergmann and Hammerschmidt, 2006), which in *S. pneumoniae* contain residues of phosphorylcholine (Bergmann and Hammerschmidt, 2006). Using proteomics others have shown that loss of *ccpA* caused changes in the amounts of several cell wall-associated proteins (Iyer *et al.*, 2005). A good correlation between our expression data and the wall fraction protein levels was observed for some proteins (Iyer *et al.*, 2005), but for other proteins no significant

regulation at the transcriptional level was detected. Although we cannot rule out the possibility that this is due to interspecies variation or translational and post-translation regulation, in light of our results it is reasonable to speculate that, rather than altering the protein level, CcpA is somehow affecting the tethering of the proteins to the cell wall, as we showed for capsule attachment. CcpA-dependent effects on the levels of several NDP-activated precursors of wall polysaccharides (Fig. 6.5) further strengthen the role of CcpA in shaping the cell wall decoration. This unforeseen function of CcpA might be crucial in the host-pneumococcal interaction, which is heavily dependent on cell wall phosphorylcholine and associated proteins (reviewed in Kadioglu *et al.*, 2008). Future studies on cell-surface proteome should be performed to address this issue in more detail.

Of the promoters differentially regulated in the *ccpA* mutant *circa* 42% are presumably subject to direct regulation by CcpA, as denoted by the presence of a *cre* sequence. This value is in good agreement with the 38% previously determined using the Tn-seq method to evaluate genetic interactions (van opijnen *et al.*, 2009). Still, a large percentage of the regulated promoters lack a canonical *cre* site. CcpA influenced the transcript level of 22 other transcriptional regulators, and thereby indirectly affects genes that are under the control of these regulators. Interestingly, we found that CcpA-responsive genes are also part of other regulatory networks. About 15 genes, mainly involved in amino acid and carbohydrate metabolism, but also the virulence gene *pcpA*, are commonly regulated by the nutritional regulator CodY and CcpA (Hendriksen *et al.*, 2008). Additionally, CcpA was found to share many gene targets with two-component systems regulatory networks, including those of CiaRH (Halfmann *et al.*, 2007), TCS04 (McCluskey *et al.*, 2004), TCS06 (Standish *et al.*, 2007), TCS08 (McKessar and Hakenbeck, 2007), and TCS09 (Hendriksen *et al.*, 2007). Recent

studies in *S. pyogenes* have highlighted the importance of a combination of independent transcriptional regulators to coordinate gene expression during infection (Shelburne *et al.*, 2010; Kietzman and Caparon, 2010). In this light, our data opens new avenues to explore how *S. pneumoniae* virulence is shaped by co-regulation of independent transcriptional regulators.

Factors controlling the interaction between pathogens and their host are of utmost importance for *in vivo* fitness and persistence in adverse host niches. Previously, the role of the transcriptional regulator CcpA in the physiology of the pneumococcus has been underappreciated. In this work we resorted to a combined transcriptome and metabolite profiling approach to demonstrate that CcpA is a master regulator involved in varied cellular processes in *S. pneumoniae*. We have ascertained that *S. pneumoniae* optimizes basic metabolic processes, modulates expression of virulence factors and most likely tunes association of macromolecules with the cell wall in a CcpA-mediated manner. The observed carbohydrate-dependency of the CcpA regulatory network indicates a key role in adjusting to specific nutritional cues within host niches. Exploring the unveiled links between CcpA and other regulators will certainly contribute to an improved understanding on the ability of *S. pneumoniae* to colonize and cause disease. The insights gained thus far from this comprehensive analysis foresee CcpA as a key factor in the interaction between *S. pneumoniae* and its host.

Acknowledgements

SM Carvalho helds a fellowship SFRH/BD/35947/2007 from Fundação para a Ciência e a Tecnologia (FCT). This work was funded by FCT and FEDER, projects PTDC/BIA-MIC/099963/2008 and PTDC/SAU-MII/100964/2008 and through grant PEst-OE/EQB/LA0004/2011. We would like to thank Dr. Luís Fonseca for assistance in the determination of substrate consumption rates. The authors are thankful to Dr. Karina Xavier and Dr. Rasmus Larsen for critically reading the manuscript that originated this chapter. SM Carvalho and AR Neves would like to thank Prof. H Santos for all the support provided during the course of this work.

Author's Contribution

Performed the experiments: SM Carvalho and T Kloosterman. T Kloosterman performed the microarray experiments, real time quantitative RT-PCRs and *in silico* microarray analysis and *cre* site prediction. Conceived and designed the experiments: SM Carvalho, T Kloosterman, OP Kuipers and AR Neves. Analyzed the data: SM Carvalho, T Kloosterman and AR Neves.

Chapter 7

Overview and concluding remarks

Chapter 7 – Contents

In 1928 Alexander Fleming discovered the world's first antibiotic, penicillin. Since then, several other natural antibiotics were isolated and broad-spectrum semi-synthetic antibiotics were produced. Antibiotics have saved millions of lives since the groundbreaking discovery of penicillin. However, their inappropriate use combined with the natural capacity of microorganisms to take up foreign DNA has dramatically increased the number of antibiotic resistant pathogens. *S. pneumoniae*, a common asymptomatic commensal of the nasopharynx, is among those microorganisms. In young children, the elderly and immune-compromised people the pneumococcus is a leading cause of bacterial meningitis, pneumonia, septicemia, and otitis media. With widespread antibiotic resistance and re-emergence of non-type vaccine strains, it is urgent to find new targets for the development of novel therapeutic and preventive drugs. One such opportunity is offered by the recent findings that link pathogenesis to carbohydrate metabolism.

The work presented in this thesis contributes to the understanding of basic metabolic processes, in particular, sugar metabolism and its role in pneumococcal virulence.

Glucose and galactose as carbon sources for growth of *S. pneumoniae*

Glucose is the preferred carbon source of many Gram-positive microorganisms. A recent study showed that Glc, among thirty two carbohydrate sources, was the one supporting fastest growth of strain DP1004, a rough derivative of strain D39 (Bidossi *et al.*, 2012). Even though competition assays were not performed, the data point out Glc as the preferred sugar of *S. pneumoniae*. In the human host, Glc is present in the blood and in the inflamed lungs of hyperglycemic individuals, but is scarce in the nasopharyngeal milieu

(Philips *et al.*, 2003; Shelburne *et al.*, 2008a). In this light, it is tempting to suggest that during infection, an increased availability of Glc would enable fast growth of *S. pneumoniae* leading to exacerbated disease.

Galactose is generally slowly metabolized by bacteria (reviewed in Deutscher *et al.*, 2006). In our and other studies the use of Gal as single carbon source reduced the growth rate of *S. pneumoniae* by at least 50% of that observed on Glc (Chapter 6) (Bidossi *et al.*, 2012). Despite being a slowly metabolized carbohydrate, biomass and energetic yields on Gal are similar (or higher) to those registered on Glc (Chapter 6) (Bidossi *et al.*, 2012). In this respect, Gal appears as a good carbon source to support avirulent colonization. Interestingly, Gal is one of the most abundant carbohydrates released during the deglycosylation of human mucins by pneumococcal exoglycosidases (King *et al.*, 2006). Mucins are heavily glycosylated proteins found in the mucus coating the surface of epithelial cells that line the cavities of the body, including the nasopharynx, which is the colonization niche of *S. pneumoniae* (Rose and Voynow, 2006; Yesilkaya *et al.*, 2008; Shelburne *et al.*, 2008a).

S. pneumoniae possesses the genes encoding the specific steps of the metabolic routes generally used for Gal catabolism in other *Streptococcaceae*, *i. e.* the Leloir and the tagatose 6-phosphate pathways (Thomas *et al.*, 1980; Abranches *et al.*, 2004; Neves *et al.*, 2010). In this work we have not performed a detailed biochemical characterization of the pathways, but our findings provide strong evidence for the simultaneous operation of both pathways during growth of *S. pneumoniae* on Gal (Chapter 6). Indeed, the presence of the intermediates α-Gal1P of the Leloir pathway and TBP of the tagatose 6-phosphate pathway, as well as the elevated expression levels of the genes *galM*, *galK*, *galT-2* (Leloir pathway) and *lacABCD* (tagatose 6-phosphate pathway) on Gal fully corroborate this view (Fig. 7.1) (Chapter 6). Moreover, the accumulation of TBP during Gal

metabolism clearly indicates the existence of Gal-PTS transporters in *S. pneumoniae*. This observation is in good agreement with other studies supporting the involvement of PTS systems in the uptake of Gal by *S. pneumoniae* (Kaufman and Yother, 2007; Bidossi *et al.*, 2012). Even though the simultaneous operation of both pathways for Gal dissimilation represents an additional energetic cost, this behavior is not unique for *S. pneumoniae*. In other *Streptococcaceae*, the occurrence and use of the Leloir and/or the tagatose 6-phosphate pathway for galactose utilization is strain-dependent. For instance, in *S. mutans* UA159 both pathways are required for efficient galactose utilization (Abranches *et al.*, 2004). Generally laboratorial *L. lactis* strains harbor the Leloir pathway, whereas dairy isolates possess and express both (Neves *et al.*, 2010). Interestingly, the relative efficacy of each pathway in the degradation of the sugar has yet to be established.

In *S. pneumoniae*, the metabolism of Glc is typically homofermentative, yielding lactate as major end-product; additionally, minor amounts of formate were also detected (Fig. 7.1). On the other hand, the metabolism of Gal was shifted towards mixed-acid fermentation with lactate, formate, acetate and ethanol as end-products (Fig. 7.1). The production of mixed-acid end-products on Gal is a behavior displayed by many *Streptococcaceae* (Steele *et al.*, 1954; Pierce, 1957; Thomas *et al.*, 1980; Abranches *et al.*, 2004; Neves *et al.*, 2010). The metabolic shift occurs due to higher flux through pyruvate formate-lyase (PFL) when Gal is used as carbon source (Fig. 7.1). PFL is activated post-translationally via a PFL-activating enzyme (PFL-AE) (Melchiorsen *et al.*, 2000; Buis and Broderick, 2005). The genome of *S. pneumoniae* possesses two copies of *pfl* (*spd_0420* and *spd_0235*) and *pfl-ae* (*spd_1774* and *spd_0229*) (Tettelin *et al.*, 2001; Hoskins *et al.*, 2001; Lanie *et al.*, 2007). In this work, we assigned *spd_0420* and *spd_1774* as coding for the functional pyruvate formate-lyase (PFL) and pyruvate formate-

lyase activating enzyme (PFL-AE) in *S. pneumoniae*, respectively; mutants of these genes were not able to produce formate, acetate and ethanol (Chapter 5). Gene duplication has long been considered to play a major role in evolution. Duplication of *pfl* and *pfl-ae* is not exclusive of *S. pneumoniae*. In the genome of *S. mutans* UA159 and *S. pyogenes* MGAS5005, two copies of each *pfl* and *pfl-ae* are also present (Ajdic *et al.*, 2002; Sumby *et al.*, 2005). Interestingly, the alignment of the amino acid sequences of the paralogous proteins in each strain indicated low number of identical residues (alignments performed with ClustalW, data not shown). This might explain why SPD_0235 and SPD_0229, the SPD_0420 and SPD_1774 paralogs, respectively, lost the function of PFL and PFL-AE. It is worth noting that the functional pneumococcal PFL and PFL-AE share high homology with a single copy of these genes in the other streptococci, whereas SPD_0235 and SPD_0229 share homology with the other copy. This might indicate that the gene duplication event preceded speciation.

Inactivation of the non-functional PFL and PFL-AE copies in *S. pneumoniae* did not produce a clear phenotype under the conditions studied (Chapter 5) (Yesilkaya *et al.*, 2009 on the CD). This genetic flexibility may allow for the arousal of new mutations leading to increased fitness of bacteria, or even potentiate the appearance of new functions. The regulatory programs involved in the evolution of paralogous proteins and their role in the evolutionary innovation at the biochemical level currently receive considerable attention (Martínez-Núñez *et al.*, 2010).

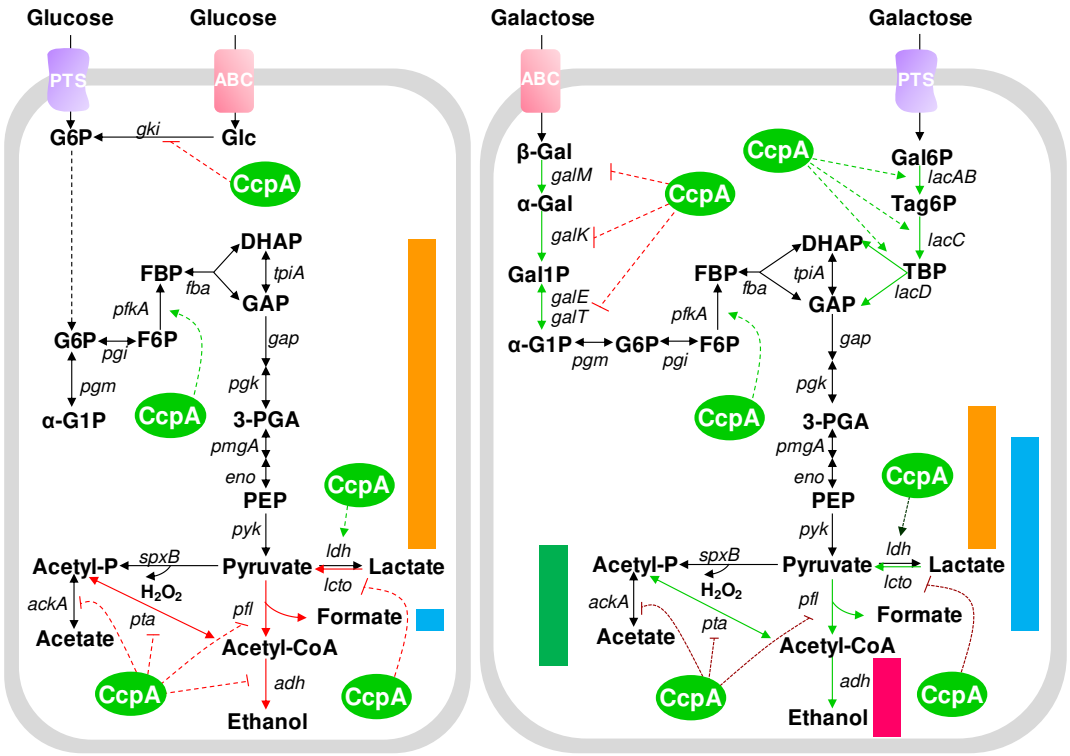

Fig. 7.1. Schematic representation of carbon catabolite control by CcpA during growth on glucose and galactose by *S. pneumoniae* D39. The levels of end-products (in µmol mg dw^{-1}) can be appreciated from the bar sizes: (■), lactate; (■), formate; (■), acetate; (■), ethanol. Green solid arrows: overexpression of the genes on Gal as compared to Glc; Red solid arrows: underexpression of the genes on Glc as compared to Gal. Green dashed arrows: activation by CcpA; Dark green dotted dashed arrows: alleviation of activation by CcpA on Gal as compared to Glc; Red dashed arrows, repression by CcpA; Dark red dotted arrows: alleviation of repression by CcpA in Gal as compared to Glc; The *cre* site position in promoter region of genes or operons encoding for activities downstream of pyruvate is coherent with the type of regulation. The intracellular reactions depicted are catalyzed by the following enzymes (the genes that code for the enzymes are shown in parenthesis): glucokinase (*gki*), phosphoglucose isomerase (*pgi*), 6-phosphofructokinase (*pfkA*), fructose 1,6-bisphosphate aldolase (*fba*), triosephosphate isomerase (*tpiA*), glyceraldehyde 3-phosphate dehydrogenase (*gap*), phosphoglycerate kinase (*pgk*), phosphoglyceromutase (*gpmA*), enolase (*eno*), pyruvate

kinase (*pyk*), galactose 6-phosphate isomerase (*lacAB*), tagatose 6-phosphate kinase (*lacC*), tagatose 1,6-bisphosphate aldolase (*lacD*), galactose mutarotase (*galM*), galactokinase (*galK*), galactose 1-phosphate uridylyltransferase (*galT*), UDP-galactose 4-epimerase (*galE*), α-phosphoglucomutase (*pgm*); pyruvate oxidase (*spxB*); pyruvate formate-lyase (*pfl*); bifunctional acetaldehyde-CoA/alcohol dehydrogenase (*adh*); phosphotransacetylase (*pta*); acetate kinase (*ackA*); L-lactate dehydrogenase (*ldh*); lactate oxidase (*lcto*). Abbreviations: Glc, glucose; G6P, glucose 6-phosphate; F6P, fructose 6-phosphate; FBP, fructose 1,6-bisphosphate; GAP, glyceraldehyde 3-phosphate; DHAP, dihydroxyacetone phosphate; 3-PGA, 3-phosphoglycerate; PEP, phospho*enol*pyruvate; Gal, galactose; Gal6P, galactose 6-phosphate; Gal1P, galactose 1-phosphate; Tag6P, tagatose 6-phosphate; TBP, tagatose 1,6-bisphosphate; α-G1P, α-glucose 1-phosphate.

Regulation of glucose and galactose metabolism in *S. pneumoniae*

It is well established that the catabolism of Gal in members of the *Streptococcaceae* originates a mixed-acid end-product profile (Chapters 5 and 6) (Steele *et al.*, 1954; Pierce, 1957; Thomas *et al.*, 1980; Abranches *et al.*, 2004; Neves *et al.*, 2010). However, the relative amount of products varies between species and even strains within the same species, probably due to disparate allosteric and transcriptional control exerted over the enzymes in glycolysis and downstream of pyruvate (Thomas *et al.*, 1980; Yamada *et al.*, 1985; Yamada and Carlsson, 1975a; Garrigues *et al.*, 1997; Asanuma *et al.*, 2004; Abranches *et al.*, 2008; Lopez de Felipe and Gaudu, 2009). The role of the global regulator of gene expression CcpA in the fermentation type displayed by *S. pneumoniae* on Glc and Gal will be discussed in the present section.

In *S. pneumoniae*, during growth on Glc CcpA favors homolactic fermentation as evidenced from our transcriptomic, *cre* site prediction and metabolic data. Indeed, on Glc CcpA represses the genes implicated in mixed-

acid fermentation (*pfl*, *pta*, *ackA* and *adh*) and activates *ldh*, thus promoting homolactic fermentation (Fig. 7.1, Chapter 6). The position of predicted *cre* sites in the promoter regions upstream of the genes *pfl*, *pta*, *ackA* and *adh* is consistent with repression by CcpA, whereas the position of the predicted *cre* upstream the promoter of the operon containing *ldh* and the glycolytic gene *pfkA*, is coherent with activation by CcpA (Chapter 6). Furthermore, inactivation of *ccpA* changed the fermentation from homolactic to a mixed-acid profile (Chapter 6). This type of regulation by CcpA, promoting homolactic metabolism, is common among the *Streptococcaceae* (Luesink *et al*., 1998; Gaudu *et al*., 2003; Asanuma *et al*., 2004; Zomer *et al*., 2007; Abranches *et al*., 2008; Lopez de Felipe and Gaudu, 2009). In these fermentative microorganisms lactate dehydrogenase is probably the most efficient activity in the anaerobic regeneration of the reducing equivalents generated in glycolysis (reviewed in Garvie *et al*., 1980). Therefore, the concerted control exerted by CcpA in the presence of a fast metabolizable sugar ensures metabolic efficacy.

On Gal, CcpA represses the genes coding for the enzymes of the Leloir pathway and activates those of the tagatose 6-phosphate pathway (Fig. 7.1) (Luesink *et al*., 1998). Genes encoding the Leloir and tagatose 6-phosphate pathways are frequently organized in operon-like structures and are thus prone to coordinated regulation. Curiously, in *S. pneumoniae* the Leloir genes are scattered in the chromosome. Nevertheless, *galM* possesses a *cre* site downstream its promoter region, which position is consistent with repression by CcpA; for *galKT* a clear promoter was not determined but a *cre* site near the starting codon of the *galK* gene was detected (Chapter 6). In contrast, the tagatose 6-phosphate pathway genes are organized in a single transcriptional unit, *lacABCD*. A *cre* site was not predicted upstream of the promoter region of this operon (Chapter 6).

Surprisingly, the Leloir genes, which are under the negative control of CcpA irrespectively of the sugar used for growth, appeared strongly upregulated on Gal compared to Glc in strain D39 and its *ccpA* mutant. This finding indicates the existence of CcpA-independent Gal-dependent regulatory mechanisms. Overexpression of the Leloir and tagatose 6-phosphate genes on Gal as compared to Glc was also observed in *S. mutans* (Abranches *et al.*, 2008).

The transcriptional regulatory effect of CcpA on the enzymes downstream of pyruvate is similar on Gal and Glc, except for a slight derepression of the mixed-acid genes and a small alleviation of the *ldh* activation on the former sugar (Fig. 7.1). Unexpectedly, the inactivation of *ccpA* rendered a more homolactic profile on Gal. As for expression of the Leloir genes, CcpA-independent Gal-dependent control of mixed-acid fermentation genes seems to be in effect in *S. pneumoniae*. Increased expression of mixed-acid genes on Gal as compared to Glc is not unprecedented. In *S. mutans* and *L. lactis*, *pfl* expression is strongly activated on Gal when compared to Glc (Melchiorsen *et al.*, 2000; Abranches *et al.*, 2008). Surprising is the fact that in *S. pneumoniae* upregulation of the mixed-acid genes (*pfl*, *pfl-ae*, *pta*) on Gal relative to Glc is lost when *ccpA* is inactivated (Chapter 6). This leads us to propose an indirect contribution of CcpA to the mixed-acid profile of D39 on Gal (Fig. 7.1). A likely scenario could involve cross-talk of CcpA with other regulatory proteins. Of note is the considerable number of genes affected by CcpA that are also targets for two-component systems involved in sugar metabolism, such as CiaRH, TCS08 and TCS09 (Chapter 6) (McKessar and Hakenbeck, 2007; Hendriksen *et al.*, 2007; Halfmann *et al.*, 2007). The importance of co-regulation by independent transcriptional regulators to coordinate gene expression has been highlighted in recent studies (Kietzman and Caparon, 2010; Shelburne *et al.*, 2010).

Independently of Glc or Gal, in *S. pneumoniae* CcpA promotes homolactic fermentation as denoted by the strong activation of *ldh* (Fig. 7.1). An interesting feature on Glc is the substantial repression of *gki* exerted by CcpA. The gene encodes glucokinase, which catalyzes the conversion of Glc into G6P, a step essential for Glc dissimilation via non-PTS routes. On Gal, CcpA activates the PTS-dependent route (tagatose 6-phosphate pathway), while repressing the Leloir pathway. In view of the results, sugar uptake via PTSs seems to be highly favored by CcpA. PTS uptake systems are more efficient in energetic terms than other classes of transporters and provide a typical PTS-mediated signal transduction pathway for CcpA regulation (reviewed in Deutscher *et al.*, 2006). CcpA regulation in *S. pneumoniae* thus seems to comply with the essence of catabolite control, which is to coordinate metabolic operation ensuring a maximal profit for growth.

Besides its role in determining the type of fermentation exhibited by *S. pneumoniae*, CcpA influences the expression of genes involved in a multitude of cellular functions. Up to 19% of the ORFs in the genome of strain D39 were affected by CcpA, thus confirming CcpA as a global regulator of gene expression in the pneumococcus. The pleiotropic effect of this regulator has also been shown for other pathogenic streptococci, namely *S. mutans* and *S. pyogenes* (Abranches *et al.*, 2008; Shelburne *et al.*, 2008b). In Gram-positive bacteria the repressing function of CcpA is mainly mediated by Glc, which is normally the preferred sugar (reviewed in Deutscher *et al.*, 2006; Görke and Stülke, 2008). Our work shows that in *S. pneumoniae* Gal, a less preferred sugar, elicits CcpA-dependent regulation to an extent similar to that of Glc (Chapter 6). In *B. subtilis*, the extent of CcpA-dependent catabolite repression exerted by different sugars was found to correlate with the amount of $HPr_{(Ser46)}$~P in the cell and thus presumably depends on the size of the glycolytic metabolite pools (Singh *et al.*, 2008). The glycolytic

intermediates FBP and G6P induce HPrK activity and consequently phosphorylation of HPr at Ser46, as well as the formation of the complex CcpA/ $HPr_{(Ser46)}$~P. In agreement with this hypothesis is the identical accumulation of FBP and G6P during mid-exponential growth of *S. pneumoniae* on Gal and Glc (Chapter 6). In the closely related *S. mutan*s, the CcpA regulon on Gal was about 2 times smaller than that on Glc (Abranches *et al*., 2008; Zeng and Burne, 2010). Interestingly, in *S. mutans* the levels of FBP and G6P on Gal were 2.5 to 4.5-fold lower than those on Glc (Abbe *et al*., 1982). In view of ours and other results, a positive correlation between upper glycolytic intermediates and the extent of catabolite repression in the *Streptococcaceae* is also likely.

Direct regulation of gene expression via CcpA is performed through binding of the protein to *cis-cre* operator sequences. The position of the *cre* site in the promoter region of the regulated gene dictates the regulation signal. Thus, it is expected that the response signal of genes prone to direct regulation by CcpA is the same irrespectively of the sugar source, but the magnitude might vary in a sugar-dependent manner. In *S. pneumoniae*, a good example of this notion is offered by the CcpA-mediated responses of the mixed-acid genes (*pfl*, *pfl-ae*, *pta*, *ackA*) and *ldh* during growth on Glc or Gal (Fig. 7.1).

In summary, CcpA is a master regulator of gene expression in *S. pneumoniae*. Moreover, the global regulator was found to have a prominent role in shaping fermentative metabolism in this human pathogen.

Metabolic responses of *S. pneumoniae* to oxygen

S. pneumoniae is a non-respiring, fermentative organism that tolerates oxygen. The bacterium thrives in micro-environments highly exposed to oxygen, such as the outer layer of mucosal secretions lining the surface of epithelial respiratory tract cells. The deeper the pneumococcus penetrates into the mucus layers, the less exposed to oxygen it becomes. In blood, *S. pneumoniae* encounters a *"quasi"* oxygen depleted environment, since oxygen is mostly bound to haemoglobin (LeMessurier *et al.*, 2006). Hence, the human host provides a range of environments that vary for oxygen availability. Consequently, understanding how oxygen impacts on the physiology of *S. pneumoniae* is essential to comprehend how the pathogen interacts with its host.

In *S. pneumoniae*, the sensitivity to oxygen seems to be strain-dependent (Auzat *et al.*, 1999; Yu *et al.*, 2001; Chapuy-Regaud *et al.*, 2001; Taniai *et al.*, 2008). Strain 0100993 (serotype 3) displayed a 2.3-fold decrease in biomass yield and a small increment in growth rate under aerobic conditions relatively to anaerobiosis (Yu *et al.*, 2001), whereas the growth parameters of strain CP1015, a non-encapsulated derivative of strain D39, remained unaffected by the presence of oxygen (Auzat *et al.*, 1999; Chapuy-Regaud *et al.*, 2001). In Chapter 2, we describe biomass reductions of about 3 and 16 times for strains D39 and R6, respectively, when oxygen was provided continuously (40% partial air tension) during growth, as compared to semi-aerobic (50-60% initial air tension) or anaerobic conditions (argon atmosphere). Moreover, oxygen stimulated the growth rate of both strains (Chapter 2). In general, oxygen seems to have a detrimental effect on the biomass yield of pneumococcal strains. The ability of catalase-negative *Streptococcaceae* to survive in aerobic environments depends on the presence of flavin-type NADH oxidases (*e.g.* NOX), NADH peroxidases

and enzymes capable of detoxifying the cell from molecular oxygen (*e.g.* superoxide dismutases) (Higuchi *et al.*, 1993; Poyart *et al.*, 1995; Gibson *et al.*, 2000; Neves *et al.*, 2002b). *S. pneumoniae* is seemingly equipped with superoxide dismutase(s) and NADH oxidase(s), but NADH peroxidases have so far not been identified (Poyart *et al.*, 1998; Yesilkaya *et al.*, 2000). Multiple copies of *nox* genes are not uncommon in the *Streptococcaceae* (Higuchi *et al.*, 1999; Neves *et al.*, 2002b; Wegmann *et al.*, 2007; Aikawa *et al.*, 2012), but *S. pneumoniae* possesses a single enzyme, which reduces O_2 to water at the expense of NADH (Auzat *et al.*, 1999).

Besides the role in detoxification of O_2, in dairy *Streptococcaceae*, NADH oxidase has a preponderant role in the re-direction of carbon fluxes during the aerobic metabolism of Glc (Neves *et al.*, 2002a). In *L. lactis* NADH oxidase, the expression of which is induced by oxygen, alleviates the need for regeneration of NADH at the level of lactate dehydrogenase, allowing a shift from lactate to acetate production (Neves *et al.*, 2002a). In *S. pneumoniae*, lactate is the major end-product of Glc metabolism under anoxic or hypoxic conditions (Fig. 7.2) (Chapter 2). On the other hand, when oxygen is abundant, a switch from lactate to acetate and H_2O_2 occurs (Fig. 7.2; Chapter 2). The high production of H_2O_2 combined with the fact that in *S. pneumoniae* the *nox* gene is apparently not induced by oxygen (Auzat *et al.*, 1999) minimize the role of the H_2O-producing NADH oxidase in flux re-rerouting. In this pathogen, pyruvate oxidase (SpxB) efficiently competes with NADH oxidase for oxygen, and is the main activity responsible for acetate and H_2O_2 production under aerobic Glc metabolism. Besides NADH oxidase and pyruvate oxidase, a third oxidase, lactate oxidase, might compete for oxygen in the pneumococcus (Taniai *et al.*, 2008). In the dairy *Streptococcaceae* the activities of lactate oxidase and pyruvate oxidase are only detectable under Glc deprivation (Seki *et al.*, 2004; Goffin *et al.*, 2006). In *S.*

pneumoniae, lactate oxidase activity is independent of growth phase and Glc availability (Taniai *et al.*, 2008). The latter finding was confirmed in Chapter 2 of this work, as evident from the intense lactate utilization without Glc exhaustion under aerobic conditions. Lactate oxidase has been proposed to play a role in energy generation during aerobic growth on Glc (Taniai *et al.*, 2008). However, during efficient Glc consumption the conversion of pyruvate to lactate and back to pyruvate seems improbable and is not supported by end-product data in Chapter 2 and (Taniai *et al.*, 2008). In both datasets the concentration of H_2O_2 is around 1 mM at the onset of growth arrest, and in our study lactate increases steadily while Glc is being utilized. A considerable increment in H_2O_2 concentration (1 to ~2-5 mM), which in our study is concomitant with lactate utilization, is only observed after growth stopped (Chapter 2) (Taniai *et al.*, 2008). Interestingly, ~1 mM H_2O_2 is reported as the minimal inhibitory concentration (MIC) necessary to prevent growth of strain D39 (Pericone *et al.*, 2003). It seems likely that growth arrest while Glc is still plentiful is a consequence of H_2O_2 accumulation in the medium. In view of the results we propose that lactate oxidase activity has an important role in energy generation and maintenance processes when Glc is limiting or its utilization impaired due to a stressful condition, such as that presented by H_2O_2 induced cell damage. Indeed, the increase in lactate oxidase activity at the onset of growth arrest observed by Taniai *et al.* (2008) is in agreement with our hypothesis. Our view is further supported by the lack of H_2O_2 accumulation in a D39*spxB*$^-$ mutant strain while Glc was available in the growth medium, strongly suggesting that lactate oxidase was not active. In accordance, Taniai *et al.* (2008) show that H_2O_2 production in their *spxB* mutant is more accentuated after Glc consumption. Considering the data, a plausible possibility is Glc-mediated repression of the lactate oxidase gene. In *L. plantarum*, *poxB*, the lactate oxidase encoding gene, is directly repressed by CcpA in a Glc-dependent manner

(Lorquet *et al.*, 2004). In Chapter 6 we show that *lcto*, codifying the pneumococcal lactate oxidase, is under the negative control of CcpA in the presence of Glc. This regulation is most likely direct, as a *cre* site was identified downstream the promoter region of *lcto*. Interestingly, in the closely related *L. lactis* the production of lactate as major end-product of aerobic Glc metabolism was ensured by CcpA-mediated repression of *pta* and *ack* genes (mixed-acid) (Lopez de Felipe and Gaudu, 2009). In Chapter 6 we demonstrated that the mixed-acid genes are under the influence of CcpA, hence a role of CcpA in the regulation of aerobic metabolism in *S. pneumoniae* should not be disregarded.

Under aerobic conditions, PFL activity is not expected due to oxygen-induced PFL inactivation (Yamada *et al.*, 1985; Melchiorsen *et al.*, 2000; Takahashi-Abbe *et al.*, 2003; Buis and Broderick, 2005). In agreement, in the presence of abundant oxygen formate is not produced from the metabolism of Glc by *S. pneumoniae* (Chapter 2). Under low oxygen tensions (semi-aerobic conditions) minor amounts of formate were detected in the growth medium, suggesting that the pneumococcal PFL is more resistant to oxygen than that of *E. coli* (Knappe *et al.*, 1993). Similar observations have been reported for other *Streptococcaceae*, such as *L. lactis* (Arnau *et al.*, 1997).

The behavior of *S. pneumoniae* in aerobiosis most likely represents a competitive advantage in the nasopharynx, where oxygen approximates atmospheric levels. Indeed, in this aerobic environment *S. pneumoniae* co-inhabits with other microorganisms, and possibly inhibits the growth of competitors by producing H_2O_2 (Pericone *et al.*, 2000). The homolactic behavior in semi-aerobic or anaerobic conditions suits the lifestyle of the pneumococcus in the deeper layers of the mucus and blood. In such niches, few major competitors are present, and the bacterium's prime goal is to use the nutrients for fast growth.

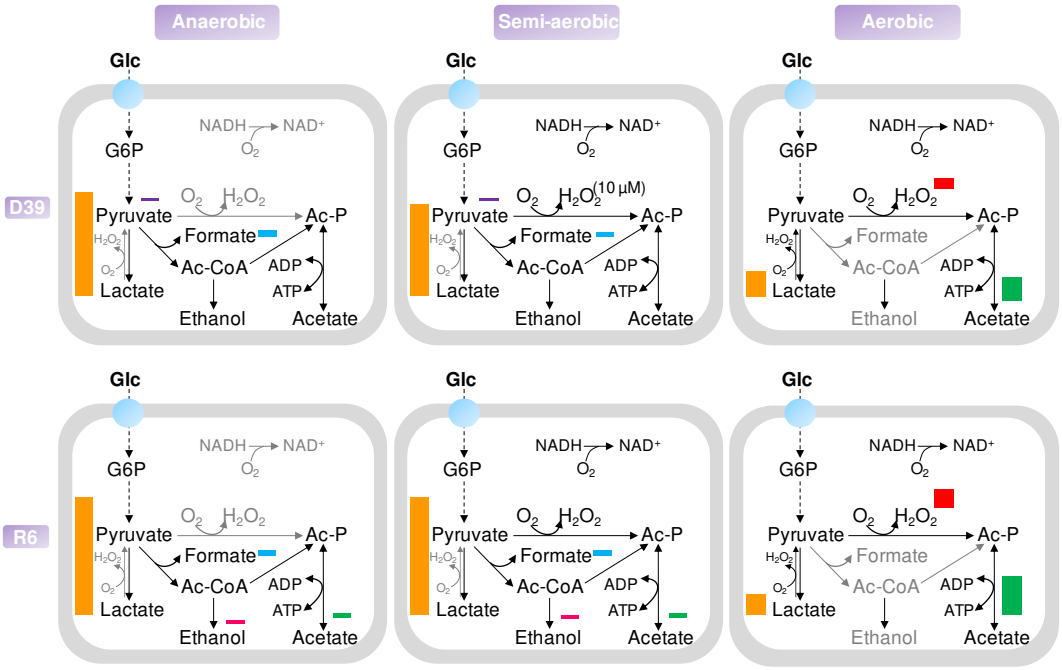

Fig. 7.2. Schematic representation of end-products resulting from glucose metabolism under anaerobic, semi-aerobic and aerobic conditions in *S. pneumoniae* D39 and R6. Pyruvate is the substrate of three competing enzymes: lactate dehydrogenase, pyruvate formate-lyase and pyruvate oxidase. Homolactic fermentation reduces pyruvate into lactate, through lactate dehydrogenase (LDH), whereas mixed-acid fermentation leads to formate, acetate and ethanol. Oxygen might be consumed at the level of lactate oxidase (LOX), pyruvate oxidase (SpxB) or H_2O-NADH oxidase (NOX). The levels of end-products (in µmol mg dw^{-1}) can be appreciated from the bar sizes: (■), lactate; (■), formate; (■), acetate; (■), ethanol. Abbreviations: Ac-P, acetyl-phosphate; Ac-CoA, acetyl-coenzyme A; G6P, glucose 6-phosphate. In strain R6 grown under semi-aerobic conditions H_2O_2 was not experimentally determined.

Pyruvate oxidase is a key enzyme in the sugar metabolism of *S. pneumoniae*

The pneumococcal pyruvate oxidase (SpxB) catalyses the conversion of pyruvate, O_2 and inorganic phosphate (P_i) into acetyl-phosphate, CO_2 and H_2O_2 and requires FAD, thiamin diphosphate and Mg^{2+} as cofactors (Spellerberg *et al.*, 1996). Homologues of this enzyme are present in other *Streptococcaceae* species (*e.g. S. sanguinis* and *S. gordonii*) and other *Lactobacillales* (*e.g. L. plantarum*) (Spellerberg *et al.*, 1996; Goffin *et al.*, 2006; Chen *et al.*, 2011; Zheng *et al.*, 2011c). The crystal structure and the mechanism of catalysis of the *L. plantarum* SpxB have been elucidated, (Tittmann *et al.*, 2005), and the data were used to propose a structural model of the pneumococcal SpxB (Ramos-Montañez *et al.*, 2008). The products of pyruvate oxidase activity, acetyl-phosphate and H_2O_2, play relevant physiological roles. Acetyl-phosphate is a high energy compound that serves as phosphoryl donor for the production of acetate and ATP via acetate kinase (Pericone *et al.*, 2003). Production of hydrogen peroxide can present a competitive advantage within microbial comunities. A number of streptococci, including *S. pneumoniae*, are able to produce H_2O_2 in concentrations that are inhibitory to other co-inhabitants (Pericone, 2000; Regev-Yochay *et al.*, 2006; Chen *et al.*, 2011). Besides this inhibitory effect, H_2O_2 produced by *S. pneumoniae* also has cytotoxic effects on human cells (Braun *et al.*, 2002). H_2O_2 does not only damage surrounding cells but also the pneumococcus itself. It can influence the composition of the cell membrane through modulation of fatty-acid biosynthesis protein F (FabF) activity and might cause oxidative stress and genetic instability in the pneumococcus (Pericone *et al.*, 2000; Pericone *et al.*, 2003; Pesakhov *et al.*, 2007; Benisty *et al.*, 2010). Finally, the amount of H_2O_2 produced presumably correlates with increased

mutation frequency in the opaque to transparent phenotypic variation in *S. pneumoniae* (Ramos-Montañez *et al.*, 2008).

SpxB is assumed to have a relevant role in central metabolism (Spellerberg *et al.*, 1996; Ramos-Montañez *et al.*, 2008; Taniai *et al.*, 2008). In Chapters 2 and 4 we show that at least for sugar metabolism this is the case. First, we describe the pivotal role of pyruvate oxidase in the shift from lactate to acetate and H_2O_2 production during the aerobic metabolism of Glc in *S. pneumoniae* (Chapter 2). Second, we show that *spxB* inactivation in strain D39 affects growth rate, end-product profiles (H_2O_2 and pyruvate accumulation), levels of intracellular metabolites (particularly FBP, G6P and acetyl-phosphate) and capsule amount during semi-aerobic Glc metabolism (Chapter 4). Third, we describe an alteration in the sugar utilization capabilities of strain D39 as a consequence of *spxB* inactivation (Chapter 4).

SpxB affects negatively the utilization of N-acetylglucosamine and sugars potentially present in bacterial capsules or host glycans (rhamnose, glucuronic acid and gluconic acid) (Chapter 4). The utilization of host glycans as nutritional sources for pneumococcal growth is supported by recent studies (Burnaugh *et al.*, 2008; Yesilkaya *et al.*, 2008; Marion *et al.*, 2012). Interestingly, pathways implicated in the transport and utilization of these sugars were strongly repressed in strain D39 relative to the *spxB* mutant when grown on Glc (Chapter 4). These results led us to hypothesize that in specific microenvironments where oxygen and Glc are available, *e.g.* lungs during infection (Philips *et al.*, 2003), SpxB produces a signal involved in repression of the catabolic pathways of alternative sugars, allowing for rapid proliferation of the pneumococcus through the utilization of the preferred substrate. We speculate that regulatory proteins could be involved in this mechanism, but such a connection has yet to be found.

At this stage our findings prompt further investigations as to the mechanisms that link SpxB with repression of sugar catabolic genes and capsule synthesis. In particular, the identification of the molecular signals and any specific regulators involved are of great interest.

Impact of sugar metabolism on virulence

The adaptation of *S. pneumoniae* to certain environmental cues results in expression of virulence factors. Accumulating evidence reveals that inactivation of proteins involved in central metabolic processes leads to attenuation of virulence. Among others, examples include PFL (Chapter 5), SpxB (Ramos-Montañez *et al.*, 2008) and CcpA (Giammarinaro and Paton, 2002; Iyer *et al.*, 2005). In this thesis we show that CcpA affects a large fraction of the genome of *S. pneumoniae*, including genes coding for classical virulence factors and biosynthetic pathways of cell surface components (Chapter 6). All together, this could explain the avirulent phenotypes of *ccpA* mutants (Giammarinaro and Paton, 2002; Iyer *et al.*, 2005). Our data show that capsule synthesis is unaffected by *ccpA* deletion, independently of the sugar (Glc or Gal) used for growth. In agreement, a regulation of capsule expression by CcpA was not reported in other studies (Iyer *et al.*, 2005; van Opijnen *et al.*, 2009). In contrast, Giammarinaro and Paton (2002) proposed that the avirulent behavior of a *ccpA* mutant most likely was due to impaired capsule production. However, in this study capsule amount was not quantified (Giammarinaro and Paton, 2002). An explanation for the dissimilar results is difficult to put forward, but difference in strain handling and manipulation cannot be disregarded.

Rather than affecting capsule amount *per se*, CcpA affects the attachment of capsule to the cell wall or membrane (Fig. 7.3; Chapter 6). CcpA influences the

synthesis of the cell wall component phosphorylcholine via repression of the *lic1* operon involved in synthesis of CDP-Cho and CDP-ribitol, which are the precursors of the teichoic acid (Fig. 7.3). In accordance, the levels of CDP-choline are lower in D39 than in the *ccpA* mutant (Fig. 7.3; Chapter 6). Phosphorylcholine is the anchor molecule for choline-binding proteins, well known virulence factors in *S. pneumoniae* (reviewed in Bergmann and Hammerschmidt, 2006; Kadioglu *et al.*, 2008). Interestingly, genes coding for the choline-binding proteins *pspA* and *pcpA* were also repressed by CcpA. In this light, CcpA seemingly affects the binding of cell wall proteins to the cell wall. The predicted involvement of CcpA in modulating the cell surface of *S. pneumoniae* places the regulator at the core of host-pathogen interactions. To substantiate this assumption an in-depth analysis of the cell-surface proteome should be performed.

Phase variation of capsule expression is among the most remarkable mechanisms associated with pneumococcal adaptation and virulence of this pathogen. In this process, switching between opaque and transparent phenotypes is observed in response to environmental cues (Kim *et al.*, 1999; Weiser *et al.*, 2001). Transparent phenotypes produce less capsule, more cell wall teichoic acids, and more choline-binding protein A (CbpA) than opaque variants. Moreover, *spxB* expression is higher in transparent variants (Overweg *et al.*, 2000; Li-Korotky *et al.*, 2009). Considering their metabolic traits, transparent variants are better adapted for colonization, whereas opaque variants perform better in infection (Kim and Weiser, 1998; Kim *et al.*, 1999; Nelson *et al.*, 2007). Indeed, transparent phenotypes are especially located in close contact with the mucosal surfaces of epithelial cells (*e.g.* in the nasopharynx) or in biofilms, whereas opaque phenotypes are predominantly found in blood or watery niches (Ogunniyi *et al.*, 2002; Hammerschmidt *et al.*, 2005; McEllistrem *et al.*, 2007, Allegrucci and Sauer, 2008).

Despite recent studies showing the involvement of the CpsA-D proteins in capsule production, the overall molecular mechanism by which this system controls capsule synthesis is not completely understood (reviewed in Yother, 2011; Chapter 1). Moreover, the regulation of capsule transcription remains controversial. In *S. pneumoniae*, polymorphisms in the *cps* promoter region and genetic mobile elements in the region between *dexB* and *cpsA* genes (point mutations, RUP elements, IS sequences) are proposed to influence the promoter strength, the binding of regulatory proteins to the promoter, and to promote sequence rearrangements (Moscoso and Garcia, 2009). However, proteins involved in the regulation of capsule expression are largely unknown.

The higher expression of *spxB* in transparent as compared to opaque variants is well documented (Overweg *et al.*, 2000), however the effect of the enzyme on capsule synthesis had not been investigated. Deletion of *spxB* or a reduction in its activity is reported to induce opaque-like or mucoid phenotypes (Overweg *et al.*, 2000; Ramos-Montañez *et al.*, 2008; Allegrucci and Sauer, 2008). In Chapter 4 we show that loss of *spxB* in strain D39 indeed renders an opaque-like phenotype. Importantly, we went on to demonstrate that this phenotype is a consequence of increased capsule production (Fig. 7.3; Chapter 4). Based on the data of Chapter 4, we propose that SpxB is involved in the signal transduction cascade adjusting the amount of capsule in *S. pneumoniae*, and that this connection is most likely related to oxygen sensing. In accordance, capsule synthesis was shown to respond to changes in oxygen availability (Weiser *et al.*, 2001). How this signalling mechanism occurs is still to be elucidated. Known is the inhibitory effect of H_2O_2, the product of SpxB activity, on FabF activity, which ultimately results in changes in membrane fatty-acid composition (Benisty *et al.*, 2010). Capsule synthesis is tightly interconnected with peptidoglycan synthesis and is partly regulated by membrane proteins (reviewed in Yother, 2011; Chapter

1). Hence, it is possible that disturbances in the membrane or cell wall influence capsule synthesis. Interestingly, in Chapter 4 the TEM studies indicate subtle modifications in the membrane of the *spxB* mutants.

Overall, our results highlight a relevant role of a sugar metabolic enzyme (SpxB) and a global regulator of gene expression (CcpA) in the expression of virulence factors.

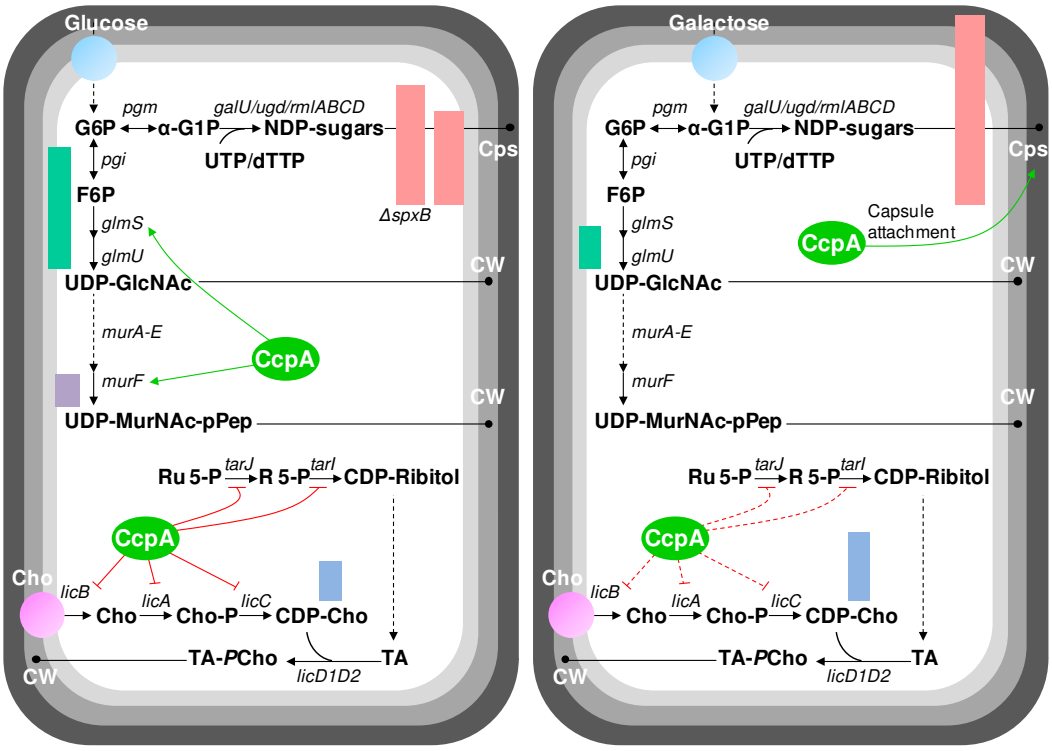

Fig. 7.3. Schematic representation of the pathways involved in production of structural virulence factors (peptidoglycan, *P*Cho cell wall, capsule) and catabolite control exerted by CcpA. A comparison between growth on Glc and Gal is depicted. The levels of intracellular metabolites can be appreciated from the bar sizes: (■), UDP-GlcNAc; (■), UDP-MurNAc-pPep; (■), CDP-Cho. The bar size of GlcUA, (■) is in a different scale and should not be compared with the bars of the other metabolites. Green arrows indicate activation by CcpA; Red arrows indicate repression by CcpA; Red dashed arrows indicate alleviation of repression by CcpA on Gal as compared to Glc; Of all the genes affected by CcpA only the *lic1* (*tarIJlicABC*) operon exhibits a possible *cre* site (inside *tarJ*). The intracellular reactions depicted are catalyzed by the following enzymes (the genes that code for the enzymes are in parenthesis): phosphoglucose isomerase (*pgi*), α-phosphoglucomutase (*pgm*), glucose 1-P uridylyltransferase (*galU*), UDP-Glc dehydrogenase (*ugd*), glucose 1-P thymidylyltransferase CpsL (*rmlA*), dTDP-glc 4,6-dehydratase CpsN (*rmlB*), dTDP-4-keto-6-deoxy-D-glucose 3,5-epimerase CpsM (*rmlC*), dTDP-4-keto-L-rhamnose reductase CpsO (*rmlD*), D-fructose 6-phosphate

amidotransferase (*glmS*), UDP-N-acetylglucosamine pyrophosphorylase (*glmU*), UDP-N-acetylglucosamine 1-carboxyvinyltransferase (*murA*), UDP-N-acetyl*enol*pyruvoyl-glucosamine reductase (*murB*), UDP-N-acetylmuramate-L-alanine ligase (*murC*), UDP-N-acetylmuramoyl-L-alanyl-D-glutamate synthetase (*murD*), UDP-N-acetylmuramoylalanyl-D-glutamate-2,6-diaminopimelate ligase (*murE*), UDP-N-acetylmuramoylalanyl-D-glutamyl-2, 6-diaminopimelate--D-alanyl-D-alanyl ligase (*murF*), alcohol dehydrogenase, zinc-containing (*tarJ*), 2-C-methyl-D-erythritol 4-phosphate cytidylyltransferase (*tarI*), protein LicB (*licB*), choline kinase or LicA (*pck*), CTP:phosphocholine cytidylyltransferase (*licC*), phosphotransferase LicD1 (*licD1*), phosphotransferase LicD2 (*licD2*). Abbreviations: G6P, glucose 6-phosphate; α-G1P, α-glucose 1-phosphate; F6P, fructose 6-phosphate; UDP-GlcNAc, UDP-N-acetylglucosamine; UDP-MurNAc-pPep, UDP-N-acetylmuramoyl-pentapeptide; Ru 5-P, ribulose 5-phosphate; R 5-P, ribitol 5-phosphate; Cho, choline; CDP-Cho, CDP-choline; Cho-P, choline phosphate; *P*Cho, phosphorylcholine; TA, teichoic acid; GlcUA, glucuronic acid.

Link between uracil and capsule, the major virulence factor of *S. pneumoniae*

In Chapter 3 we described the isolation of an irreversible D39 spontaneous mutant (D39SM), similar to a transparent variant. The underproducing capsule phenotype (transparent) resulted from a mutation in the promoter region of the *cps locus* (Chapter 3). The underproducing capsule phenotype provided a growth advantage to this strain, *i.e.* was beneficial, in conditions deprived of uracil (Chapter 3). The genomic mutation rate that generates beneficial mutations in *S. pneumoniae* during single-colony serial transfer is in the order of 4.8×10^{-4} per genome per generation, a value similar to that previously found for *E. coli* (Perfeito *et al.*, 2007; Stevens and Sebert, 2011). These studies support the idea that the number of genes mutating during bacterial adaptation is higher than previously imagined, which has negative implications in the emergence of antibiotic-resistant strains (Perfeito *et al.*, 2007; Stevens and

Sebert, 2011). In the case of *S. pneumoniae*, the spread of beneficial mutations may be exacerbated by the fact that this organism is naturally competent (Stevens and Sebert, 2011). We hypothesize that the mutations acquired by our D39SM strain most likely resulted from adaptation to deprivation of a nutrient required for capsule production, *e.g.* uracil, and thus is beneficial in conditions in which that nutrient is missing (Chapter 3).

In Chapter 3 we show that the pyrimidine nucleobase uracil plays a determinant role in the physiology of the pneumococcus. Uracil is involved in central carbon metabolism as the high energy molecule used to activate the sugar precursors for the biosynthesis of structural polysaccharides in lactic acid bacteria (reviewed in Kilstrup *et al.*, 2005). In *S. pneumoniae*, UDP-sugars are the building blocks for capsule synthesis (Bentley *et al.*, 2006). Altered synthesis of polysaccharides in response to variation in pyrimidine concentrations are documented in the literature. In *E. coli*, synthesis of the cellulose exopolysaccharide changes in response to variation in pyrimidine availability (Garavaglia *et al.*, 2012). Interestingly, inactivation of genes belonging to the *de novo* synthesis of UMP impairs cellulose production, which can be triggered by addition of exogenous uracil (Garavaglia *et al.*, 2012). In *Vibrio cholerae*, pyrimidines play an important role in the control of exopolysaccharide production and biofilm formation, via the regulator CytR, which represses nucleosides uptake and catabolism when these are scarce (Haugo and Watnick, 2002; Garavaglia *et al.*, 2012). In *Pseudomonas fluorescens*, a spontaneous mutation in a gene of the *de novo* synthesis of pyrimidines, *carB*, affects the proportion of capsulated to non-encapsulated subpopulations, by a molecular mechanism yet to be discovered (Beaumont *et al.*, 2009; Garavaglia *et al.*, 2012). In a *S. thermophilus* galactose-fermenting mutant strain, displaying increased activities of the Leloir genes, exopolysaccharide production was enhanced by overexpressing *galU*, that

codes for the enzyme that converts α-G1P to UDP-Glc at the expense of UTP (Levander *et al.*, 2002). Deletions in *galU* lead to a substantial decrease in capsule amounts, growth defects and attenuation of virulence in *S. pneumoniae* (Mollerach *et al.*, 1998; Hardy *et al.*, 2000; Hardy *et al.*, 2001). In view of these results, it is conceivable that capsule production in *S. pneumoniae* is affected by uracil availability. Our studies show that capsule expression and production is slightly but consistently higher in uracil-containing as compared to uracil-deprived medium (Chapter 3). Moreover, uracil shows no effect on strains that have no capsule or that exhibit low capsule levels, such as R6 or D39SM (Chapters 2 and 3). Therefore, the idea that in the human host uracil may be involved in the signalling cascade controlling capsule production is not unreasonable.

A connection between uracil metabolism, the pathways for pyrimidine synthesis and the production of capsule was unveiled in this thesis. Deciphering the molecular mechanisms associated to these processes is a goal for future investigations. In particular, addressing questions such as “is uracil a signal for capsule production?”, “how does *S. pneumoniae* take advantage of uracil sources in the host?”, and “what are the mechanisms integrating capsule production and pyrimidine metabolism?” is of great interest.

In summary, the work described in this thesis represents a significant contribution to the understanding of central metabolism, and in particular sugar metabolism and provides clues regarding the relation of these pathways to virulence in *S. pneumoniae*. The scarcity of data on metabolic pathways and their regulation in *S. pneumoniae* has so far hampered a comprehensive understanding of the connections between these processes. In the long run, we expect that the insights gained form this work will be critical to unveil interdependences between carbohydrate metabolism and pneumococcal

pathogenesis required to advance our knowledge into new possible ways to combat this deadly pathogen.

The data generated here is already being used to generate descriptive and predictive models of *S. pneumoniae* metabolism. We expect that such mathematical representations will contribute to deepen our understanding of how a functional state arises from the components, and ultimately will facilitate the identification of novel targets for alternative therapeutic and preventive drugs.

References

Abbe,K., Takahashi,S., and Yamada,T. (1982) Involvement of oxygen-sensitive pyruvate formate-lyase in mixed-acid fermentation by *Streptococcus mutans* under strictly anaerobic conditions. *J Bacteriol* **152**: 175-182.

Abeyta,M., Hardy,G.G., and Yother,J. (2003) Genetic alteration of capsule type but not PspA type affects accessibility of surface-bound complement and surface antigens of *Streptococcus pneumoniae*. *Infect Immun* **71**: 218-225.

Abranches,J., Chen,Y.Y., and Burne,R.A. (2004) Galactose metabolism by *Streptococcus mutans*. *Appl Environ Microbiol* **70**: 6047-6052.

Abranches,J., Nascimento,M.M., Zeng,L., Browngardt,C.M., Wen,Z.T., Rivera,M.F., and Burne,R.A. (2008) CcpA regulates central metabolism and virulence gene expression in *Streptococcus mutans*. *J Bacteriol* **190**: 2340-2349.

Aikawa,C., Furukawa,N., Watanabe,T., Minegishi,K., Furukawa,A., Eishi,Y. *et al.* (2012) Complete genome sequence of the serotype k *Streptococcus mutans* strain LJ23. *J Bacteriol* **194**: 2754-2755.

Ajdic,D., McShan,W.M., McLaughlin,R.E., Savic,G., Chang,J., Carson,M.B. *et al.* (2002) Genome sequence of *Streptococcus mutans* UA159, a cariogenic dental pathogen. *Proc Natl Acad Sci U S A* **99**: 14434-14439.

Allegrucci,M., and Sauer,K. (2008) Formation of *Streptococcus pneumoniae* non-phase-variable colony variants is due to increased mutation frequency present under biofilm growth conditions. *J Bacteriol* **190**: 6330-6339.

Alloing,G., de,P.P., and Claverys,J.P. (1994) Three highly homologous membrane-bound lipoproteins participate in oligopeptide transport by the Ami system of the Gram-positive *Streptococcus pneumoniae*. *J Mol Biol* **241**: 44-58.

Alloing,G., Granadel,C., Morrison,D.A., and Claverys,J.P. (1996) Competence pheromone, oligopeptide permease, and induction of competence in *Streptococcus pneumoniae*. *Mol Microbiol* **21** : 471-478.

AlonsoDeVelasco,E., Verheul,A.F., Verhoef,J., and Snippe,H. (1995) *Streptococcus pneumoniae*: virulence factors, pathogenesis, and vaccines. *Microbiol Rev* **59**: 591-603.

Amon,J., Titgemeyer,F., and Burkovski,A. (2010) Common patterns - unique features: nitrogen metabolism and regulation in Gram-positive bacteria. *FEMS Microbiol Rev* **34**: 588-605.

References

Andersen,H.W., Solem,C., Hammer,K., and Jensen,P.R. (2001) Twofold reduction of phosphofructokinase activity in *Lactococcus lactis* results in strong decreases in growth rate and in glycolytic flux. *J Bacteriol* **183**: 3458-3467.

Arnau,J., Jorgensen,F., Madsen,S.M., Vrang,A., and Israelsen,H. (1997) Cloning, expression, and characterization of the *Lactococcus lactis pfl* gene, encoding pyruvate formate-lyase. *J Bacteriol* **179**: 5884-5891.

Asanuma,N., Iwamoto,M., and Hino,T. (1999) Structure and transcriptional regulation of the gene encoding pyruvate formate-lyase of a ruminal bacterium, *Streptococcus bovis*. *Microbiology* **145 (Pt 1)**: 151-157.

Asanuma,N., Yoshii,T., and Hino,T. (2004) Molecular characterization of CcpA and involvement of this protein in transcriptional regulation of lactate dehydrogenase and pyruvate formate-lyase in the ruminal bacterium *Streptococcus bovis*. *Appl Environ Microbiol* **70**: 5244-5251.

Auzat,I., Chapuy-Regaud,S., Le,B.G., Dos,S.D., Ogunniyi,A.D., Le,T., I *et al.* (1999) The NADH oxidase of *Streptococcus pneumoniae*: its involvement in competence and virulence. *Mol Microbiol* **34**: 1018-1028.

Avery,O.T., Macleod,C.M., and McCarty,M. (1944) Studies on the chemical nature of the substance inducing transformation of pneumococcal types: induction of transformation by a desoxyribonucleic acid fraction isolated from pneumococcus type III. *J Exp Med* **79**: 137-158.

Baerends,R.J., Smits,W.K., de,J.A., Hamoen,L.W., Kok,J., and Kuipers,O.P. (2004) Genome2D: a visualization tool for the rapid analysis of bacterial transcriptome data. *Genome Biol* **5**: R37.

Balachandran,P., Hollingshead,S.K., Paton,J.C., and Briles,D.E. (2001) The autolytic enzyme LytA of *Streptococcus pneumoniae* is not responsible for releasing pneumolysin. *J Bacteriol* **183**: 3108-3116.

Béal,C., Louvet,P., Corrieu,G. (1989) Influence of controlled pH and temperature on the growth and acidification of pure cultures of *Streptococcus thermophilus* 404 and *Lactobacillus bulgaricus* 398. *Appl Microbiol Biotechnol* **32**: 148-154.
Beaumont,H.J., Gallie,J., Kost,C., Ferguson,G.C., and Rainey,P.B. (2009) Experimental evolution of bet hedging. *Nature* **462**: 90-93.

Belanger,A.E., Clague,M.J., Glass,J.I., and LeBlanc,D.J. (2004) Pyruvate oxidase is a determinant of Avery's rough morphology. *J Bacteriol* **186**: 8164-8171.

Bender,G.R., Thibodeau,E.A., and Marquis,R.E. (1985) Reduction of acidurance of streptococcal growth and glycolysis by fluoride and Gramicidin. *J Dent Res* **64**: 90-95.

Bender,M.H., and Yother,J. (2001) CpsB is a modulator of capsule-associated tyrosine kinase activity in *Streptococcus pneumoniae*. *J Biol Chem* **276**: 47966-47974.

Bender,M.H., Cartee,R.T., and Yother,J. (2003) Positive correlation between tyrosine phosphorylation of CpsD and capsular polysaccharide production in *Streptococcus pneumoniae*. *J Bacteriol* **185**: 6057-6066.

Benisty,R., Cohen,A.Y., Feldman,A., Cohen,Z., and Porat,N. (2010) Endogenous H_2O_2 produced by *Streptococcus pneumoniae* controls FabF activity. *Biochim Biophys Acta* **1801**: 1098-1104.

Bentley,S.D., Aanensen,D.M., Mavroidi,A., Saunders,D., Rabbinowitsch,E., Collins,M. *et al.* (2006) Genetic analysis of the capsular biosynthetic locus from all 90 pneumococcal serotypes. *PLoS Genet* **2**: e31.

Bergmann,S., Rohde,M., Chhatwal,G.S., and Hammerschmidt,S. (2001) α-Enolase of *Streptococcus pneumoniae* is a plasmin(ogen)-binding protein displayed on the bacterial cell surface. *Mol Microbiol* **40**: 1273-1287.

Bergmann,S., Wild,D., Diekmann,O., Frank,R., Bracht,D., Chhatwal,G.S., and Hammerschmidt,S. (2003) Identification of a novel plasmin(ogen)-binding motif in surface displayed alpha-enolase of *Streptococcus pneumoniae*. *Mol Microbiol* **49**: 411-423.

Bergmann,S., and Hammerschmidt,S. (2006) Versatility of pneumococcal surface proteins. *Microbiology* **152** : 295-303.

Berry,A.M., and Paton,J.C. (2000) Additive attenuation of virulence of *Streptococcus pneumoniae* by mutation of the genes encoding pneumolysin and other putative pneumococcal virulence proteins. *Infect Immun* **68**: 133-140.

Bhasin,N., Albus,A., Michon,F., Livolsi,P.J., Park,J.S., and Lee,J.C. (1998) Identification of a gene essential for O-acetylation of the *Staphylococcus aureus* type 5 capsular polysaccharide. *Mol Microbiol* **27**: 9-21.

Bidossi,A., Mulas,L., Decorosi,F., Colomba,L., Ricci,S., Pozzi,G. *et al.* (2012) A functional genomics approach to establish the complement of carbohydrate transporters in *Streptococcus pneumoniae*. *PLoS One* **7**: e33320.

Bijlsma,J.J., Burghout,P., Kloosterman,T.G., Bootsma,H.J., de,J.A., Hermans,P.W., and Kuipers,O.P. (2007) Development of genomic array footprinting for identification of

conditionally essential genes in *Streptococcus pneumoniae*. *Appl Environ Microbiol* **73**: 1514-1524.

Blumenkrantz,N., and Asboe-Hansen,G. (1973) New method for quantitative determination of uronic acids. *Anal Biochem* **54**: 484-489.

Boels,I.C., Ramos,A., Kleerebezem,M., and de Vos,W.M. (2001) Functional analysis of the *Lactococcus lactis galU* and *galE* genes and their impact on sugar nucleotide and exopolysaccharide biosynthesis. *Appl Environ Microbiol* **67**: 3033-3040.

Bogaert,D., De Groot,R., and Hermans,P.W. (2004) *Streptococcus pneumoniae* colonisation: the key to pneumococcal disease. *Lancet Infect Dis* **4**: 144-154.

Braun,J.S., Sublett,J.E., Freyer,D., Mitchell,T.J., Cleveland,J.L., Tuomanen,E.I., and Weber,J.R. (2002) Pneumococcal pneumolysin and H_2O_2 mediate brain cell apoptosis during meningitis. *J Clin Invest* **109**: 19-27.

Brooks,A.N., Turkarslan,S., Beer,K.D., Lo,F.Y., Baliga,N.S. (2011) Adaptation of cells to new environments. *Wiley Interdiscip Rev Syst Biol Med* **3**: 544-61.

Brückner,R., and Titgemeyer,F. (2002) Carbon catabolite repression in bacteria: choice of the carbon source and autoregulatory limitation of sugar utilization. *FEMS Microbiol Lett* **209**: 141-148.

Brugger,S.D., Hathaway,L.J., and Muhlemann,K. (2009) Detection of *Streptococcus pneumoniae* strain cocolonization in the nasopharynx. *J Clin Microbiol* **47**: 1750-1756.

Buis,J.M., and Broderick,J.B. (2005) Pyruvate formate-lyase activating enzyme: elucidation of a novel mechanism for glycyl radical formation. *Arch Biochem Biophys* **433**: 288-296.

Burnaugh,A.M., Frantz,L.J., and King,S.J. (2008) Growth of *Streptococcus pneumoniae* on human glycoconjugates is dependent upon the sequential activity of bacterial exoglycosidases. *J Bacteriol* **190**: 221-230.

Campbell,J.W., and Cronan,J.E., Jr. (2001) Bacterial fatty acid biosynthesis: targets for antibacterial drug discovery. *Annu Rev Microbiol* **55**: 305-332.

Cardozo,D.M., Nascimento-Carvalho,C.M., Souza,F.R., and Silva,N.M. (2006) Nasopharyngeal colonization and penicillin resistance among pneumococcal strains: a worldwide 2004 update. *Braz J Infect Dis* **10**: 293-304.

Cartee,R.T., Forsee,W.T., Bender,M.H., Ambrose,K.D., and Yother,J. (2005a) CpsE from type 2 *Streptococcus pneumoniae* catalyzes the reversible addition of glucose-1-phosphate to a polyprenyl phosphate acceptor, initiating type 2 capsule repeat unit formation. *J Bacteriol* **187**: 7425-7433.

Cartee,R.T., Forsee,W.T., and Yother,J. (2005b) Initiation and synthesis of the *Streptococcus pneumoniae* type 3 capsule on a phosphatidylglycerol membrane anchor. *J Bacteriol* **187**: 4470-4479.

Casadevall,A., and Pirofski,L.A. (1999) Host-pathogen interactions: redefining the basic concepts of virulence and pathogenicity. *Infect Immun* **67**: 3703-3713.

Caymaris,S., Bootsma,H.J., Martin,B., Hermans,P.W., Prudhomme,M., and Claverys,J.P. (2010) The global nutritional regulator CodY is an essential protein in the human pathogen *Streptococcus pneumoniae*. *Mol Microbiol* **78**: 344-360.

Chapuy-Regaud,S., Duthoit,F., Malfroy-Mastrorillo,L., Gourdon,P., Lindley,N.D., and Trombe,M.C. (2001) Competence regulation by oxygen availability and by Nox is not related to specific adjustment of central metabolism in *Streptococcus pneumoniae*. *J Bacteriol* **183**: 2957-2962.

Chapuy-Regaud,S., Ogunniyi,A.D., Diallo,N., Huet,Y., Desnottes,J.F., Paton,J.C. *et al.* (2003) RegR, a global LacI/GalR family regulator, modulates virulence and competence in *Streptococcus pneumoniae*. *Infect Immun* **71**: 2615-2625.

Chen,J.D., and Lacks,S.A. (1991) Role of uracil-DNA glycosylase in mutation avoidance by *Streptococcus pneumoniae*. *J Bacteriol* **173**: 283-290.

Chen,L., Ge,X., Dou,Y., Wang,X., Patel,J.R., and Xu,P. (2011) Identification of hydrogen peroxide production-related genes in *Streptococcus sanguinis* and their functional relationship with pyruvate oxidase. *Microbiology* **157**: 13-20.

Chen,Y.Y., Betzenhauser,M.J., Snyder,J.A., and Burne,R.A. (2002) Pathways for lactose/galactose catabolism by *Streptococcus salivarius*. *FEMS Microbiol Lett* **209**: 75-79.

Chiang,C., Bongiorni,C., and Perego,M. (2011) Glucose-dependent activation of *Bacillus anthracis* toxin gene expression and virulence requires the carbon catabolite protein CcpA. *J Bacteriol* **193**: 52-62.

Choi,S.K., and Saier,M.H., Jr. (2005) Regulation of *sigL* expression by the catabolite control protein CcpA involves a roadblock mechanism in *Bacillus subtilis*: potential connection between carbon and nitrogen metabolism. *J Bacteriol* **187**: 6856-6861.

References

Cieslewicz,M.J., Chaffin,D., Glusman,G., Kasper,D., Madan,A., Rodrigues,S. *et al.* (2005) Structural and genetic diversity of Group B *Streptococcus* capsular polysaccharides. *Infect Immun* **73**: 3096-3103.

Claverys,J.P., Prudhomme,M., Mortier-Barriere,I., and Martin,B. (2000) Adaptation to the environment: *Streptococcus pneumoniae*, a paradigm for recombination-mediated genetic plasticity? *Mol Microbiol* **35**: 251-259.

Cocaign-Bousquet,M., Even,S., Lindley,N.D., and Loubière,P. (2002) Anaerobic sugar catabolism in *Lactococcus lactis*: genetic regulation and enzyme control over pathway flux. *Appl Microbiol Biotechnol* **60**: 24-32.

Cocaign-Bousquet,M., Garrigues,C., Novak,L., Lindley,N.D., and Loubière,P. (1995) Rational development of a simple synthetic medium for the sustained growth of *Lactococcus lactis*. *J Appl Bacteriol* **79**: 108-116.

Cundell,D.R., Weiser,J.N., Shen,J., Young,A., and Tuomanen,E.I. (1995) Relationship between colonial morphology and adherence of *Streptococcus pneumoniae*. *Infect Immun* **63**: 757-761.

Dalia,A.B., Standish,A.J., and Weiser,J.N. (2010) Three surface exoglycosidases from *Streptococcus pneumoniae*, NanA, BgaA, and StrH, promote resistance to opsonophagocytic killing by human neutrophils. *Infect Immun* **78**: 2108-2116.

Daniely,D., Portnoi,M., Shagan,M., Porgador,A., Givon-Lavi,N., Ling,E. *et al.* (2006) Pneumococcal 6-phosphogluconate-dehydrogenase, a putative adhesin, induces protective immune response in mice. *Clin Exp Immunol* **144**: 254-263.

Dawid,S., Roche,A.M., and Weiser,J.N. (2007) The *blp* bacteriocins of *Streptococcus pneumoniae* mediate intraspecies competition both *in vitro* and *in vivo*. *Infect Immun* **75**: 443-451.

de Ruyter,P.G., Kuipers,O.P., and de Vos,W.M. (1996) Controlled gene expression systems for *Lactococcus lactis* with the food-grade inducer nisin. *Appl Environ Microbiol* **62**: 3662-3667.

De Vuyst,L., Vanderveken,F., Van de Ven,S., and Degeest,B. (1998) Production by and isolation of exopolysaccharides from *Streptococcus thermophilus* grown in a milk medium and evidence for their growth-associated biosynthesis. *J Appl Microbiol* **84**: 1059-1068.

De Vuyst,L., and Degeest,B. (1999) Heteropolysaccharides from lactic acid bacteria. *FEMS Microbiol Rev* **23**: 153-177.

Delcour,J., Ferain,T., Deghorain,M., Palumbo,E., and Hols,P. (1999) The biosynthesis and functionality of the cell-wall of lactic acid bacteria. *Antonie Van Leeuwenhoek* **76**: 159-184.

Derzelle,S., Bolotin,A., Mistou,M.Y., and Rul,F. (2005) Proteome analysis of *Streptococcus thermophilus* grown in milk reveals pyruvate formate-lyase as the major upregulated protein. *Appl Environ Microbiol* **71**: 8597-8605.

Deutscher,J., Francke,C., and Postma,P.W. (2006) How phosphotransferase system-related protein phosphorylation regulates carbohydrate metabolism in bacteria. *Microbiol Mol Biol Rev* **70**: 939-1031.

Deutscher,J. (2008) The mechanisms of carbon catabolite repression in bacteria. *Curr Opin Microbiol* **11**: 87-93.

Di Pasqua,R., Hoskins,N., Betts,G., and Mauriello,G. (2006) Changes in membrane fatty acids composition of microbial cells induced by addiction of thymol, carvacrol, limonene, cinnamaldehyde, and eugenol in the growing media. *J Agric Food Chem* **54**: 2745-2749.

Dossonnet,V., Monedero,V., Zagorec,M., Galinier,A., Perez-Martinez,G., and Deutscher,J. (2000) Phosphorylation of HPr by the bifunctional HPr Kinase/P-ser-HPr phosphatase from *Lactobacillus casei* controls catabolite repression and inducer exclusion but not inducer expulsion. *J Bacteriol* **182**: 2582-2590.

Dowson,C.G. (2004) What is the pneumococcus?. In: Tuomanen,E.I., Mitchell,T.J., Morrison,A.D. and Spratt,B.G. (Eds.) The pneumococcus (pp. 13-14). ASM Press, Washington D.C..

Duane,P.G., Rubins,J.B., Weisel,H.R., and Janoff,E.N. (1993) Identification of hydrogen peroxide as a *Streptococcus pneumoniae* toxin for rat alveolar epithelial cells. *Infect Immun* **61**: 4392-4397.

Echenique,J.R., Chapuy-Regaud,S., and Trombe,M.C. (2000) Competence regulation by oxygen in *Streptococcus pneumoniae*: involvement of *ciaRH* and *comCDE*. *Mol Microbiol* **36**: 688-696.

Egeter,O., and Brückner,R. (1996) Catabolite repression mediated by the catabolite control protein CcpA in *Staphylococcus xylosus*. *Mol Microbiol* **21**: 739-749.

Ermolaeva,M.D., White,O., and Salzberg,S.L. (2001) Prediction of operons in microbial genomes. *Nucleic Acids Res* **29**: 1216-1221.

Even,S., Lindley,N.D., and Cocaign-Bousquet,M. (2001) Molecular physiology of sugar catabolism in *Lactococcus lactis* IL1403. *J Bacteriol* **183**: 3817-3824.

Facklam,R. (2002) What happened to the streptococci: overview of taxonomic and nomenclature changes. *Clin Microbiol Rev* **15**: 613-630.

Fernebro,J., Andersson,I., Sublett,J., Morfeldt,E., Novak,R., Tuomanen,E. *et al.* (2004) Capsular expression in *Streptococcus pneumoniae* negatively affects spontaneous and antibiotic-induced lysis and contributes to antibiotic tolerance. *J Infect Dis* **189**: 328-338.

Flahaut,S., Vinogradov,E., Kelley,K.A., Brennan,S., Hiramatsu,K., and Lee,J.C. (2008) Structural and biological characterization of a capsular polysaccharide produced by *Staphylococcus haemolyticus*. *J Bacteriol* **190**: 1649-1657.

Fleischmann,R.D., Adams,M.D., White,O., Clayton,R.A., Kirkness,E.F., Kerlavage,A.R. *et al.* (1995) Whole-genome random sequencing and assembly of *Haemophilus influenzae* Rd. *Science* **269**: 496-512.

Fujita,Y. (2009) Carbon catabolite control of the metabolic network in *Bacillus subtilis*. *Biosci Biotechnol Biochem* **73**: 245-259.

Garavaglia,M., Rossi,E., and Landini,P. (2012) The pyrimidine nucleotide biosynthetic pathway modulates production of biofilm determinants in *Escherichia coli*. *PLoS One* **7**: e31252.

Garcia-Rodriguez,J.A., and Fresnadillo Martinez,M.J. (2002) Dynamics of nasopharyngeal colonization by potential respiratory pathogens. *J Antimicrob Chemother* **50 Suppl S2**: 59-73.

Garrigues,C., Loubiere,P., Lindley,N.D., and Cocaign-Bousquet,M. (1997) Control of the shift from homolactic acid to mixed-acid fermentation in *Lactococcus lactis*: predominant role of the NADH/NAD^+ ratio. *J Bacteriol* **179**: 5282-5287.

Garvie,E.I. (1980) Bacterial lactate dehydrogenases. *Microbiol Rev* **44**: 106-139.

Gaspar,P., Neves,A.R., Shearman,C.A., Gasson,M.J., Baptista,A.M., Turner,D.L. *et al.* (2007) The lactate dehydrogenases encoded by the *ldh* and *ldhB* genes in *Lactococcus lactis* exhibit distinct regulation and catalytic properties - comparative modeling to probe the molecular basis. *FEBS J* **274**: 5924-5936.

Gasson,M.J. (1983) Genetic transfer systems in lactic acid bacteria. *Antonie Van Leeuwenhoek* **49**: 275-282.

Gaudu,P., Lamberet,G., Poncet,S., and Gruss,A. (2003) CcpA regulation of aerobic and respiration growth in *Lactococcus lactis*. *Mol Microbiol* **50**: 183-192.

Gerosa,L., and Sauer,U. (2011) Regulation and control of metabolic fluxes in microbes. *Curr Opin Biotechnol* **22**: 566-575.

Giammarinaro,P., and Paton,J.C. (2002) Role of RegM, a homologue of the catabolite repressor protein CcpA, in the virulence of *Streptococcus pneumoniae*. *Infect Immun* **70**: 5454-5461.

Gibson,C.M., Mallett,T.C., Claiborne,A., and Caparon,M.G. (2000) Contribution of NADH oxidase to aerobic metabolism of *Streptococcus pyogenes*. *J Bacteriol* **182**: 448-455.

Giudicelli,S., and Tomasz,A. (1984) Attachment of pneumococcal autolysin to wall teichoic acids, an essential step in enzymatic wall degradation. *J Bacteriol* **158**: 1188-1190.

Goffin,P., Muscariello,L., Lorquet,F., Stukkens,A., Prozzi,D., Sacco,M. *et al.* (2006) Involvement of pyruvate oxidase activity and acetate production in the survival of *Lactobacillus plantarum* during the stationary phase of aerobic growth. *Appl Environ Microbiol* **72**: 7933-7940.

Gonçalves,V.M., Takagi,M., Lima,R.B., Massaldi,H., Giordano,R.C., and Tanizaki,M.M. (2003) Purification of capsular polysaccharide from *Streptococcus pneumoniae* serotype 23F by a procedure suitable for scale-up. *Biotechnol Appl Biochem* **37**: 283-287.

Görke,B., and Stülke,J. (2008) Carbon catabolite repression in bacteria: many ways to make the most out of nutrients. *Nat Rev Microbiol* **6**: 613-624.

Gray,B.M., and Musher,D.M. (2008) The history of pneumococcal disease. In: Siber,G.R., Klugman,K.P., and Mäkelä,P.H. (Eds.) Pneumococcal vaccines (pp. 3-17). ASM Press, Washington D.C..

Griffin,T.J., Gygi,S.P., Ideker,T., Rist,B., Eng,J., Hood,L., and Aebersold,R. (2002) Complementary profiling of gene expression at the transcriptome and proteome levels in *Saccharomyces cerevisiae*. *Mol Cell Proteomics* **1**: 323-333.

Grundy,F.J., Waters,D.A., Allen,S.H., and Henkin,T.M. (1993) Regulation of the *Bacillus subtilis* acetate kinase gene by CcpA. *J Bacteriol* **175**: 7348-7355.

Guerzoni,M.E., Lanciotti,R., and Cocconcelli,P.S. (2001) Alteration in cellular fatty acid composition as a response to salt, acid, oxidative and thermal stresses in *Lactobacillus helveticus*. *Microbiology* **147**: 2255-2264.

Guidolin,A., Morona,J.K., Morona,R., Hansman,D., and Paton,J.C. (1994) Nucleotide sequence analysis of genes essential for capsular polysaccharide biosynthesis in *Streptococcus pneumoniae* type 19F. *Infect Immun* **62**: 5384-5396.

Guiral,S., Henard,V., Laaberki,M.H., Granadel,C., Prudhomme,M., Martin,B., and Claverys,J.P. (2006) Construction and evaluation of a chromosomal expression platform (CEP) for ectopic, maltose-driven gene expression in *Streptococcus pneumoniae*. *Microbiology* **152**: 343-349.

Gunnewijk,M.G., and Poolman,B. (2000) Phosphorylation state of HPr determines the level of expression and the extent of phosphorylation of the lactose transport protein of *Streptococcus thermophilus*. *J Biol Chem* **275**: 34073-34079.

Hakenbeck,R., Balmelle,N., Weber,B., Gardes,C., Keck,W., and de Saizieu,A. (2001) Mosaic genes and mosaic chromosomes: intra- and interspecies genomic variation of *Streptococcus pneumoniae*. *Infect Immun* **69**: 2477-2486.

Hakenbeck,R., Brückner,R., Denapaite,D., and Maurer,P. (2012) Molecular mechanisms of beta-lactam resistance in *Streptococcus pneumoniae*. *Future Microbiol* **7**: 395-410.

Halfmann,A., Kovacs,M., Hakenbeck,R., and Brückner,R. (2007) Identification of the genes directly controlled by the response regulator CiaR in *Streptococcus pneumoniae*: five out of 15 promoters drive expression of small non-coding RNAs. *Mol Microbiol* **66**: 110-126.

Hammerschmidt,S., Wolff,S., Hocke,A., Rosseau,S., Muller,E., and Rohde,M. (2005) Illustration of pneumococcal polysaccharide capsule during adherence and invasion of epithelial cells. *Infect Immun* **73**: 4653-4667.

Hanson,B.R., Lowe,B.A., and Neely,M.N. (2011) Membrane topology and DNA-binding ability of the Streptococcal CpsA protein. *J Bacteriol* **193**: 411-420.

Hardy,G.G., Caimano,M.J., and Yother,J. (2000) Capsule biosynthesis and basic metabolism in *Streptococcus pneumoniae* are linked through the cellular phosphoglucomutase. *J Bacteriol* **182**: 1854-1863.

Hardy,G.G., Magee,A.D., Ventura,C.L., Caimano,M.J., and Yother,J. (2001) Essential role for cellular phosphoglucomutase in virulence of type 3 *Streptococcus pneumoniae*. *Infect Immun* **69**: 2309-2317.

Hathaway,L.J., Brugger,S.D., Morand,B., Bangert,M., Rotzetter,J.U., Hauser,C. *et al.* (2012) Capsule type of *Streptococcus pneumoniae* determines growth phenotype. *PLoS Pathog* **8**: e1002574.

Haugo,A.J., and Watnick,P.I. (2002) *Vibrio cholerae* CytR is a repressor of biofilm development. *Mol Microbiol* **45**: 471-483.

Hava,D.L., and Camilli,A. (2002) Large-scale identification of serotype 4 *Streptococcus pneumoniae* virulence factors. *Mol Microbiol* **45**: 1389-1406.

Hava,D.L., LeMieux,J., and Camilli,A. (2003) From nose to lung: the regulation behind *Streptococcus pneumoniae* virulence factors. *Mol Microbiol* **50**: 1103-1110.

Heinemann,M., and Sauer,U. (2010) Systems biology of microbial metabolism. *Curr Opin Microbiol* **13**: 337-343.

Henderson,B., and Martin,A. (2011) Bacterial moonlighting proteins and bacterial virulence. *Curr Top Microbiol Immunol*.

Hendriksen,W.T., Silva,N., Bootsma,H.J., Blue,C.E., Paterson,G.K., Kerr,A.R. *et al.* (2007) Regulation of gene expression in *Streptococcus pneumoniae* by response regulator 09 is strain dependent. *J Bacteriol* **189**: 1382-1389.

Hendriksen,W.T., Bootsma,H.J., Estevão,S., Hoogenboezem,T., de Jong,A., de Groot,R. *et al.* (2008) CodY of *Streptococcus pneumoniae*: link between nutritional gene regulation and colonization. *J Bacteriol* **190**: 590-601.

Herrgard,M.J., Covert,M.W., and Palsson,B.O. (2004) Reconstruction of microbial transcriptional regulatory networks. *Curr Opin Biotechnol* **15**: 70-77.

Higuchi,M., Shimada,M., Yamamoto,Y., Hayashi,T., Koga,T., and Kamio,Y. (1993) Identification of two distinct NADH oxidases corresponding to H_2O_2-forming oxidase and H_2O-forming oxidase induced in *Streptococcus mutans*. *J Gen Microbiol* **139**: 2343-2351.

Higuchi,M., Yamamoto,Y., Poole,L.B., Shimada,M., Sato,Y., Takahashi,N., and Kamio,Y. (1999) Functions of two types of NADH oxidases in energy metabolism and oxidative stress of *Streptococcus mutans*. *J Bacteriol* **181**: 5940-5947.

Hindré,T., Knibbe,C., Beslon,G., and Schneider,D. (2012) New insights into bacterial adaptation through *in vivo* and *in silico* experimental evolution. *Nat Rev Microbiol* **10**: 352-365.

Hirst,R.A., Sikand,K.S., Rutman,A., Mitchell,T.J., Andrew,P.W., and O'Callaghan,C. (2000) Relative roles of pneumolysin and hydrogen peroxide from *Streptococcus pneumoniae* in inhibition of ependymal ciliary beat frequency. *Infect Immun* **68**: 1557-1562.

Holmén,J.M., Karlsson,N.G., Abdullah,L.H., Randell,S.H., Sheehan,J.K., Hansson,G.C., and Davis,C.W. (2004) Mucins and their O-Glycans from human bronchial epithelial cell cultures. *Am J Physiol Lung Cell Mol Physiol* **287**: L824-L834.

Holmes,A.R., McNab,R., Millsap,K.W., Rohde,M., Hammerschmidt,S., Mawdsley,J.L., and Jenkinson,H.F. (2001) The *pavA* gene of *Streptococcus pneumoniae* encodes a fibronectin-binding protein that is essential for virulence. *Mol Microbiol* **41**: 1395-1408.

Holo,H., and Nes,I.F. (1995) Transformation of *Lactococcus* by electroporation. *Methods Mol Biol* **47**: 195-199.

Hoskins,J., Alborn,W.E., Jr., Arnold,J., Blaszczak,L.C., Burgett,S., DeHoff,B.S. *et al.* (2001) Genome of the bacterium *Streptococcus pneumoniae* strain R6. *J Bacteriol* **183**: 5709-5717.

Iannelli,F., Pearce,B.J., and Pozzi,G. (1999) The type 2 capsule *locus* of *Streptococcus pneumoniae*. *J Bacteriol* **181**: 2652-2654.

Ibrahim,Y.M., Kerr,A.R., McCluskey,J., and Mitchell,T.J. (2004) Control of virulence by the two-component system CiaR/H is mediated via HtrA, a major virulence factor of *Streptococcus pneumoniae*. *J Bacteriol* **186**: 5258-5266.

Inácio,J.M., Costa,C., and de Sá-Nogueira,I. (2003) Distinct molecular mechanisms involved in carbon catabolite repression of the arabinose regulon in *Bacillus subtilis*. *Microbiology* **149**: 2345-2355.

Iwami,Y., and Yamada,T. (1985) Regulation of glycolytic rate in *Streptococcus sanguis* grown under glucose-limited and glucose-excess conditions in a chemostat. *Infect Immun* **50**: 378-381.

Iyer,R., Baliga,N.S., and Camilli,A. (2005) Catabolite control protein A (CcpA) contributes to virulence and regulation of sugar metabolism in *Streptococcus pneumoniae*. *J Bacteriol* **187**: 8340-8349.

Iyer,R., and Camilli,A. (2007) Sucrose metabolism contributes to *in vivo* fitness of *Streptococcus pneumoniae*. *Mol Microbiol* **66**: 1-13.

Jedrzejas,M.J. (2001) Pneumococcal virulence factors: structure and function. *Microbiol Mol Biol Rev* **65** : 187-207.

Johansen,E., and Kibenich,A. (1992) Isolation and characterization of IS1165, an insertion sequence of *Leuconostoc mesenteroides* subsp. *cremoris* and other lactic acid bacteria. *Plasmid* **27**: 200-206.

Johnston,J.W., Briles,D.E., Myers,L.E., and Hollingshead,S.K. (2006) Mn^{2+}-dependent regulation of multiple genes in *Streptococcus pneumoniae* through PsaR and the resultant impact on virulence. *Infect Immun* **74**: 1171-1180.

Kadioglu,A., Weiser,J.N., Paton,J.C., and Andrew,P.W. (2008) The role of *Streptococcus pneumoniae* virulence factors in host respiratory colonization and disease. *Nat Rev Microbiol* **6**: 288-301.

Kaiser,M., and Sawers,G. (1995) Fnr activates transcription from the P6 promoter of the *pfl* operon *in vitro*. *Mol Microbiol* **18**: 331-342.

Karlin,S., Theriot,J., and Mrazek,J. (2004) Comparative analysis of gene expression among low G+C Gram-positive genomes. *Proc Natl Acad Sci U S A* **101**: 6182-6187.

Karlyshev,A.V., Pallen,M.J., and Wren,B.W. (2000) Single-primer PCR procedure for rapid identification of transposon insertion sites. *Biotechniques* **28**: 1078, 1080, 1082.

Kaufman,G.E., and Yother,J. (2007) CcpA-dependent and -independent control of beta-galactosidase expression in *Streptococcus pneumoniae* occurs via regulation of an upstream phosphotransferase system-encoding operon. *J Bacteriol* **189**: 5183-5192.

Keevil,C.W., Marsh,P.D., and Ellwood,D.C. (1984) Regulation of glucose metabolism in oral streptococci through independent pathways of glucose 6-phosphate and glucose 1-phosphate formation. *J Bacteriol* **157**: 560-567.

Kietzman,C.C., and Caparon,M.G. (2010) CcpA and LacD.1 affect temporal regulation of *Streptococcus pyogenes* virulence genes. *Infect Immun* **78**: 241-252.

Kilstrup,M., Hammer,K., Ruhdal,J.P., and Martinussen,J. (2005) Nucleotide metabolism and its control in lactic acid bacteria. *FEMS Microbiol Rev* **29**: 555-590.

Kim,J.H., Yang,Y.K., and Chambliss,G.H. (2005) Evidence that *Bacillus* catabolite control protein CcpA interacts with RNA polymerase to inhibit transcription. *Mol Microbiol* **56**: 155-162.

Kim,J.O., and Weiser,J.N. (1998) Association of intrastrain phase variation in quantity of capsular polysaccharide and teichoic acid with the virulence of *Streptococcus pneumoniae*. *J Infect Dis* **177**: 368-377.

Kim,J.O., Romero-Steiner,S., Sorensen,U.B., Blom,J., Carvalho,M., Barnard,S. *et al.* (1999) Relationship between cell surface carbohydrates and intrastrain variation on opsonophagocytosis of *Streptococcus pneumoniae*. *Infect Immun* **67**: 2327-2333.

King,S.J., Hippe,K.R., Gould,J.M., Bae,D., Peterson,S., Cline,R.T. *et al.* (2004) Phase variable desialylation of host proteins that bind to *Streptococcus pneumoniae in vivo* and protect the airway. *Mol Microbiol* **54**: 159-171.

King,S.J., Hippe,K.R., and Weiser,J.N. (2006) Deglycosylation of human glycoconjugates by the sequential activities of exoglycosidases expressed by *Streptococcus pneumoniae*. *Mol Microbiol* **59**: 961-974.

King,S.J. (2010) Pneumococcal modification of host sugars: a major contributor to colonization of the human airway? *Mol Oral Microbiol* **25**: 15-24.

Kloosterman,T.G., Bijlsma,J.J., Kok,J., and Kuipers,O.P. (2006a) To have neighbour's fare: extending the molecular toolbox for *Streptococcus pneumoniae*. *Microbiology* **152**: 351-359.

Kloosterman,T.G., Hendriksen,W.T., Bijlsma,J.J., Bootsma,H.J., van Hijum,S.A., Kok,J. *et al.* (2006b) Regulation of glutamine and glutamate metabolism by GlnR and GlnA in *Streptococcus pneumoniae*. *J Biol Chem* **281**: 25097-25109.

Kloosterman,T.G., Witwicki,R.M., van der Kooi-Pol MM, Bijlsma,J.J., and Kuipers,O.P. (2008) Opposite effects of Mn^{2+} and Zn^{2+} on PsaR-mediated expression of the virulence genes *pcpA*, *prtA*, and *psaBCA* of *Streptococcus pneumoniae*. *J Bacteriol* **190**: 5382-5393.

Knappe,J., and Sawers,G. (1990) A radical-chemical route to acetyl-CoA: the anaerobically induced pyruvate formate-lyase system of *Escherichia coli*. *FEMS Microbiol Rev* **6**: 383-398.

Knappe,J., Elbert,S., Frey,M., and Wagner,A.F. (1993) Pyruvate formate-lyase mechanism involving the protein-based glycyl radical. *Biochem Soc Trans* **21 (Pt 3)**: 731-734.

Kolter,R., Siegele,D.A., and Tormo,A. (1993) The stationary phase of the bacterial life cycle. *Annu Rev Microbiol* **47**: 855-874.

Krüger,S., Gertz,S., and Hecker,M. (1996) Transcriptional analysis of *bglPH* expression in *Bacillus subtilis*: evidence for two distinct pathways mediating carbon catabolite repression. *J Bacteriol* **178**: 2637-2644.

Kuipers,O.P., de Ruyter,P., Kleerebezem,M., and de Vos,W. (1998) Quorum sensing-controlled gene expression in lactic acid bacteria. *J Biotechnol* **64**: 15-21.

Lanie,J.A., Ng,W.L., Kazmierczak,K.M., Andrzejewski,T.M., Davidsen,T.M., Wayne,K.J. *et al.* (2007) Genome sequence of Avery's virulent serotype 2 strain D39 of *Streptococcus pneumoniae* and comparison with that of unencapsulated laboratory strain R6. *J Bacteriol* **189**: 38-51.

Lau,G.W., Haataja,S., Lonetto,M., Kensit,S.E., Marra,A., Bryant,A.P. *et al.* (2001) A functional genomic analysis of type 3 *Streptococcus pneumoniae* virulence. *Mol Microbiol* **40**: 555-571.

Lee,C.J., Banks,S.D., and Li,J.P. (1991) Virulence, immunity, and vaccine related to *Streptococcus pneumoniae*. *Crit Rev Microbiol* **18**: 89-114.

Leenhouts,K., Buist,G., Bolhuis,A., ten Berge,A., Kiel,J., Mierau,I. *et al.* (1996) A general system for generating unlabelled gene replacements in bacterial chromosomes. *Mol Gen Genet* **253**: 217-224.

LeMessurier,K.S., Ogunniyi,A.D., and Paton,J.C. (2006) Differential expression of key pneumococcal virulence genes *in vivo*. *Microbiology* **152**: 305-311.

Levander,F., Svensson,M., and Radstrom,P. (2002) Enhanced exopolysaccharide production by metabolic engineering of *Streptococcus thermophilus*. *Appl Environ Microbiol* **68**: 784-790.

Levy,M. (2005) Pathophysiology of oxygen delivery in respiratory failure. *Chest* **128**: 547S-553S.

Li-Korotky,H.S., Lo,C.Y., Zeng,F.R., Lo,D., and Banks,J.M. (2009) Interaction of phase variation, host and pressure/gas composition: pneumococcal gene expression of PsaA, SpxB, Ply and LytA in simulated middle ear environments. *Int J Pediatr Otorhinolaryngol* **73**: 1417-1422.

Limoli,D.H., Sladek,J.A., Fuller,L.A., Singh,A.K., and King,S.J. (2011) BgaA acts as an adhesin to mediate attachment of some pneumococcal strains to human epithelial cells. *Microbiology* **157**: 2369-2381.

Linares,D.M., Kok,J., and Poolman,B. (2010) Genome sequences of *Lactococcus lactis* MG1363 (revised) and NZ9000 and comparative physiological studies. *J Bacteriol* **192**: 5806-5812.

Lindner,C., Galinier,A., Hecker,M., and Deutscher,J. (1999) Regulation of the activity of the *Bacillus subtilis* antiterminator LicT by multiple PEP-dependent, enzyme I- and HPr-catalysed phosphorylation. *Mol Microbiol* **31**: 995-1006.

Lindner,C., Hecker,M., Le,C.D., and Deutscher,J. (2002) *Bacillus subtilis* mutant LicT antiterminators exhibiting enzyme I- and HPr-independent antitermination affect catabolite repression of the *bglPH* operon. *J Bacteriol* **184**: 4819-4828.

Livak,K.J., and Schmittgen,T.D. (2001) Analysis of relative gene expression data using real-time quantitative PCR and the $2^{-\Delta\Delta C}_{T}$ method. *Methods* **25**: 402-408.

Llull,D., Lopez,R., and Garcia,E. (2001) Genetic bases and medical relevance of capsular polysaccharide biosynthesis in pathogenic streptococci. *Curr Mol Med* **1**: 475-491.

Lopez de Felipe,F., and Gaudu,P. (2009) Multiple control of the acetate pathway in *Lactococcus lactis* under aeration by catabolite repression and metabolites. *Appl Microbiol Biotechnol* **82**: 1115-1122.

López,R., and Garcia,E. (2004) Recent trends on the molecular biology of pneumococcal capsules, lytic enzymes, and bacteriophage. *FEMS Microbiol Rev* **28**: 553-580.

López,R. (2006) Pneumococcus: the sugar-coated bacteria. *Int Microbiol* **9**: 179-190.

Lorca,G.L., Barabote,R.D., Zlotopolski,V., Tran,C., Winnen,B., Hvorup,R.N. *et al.* (2007) Transport capabilities of eleven Gram-positive bacteria: comparative genomic analyses. *Biochim Biophys Acta* **1768**: 1342-1366.

Lorquet,F., Goffin,P., Muscariello,L., Baudry,J.B., Ladero,V., Sacco,M. *et al.* (2004) Characterization and functional analysis of the *poxB* gene, which encodes pyruvate oxidase in *Lactobacillus plantarum*. *J Bacteriol* **186**: 3749-3759.

Luesink,E.J., van Herpen,R.E., Grossiord,B.P., Kuipers,O.P., and de Vos,W.M. (1998) Transcriptional activation of the glycolytic *las* operon and catabolite repression of the *gal* operon in *Lactococcus lactis* are mediated by the catabolite control protein CcpA. *Mol Microbiol* **30**: 789-798.

Lulko,A.T., Buist,G., Kok,J., and Kuipers,O.P. (2007) Transcriptome analysis of temporal regulation of carbon metabolism by CcpA in *Bacillus subtilis* reveals additional target genes. *J Mol Microbiol Biotechnol* **12**: 82-95.

Magee,A.D., and Yother,J. (2001) Requirement for capsule in colonization by *Streptococcus pneumoniae*. *Infect Immun* **69**: 3755-3761.

Maguin,E., Prevost,H., Ehrlich,S.D., and Gruss,A. (1996) Efficient insertional mutagenesis in lactococci and other Gram-positive bacteria. *J Bacteriol* **178**: 931-935.

Mahr,K., Hillen,W., and Titgemeyer,F. (2000) Carbon catabolite repression in *Lactobacillus pentosus*: analysis of the *ccpA* region. *Appl Environ Microbiol* **66**: 277-283.

Manco,S., Hernon,F., Yesilkaya,H., Paton,J.C., Andrew,P.W., and Kadioglu,A. (2006) Pneumococcal neuraminidases A and B both have essential roles during infection of the respiratory tract and sepsis. *Infect Immun* **74**: 4014-4020.

Margolis,E., Yates,A., and Levin,B.R. (2010) The ecology of nasal colonization of *Streptococcus pneumoniae*, *Haemophilus influenzae* and *Staphylococcus aureus*: the role of competition and interactions with host's immune response. *BMC Microbiol* **10**: 59.

Marion,C., Burnaugh,A.M., Woodiga,S.A., and King,S.J. (2011) Sialic acid transport contributes to pneumococcal colonization. *Infect Immun* **79**: 1262-1269.

Marion,C., Stewart,J.M., Tazi,M.F., Burnaugh,A.M., Linke,C.M., Woodiga,S.A., and King,S.J. (2012) *Streptococcus pneumoniae* can utilize multiple sources of hyaluronic acid for growth. *Infect Immun* **80**: 1390-1398.

Martin,B., Prudhomme,M., Alloing,G., Granadel,C., and Claverys,J.P. (2000) Cross-regulation of competence pheromone production and export in the early control of transformation in *Streptococcus pneumoniae*. *Mol Microbiol* **38**: 867-878.

Martínez-Núñez,M.A., Perez-Rueda,E., Gutierrez-Rios,R.M., and Merino,E. (2010) New insights into the regulatory networks of paralogous genes in bacteria. *Microbiology* **156**: 14-22.

Maruyama,Y., Nakamichi,Y., Itoh,T., Mikami,B., Hashimoto,W., and Murata,K. (2009) Substrate specificity of streptococcal unsaturated glucuronyl hydrolases for sulfated glycosaminoglycan. *J Biol Chem* **284**: 18059-18069.

Massaldi,H., Bessio,M.I., Suarez,N., Texeira,E., Rossi,S., and Ferreira,F. (2010) Features of bacterial growth and polysaccharide production of *Streptococcus pneumoniae* serotype 14. *Biotechnol Appl Biochem* **55**: 37-43.

McCluskey,J., Hinds,J., Husain,S., Witney,A., and Mitchell,T.J. (2004) A two-component system that controls the expression of pneumococcal surface antigen A (PsaA) and regulates virulence and resistance to oxidative stress in *Streptococcus pneumoniae*. *Mol Microbiol* **51**: 1661-1675.

McEllistrem,M.C., Ransford,J.V., and Khan,S.A. (2007) Characterization of *in vitro* biofilm-associated pneumococcal phase variants of a clinically relevant serotype 3 clone. *J Clin Microbiol* **45**: 97-101.

McKessar,S.J., and Hakenbeck,R. (2007) The two-component regulatory system TCS08 is involved in cellobiose metabolism of *Streptococcus pneumoniae* R6. *J Bacteriol* **189**: 1342-1350.

Meiattini,F. (1988) Inorganic peroxides. In: Bergmeyer,H.U., Bergmeyer,J., and Grabl,M. (Eds.) Methods of enzymatic analysis (Vol. VII, pp. 566-571). Verlag-Chemie, Weinheim, Germany.

Melchiorsen,C.R., Jokumsen,K.V., Villadsen,J., Johnsen,M.G., Israelsen,H., and Arnau,J. (2000) Synthesis and posttranslational regulation of pyruvate formate-lyase in *Lactococcus lactis*. *J Bacteriol* **182**: 4783-4788.

Melchiorsen,C.R., Jensen,N.B., Christensen,B., Vaever,J.K., and Villadsen,J. (2001) Dynamics of pyruvate metabolism in *Lactococcus lactis*. *Biotechnol Bioeng* **74**: 271-279.

Mercade,M., Lindley,N.D., and Loubiere,P. (2000) Metabolism of *Lactococcus lactis* subsp. *cremoris* MG 1363 in acid stress conditions. *Int J Food Microbiol* **55**: 161-165.

Mitchell,A.M., and Mitchell,T.J. (2010) *Streptococcus pneumoniae*: virulence factors and variation. *Clin Microbiol Infect* **16**: 411-418.

Mitchell,T.J. (2003) The pathogenesis of streptococcal infections: from tooth decay to meningitis. *Nat Rev Microbiol* **1**: 219-230.

Miwa,Y., Nakata,A., Ogiwara,A., Yamamoto,M., and Fujita,Y. (2000) Evaluation and characterization of catabolite-responsive elements (*cre*) of *Bacillus subtilis*. *Nucleic Acids Res* **28**: 1206-1210.

Mollerach,M., López,R., and Garcia,E. (1998) Characterization of the *galU* gene of *Streptococcus pneumoniae* encoding a uridine diphosphoglucose pyrophosphorylase: a gene essential for capsular polysaccharide biosynthesis. *J Exp Med* **188**: 2047-2056.

Monedero,V., Kuipers,O.P., Jamet,E., and Deutscher,J. (2001) Regulatory functions of serine-46-phosphorylated HPr in *Lactococcus lactis*. *J Bacteriol* **183**: 3391-3398.

Morona,J.K., Paton,J.C., Miller,D.C., and Morona,R. (2000) Tyrosine phosphorylation of CpsD negatively regulates capsular polysaccharide biosynthesis in *Streptococcus pneumoniae*. *Mol Microbiol* **35**: 1431-1442.

Morona,J.K., Morona,R., Miller,D.C., and Paton,J.C. (2002) *Streptococcus pneumoniae* capsule biosynthesis protein CpsB is a novel manganese-dependent phosphotyrosine-protein phosphatase. *J Bacteriol* **184**: 577-583.

Morona,J.K., Morona,R., Miller,D.C., and Paton,J.C. (2003) Mutational analysis of the carboxy-terminal (YGX)4 repeat domain of CpsD, an autophosphorylating tyrosine kinase required for capsule biosynthesis in *Streptococcus pneumoniae*. *J Bacteriol* **185**: 3009-3019.

Morona,J.K., Miller,D.C., Morona,R., and Paton,J.C. (2004) The effect that mutations in the conserved capsular polysaccharide biosynthesis genes *cpsA*, *cpsB*, and *cpsD* have on virulence of *Streptococcus pneumoniae*. *J Infect Dis* **189**: 1905-1913.

Morona,J.K., Morona,R., and Paton,J.C. (2006) Attachment of capsular polysaccharide to the cell wall of *Streptococcus pneumoniae* type 2 is required for invasive disease. *Proc Natl Acad Sci U S A* **103**: 8505-8510.

Moscoso,M., and Garcia,E. (2009) Transcriptional regulation of the capsular polysaccharide biosynthesis *locus* of *Streptococcus pneumoniae*: a bioinformatic analysis. *DNA Res* **16**: 177-186.

Navarro Llorens,J.M., Tormo,A., and Martinez-Garcia,E. (2010) Stationary phase in Gram-negative bacteria. *FEMS Microbiol Rev* **34**: 476-495.

Neef,J., Andisi,V.F., Kim,K.S., Kuipers,O.P., and Bijlsma,J.J. (2011) Deletion of a cation transporter promotes lysis in *Streptococcus pneumoniae*. *Infect Immun* **79**: 2314-2323.

Neijssel,O.M., Snoep,J.L., and Teixeira de Mattos,M.J. (1997) Regulation of energy source metabolism in streptococci. *Soc Appl Bacteriol Symp Ser* **26**: 12S-19S.

Nelson,A.L., Roche,A.M., Gould,J.M., Chim,K., Ratner,A.J., and Weiser,J.N. (2007) Capsule enhances pneumococcal colonization by limiting mucus-mediated clearance. *Infect Immun* **75**: 83-90.

Nelson,D.L., and Cox,M.M. (2000) Lehninger, Principles of Biochemistry, 3rd edition (pp. 527-566). Worth Publishers, New York.

Nessler,S., Fieulaine,S., Poncet,S., Galinier,A., Deutscher,J., and Janin,J. (2003) HPr kinase/phosphorylase, the sensor enzyme of catabolite repression in Gram-positive bacteria: structural aspects of the enzyme and the complex with its protein substrate. *J Bacteriol* **185**: 4003-4010.

Neuhaus,F.C., and Baddiley,J. (2003) A continuum of anionic charge: structures and functions of D-alanyl-teichoic acids in Gram-positive bacteria. *Microbiol Mol Biol Rev* **67**: 686-723.

Neves,A.R., Ramos,A., Nunes,M.C., Kleerebezem,M., Hugenholtz,J., de Vos,W.M. *et al.* (1999) *In vivo* nuclear magnetic resonance studies of glycolytic kinetics in *Lactococcus lactis*. *Biotechnol Bioeng* **64**: 200-212.

Neves,A.R., Ventura,R., Mansour,N., Shearman,C., Gasson,M.J., Maycock,C. *et al.* (2002a) Is the glycolytic flux in *Lactococcus lactis* primarily controlled by the redox charge? Kinetics of NAD^+ and NADH pools determined *in vivo* by ^{13}C-NMR. *J Biol Chem* **277**: 28088-28098.

Neves,A.R., Ramos,A., Costa,H., van Swam II, Hugenholtz,J., Kleerebezem,M. *et al.* (2002b) Effect of different NADH oxidase levels on glucose metabolism by *Lactococcus lactis*: kinetics of intracellular metabolite pools determined by *in vivo* nuclear magnetic resonance. *Appl Environ Microbiol* **68**: 6332-6342.

Neves,A.R., Pool,W.A., Kok,J., Kuipers,O.P., and Santos,H. (2005) Overview on sugar metabolism and its control in *Lactococcus lactis* - the input from *in vivo* NMR. *FEMS Microbiol Rev* **29**: 531-554.

Neves,A.R., Pool,W.A., Castro,R., Mingote,A., Santos,F., Kok,J. *et al.* (2006) The α-phosphoglucomutase of *Lactococcus lactis* is unrelated to the α-D-phosphohexomutase superfamily and is encoded by the essential gene *pgmH*. *J Biol Chem* **281**: 36864-36873.

Neves,A.R., Pool,W.A., Solopova,A., Kok,J., Santos,H., and Kuipers,O.P. (2010) Towards enhanced galactose utilization by *Lactococcus lactis*. *Appl Environ Microbiol* **76**: 7048-7060.

Nicoloff,H., Elagoz,A., Arsène-Ploetze,F., Kammerer,B., Martinussen,J., and Bringel,F. (2005) Repression of the *pyr* operon in *Lactobacillus plantarum* prevents its ability to grow at low carbon dioxide levels. *J Bacteriol* **187**: 2093-2104.

Nieto,C., Espinosa,M., and Puyet,A. (1997) The maltose/maltodextrin regulon of *Streptococcus pneumoniae*. Differential promoter regulation by the transcriptional repressor MalR. *J Biol Chem* **272**: 30860-30865.

Nnyepi,M.R., Peng,Y., and Broderick,J.B. (2007) Inactivation of *E. coli* pyruvate formate-lyase: role of AdhE and small molecules. *Arch Biochem Biophys* **459**: 1-9.

O'Donovan,G.A., and Neuhard,J. (1970) Pyrimidine metabolism in microorganisms. *Bacteriol Rev* **34**: 278-343.

Obaro,S., and Adegbola,R. (2002) The pneumococcus: carriage, disease and conjugate vaccines. *J Med Microbiol* **51**: 98-104.

Oggioni,M.R., Trappetti,C., Kadioglu,A., Cassone,M., Iannelli,F., Ricci,S. *et al.* (2006) Switch from planktonic to sessile life: a major event in pneumococcal pathogenesis. *Mol Microbiol* **61**: 1196-1210.

Ogunniyi,A.D., Giammarinaro,P., and Paton,J.C. (2002) The genes encoding virulence-associated proteins and the capsule of *Streptococcus pneumoniae* are upregulated and differentially expressed *in vivo*. *Microbiology* **148**: 2045-2053.

Orihuela,C.J., Gao,G., McGee,M., Yu,J., Francis,K.P., and Tuomanen,E. (2003) Organ-specific models of *Streptococcus pneumoniae* disease. *Scand J Infect Dis* **35**: 647-652.

Orihuela,C.J., Radin,J.N., Sublett,J.E., Gao,G., Kaushal,D., and Tuomanen,E.I. (2004a) Microarray analysis of pneumococcal gene expression during invasive disease. *Infect Immun* **72**: 5582-5596.

Orihuela,C.J., Gao,G., Francis,K.P., Yu,J., and Tuomanen,E.I. (2004b) Tissue-specific contributions of pneumococcal virulence factors to pathogenesis. *J Infect Dis* **190**: 1661-1669.

Overweg,K., Pericone,C.D., Verhoef,G.G., Weiser,J.N., Meiring,H.D., de Jong,A.P. *et al.* (2000) Differential protein expression in phenotypic variants of *Streptococcus pneumoniae*. *Infect Immun* **68**: 4604-4610.

Papagianni,M., Avramidis,N., and Filiousis,G. (2007) Glycolysis and the regulation of glucose transport in *Lactococcus lactis* spp. *lactis* in batch and fed-batch culture. *Microb Cell Fact* **6**: 16.

Paton,J.C., Andrew,P.W., Boulnois,G.J., and Mitchell,T.J. (1993) Molecular analysis of the pathogenicity of *Streptococcus pneumoniae*: the role of pneumococcal proteins. *Annu Rev Microbiol* **47**: 89-115.

Patrick,S., Blakely,G.W., Houston,S., Moore,J., Abratt,V.R., Bertalan,M. *et al.* (2010) Twenty-eight divergent polysaccharide *loci* specifying within- and amongst-strain capsule diversity in three strains of *Bacteroides fragilis*. *Microbiology* **156**: 3255-3269.

Perfeito,L., Fernandes,L., Mota,C., and Gordo,I. (2007) Adaptive mutations in bacteria: high rate and small effects. *Science* **317**: 813-815.

Pericone,C.D., Overweg,K., Hermans,P.W., and Weiser,J.N. (2000) Inhibitory and bactericidal effects of hydrogen peroxide production by *Streptococcus pneumoniae* on other inhabitants of the upper respiratory tract. *Infect Immun* **68**: 3990-3997.

Pericone,C.D., Bae,D., Shchepetov,M., McCool,T., and Weiser,J.N. (2002) Short-sequence tandem and nontandem DNA repeats and endogenous hydrogen peroxide production contribute to genetic instability of *Streptococcus pneumoniae*. *J Bacteriol* **184**: 4392-4399.

Pericone,C.D., Park,S., Imlay,J.A., and Weiser,J.N. (2003) Factors contributing to hydrogen peroxide resistance in *Streptococcus pneumoniae* include pyruvate oxidase (SpxB) and avoidance of the toxic effects of the fenton reaction. *J Bacteriol* **185**: 6815-6825.

Pesakhov,S., Benisty,R., Sikron,N., Cohen,Z., Gomelsky,P., Khozin-Goldberg,I. *et al.* (2007) Effect of hydrogen peroxide production and the Fenton reaction on membrane composition of *Streptococcus pneumoniae*. *Biochim Biophys Acta* **1768**: 590-597.

Pettigrew,M.M., Gent,J.F., Revai,K., Patel,J.A., and Chonmaitree,T. (2008) Microbial interactions during upper respiratory tract infections. *Emerg Infect Dis* **14**: 1584-1591.

Philips,B.J., Meguer,J.X., Redman,J., and Baker,E.H. (2003) Factors determining the appearance of glucose in upper and lower respiratory tract secretions. *Intensive Care Med* **29**: 2204-2210.

Pierce,W.A., Jr. (1957) Glucose and galactose metabolism in *Streptococcus pyogenes*. *J Bacteriol* **74**: 186-193.

Poolman,B., and Konings,W.N. (1993) Secondary solute transport in bacteria. *Biochim Biophys Acta* **1183**: 5-39.

Postma,P.W., Lengeler,J.W., and Jacobson,G.R. (1993) Phosphoenolpyruvate: carbohydrate phosphotransferase systems of bacteria. *Microbiol Rev* **57**: 543-594.

Potvin,B.W., Kelleher,R.J., Jr., and Gooder,H. (1975) Pyrimidine biosynthetic pathway of *Bacillus subtilis*. *J Bacteriol* **123**: 604-615.

Poyart,C., Berche,P., and Trieu-Cuot,P. (1995) Characterization of superoxide dismutase genes from Gram-positive bacteria by polymerase chain reaction using degenerate primers. *FEMS Microbiol Lett* **131**: 41-45.

Poyart,C., Quesne,G., Coulon,S., Berche,P., and Trieu-Cuot,P. (1998) Identification of streptococci to species level by sequencing the gene encoding the manganese-dependent superoxide dismutase. *J Clin Microbiol* **36**: 41-47.

Pracht,D., Elm,C., Gerber,J., Bergmann,S., Rohde,M., Seiler,M. *et al.* (2005) PavA of *Streptococcus pneumoniae* modulates adherence, invasion, and meningeal inflammation. *Infect Immun* **73**: 2680-2689.

Presecan-Siedel,E., Galinier,A., Longin,R., Deutscher,J., Danchin,A., Glaser,P., and Martin-Verstraete,I. (1999) Catabolite regulation of the *pta* gene as part of carbon flow pathways in *Bacillus subtilis*. *J Bacteriol* **181**: 6889-6897.

Price,C.E., Zeyniyev,A., Kuipers,O.P., and Kok,J. (2011) From meadows to milk to mucosa - adaptation of *Streptococcus* and *Lactococcus* species to their nutritional environments. *FEMS Microbiol Rev*.

Quatravaux,S., Remize,F., Bryckaert,E., Colavizza,D., and Guzzo,J. (2006) Examination of *Lactobacillus plantarum* lactate metabolism side effects in relation to the modulation of aeration parameters. *J Appl Microbiol* **101**: 903-912.

Ramos-Montañez,S., Tsui,H.C., Wayne,K.J., Morris,J.L., Peters,L.E., Zhang,F. *et al.* (2008) Polymorphism and regulation of the *spxB* (pyruvate oxidase) virulence factor gene by a CBS-HotDog domain protein (SpxR) in serotype 2 *Streptococcus pneumoniae*. *Mol Microbiol* **67**: 729-746.

Ramos-Montañez,S., Kazmierczak,K.M., Hentchel,K.L., and Winkler,M.E. (2010) Instability of *ackA* (acetate kinase) mutations and their effects on acetyl phosphate and ATP amounts in *Streptococcus pneumoniae* D39. *J Bacteriol* **192**: 6390-6400.

Ramos,A., Boels,I.C., de Vos,W.M., and Santos,H. (2001) Relationship between glycolysis and exopolysaccharide biosynthesis in *Lactococcus lactis*. *Appl Environ Microbiol* **67**: 33-41.

Daran-Lapujade,P., Rossell,S., van Gulik,W.M., Luttik,M.A., de Groot,M.J., Slijper,M. *et al.* (2007) The fluxes through glycolytic enzymes in *Saccharomyces cerevisiae* are predominantly regulated at posttranscriptional levels. *Proc Natl Acad Sci U S A* **104**: 15753-15758.

Rees,D.C., Johnson,E., and Lewinson,O. (2009) ABC transporters: the power to change. *Nat Rev Mol Cell Biol* **10**: 218-227.

Regev-Yochay,G., Trzcinski,K., Thompson,C.M., Malley,R., and Lipsitch,M. (2006) Interference between *Streptococcus pneumoniae* and *Staphylococcus aureus*: *in vitro* hydrogen peroxide-mediated killing by *Streptococcus pneumoniae*. *J Bacteriol* **188**: 4996-5001.

Regev-Yochay,G., Trzcinski,K., Thompson,C.M., Lipsitch,M., and Malley,R. (2007) SpxB is a suicide gene of *Streptococcus pneumoniae* and confers a selective advantage in an *in vivo* competitive colonization model. *J Bacteriol* **189**: 6532-6539.

Reizer,J., and Panos,C. (1980) Regulation of beta-galactoside phosphate accumulation in *Streptococcus pyogenes* by an expulsion mechanism. *Proc Natl Acad Sci U S A* **77**: 5497-5501.

Ring,A., Weiser,J.N., and Tuomanen,E.I. (1998) Pneumococcal trafficking across the blood-brain barrier. Molecular analysis of a novel bidirectional pathway. *J Clin Invest* **102**: 347-360.

Rose,M.C., and Voynow,J.A. (2006) Respiratory tract mucin genes and mucin glycoproteins in health and disease. *Physiol Rev* **86**: 245-278.

Rosenow,C., Maniar,M., and Trias,J. (1999) Regulation of the α-galactosidase activity in *Streptococcus pneumoniae*: characterization of the raffinose utilization system. *Genome Res* **9**: 1189-1197.

Saluja,S.K., and Weiser,J.N. (1995) The genetic basis of colony opacity in *Streptococcus pneumoniae*: evidence for the effect of box elements on the frequency of phenotypic variation. *Mol Microbiol* **16**: 215-227.

Sanders,J.W., Venema,G., Kok,J., and Leenhouts,K. (1998) Identification of a sodium chloride-regulated promoter in *Lactococcus lactis* by single-copy chromosomal fusion with a reporter gene. *Mol Gen Genet* **257**: 681-685.

Sauter,M., and Sawers,R.G. (1990) Transcriptional analysis of the gene encoding pyruvate formate-lyase-activating enzyme of *Escherichia coli*. *Mol Microbiol* **4**: 355-363.

Sawers,G., and Watson,G. (1998) A glycyl radical solution: oxygen-dependent interconversion of pyruvate formate-lyase. *Mol Microbiol* **29**: 945-954.

Schleifer,K.H., Kraus,J., Dvorak,C., kilpper-Bälz,R., Colins,M.D., and Fisher,W. (1985) Transfer of *Streptococcus lactis* and related species to the genus *Lactococcus* gen. nov. *System Appl Microbiol* **6**: 183-95.

Schumacher,M.A., Allen,G.S., Diel,M., Seidel,G., Hillen,W., and Brennan,R.G. (2004) Structural basis for allosteric control of the transcription regulator CcpA by the phosphoprotein HPr-Ser46-P. *Cell* **118**: 731-741.

Schumacher,M.A., Seidel,G., Hillen,W., and Brennan,R.G. (2007) Structural mechanism for the fine-tuning of CcpA function by the small molecule effectors glucose 6-phosphate and fructose 1,6-bisphosphate. *J Mol Biol* **368**: 1042-1050.

Sebert,M.E., Palmer,L.M., Rosenberg,M., and Weiser,J.N. (2002) Microarray-based identification of *htrA*, a *Streptococcus pneumoniae* gene that is regulated by the CiaRH two-component system and contributes to nasopharyngeal colonization. *Infect Immun* **70**: 4059-4067.

Sebert,M.E., Patel,K.P., Plotnick,M., and Weiser,J.N. (2005) Pneumococcal HtrA protease mediates inhibition of competence by the CiaRH two-component signaling system. *J Bacteriol* **187**: 3969-3979.

Sedewitz,B., Schleifer,K.H., and Gotz,F. (1984) Physiological role of pyruvate oxidase in the aerobic metabolism of *Lactobacillus plantarum*. *J Bacteriol* **160**: 462-465.

Seidel,G., Diel,M., Fuchsbauer,N., and Hillen,W. (2005) Quantitative interdependence of coeffectors, CcpA and *cre* in carbon catabolite regulation of *Bacillus subtilis*. *FEBS J* **272**: 2566-2577.

Seidl,K., Stucki,M., Ruegg,M., Goerke,C., Wolz,C., Harris,L. *et al.* (2006) *Staphylococcus aureus* CcpA affects virulence determinant production and antibiotic resistance. *Antimicrob Agents Chemother* **50**: 1183-1194.

Seki,M., Iida,K., Saito,M., Nakayama,H., and Yoshida,S. (2004) Hydrogen peroxide production in *Streptococcus pyogenes*: involvement of lactate oxidase and coupling with aerobic utilization of lactate. *J Bacteriol* **186**: 2046-2051.

Severin,A., Horne,D., and Tomasz,A. (1997) Autolysis and cell wall degradation in a choline-independent strain of *Streptococcus pneumoniae*. *Microb Drug Resist* **3**: 391-400.

Shafeeq,S., Kloosterman,T.G., and Kuipers,O.P. (2011) CelR-mediated activation of the cellobiose-utilization gene cluster in *Streptococcus pneumoniae*. *Microbiology* **157**: 2854-2861.

Sheehan,J.K., Richardson,P.S., Fung,D.C., Howard,M., and Thornton,D.J. (1995) Analysis of respiratory mucus glycoproteins in asthma: a detailed study from a patient who died in status asthmaticus. *Am J Respir Cell Mol Biol* **13**: 748-756.

Shelburne,S.A., Davenport,M.T., Keith,D.B., and Musser,J.M. (2008a) The role of complex carbohydrate catabolism in the pathogenesis of invasive streptococci. *Trends Microbiol* **16**: 318-325.

Shelburne,S.A., Olsen,R.J., Suber,B., Sahasrabhojane,P., Sumby,P., Brennan,R.G., and Musser,J.M. (2010) A combination of independent transcriptional regulators shapes bacterial virulence gene expression during infection. *PLoS Pathog* **6**: e1000817.

Shelburne,S.A., III, Keith,D., Horstmann,N., Sumby,P., Davenport,M.T., Graviss,E.A. *et al.* (2008b) A direct link between carbohydrate utilization and virulence in the major human pathogen group A Streptococcus. *Proc Natl Acad Sci U S A* **105**: 1698-1703.

Sicard,A.M. (1964) A new synthetic medium for *Diplococcus pneumoniae*, and its use for the study of reciprocal transformations at the *amiA locus*. *Genetics* **50**: 31-44.

Simmonds,R.J., and Harkness,R.A. (1981) High-performance liquid chromatographic methods for base and nucleoside analysis in extracellular fluids and in cells. *J Chromatogr* **226**: 369-381.

Singh,K.D., Schmalisch,M.H., Stülke,J., and Görke,B. (2008) Carbon catabolite repression in *Bacillus subtilis*: quantitative analysis of repression exerted by different carbon sources. *J Bacteriol* **190**: 7275-7284.

Snoep,J.L., de Graef,M.R., Westphal,A.H., de Kok,A., Teixeira de Mattos,M.J., and Neijssel,O.M. (1993) Differences in sensitivity to NADH of purified pyruvate dehydrogenase complexes of *Enterococcus faecalis*, *Lactococcus lactis*, *Azotobacter vinelandii* and *Escherichia coli*: implications for their activity *in vivo*. *FEMS Microbiol Lett* **114**: 279-283.

Solopova,A., Bachmann,H., Teusink,B., Kok,J., Neves,A.R., and Kuipers,O.P. (2012) A specific mutation in the promoter region of the silent *cel* cluster accounts for the appearance of lactose-utilizing *Lactococcus lactis* MG1363. *Appl Environ Microbiol* **78**: 5612-5621.

Song,J.H., Ko,K.S., Lee,J.Y., Baek,J.Y., Oh,W.S., Yoon,H.S. *et al.* (2005) Identification of essential genes in *Streptococcus pneumoniae* by allelic replacement mutagenesis. *Mol Cells* **19**: 365-374.

Song,J.H., Dagan,R., Klugman,K.P., and Fritzell,B. (2012) The relationship between pneumococcal serotypes and antibiotic resistance. *Vaccine* **30**: 2728-2737.

Spellerberg,B., Cundell,D.R., Sandros,J., Pearce,B.J., Idanpaan-Heikkila,I., Rosenow,C., and Masure,H.R. (1996) Pyruvate oxidase, as a determinant of virulence in *Streptococcus pneumoniae*. *Mol Microbiol* **19**: 803-813.

Standish,A.J., Stroeher,U.H., and Paton,J.C. (2007) The pneumococcal two-component signal transduction system RR/HK06 regulates CbpA and PspA by two distinct mechanisms. *J Bacteriol* **189**: 5591-5600.

Steele,R.H., White,A.G., and Pierce,W.A., Jr. (1954) The fermentation of galactose by *Streptococcus pyogenes*. *J Bacteriol* **67**: 86-89.

Steinmoen,H., Knutsen,E., and Havarstein,L.S. (2002) Induction of natural competence in *Streptococcus pneumoniae* triggers lysis and DNA release from a subfraction of the cell population. *Proc Natl Acad Sci U S A* **99**: 7681-7686.

Stevens,K.E., and Sebert,M.E. (2011) Frequent beneficial mutations during single-colony serial transfer of *Streptococcus pneumoniae*. *PLoS Genet* **7**: e1002232.

Stülke,J., Arnaud,M., Rapoport,G., and Martin-Verstraete,I. (1998) PRD-a protein domain involved in PTS-dependent induction and carbon catabolite repression of catabolic operons in bacteria. *Mol Microbiol* **28**: 865-874.

Sumby,P., Porcella,S.F., Madrigal,A.G., Barbian,K.D., Virtaneva,K., Ricklefs,S.M. *et al.* (2005) Evolutionary origin and emergence of a highly successful clone of serotype M1 Group A *Streptococcus* involved multiple horizontal gene transfer events. *J Infect Dis* **192**: 771-782.

Takahashi-Abbe,S., Abe,K., and Takahashi,N. (2003) Biochemical and functional properties of a pyruvate formate-lyase (PFL)-activating system in *Streptococcus mutans*. *Oral Microbiol Immunol* **18**: 293-297.

Takahashi,N., Abbe,K., Takahashi-Abbe,S., and Yamada,T. (1987) Oxygen sensitivity of sugar metabolism and interconversion of pyruvate formate-lyase in intact cells of *Streptococcus mutans* and *Streptococcus sanguis*. *Infect Immun* **55**: 652-656.

Takahashi,N., Iwami,Y., and Yamada,T. (1991) Metabolism of intracellular polysaccharide in the cells of *Streptococcus mutans* under strictly anaerobic conditions. *Oral Microbiol Immunol* **6**: 299-304.

Taniai,H., Iida,K., Seki,M., Saito,M., Shiota,S., Nakayama,H., and Yoshida,S. (2008) Concerted action of lactate oxidase and pyruvate oxidase in aerobic growth of *Streptococcus pneumoniae*: role of lactate as an energy source. *J Bacteriol* **190**: 3572-3579.

Terra,V.S., Homer,K.A., Rao,S.G., Andrew,P.W., and Yesilkaya,H. (2010) Characterization of novel β-galactosidase activity that contributes to glycoprotein degradation and virulence in *Streptococcus pneumoniae*. *Infect Immun* **78**: 348-357.

Tettelin,H., Nelson,K.E., Paulsen,I.T., Eisen,J.A., Read,T.D., Peterson,S. *et al.* (2001) Complete genome sequence of a virulent isolate of *Streptococcus pneumoniae*. *Science* **293**: 498-506.

Thevelein,J.M., and Hohmann,S. (1995) Trehalose synthase: guard to the gate of glycolysis in yeast? *Trends Biochem Sci* **20**: 3-10.

Thomas,T.D., Turner,K.W., and Crow,V.L. (1980) Galactose fermentation by *Streptococcus lactis* and *Streptococcus cremoris*: pathways, products, and regulation. *J Bacteriol* **144**: 672-682.

Thompson,J., and Saier,M.H., Jr. (1981) Regulation of methyl-beta-d-thiogalactopyranoside 6-phosphate accumulation in *Streptococcus lactis* by exclusion and expulsion mechanisms. *J Bacteriol* **146**: 885-894.

Throup,J.P., Koretke,K.K., Bryant,A.P., Ingraham,K.A., Chalker,A.F., Ge,Y. *et al.* (2000) A genomic analysis of two-component signal transduction in *Streptococcus pneumoniae*. *Mol Microbiol* **35**: 566-576.

Tittmann,K., Wille,G., Golbik,R., Weidner,A., Ghisla,S., and Hubner,G. (2005) Radical phosphate transfer mechanism for the thiamin diphosphate- and FAD-dependent pyruvate oxidase from *Lactobacillus plantarum*. Kinetic coupling of intercofactor electron transfer with phosphate transfer to acetyl-thiamin diphosphate via a transient FAD semiquinone/hydroxyethyl-ThDP radical pair. *Biochemistry* **44**: 13291-13303.

Tobisch,S., Zuhlke,D., Bernhardt,J., Stülke,J., and Hecker,M. (1999) Role of CcpA in regulation of the central pathways of carbon catabolism in *Bacillus subtilis*. *J Bacteriol* **181**: 6996-7004.

Tomasz,A. (1964) A chemically defined medium for *Streptococcus pneumoniae*. *Bacteriol Proc* **64**: 29.

Tomasz,A. (1967) Choline in the cell wall of a bacterium: novel type of polymer-linked choline in Pneumococcus. *Science* **157**: 694-697.

Tomasz,A., Albino,A., and Zanati,E. (1970) Multiple antibiotic resistance in a bacterium with suppressed autolytic system. *Nature* **227**: 138-140.

Tortosa,P., Declerck,N., Dutartre,H., Lindner,C., Deutscher,J., and Le,C.D. (2001) Sites of positive and negative regulation in the *Bacillus subtilis* antiterminators LicT and SacY. *Mol Microbiol* **41**: 1381-1393.

Trappetti,C., Kadioglu,A., Carter,M., Hayre,J., Iannelli,F., Pozzi,G. *et al.* (2009) Sialic acid: a preventable signal for pneumococcal biofilm formation, colonization, and invasion of the host. *J Infect Dis* **199**: 1497-1505.

Tsui,F.P., Egan,W., Summers,M.F., Byrd,R.A., Schneerson,R., and Robbins,J.B. (1988) Determination of the structure of the *Escherichia coli* K100 capsular polysaccharide, cross-reactive with the capsule from type b *Haemophilus influenzae*. *Carbohydr Res* **173**: 65-74.

Turnbough,C.L., Jr., and Switzer,R.L. (2008) Regulation of pyrimidine biosynthetic gene expression in bacteria: repression without repressors. *Microbiol Mol Biol Rev* **72**: 266-300.

Tuomanen,E. (2006) *Streptococcus pneumoniae*. In: Dworkin,M., Falkow,S., Rosenberg,E., Schleifer,K., and Stackebrandt, E. (Eds.) The Prokaryotes (pp. 149-162). Springer Science + Business Media, New York.

Van Niel,E.W., Palmfeldt,J., Martin,R., Paese,M., and Hahn-Hagerdal,B. (2004) Reappraisal of the regulation of lactococcal L-lactate dehydrogenase. *Appl Environ Microbiol* **70**: 1843-1846.

Van Opijnen,T., Bodi,K.L., and Camilli,A. (2009) Tn-seq: high-throughput parallel sequencing for fitness and genetic interaction studies in microorganisms. *Nat Methods* **6**: 767-772.

Ventura,C.L., Cartee,R.T., Forsee,W.T., and Yother,J. (2006) Control of capsular polysaccharide chain length by UDP-sugar substrate concentrations in *Streptococcus pneumoniae*. *Mol Microbiol* **61**: 723-733.

Vey,J.L., Yang,J., Li,M., Broderick,W.E., Broderick,J.B., and Drennan,C.L. (2008) Structural basis for glycyl radical formation by pyruvate formate-lyase activating enzyme. *Proc Natl Acad Sci U S A* **105**: 16137-16141.

Waite,R.D., Struthers,J.K., and Dowson,C.G. (2001) Spontaneous sequence duplication within an open reading frame of the pneumococcal type 3 capsule *locus* causes high-frequency phase variation. *Mol Microbiol* **42**: 1223-1232.

Waite,R.D., Penfold,D.W., Struthers,J.K., and Dowson,C.G. (2003) Spontaneous sequence duplications within capsule genes *cap8E* and *tts* control phase variation in *Streptococcus pneumoniae* serotypes 8 and 37. *Microbiology* **149**: 497-504.

Warner,J.B., and Lolkema,J.S. (2003) CcpA-dependent carbon catabolite repression in bacteria. *Microbiol Mol Biol Rev* **67**: 475-490.

Wartha,F., Beiter,K., Albiger,B., Fernebro,J., Zychlinsky,A., Normark,S., and Henriques - Normark,B. (2007) Capsule and D-alanylated lipoteichoic acids protect *Streptococcus pneumoniae* against neutrophil extracellular traps. *Cell Microbiol* **9**: 1162-1171.

Watson,D.A., Musher,D.M., Jacobson,J.W., and Verhoef,J. (1993) A brief history of the pneumococcus in biomedical research: a panoply of scientific discovery. *Clin Infect Dis* **17**: 913-924.

Wegmann,U., O'Connell-Motherway,M., Zomer,A., Buist,G., Shearman,C., Canchaya,C. *et al.* (2007) Complete genome sequence of the prototype lactic acid bacterium *Lactococcus lactis* subsp. *cremoris* MG1363. *J Bacteriol* **189**: 3256-3270.

Weidner,G., and Sawers,G. (1996) Molecular characterization of the genes encoding pyruvate formate-lyase and its activating enzyme of *Clostridium pasteurianum*. *J Bacteriol* **178**: 2440-2444.

Weiser,J.N., Austrian,R., Sreenivasan,P.K., and Masure,H.R. (1994) Phase variation in pneumococcal opacity: relationship between colonial morphology and nasopharyngeal colonization. *Infect Immun* **62**: 2582-2589.

Weiser,J.N., Bae,D., Epino,H., Gordon,S.B., Kapoor,M., Zenewicz,L.A., and Shchepetov,M. (2001) Changes in availability of oxygen accentuate differences in capsular polysaccharide expression by phenotypic variants and clinical isolates of *Streptococcus pneumoniae*. *Infect Immun* **69**: 5430-5439.

Weiser,J.N., and Kapoor,M. (1999) Effect of intrastrain variation in the amount of capsular polysaccharide on genetic transformation of *Streptococcus pneumoniae*: implications for virulence studies of encapsulated strains. *Infect Immun* **67**: 3690-3692.

Weiser,J.N. (2010) The pneumococcus: why a commensal misbehaves. *J Mol Med (Berl)* **88**: 97-102.

White,A.G., Steele,R.H., and Pierce,W.A., Jr. (1955) The effect of pH on the fermentation of glucose and galactose by *Streptococcus pyogenes*. *J Bacteriol* **70**: 82-86.

Wolfe,A.J. (2010) Physiologically relevant small phosphodonors link metabolism to signal transduction. *Curr Opin Microbiol* **13**: 204-209.

Wolin,M.J. (1964) Fructose 1,6-diphosphate requirement of streptococcal lactic dehydrogenases. *Science* **146**: 775-777.

Xayarath,B., and Yother,J. (2007) Mutations blocking side chain assembly, polymerization, or transport of a Wzy-dependent *Streptococcus pneumoniae* capsule are

lethal in the absence of suppressor mutations and can affect polymer transfer to the cell wall. *J Bacteriol* **189**: 3369-3381.

Yamada,T., and Carlsson,J. (1975) Glucose-6-phosphate-dependent pyruvate kinase in *Streptococcus mutans*. *J Bacteriol* **124**: 562-563.

Yamada,T., and Carlsson,J. (1975) Regulation of lactate dehydrogenase and change of fermentation products in streptococci. *J Bacteriol* **124**: 55-61.

Yamada,T., Takahashi-Abbe,S., and Abbe,K. (1985) Effects of oxygen on pyruvate formate-lyase in situ and sugar metabolism of *Streptococcus mutans* and *Streptococcus sanguis*. *Infect Immun* **47**: 129-134.

Yamamoto,Y., Sato,Y., Takahashi-Abbe,S., Takahashi,N., and Kizaki,H. (2000) Characterization of the *Streptococcus mutans* pyruvate formate-lyase (PFL)-activating enzyme gene by complementary reconstitution of the *in vitro* PFL-reactivating system. *Infect Immun* **68**: 4773-4777.

Yesilkaya,H., Kadioglu,A., Gingles,N., Alexander,J.E., Mitchell,T.J., and Andrew,P.W. (2000) Role of manganese-containing superoxide dismutase in oxidative stress and virulence of *Streptococcus pneumoniae*. *Infect Immun* **68**: 2819-2826.

Yesilkaya,H., Manco,S., Kadioglu,A., Terra,V.S., and Andrew,P.W. (2008) The ability to utilize mucin affects the regulation of virulence gene expression in *Streptococcus pneumoniae*. *FEMS Microbiol Lett* **278**: 231-235.

Yesilkaya,H., Spissu,F., Carvalho,S.M., Terra,V.S., Homer,K.A., Benisty,R. *et al.* (2009) Pyruvate formate lyase is required for pneumococcal fermentative metabolism and virulence. *Infect Immun* **77**: 5418-5427.

Yother,J. (2011) Capsules of *Streptococcus pneumoniae* and other bacteria: paradigms for polysaccharide biosynthesis and regulation. *Annu Rev Microbiol* **65**: 563-581.

Yu,J., Bryant,A.P., Marra,A., Lonetto,M.A., Ingraham,K.A., Chalker,A.F. *et al.* (2001) Characterization of the *Streptococcus pneumoniae* NADH oxidase that is required for infection. *Microbiology* **147**: 431-438.

Yum,D.Y., Lee,B.Y., and Pan,J.G. (1999) Identification of the *yqhE* and *yafB* genes encoding two 2, 5-diketo-D-gluconate reductases in *Escherichia coli*. *Appl Environ Microbiol* **65**: 3341-3346.

Zaritsky,A., Parola,A.H., Abdah,M., and Masalha,H. (1985) Homeoviscous adaptation, growth rate, and morphogenesis in bacteria. *Biophys J* **48**: 337-339.

Zeng,L., Das,S., and Burne,R.A. (2010) Utilization of lactose and galactose by *Streptococcus mutans*: transport, toxicity, and carbon catabolite repression. *J Bacteriol* **192**: 2434-2444.

Zeng,L., and Burne,R.A. (2010) Seryl-phosphorylated HPr regulates CcpA-independent carbon catabolite repression in conjunction with PTS permeases in *Streptococcus mutans*. *Mol Microbiol* **75**: 1145-1158.

Zhang,G., Mills,D.A., and Block,D.E. (2009) Development of chemically defined media supporting high-cell-density growth of lactococci, enterococci, and streptococci. *Appl Environ Microbiol* **75**: 1080-1087.

Zheng,L., Itzek,A., Chen,Z., and Kreth,J. (2011a) Environmental influences on competitive hydrogen peroxide production in *Streptococcus gordonii*. *Appl Environ Microbiol* **77**: 4318-4328.

Zheng,L., Chen,Z., Itzek,A., Ashby,M., and Kreth,J. (2011b) Catabolite control protein A controls hydrogen peroxide production and cell death in *Streptococcus sanguinis*. *J Bacteriol* **193**: 516-526.

Zheng,L.Y., Itzek,A., Chen,Z.Y., and Kreth,J. (2011c) Oxygen dependent pyruvate oxidase expression and production in *Streptococcus sanguinis*. *Int J Oral Sci* **3**: 82-89.

Zhu,J., and Shimizu,K. (2004) The effect of *pfl* gene knockout on the metabolism for optically pure D-lactate production by *Escherichia coli*. *Appl Microbiol Biotechnol* **64**: 367-375.

Zomer,A.L., Buist,G., Larsen,R., Kok,J., and Kuipers,O.P. (2007) Time-resolved determination of the CcpA regulon of *Lactococcus lactis* subsp. cremoris MG1363. *J Bacteriol* **189**: 1366-1381.

ITQB-UNL | Av. da República, 2780-157 Oeiras, Portugal
Tel (+351) 214 469 100 | Fax (+351) 214 411 277

www.itqb.unl.pt